UNIVERSITEIT VAN PRETORIA
UNIVERSITY OF PRETORIA
YUNIBESITHI YA PRETORIA

Establishment of serological assays to investigate the incidence of West Nile and Wesselsbron flavivirus infections in Africa

by

Carla Lourens

Submitted in partial fulfilment of the requirements for the degree

MSc Medical Virology

Faculty of Health Sciences

Department of Medical Virology

University of Pretoria

South Africa

Supervisor: Prof Marietjie Venter

Co-Supervisor: Dr Adriano Mendes

August 2023

Declaration

I, **Carla Lourens**, declare that the dissertation, which I hereby submit for the degree Master of Science, is my own original work followed from research carried out in the **Department of Medical Virology**, University of Pretoria, under the supervision of **Prof. Marietjie Venter** and co-supervision of **Dr Adriano Mendes**. These results have not previously been submitted by me for a degree at this, or any other tertiary institution.

Signed: 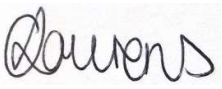

Date: 12 June 2023

Acknowledgements

My sincere gratitude and thanks to:

- My supervisor, Prof Marietjie Venter for providing me the incredible opportunity to learn from her and work on a very exciting project. She helped me grow as a scientist, by challenging me to think more critically and expand my knowledge.
- Dr Adriano Mendes, my co-supervisor, for his invaluable advice, continuous support, and patience during my MSc study. His knowledge and experience encouraged me throughout my project.
- Dr June Williams and all other veterinarians who was an integral part of the project and provided us with animal samples for testing.
- Our collaborators at Wageningen University & Research in the Netherlands, Dr Paul Wichgers-Schreur and Prof Jeroen Kortekaas, for providing us with the recombinant WNV and WSLB NS1 proteins.
- Dr Benjamin Gutjahr from Friedrich-Loeffler Institute in Germany, who assisted in the ELISA development and interpretation.
- Our ANDEMIA partners, Dr Andrea Bernasconi and Dr Clarence Yah, for the training on statistics and R programming.
- Fellow ZARV members, who assisted in processing the diagnostic samples as well as allowing me to bounce ideas back and forth, regarding my project.
- A special thank you to Miss Caitlin MacIntyre, whose willingness to lend a hand when needed and her endless support, has made a significant difference in my life. Her positivity and can-do attitude are infectious and I am grateful to have worked beside her.

I could not have done this without:

- My loving parents, Jacques and Annatjie, and sister, Lizé, for without your support I couldn't have done it, both emotional and financial. Your constant encouragement and belief have given me the motivation to persevere through the challenges and difficulties. Your willingness to lend an ear and provide emotional support whenever I needed it, gave me the strength to keep pushing forward. Thank you for setting a high standard for hard work and instilling good values to ensure I succeed. As I continue forward in my career, I will carry these lessons and values that you have taught me always. I will continue to make you proud and turn my dreams into a reality!

The following are thanked for funding:

- The running costs of this project were partially funded by the Long-term EU-Africa research and innovation Partnership on food and nutrition security and sustainable Agriculture (LEAP-Agri) grant: Research Network (LEARN) on Arboviral Zoonoses which is an EU/NRF facilitated grant (grant number: 115574). I also thank them for a bursary that helped me fund two years of my studies.

- The human aspects of the project were funded by the German Federal Ministry of Education and Research via a program called Research Networks for Health Innovations in Sub-Saharan Africa for the ANDEMIA project (grant number: 01KA1606) and the G7 Global Health Fund of the Robert Koch Institute through Dr Fabian Leendertz (grant number: ZMVI1-2517GHP703).

- I would like to thank the Poliomyelitis research foundation for awarding me a MSc bursary (grant number: 21-34)

- University of Pretoria Postgraduate bursary for their financial support in their form of student bursaries

Table of Contents

Abbreviations

%	Percentage
°C	Degree Celsius
µL	Microliter
µM	Micromolar
g	Grams

A

Abs	Antibodies
ABTS	2,2'-Azinobis [3-ethylbenzothiazoline-6-sulfonic acid]-diammonium salt
AFDUC	Acute febrile disease of unexplained cause
AHSV	African Horse Sickness Virus
ALF	Alfuy Virus
ANDEMIA	African Network for Improved Diagnostics, Epidemiology and Management of Infectious Agents
AUC	Area under the curve

B

BAGV	Bagaza Virus
BEVS	Baculovirus expression vector system
bp	Basepair
BSL3	Biosafety level 3

C

C	Capsid
CDC	Centers for Disease Control and Prevention
cDNA	Complimentary DNA
cGAS	Cyclic GMP-AMP synthase
CI	Confidence interval
CNS	Central nervous system
CO_2	Carbon dioxide
CPC	Cloned plasmid control
CPE	Cytopathic effect
CSF	Cerebrospinal fluid
CT	Cycle threshold
CVZ	Centre for Viral Zoonosis

D

DALLRD	Department of Agriculture, Land Reform and Rural Development
DEET	N, N-Diethyl-metatoluamide
DENV	Dengue Virus
DNA	Deoxyribonucleic acid
dsRNA	Double-stranded RNA

E

E	Envelope
EDTA	Ethylenediaminetetraacetic acid
EEV	Equine encephalitis

EIP	Extrinsic incubation period
ELISA	Enzyme linked immunosorbent assay
EMEM	Eagle's minimum essential media
ER	Endoplasmic reticulum

F

Fc	Fragment crystallisable region
FCS	Foetal calf serum
FRET	Fluorescence resonance energy transfer

H

H_2O	Hydrogen dioxide/water
HA	Hemagglutination inhibiting test
His-tag	Polyhistidine tag
HIV	Human immunodeficiency virus
HRP	Horse radish peroxidase

I

IFA	Immunofluorescence assay
IFN	Interferons
IgG	Immunoglobulin G
IgM	Immunoglobulin M
ISR	Immune status ratio

J

J	Youden Index
JE	Japanese encephalitis
JEV	Japanese encephalitis virus

K

kb	Kilobases
kDa	Kilodaltons
km	Kilometre
KOK	Kokobera Virus
KUN	Kunjin Virus
KZN	KwaZulu-Natal

L

LoD	Limit of detection

M

M	Membrane
MEM	Minimum essential media
Micro-VNT	Micro virus neutralisation test
MIDV	Middelburg Virus
Min	Minutes
mL	Millilitre
mRNA	Messenger RNA
MVE	Murray Valley encephalitis

N

NCA	Normal cell antigen
ng	Nanogram
NICD	National Institute for Communicable Diseases
nm	Nanometre
NS	Non-structural
NS5MTase	N-terminal methyltransferase
NS4RdRp	C-terminal RNA dependent RNA polymerase
NTC	Non-template control

O

OBP	Onderstepoort Biological Products
OD	Optical density
OH	One Health
OR	Odds ratio
ORF	Open reading frame

P

P	Passage
PBS	Phosphate buffered saline
PCR	Polymerase chain reaction
pH	Potential of hydrogen
prM	Pre-membrane
PRNT	Plaque reduction neutralisation test
PRR	Pattern recognition receptors

Q

qRT-PCR	Quantitative reverse transcription polymerase chain reaction

R

RIG-I	Retinoic acid inducible gene I
RNA	Ribonucleic acid
ROC	Receiver operating curve
rpm	Revolutions per minute
RT-PCR	Reverse transcription polymerase chain reaction
RVF	Rift Valley Fever

S

s	Seconds
SA	South Africa
SDS	Sodium dodecyl sulfate
SHUV	Shuni Virus
SINV	Sindbis Virus
SLE	Saint Louis encephalitis
SSA	Sub-Saharan Africa
ssRNA	Single-stranded RNA
STR	Stratford Virus
SUD	Sudden unexpected death

T

TAC	TaqMan array card
TAE	Tris-acetate EDTA
TBEV	Tick borne encephalitis
TCID	Median tissue culture infectious doseTLRToll-like receptors
TMB	3,3',5,5'-Tetramethylbenzidine

U

U	Units
UP	University of Pretoria
USA	United States of America
USU	Usutu Virus
UTR	Untranslated region

V

V	Volts
VNT	Virus neutralisation test

W

WNRA	West Nile antigen
WNV	West Nile Virus
WOAH	World Organization for Animal Health
WSLB	Wesselsbron Virus
WUR	Wageningen University and Research

Y

YFV	Yellow Fever Virus

Z

ZARV	Zoonotic arbo and respiratory virus research group
ZIKV	Zika Virus
ZRU	Zoonotic Research Unit
ZRUA	Zoonotic Research Unit ANDEMIA

List of Figures

Appendix

List of Tables

Chapter 7

Appendix

Conferences and Meeting Procedures

Lourens C, MacIntyre CDM, Mendes A, Venter M. Surveillance of West Nile virus in horses and humans in South Africa for 2021. Faculty of Health Science Faculty Day 2022, University of Pretoria, South Africa, 23 August 2022. (Poster)

Lourens C, MacIntyre CDM, Mendes A, Venter M. Surveillance of West Nile virus in horses and humans in South Africa for 2021. Southern African Society for Veterinary Epidemiology and Preventive Medicine (SASVEPM) 2022, East London Convention Center, South Africa, 24 August 2022. (Poster)

Annual Department of Medical Virology Journal Club and Research Report oral presentations.

Publications

MacIntyre CDM, **Lourens C**, Mendes A, Venter M. West Nile Virus, a missed cause of acute fever of unknown cause and neurological infections among hospitalized patients in South Africa. Submitted to Viruses.

Lourens C, MacIntyre CDM, Mendes A, Venter M. Genomic and serological surveillance of WNV virus in animals presenting with neurological disease in South Africa, 2017-2022. To be submitted.

Lourens C, MacIntyre CDM, Mendes A, Pretorius, M, Venter M. Wesselsbron virus identified in animals presenting with neurological signs in South Africa. To be submitted to Viruses.

Abstract

West Nile virus (WNV) and Wesselsbron virus (WSLB) are endemic to South Africa and considered to be the most important flaviviruses circulating in this country. Both viruses are arboviruses, with WNV transmitted by *Culex* mosquitoes and *Aedes* mosquitoes responsible for the spread of WSLB. Although up to 80% of WNV infections are thought to be asymptomatic in humans and sensitive animals such as horses, in 20% of cases clinical signs associated with fever or neurological signs infections occur. West Nile virus causes severe disease in up to 90% of clinical cases in equines, with neurological signs such as ataxia, recumbency, hind leg paralysis and blindness with >35% of cases being fatal. In humans, 20% of cases present with a rash and fever of which <1% of cases presenting with neurological signs, such as headache, convulsions and in severe cases, meningitis, or encephalitis and 10% of severe cases being fatal. To date WSLB mostly infects livestock, resulting in abortion or congenital malformations, while humans have reported flu-like symptoms. A single case of meningoencephalitis was reported. Other flaviviruses detected in South Africa include Usutu virus, Bagaza virus and Banzi virus.

Viraemia of flaviviruses is short, which results in several cases being missed by molecular assays. Thus, combining molecular and immunoglobulin M (IgM) serological assays, results in a better overview of the incidence of these viruses. Commercial enzyme linked immunosorbent assays (ELISAs) are available for WNV but are expensive and need to be imported. For WSLB, no commercial ELISAs are available. Surveillance studies in South Africa has indicated that WNV circulate annually during late summer and autumn in South Africa in birds and are transmitted by mosquitoes to horses, wildlife and some domestic animals and humans. Wesselsbron cases are rarely reported outside of outbreak situations. The incidence of cases in animals and humans is not well defined partially due to a lack of available diagnostic assays for different species.

The study aimed to investigate the molecular epidemiology of WNV and WSLB in South Africa. The burden of WNV and its association with neurological disease was identified through syndromic surveillance in animals and humans using available serological tools. Additionally, ELISAs were developed testing for immunoglobulin G

(IgG) and IgM antibodies in equines, humans, cattle, and a species-independent assay for WNV and WSLB using the non-structural 1 (NS1) antigen, which differs from the commercial ELISAs available that targets the envelope (E) protein.

Chapter 1 provides an in-depth overview of arboviruses, focusing on flaviviruses specifically and then taking a closer look at WNV and WSLB to highlight the importance of the viruses as a pathogen of medical and veterinary importance. Diagnostic methods to determine the incidence of these viruses are also discussed.

Chapter 2 describes the validation of a one-step real-time reverse transcription polymerase chain reaction (RT-PCR) to detect WSLB in samples subjected to testing and to ensure it can detect new cases of the virus.

In chapter 3, hospitalised cases in humans at sentinel hospitals in Gauteng and Mpumalanga were investigated during the same time by screening acute fevers with or without neurological signs to investigate the incidence and epidemiology of human cases. All samples were subjected to molecular testing with the LCD-Chipron assay (CHIP), as well as serological testing with a commercial WNV IgM ELISA kit from Euroimmun. In total, 1/216 samples tested positive for WNV with the ChIP assay, but further testing could not confirm this result. With regards to the serological testing, 12/116 tested positive for WNV and confirmed with neutralisation assays in January-June 2021, while 1/15 samples tested positive in January-April 2022. This resulted in an average positivity rate of 8.45% for 2021 and 2.44% for 2022. Samples that tested positive on IgM assay, but negative on neutralisation assay, were subjected to testing for WSLB, but no positive samples were detected. The IgM positive cases obtained from the human testing, aid in establishing molecular and serological epidemiology trends for these two flaviviruses in South Africa as well as contributing to the description of the disease.

In chapter 4, an established surveillance system to detect arboviruses in horses, livestock and wildlife with unexplained neurological disease or fever was used to detect flavivirus circulation and describe the incidence and epidemiology of cases between 2021-2022. In total, 338 animal samples were submitted, 197 in 2021; 141 in

2022, for testing and included samples from equines, wildlife, livestock, domestic, and avian species. All samples were subjected to screening with a panflavi real-time RT-PCR to detect the presence of flaviviruses. In total, 166/231 available serum samples from equines were subjected to testing with the commercial WNV IgM Equine ELISA for the whole year, as part of routine surveillance. (77/120 in 2021, 89/111 in 2022) One equine sample tested positive for WNV, and another sample tested positive for WSLB by nested flavivirus RT-PCR and confirmed by sequencing. In addition, an avian sample also tested positive for WSLB using RT-PCR in 2022. In total 10/166 (6.02%) tested positive for WNV IgM antibodies and were confirmed with neutralisation assays. This resulted in a positivity rate of 7.5% for 2021 and 1% for 2022. In 2021, there was a higher incidence of WNV by nearly 80% compared to 2022. All cattle samples submitted between 2012-2022 were screened with neutralisation assays for WNV and WSLB to detect any positive cases that can be used to validate the in-house cattle ELISA. Between 2012 and 2022, 139 livestock samples were submitted. Only 29/139 samples were plasma samples, while only 23/29 were available for screening. With regards to the WNV neutralisation assays, 7/139 (5.04%) livestock samples had neutralising antibodies against WNV. For WSLB, 7/139 (5.04%) of the livestock samples had neutralising antibodies against WSLB.

Chapter 5 shows the expression of recombinant WNV and WSLB NS1 proteins using the baculovirus system. Transfection of the recombinant baculovirus and subsequent replication of the virus was confirmed by PCR of the flavivirus NS1 gene. It wasn't possible to distinguish the protein on a sodium dodecyl-sulfate polyacrylamide gel electrophoresis (SDS-PAGE) gel from the background. After 3 passages, the protein was purified and ran on an SDS-PAGE gel. For WNV, a protein with a concentration of 0.55 mg/mL was obtained and a faint band was visible on the gel. For WSLB, a protein with a concentration of 0.14 mg/mL was measured using a Nanodrop but no visible band could be seen on the SDS-PAGE gel.

Chapter 6 and 7 show the development, optimisation, and validation of in-house serological assays for WNV and WSLB in both horses and humans using a baculovirus expressed antigen obtained from Wageningen University and Research (WUR) in the Netherlands. The in-house expressed NS1 antigen was intended for the use of the assay developments, but as discovered in Chapter 5, was unsuccessful. The IgG and

IgM assays against the NS1 protein of WNV and WSLB were evaluated, optimised and validated. The sensitivity and specificity of the assays were determined using statistical software, MedCalc. Although the commercial WNV ELISAs for humans and equines were determined to be more sensitive than our in-house assay, the discrepancy between sensitivity and specificity can be due to the different target antigen, E protein vs NS1 protein, as well as using baculovirus expressed antigen that might not be compatible with commercially available antibodies.

This study highlights the importance of establishing sensitive molecular and serological assays for arbovirus surveillance. Implementation of both molecular and serological screening suggests that flaviviruses continue to be an under-appreciated burden in South Africa. Surveillance in humans with acute febrile disease of unknown cause (AFDUC) and/or neurological signs helped to define the burden of disease and indicated an increased risk for WNV associated hospitalisations in summer and late autumn in South Africa suggesting that the virus is still missed likely due to a lack of clinical awareness of the potential risk for more severe disease. Active surveillance at the animal-human interface may aid in early detection and predicting outbreaks and may assist in the prevention, detection, and control of these arboviruses at both the local and international levels.

Chapter 1: Literature review

1.1 Arboviruses

1.1.1 Background

Viral diseases have emerged dramatically over the last few years, resulting in epidemics affecting humans. The majority of emerging viruses are vector borne or zoonotic, meaning that the virus is transmitted from animals and able to jump species to ultimately infect humans (Aspock et al., 2008). Arthropod borne viruses or arboviruses have been some of the most important emerging and reemerging diseases of the past number of decades, possibly due to climate change (Aspock, 2008). Arboviruses are a group of viruses that replicate in both arthropod vectors and vertebrate hosts (Burt et al., 2014). Arboviruses do not belong to a distinct taxonomic group but are rather grouped together based on their similar lifecycle and transmission patterns (Jones et al., 2020). The vast majority of arboviruses have a ribonucleic acid (RNA) genome and are able to rapidly adapt to changing host and environmental factors (Beckham and Tyler, 2015). Transmission between hosts is facilitated by insect vectors like sandflies, midges, mosquitoes, and ticks while vertebrate hosts act as amplification or reservoir hosts (Shope and Meegan, 1997).

There are 534 arboviruses registered in the International Catalogue of Arboviruses (Madewell, 2020). Of all the registered arboviruses, 134 have caused illnesses in humans (Madewell, 2020). Arboviruses are taxonomically diverse encompassing eight families and 14 genera (Gubler, 2002). There are five genera that are most associated with zoonotic arbovirus infections - alphavirus (*Togaviridae* family), flavivirus (*Flaviviridae* family), orthobunyavirus, nairovirus and phlebovirus (*Bunyavirales* family) (Venter, 2018; Abudurexiti, 2019). Some of the most important arboviruses include West Nile (WNV), Zika (ZIKV), Yellow Fever (YFV), Dengue (DENV)and Japanese Encephalitis virus (JEV), which are all members of the Flaviviridae family (Venter, 2018).

Arboviruses are geographically distributed over all the continents (Figure 1.1), with the number of arboviruses in an area increasing towards the equator, with the majority found in subtropical and tropical climate conditions to allow for the transmission of cold-blooded arthropods (Aspock et al., 2008). The limiting factors that influence the

geographical occurrence of arboviruses include temperature, rainfall patterns and humidity (Gubler, 2002).

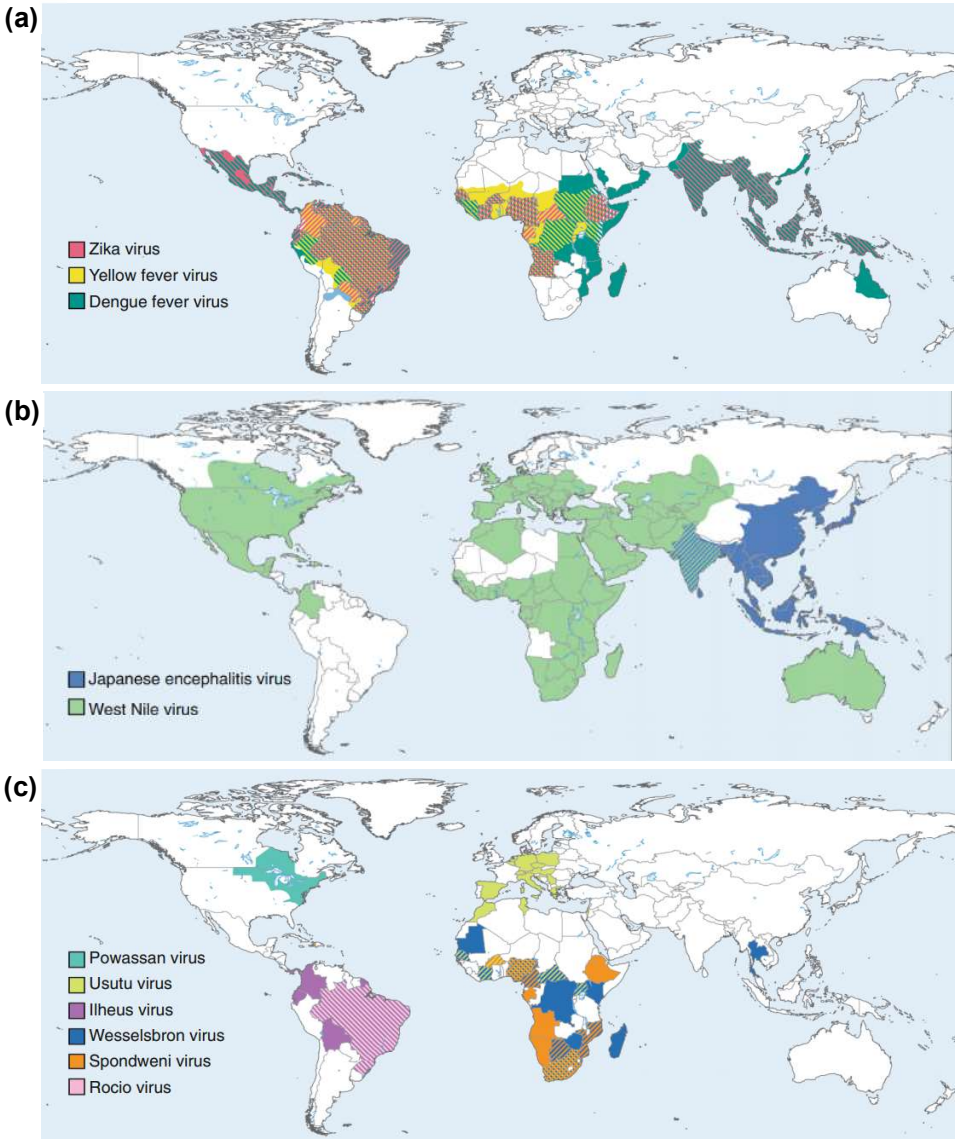

Figure 1.1: Distribution of major flaviviruses. **(a)** The global transmission of *Aedes*-transmitted flaviviruses including ZIKV, YFV and DENV. **(b)** Incidence of JEV and WNV globally and **(c)** The approximate geographic locations of flaviviruses with the potential for emergence in human populations. Adapted from (Pierson and Diamond, 2020).

Arboviruses are all dependent on vertebrate hosts to maintain them in nature (Kuno, 1998). Humans for the most part, are considered to be dead-end hosts, meaning that they do not play a role in the transmission cycle, with the exception of some like DENV, YFV and ZIKV, which uses humans as reservoir hosts in urban settings (Gubler, 2002; Weaver, 2004). The most common arthropod vector families

are *Ixoxidae* (hard ticks), *Argasidae* (soft ticks), *Culicidae/Anophelinae* (mosquitoes), *Psychodidae/Phlebotominae* (sandflies) and *Ceratopogonidae* (gnats) (Jupp, 2014).

1.1.2 Life cycle of arboviruses

The basic life cycle of arboviruses depends on the virus being transmitted by a blood-sucking arthropod to a vertebrate host, causing viraemia in the host (Pierson and Diamond, 2020). This viraemic period is usually short and during this time, another arthropod vector can be infected when biting the infected host (Aspock et al., 2008). More than one host is often involved where the reservoir host develop viraemia to a high concentration to transmit the virus back to the vector. It is not definite that a host will fall ill, meaning that the host can be asymptomatic. It is also possible that the disease can be transmitted to a human host, who is sometimes the only host and other times known as the dead-end host due to low viremia levels (Pierson and Diamond, 2020).

The virus is ingested by the arthropod during a blood meal and infects the midgut's epithelial lining (Wu et al., 2019). The temperature has a big influence on the length of the extrinsic incubation period, where increased temperature can result in shorter extrinsic incubation period (EIP) and/or an increase of viral replication, which will increase transmission rates (Coffey et al., 2013). The first replication of the virus takes place in the extravascular tissues. The suitability of a vertebrate species to act as a host and maintenance of the cycle depends mainly on the virus concentration reached during viraemia, as well as the length of viraemia (Aspock et al., 2008). Several factors influence the susceptibility of a vector, as well as a host (Liang et al., 2015).

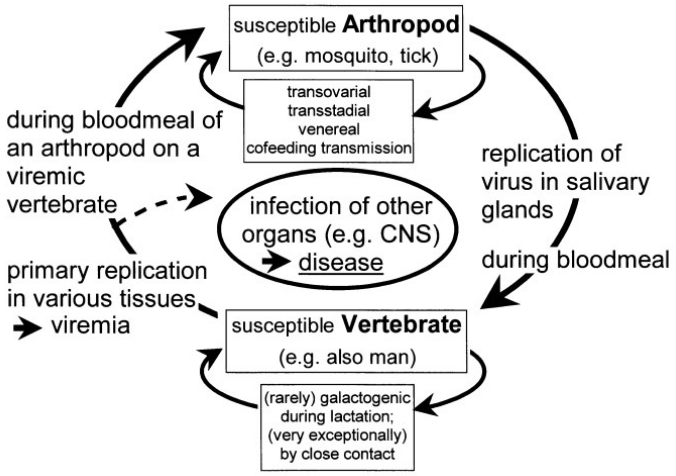

Figure 1.2: The arbovirus life cycle. Adapted from (Aspock et al., 2008).

1.2. Flaviviruses

The family Flaviviridae is divided into three genera, namely the *Flavivirus, Pestivirus*, and *Hepacivirus*, many of whose members are accountable for a considerable proportion of morbidity and mortality worldwide, both in humans and animals (Schweitzer, 2009).

1.2.1 Background and phylogeny

The flavivirus genus is classified under the *Flaviviridae* family and is made up of small, enveloped viruses that contain single-stranded positive sense non-segmented ribonuclease acid (RNA) genomes, which is approximately 11 kilobases (kb) in length (Lindebach and Rice, 2003). The flavivirus genus consists of more than 70 members, with some of the most important being DENV, WNV, Japanese Encephalitis virus (JEV) and YFV (Mazeaud et al., 2018). These viruses can all cause serious human illnesses (Tomar, 2017). More attention has been given to flaviviruses, due to their re-emergence in different areas of the world (Gould et al., 2017). The fact that there are increasing YFV transmission events in urban environments, despite the availability of a vaccine is exemplary of the impact on global health (Pierson and Diamond,2020). The diverse arthropod vectors, disease characteristics and wide geographic distribution of flaviviruses, makes it important to develop tools to identify them (Holbrook, 2017).

The JEV serogroup is made up of eight species and twosubtypes (MacKenzie et al., 2002). The serogroup was defined based on cross-neutralisation tests using polyclonal sera and include the Japanese encephalitis (JE), St. Louis encephalitis (SLE), West Nile, Murray Valley encephalitis (MVE), Kunjin (KUN), Alfuy (ALF), Koutango (KOU), Usutu (USU), Kokobera (KOK), and Stratford (STR) viruses (Poidinger et al., 1996). These viruses vary widely in their ability to infect human and animal species, as well as the disease characteristics produced (Schweitzer et al., 2009). Being of global importance, the viruses that are part of this serogroup are endemic on all continents, apart from the Antarctic (Habarugira, 2020). Infection results in symptoms ranging from febrile illness, with or without a rash and with or without myalgia, to a meningo-encephalitis with significant mortality; however, most infections are subclinical or inapparent (MacKenzie et al., 2002). The members of this group all have a natural maintenance cycle that mostly alternate between birds and mosquitoes (WNV), while some uses pigs (JEV), rodents or domestic animals (WSLB) as vertebrate hosts (MacKenzie, 2002; Gubler, 2007). Table 1.1 shows the transmission routes and

disease caused by flaviviruses.

Table 1.1: Transmission routes and diseases caused by flaviviruses. Adapted from (Pierson and Diamond, 2020).

Virus	Antigenic group	Primary geographic distribution	Zoonotic reservoir (host)	Transmission vector and route	Human disease	No of human infections
Bagaza virus	Ntaya	Africa Europe India	Birds	*Cx*. univittatus*	Unknown	Unknown
Banzi virus	Uganda S	Africa	Rodents	*Cx. rubinotus*	Febrile illness	Unkown
Dengue	Dengue	South America Central America North America Asia Australia Africa	Non-human primate (sylvatic cycle)	*A**. Aegypti* *A. albopictus*	Dengue fever Severe dengue	390 million infections per year
Ilheus	Japanese encephalitis	South America Central America	Birds Non-human primates Horses	*Cx. Pipiens, Ochlerotatus serratus, Sabethes, Haemagogus*	Febrile syndrome Encephalitis	Unknown
Japanese Encephalitis	Japanese encephalitis	Asia Australia	Birds Pigs	*Cx.tritaeniorhynchus, Cx. Annulirostris*	Febrile syndrome Meningitis Encephalitis	70 000 cases per year
Powassan	Tick-borne flavivirus	North America Eastern Europe	Rodents Lagomorphs Deer	*I***. cookei* *I. scapularis*	Febrile syndrome Meningitis Encephalitis	Hundreds
Rocio	Japanese encephalitis	South America (Brazil only)	Birds	*Cx. pipiens* *Cx. tarsalis* *Psorophora ferox*	Febrile syndrome Encephalitis	Unknown
Spondweni	Spondweni	Africa North America	Non-human primates (sylvatic cycle)	*Aedes* *Culex* *Eretmapodites* and *Mansonia*	Febrile syndrome Vascular leakage Neurological impairment	Unknown

Table 1.1 cont.: Transmission routes and diseases caused by flaviviruses. Adapted from (Pierson and Diamond, 2020).

Virus	Antigenic group	Primary geographic distribution	Zoonotic reservoir (host)	Transmission vector and route	Human disease	No of human infections
Usutu	Japanese encephalitis	Africa Europe	Birds	*Cx. pipiens*	Febrile syndrome Meningitis Encephalitis Acute flaccid paralysis	Hundreds to thousands
Wesselsbron	Yellow fever	Africa	Cattle Sheep Rats	*Aedes spp.*	Febrile syndrome	Unknown
West Nile	Japanese encephalitis	North America Middle East Africa Europe Australia	Birds	*Cx. pipiens* *Cx. tarsalis*	Febrile syndrome Meningitis Encephalitis Acute flaccid paralysis	<10 000 cases per year
Yellow fever	Yellow fever	Africa South America	Non-human primates (sylvatic cycle)	*A. aegypti*	Febrile syndrome Liver failure Haemorrhagic syndrome	130 000 severe cases per year
Zika	Spondweni	Central America South America Africa Asia North America	Non-human primates (sylvatic)	*A. aegypti* *A. albopictus* Sexual transmission Vertical transmission	Febrile syndrome Guillain-Barre syndrome Congenital anomaly Microcephaly	Thousands to millions depending on the year

**Cx*: Culex ***A:* Aedes ****I:* Ixodes

1.2.2 Viral genome morphogenesis

Flaviviruses share a common structure, with the mature enveloped flavivirus virion displaying icosahedral symmetry, a spherical shape, and a diameter of roughly 50 nanometres (nm) diameter (Pierson, 2020).

1.2.2.1 Untranslated region

The genome of flaviviruses is of positive polarity, meaning that the viral genomic RNA acts as a messenger RNA and is immediately translated (Pierson and Diamond, 2020). The genome has a single open reading frame (ORF) that is flanked by a structured 5' untranslated region (UTR) and 3' UTR region (Blazevic et al., 2016). It has been demonstrated that the 5' UTR and 3' UTR are involved in both host and viral protein interactions (Pierson and Diamond, 2020). Three structural proteins are encoded for by the amino terminus of the genome and make up the virus particle – capsid (C), membrane (M), with pre-membrane (prM) as its precursor, and envelope (E) protein (Blazevic et al., 2016). The genome also encodes for seven non-structural proteins and is essential for viral replication (Mukhopadhyay et al., 2005).

1.2.2.2 Structural proteins of flaviviruses

The structural pre-membrane (prM/M) and envelope (E) proteins are arranged in icosahedral lattices at the virion surface and differ between a mature and immature virion(Blazevic et al., 2016). The prM/M and E proteins play an integral part in viral morphogenesis (Mukhopadhyay et al., 2005). The E protein mediates the virus entry step in the replication cycle (Mukhopadhyay, 2005). Its structure was first solved for tick-borne encephalitis (TBEV), which was followed by DENV, WNV and ZIKV (Zhang et al., 2004). The structure of the E protein is made up of three domains (E-DI, E-DII and E-DIII) that are attached to the viral membrane through a helical stem and two antiparallel transmembrane domains (Mukhopadhyay et al., 2005). The prM assists in the folding of the E protein in the endoplasmic reticulum (ER) (Mukhopadhyay, 2005). To avoid any conformational changes to the E protein, the prM is incorporated into the viral envelope during the virion morphogenesis process (Modis et al., 2003). For maturation of the virion particle, the prM is cleaved to M when the immature virions are transported through the Golgi network (Modis et al., 2003). When mature, 90 E dimers are incorporated and arranged in a specific herringbone pattern (Pierson, 2020). The capsid protein is a small helical protein that binds to either viral nucleic acids or host lipids and allows for the incorporation of the viral genome into the virions (Mukhopadhyay et al., 2005).

1.2.2.3 Non-structural proteins

The RNA genome encodes for seven non-structural (NS) proteins – NS1, NS2A, NS2B, NS3, NS4A, NS4B and NS5 (Weissenbock et al., 2010). The NS1 protein [≈46 kilodaltons (kDa)] is usually found within cells but is also found on the cell surface or

secreted from mammalian cells (Mackenzie et al., 1996; Lindebach and Rice, 2003). The NS1 glycoprotein is made up of two or three N-linked-glycosylation sites and have 12 conserved cysteines that form disulphide bonds (Lindebach and Rice, 2003). It has been determined that NS1 plays an integral role in RNA replication and during infection; a strong humoral response is mounted against this protein (Mackenzie et al., 1996; Lindebach, 2003). The NS2A protein is relatively small (≈22 kDa) and is a hydrophobic protein (Lindebach and Rice, 2003). The function of the NS2A protein is to mediate the shift between viral RNA packaging and RNA replication (Khromykh et al., 2001). The NS2B protein (≈14 kDa) is a membrane associated protein and is a co-factor for the serine protease required by NS3 (Droll et al., 2000). The NS2B protein forms a complex with NS3 and is a necessary co-factor for the serine protease in NS3 (Lindebach and Rice, 2003). The NS3 protein (≈70 kDa) is a large, multi-functional protein that makes use of several enzymatic activity to cap viral RNA and is involved in RNA replication (Bollati et al., 2010). The NS3 protein is associated with membranes through interactions with NS2B (Lindebach and Rice, 2003). The NS4A and NS4B proteins (≈16 and 27 kDa respectively) are small, hydrophobic proteins (Lindebach and Rice, 2003). The NS4A protein plays a role in membrane rearrangement by translocating the NS4B protein into the endoplasmic reticulum (ER) lumen, where NS4B, which is a transmembrane protein, interferes with interferon signaling (Lindebach and Rice, 2003). The largest protein of all the NS proteins is the NS5 protein (≈103 kDa) (Lindebach, 2003). It is a well-conserved, multifunctional protein and is made up of anN-terminal methyltransferase (NS5MTase) domain and a C-terminal RNA dependentRNA polymerase (NS5RdRp) domain (Bollati et al., 2010). The N-terminal of the NS5protein plays a role in viral capping, while the C-terminal aids in RNA replication (Bollatiet al., 2010). Figure 1.3 illustrates the flavivirus genome composition.

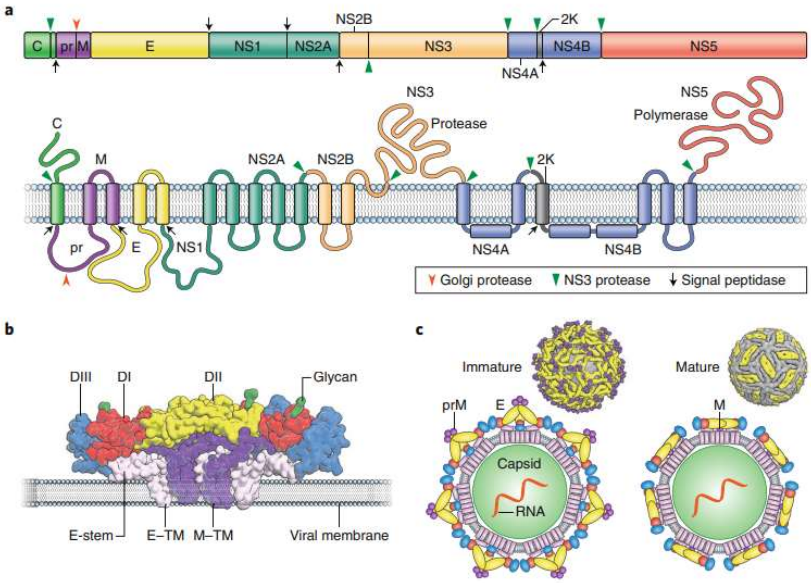

Figure 1.3: Organisation and structure of flaviviruses. (a) Flaviviruses encode a single open reading frame that is translated at the ER into a polyprotein, which is subsequently cleaved by viral and host cell proteases. This processing results in 10 functional proteins including the three structural proteins, C, prM and E, and seven non-structural proteins. The NS4A exists in two forms that differ with respect to cleavage of the 2 K domain at its carboxy terminus. (b) Flavivirus E proteins are elongated three-domain structures tethered to the viral membrane by a stem and two antiparallel transmembrane domains. The E protein domains are indicated in red, yellow and blue (DI–III, respectively). The M protein, also attached to the viral membrane by two transmembrane domains, is shown in purple. (c) The distinct arrangement of E proteins on immature (left) and mature (right) forms of the virion are depicted. Adapted from (Pierson and Diamond, 2020).

1.3 Virus entry

The initial step of virus entry is the binding of the E glycoprotein to cellular receptors (Pierson and Diamond, 2020). Flaviviruses must recognise specific receptors for cell entry, but this can vary between different host species (Smit et al., 2011). Negatively charged glycosaminoglycans, like heparan sulphate, are expressed on the cell surface and are utilised by several flaviviruses as a low-affinity attachment factor (Mukhopadhyay et al., 2005). The interactions of glycosaminoglycans allow for the concentration of the virus at the cell surface and this is mediated by the DII domain of the E-protein (Mukhopadhyay et al., 2005). The attachment factors on the host cell membrane are responsible for initiating fusion with the E protein of the virus and are transported into the endosome (Pierson and Diamond, 2020).

Flaviviruses enter the cell through clathrin-mediated endocytosis (Smit et al., 2011). The virus particles diffuse along the surface to a pre-existing clathrin-coated pit by either binding to the entry receptor, which is localised to clathrin hotspots at the cell surface or being transported to the pre-existing clathrin-coated pit (Smit et al., 2011).

The plasma membrane in the pit folds back on itself to form a clathrin-coated vesicle (Smit, 2011). The vesicle is then transported from the plasma membrane, and the clathrin coat released from the vesicle (Pierson and Diamond, 2020). Different cell entries have been recorded for different virus strains and cell types (Pierson, 2020). The endocytic vesicle that carries the virus is delivered to early endosomes, which in turn matures into a late endosome (Smit et al., 2011). Figure 1.4 represents the flavivirus replication cycle.

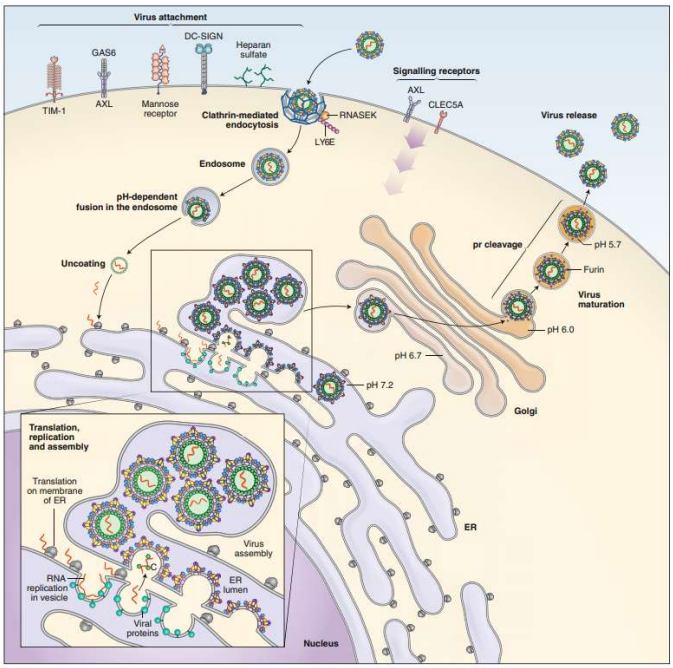

Figure 1.4: The flavivirus replication cycle. Flaviviruses infect mammalian cells via interactions with multiple types of host attachment factors, including molecules that bind to the viral membrane or virion-associated N-linked carbohydrates. Interactions with cell-surface host factors, may also initiate signalling pathways that modulate the host immune response. Virions are internalised by clathrin-dependent mechanisms. Viral fusion with host membranes occurs in the endosome in a low pH-dependent manner. Viral RNA replication occurs on membranes of the host reorganized through the actions of the non-structural proteins. These virus-induced membrane structures spatially coordinate viral genomic RNA replication and virion morphogenesis. Virus particles assemble at and bud into the ER and traffic out of the cell. Virion maturation occurs during egress. Adapted from (Pierson and Diamond, 2020).

A low pH environment is required in the endosome, to allow for fusion between the viral membrane and the endosomal membrane (Laureti et al., 2018). Following fusion, the nucleocapsid is released into the cell cytosol (Laureti, 2018). It has been reported that the additionof a hydrogen cation to histidine residues triggers the conformational change of the E protein where the E homodimers are dissociated into monomers (Smit et al., 2011). This leads to the outward projection of DII and exposure of the fusion

loop at the DII to the target membrane (Mukhopadhyay et al., 2005). The E protein inserts its fusion loop into the membrane and three copies of E interact with each other to form a trimer (Pierson and Diamond, 2020). The DII is then believed to fold back on the trimer, resulting in a hairpin-like configuration (Pierson and Diamond, 2020). The energy that is released by the conformational changes allows for fusion (Pierson and Diamond, 2020). Finally, a fusion pore is formed and enlarged, after which the nucleocapsid is released into the cell cytosol (Smit et al., 2011; Laureti et al., 2018; Pierson and Diamond, 2020).

1.4 Viral replication

The genomic RNA of flaviviruses encodes for a single ORF, that is flanked by a 5' end and 3' end UTR, responsible for viral translation, replication, and regulation of the innate immune response (Gebhard et al., 2011). After the release of the nucleocapsid in the cell cytosol, the positive-sense single-stranded RNA is translated into a polyprotein, which is subsequently cleaved into structural and non-structural proteins (Pierson and Diamond, 2020). The replication process takes place at the surface of the endoplasmic reticulum in cytoplasmic viral factories (Lorenz et al., 2002). Using the single-stranded RNA (ssRNA) as a template, a double-stranded RNA (dsRNA) genome is synthesised. The dsRNA genome is then replicated, providing more viral ssRNA genomes (Pierson and Diamond, 2020). The assembly of the virus takes place in the endoplasmic reticulum (Lorenz et al., 2002). The virion buds at the endoplasmic reticulum and is transported into the Golgi apparatus (Piersonand Diamond, 2020). The prM protein is then cleaved, resulting in a mature virion (Pierson and Diamond, 2020). The mature virions are released by exocytosis (Pierson and Diamond, 2020).

1.5 Immune response to flavivirus infections

The flavivirus life cycle is confined within the host cell cytoplasm (Pierson and Diamond, 2020). The host cell is equipped with pattern recognition receptors (PRRs) distributed within the endosomal compartments and cytoplasm, which are able to detect and respond to viral RNA and infected cells (van Leur et al., 2021). The first line of defense is the innate immune response, which is rapid and required to establish adaptive immunity, which is long-lasting immunological memory (van Leur et al., 2021). To trigger an effective immune response, detection of invading virus molecules by the PRRs are required, as well as the PRRs activating the synthesis and secretionof type I interferons (IFNs) (van Leur et al., 2021). Briefly, the innate immune activation

starts by recognition of the flaviviral dsRNA or ssRNA in the cytoplasm by retinoic acid-inducible gene I (RIG-I), or endosomes by toll-like receptor (TLRs) (van Leur et al., 2021). Flaviviruses have developed multiple routes of intervention in either the nuclear factor kappa B (NFκB) pathway or the interferon regulatory factors (IRF) pathway (van Leur et al., 2021). For WNV specifically, the protease NS5 intervenes by suppressing the maturation of signal transducer and activator of transcription 2 (STAT2) and additionally NS1 can induce degradation of complement factor C4 and thus complement activation (van Leur et al., 2021).

Focusing on the antibodies specifically, neutralising antibodies are generated as a result of infection or vaccination and are critical for developing immunity to viral infections (van Leur et al., 2021). Antibody responses to flaviviruses are primarily elicited to the E, prM and NS1 proteins (Sevvana and Kuhn, 2020). The E protein is the primary target of neutralising antibodies and comprises of three domains – EDI, which contains the N-terminus, EDII that has the fusion loop to mediate endosomal fusion and EDIII, which is required for attachment to host cells (Sevvana and Kuhn, 2020). Antibodies to prM is also produced upon infection, with anti-prM antibodies dominating the B cell response (van Leur et al., 2021). The NS1 protein is multifunctional and exists in monomeric form, which participates in ER remodeling during replication associated with membranes of infected cells, and oligomeric forms that are secreted into serum during the acute infection (Glasner et al., 2018). The NS1 protein accumulates intracellularly and is secreted from infected cells, which can be found in blood serum and other body fluids (Fisher et al., 2023). Since antibodies are produced against this protein, it can be used for serology diagnosis. Figure 1.5 shows a schematic representation of the host innate immune response to flavivirus infection.

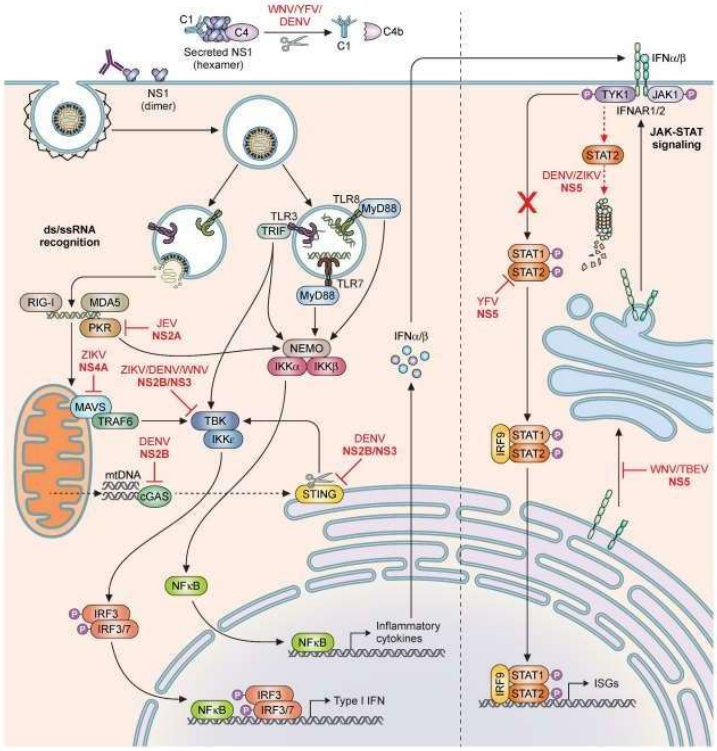

Figure 1.5: Schematic of the host innate immune response and flaviviral antagonism. Innate immune activation starts by recognition of flaviviral ds- or ssRNA either in the cytoplasm or in the endosomes. Subsequently the NFκB pathway and IRF pathways can be activated to initiate the production of Type I IFN and a range of inflammatory cytokines. Flaviviruses have developed multiple routes of intervention in both pathways. The protease NS5 and NS1 are involved in the suppression of viral infection. Adapted from van Leur, 2020.

1.6. Background and history of WNV and WSLB

1.6.1 West Nile Virus

West Nile Virus is a neurotropic flavivirus that affects the nervous system of the host and results in disease like West Nile fever and encephalitis (Colpitts et al., 2012). West Nile Virus is classified under the JEV serogroup of flaviviruses, with several viruses that share a similar transmission cycle (Gubler, 2007). The virus circulates between ornithophilic mosquitoes, specifically *Culex univittatus and C. pipiens*, and birds (Jupp, 2014). Birds are seen as the sentinels for WNV, as well as the amplifying hosts (Colpitts et al., 2012). Birds rarely show any symptoms, which can be due to their genetic resistance (Jupp, 2014; McVey et al., 2015). West Nile virus may spill over to humans or horses, but they are considered to be dead-end hosts (Venter,2018).

The first isolation of WNV in humans was from a blood specimen taken from a febrile patient in the West Nile province, Uganda in 1937 (Gubler, 2007). In the 1950s, isolation of WNV in adults in Israel were confirmed by performing neutralisation assays against various viruses (Melnick, 1951; Bernkopf et al., 1953). The virus was initially

regarded as an unimportant human and animal pathogen, since it was enzootic in Africa, Asia, and the Middle East, with some cases reported in Europe (Gubler, 2007). In 1999, individuals in New York City presented with WNV symptoms and it was confirmed that the virus was introduced to North America (Schweitzer et al., 2009; Colpitts et al., 2012). Since then, WNV can be found in several avian and mosquito species worldwide (Figure 1.6).

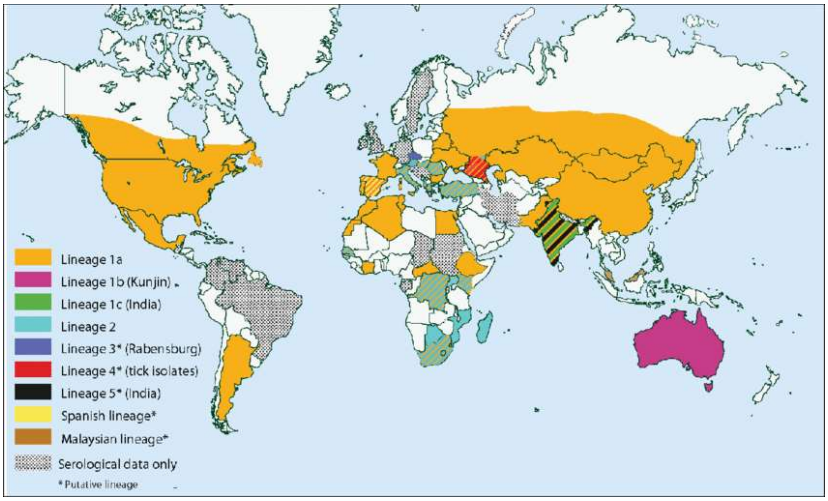

Figure 1.6: Worldwide distribution of West Nile virus. Adapted from (Ciota and Kramer, 2013).

West Nile virus is biologically diverse; up to nine lineages have been proposed (Fall, 2017). However, most human outbreaks of WN encephalitis have been attributed to lineages 1 and 2 (Fall, 2017). Lineage 1 is found in North America, North Africa, Europe and Australia and lineage 2 being endemic to South Africa and Madagascar (Venter et al., 2017b). Cases of the third and fourth lineage have been confirmed in Central and Eastern Europe, while lineage 5 has been reported in India (Lanciotti et al., 2002; Venter et al., 2017b). Lineage 6 has been described in Spain and is based on a small gene fragment (Fall, 2017). Koutango virus (lineage 7) was initially classified as a different virus but is now a distinct lineage of WNV and has shown to have a higher virulence than the lineage 1a strain in mice (Fall, 2017). Lineage 8 was isolated in Senegal in 1992 from *Culex perfuscus* and lineage 9 isolated from *Uranotaenia unguiculata* mosquitoes in Austria (Fall, 2017). Neuro-invasiveness and mildness of strain depend on the genotype and not the lineage of WNV (Burt et al., 2014).

1.6.2 Wesselsbron virus

Wesselsbron virus (WSLB) is an acute mosquito-borne virus that affects ruminants in Africa (Weyer, 2013). Wesselsbron virus is thought to be transmitted by *Aedes caballus juppi* mosquitoes and infects several domestic livestock species including camels, cattle, pigs, donkeys, and horses (Jupp and Kemp, 1998). It has also been detected in wildlife species, but it is not well-described (Weyer et al., 2013). Occasional spill over to humans have been reported, especially field workers or when handling the specimens in a laboratory (Diagne et al., 2017).

The first report of Wesselsbron was recorded in the late summer of 1954 in Merino sheep in the Wesselsbron area, Orange Free State, South Africa (Weiss et al., 1956). Mortality was observed the first week of life in newborn lambs, as well as ewes aborting at full-term pregnancy (Oymans et al., 2020). The flock was injected with a Rift Valley Fever (RVF) vaccine two weeks prior (Weiss et al., 1956). It was suspected that the attenuated RVF incorporated into the vaccine, might be causing the abortions (Weiss, 1956). The virus from the lambs was isolated and it initially appeared to be RVF but has since been shown to be a distinct species from the flavivirus family (Weiss et al., 1956). It was concluded that the virus was an undescribed agent and was given the name of Wesselsbron virus (Weiss et al., 1956). The occurrence of WSLB typically occurs simultaneously with RVF outbreaks (Venter, 2018). Due to the similarity between the clinical symptoms of WSLB and RVF, WSLB outbreaks are often mistaken for RVF, and its importance may be overlooked (Diagne et al., 2017). Two clades of WSLB in southern Africa have been identified, specifically SA and Zimbabwe, using the NS5 gene ofthe WSLB genome (Weyer et al., 2013). Clade I include isolates from South Africa and Zimbabwe, whereas clade II only includes isolates from the KwaZulu Natal (KZN) province of South Africa (Weyer et al., 2013).

1.6.3 Vectors and Hosts of WNV and WSLB

West Nile virus is primarily transmitted by the bite of an infected mosquito that acquires the virusby feeding on infected birds (Colpitts et al., 2012). There are more than 65 mosquito species that transmit WNV, with *Culex* mosquitoes, specifically *Culex univittatus* and *C. pipiens*, seen as the primary global transmission vector (Reisen et al., 2005). Other vectors include *C. quinquefasciatus, C. stigmatosoma, C. thriambus* and *C. nigripalpus* (Colpitts et al., 2012; MacIntyre et al., 2023). *Aedes* mosquitoes

have been reported for WNV vectors but are not considered primary vectors (Bowen and Nemeth, 2007). Vertical transmission of the virus has been confirmed since only females feed on animal blood (Colpitts et al., 2012). Vector preference depends on the ability to infect mosquito species, the geographical range and the mosquito's ability to feed and infect host species (Colpitts et al., 2012). West Nile virus has been identified in mosquitoes in peri-urban and conservation areas at the animal/human interface in South Africa, suggesting increasing circulation potential for those viruses between humans, wildlife, domestic animals, and avian species that are common in those areas (MacIntyre et al., 2023).

Floodwater-associated *Aedes caballus juppi* mosquitoes are responsible for transmitting WSLB to several vertebrate hosts (Kokernot et al., 1958; Weyer, 2013). Incidental isolation with unknown epidemiological importance was also made from an ixodid tick (Weyer et al., 2013). The incidence of WSLB is seasonally associated, with more infections during warmer months with high rainfall, since this favours higher mosquito populations (Heymann et al., 1958; Weyer, 2013).

Wesselsbron virus has been detected in numerous domestic livestock species including camels, cattle, pigs, donkeys, and horses (Oluwayelu et al., 2018). Evidence of WSLB infection was also reported in wild animals like zebras and ruminants (Diagne et al., 2017). Questions have been raised regarding the reservoir status of WSLB, since isolations were also made in Cape short-eared gerbil *Desmodillus auricularis* in southern Africa (Kokernot et al., 1958; Diagne et al., 2017). A few human cases have been reported, mostly from the Central African Republic, Senegal, and two neurological cases reported in SA and Senegal (Weyer, 2013; Diagne et al., 2017).

1.6.4 Factors playing a role in infections and transmission

Reservoir competence, i.e., an index that reflects the relative number of infectious mosquitoes that would be derived from feeding on each host species, is a useful measure of the relative importance of each vertebrate species (Ciota and Kramer, 2013). This value depends on the susceptibility of the vertebrate host, the concentration of infectious virus particles in the blood, and the duration of an infectious level viremia in the host (Ciota and Kramer, 2013). The relationship between rainfall and mosquito vectors is significant, since precipitation patterns influence the feeding and reproduction cycle of mosquitoes (Ciota and Kramer, 2013;Ciota, 2017; McVey et

al., 2015). In late summer and early fall, more human infections occur, due to outdoor activity (Ciota, 2017). Other types of transmission include trans-placental transmission, transmission via blood transfusions, organ donations, breast feeding and laboratory accidents (Semenza et al., 2016).

1.6.5 Epidemiology of WNV and WSLB

In the *Flaviviridae* family, there are more than 100 species that are grouped based on their antigenic groups (Schweitzer et al., 2009). There are 12 antigenic groups with a 13th antigenic group not yet assigned (Rathore and St John, 2020). Flavivirus antigenic relationships generate immune responses that are cross-reactive to multiple flaviviruses and their widespread and overlapping geographical distributions, coupled with increases in vaccination coverage, increase the likelihood of exposure to multiple flaviviruses (Rathore and St John, 2020). Depending on the antigenic properties of the viruses to which a person is exposed, flavivirus cross-reactivity can be beneficial or could promote immune pathologies (Rathore and St John, 2020).

The spread of WNV to other continents can be explained by the migration of birds, which are the potential amplifying hosts of the virus and remain viraemic for a long time (McVey et al., 2015). When mosquitoes take a blood meal from an infected bird, the virus infects and replicates in the mosquito's midgut epithelial cells, and subsequently travels to the salivary glands (Colpitts et al., 2012). In the salivary glands, the virus accumulates and results in a high viraemia (Colpitts, 2012). West Nile virus is transmitted to vertebrate hosts through an infected mosquito vector during blood-feeding (Colpitts et al., 2012). Bird-to-bird transmission has been demonstrated in the laboratory for certain species, confirming that numerous species are able to transmit the virus through direct contact (Komar et al., 2003).

Wesselsbron virus was also reportedly confirmed in several sheep in the Middelburg district of the Cape province in South Africa in 1959, where acute, subacute, chronic, and mild or abortive forms of the disease was found in older animals (Le Roux, 1959). It is widely distributed in Africa and isolates have been found in countries like Namibia, Angola, Madagascar, Botswana, Zimbabwe, Cameroon, and the Democratic Republic of Congo (Weyer et al., 2013). Thailand is the only country outside of the African continent that has reported a case of WSLB in 1966, but it was not investigated further (Gould et al., 1967). Between 2010-2011, two human cases of WSLB infection were

identified in South Africa making use of RT-PCR (Figure 1.7) (Weyer et al 2013). In limited serosurvey studies, dating from 1955 to 1978, targeting WSLB antibodies from several different African countries, a total of 547 of 2647 (nearly 21%) human specimens tested positive (McIntosh, 1980). In South Africa, serologically positive human cases were recorded along the eastern coast, with detection rates of 32% in the subtropical region of KwaZulu Natal province (Ndumu area) and 0.7% in the Eastern Cape province (Weyer, 2013). During 2008, two positive equine samples were confirmed by the Zoonotic arbo- and respiratory virus (ZARV) research group (Human, 2008). Wesselsbron virus is rare and has sporadic outbreaks, but is present in South Africa, highlighting the importance of its continuous surveillance.

The *Aedes* mosquitoes are responsible for transmitting the WSLB throughmeans of mechanical transmission (Kokernot et al., 1958). Mechanical transmission refers to the transfer of pathogens from an infected host to a susceptible host, where a biological association is not required (Foil and Gorham, 2000). Like many other arboviruses, vertical transmission is sufficient for maintaining the virus in nature (Kokernot et al., 1958).

Figure 1.7: The map displays the approximate distribution of recorded human cases of Wesselsbron disease in South Africa. Adapted from (Weyer et al., 2013).

1.7 Infection in humans and animals

1.7.1 West Nile virus

West Nile virus can manifest in humans varying from asymptomatic infection to a nondescript febrile viral syndrome to potentially fatal neurological disease (Gubler,

2007). Symptoms can be present for 2 to 5 days, but incubation periods of up to 15 days have been recorded (Pealer et al., 2003; Rudolph, 2014). Approximately 80% of WNV infections are asymptomatic, while 20% present with symptoms similar to dengue virus, and 1% lead to neuro-invasive syndrome, of which 10% may succumb (Zouet al., 2010).

West Nile virus infection in humans can result in a spectrum of diseases ranging from a febrile illness, which is called WNV fever, all the way to severe neuroinvasive disease (Bai, 2019). Common symptoms associated with WNV fever include fever, chills, malaise, headache, backache, myalgia, arthralgia, nausea, vomiting, diarrhoea, and a maculopapular rash (Zou et al., 2010). Approximately half of WNV cases is classified as WNV fever, while the other half has been classified as neuroinvasive disease (Bai, 2019). Neuroinvasive disease cases present with more severe symptoms including encephalitis, meningitis, and acute flaccid paralysis (Sejvar et al.,2008). The first report of asymmetric flaccid paralysis due to WNV infection, was in 1979, but no pathological data was taken from the patient (Madden, 2003). In 2002, there was a WNV outbreak in Houston, Texas, with patients presenting with flaccid paralysis originally attributed to Guillain-Barré syndrome (Weatherhead et al., 2015). After further assessment of these patients, it was concluded that their symptoms and motor responses were not consistent with Guillain-Barré syndrome, and it was reported to the Center for Disease Control (CDC) as WNV positive cases (Weatherhead et al., 2015). Changes in mental status associated with meningitis or encephalitis are very common,but motor weakness is often the clinical indicator of WNV infection (Weiss et al., 2001). In recent years, severe neurological illness has been reported much more frequently, together with neuromuscular manifestations (Bai, 2019).

In horses 20% to 30% of infections develop symptoms with as many as 90% of these developing severe neurological diseases (Venter et al, 2017a). Of the neurological cases 30% to 40% are fatal (Venter et al., 2017b). Neurological signs in horses include ataxia, weakness, recumbence, seizures, and muscle fasciculation (Bertram et al., 2020). Infection in wildlife can range from no clinical signs to severe neurological illness including ataxia, paresis and recumbency (Marra et al., 2004; Steyn, 2019).

Common signs in animals that have been reported include weakness, stumbling,

trembling, head tremors, inability to fly in birds or walk, and lack of awareness (Petersen et al., 2013). Unlike the observations in America and Europe where massive die-off of birds was observed following the introduction of WNV into the country, in Africa, no large-scale bird mortalities have been associated with WNV circulation, possibly due to genetic resistance in Southern African birds (McVey, 2015). Some sensitive birds in Africa, for example the blue crane, crows, blue jays and flamingo's, also show neurological signs that include loss of coordination, head tilt, tremors, weakness, and a lack of energy (Steyn et al., 2019). Table 1.2 shows the WNV outbreaks since its first isolation.

Table 1.2: A table showing notable WNV outbreaks since its first isolation in 1937

Year	Location	Description	Reference
1951-1952	Israel	123 cases with no fatalities Majority of cases in young children	Bernkopf et al., 1953
1957	Israel	Elderly group showed severe neurological manifestations	Hayes, 1989
1962	France	10 human cases developed meningitis and encephalitis	Sejvar et al., 2008
1974	South Africa	Largest African epidemic Approximately 3000 clinical cases	Hubalek and Halouzka, 1999; Jupp, 2001; Burt, 2002
1983-1984	South Africa	Epizootic involving WNV and Sindbis virus occurred in the Witwatersrand Hundreds of human cases reported	Jupp et al., 1986
1994	Algeria	Outbreak with 50 patients Eight fatalities	Hubalek and Halouzka, 1999
1996	Romania	First WNV outbreak centred in predominantly urban area 393 hospitalized cases 17 fatalities	Campbell et al., 2001
1996	Morocco	94 horses affected 42 fatalities	Benjelloun et al., 2017
1997	Tunisia	173 patients hospitalized with meningitis or meningoencephalitis 8 deaths reported >50% of patients were over 50 years of age	Sejvar et al., 2008
1998	Italy	14 horses in Tuscany confirmed as WNV positive cases 6 fatalities	Murgue et al., 2001
1999	Russia	Large outbreak of WNV with 183 serologically confirmed cases 84 cases of acute meningoencephalitis 40 fatalities >75% of patients were older than 60 years	Platonov et al., 2001
1999	USA	WNV introduced to the USA 62 confirmed human cases 7 fatalities High fatality rate in various birds	Nash et al., 2001

Table 1.2 cont: A table showing notable WNV outbreaks since its first isolation in 1937

Year	Location	Description	Reference
1998-2000	Israel	18 horses with severe neurological disease tested positive for WNV WNV identified in commercial birds in 1999 In 2000, over 400 cases of encephalitic disease confirmed 28 fatalities	Giladi et al., 2001
2000	France	76 confirmed WNV cases in horses 21 deaths reported	Murgue et al., 2000
2002	USA	Human cases reported was 4156 2354 cases were meningoencephalitis 284 fatalities reported	Sejvar et al., 2008
2003	Morocco	9 equine cases 5 deaths reported	Benjelloun et al., 2017
2008	Italy	33 clinical cases reported in horses 5 horses died Same strain as the 1998 outbreak	Monaco et al., 2010
2010	South Africa	18 confirmed positive cases in horses 8 fatalities Majority of horses showed neurological signs	Venter, 2017
2010	Greece	A total of 197 patients with neuroinvasive disease were reported 33 fatalities Advanced age and history of heart disease were associated with death	Danis et al., 2011b
2010	Spain	51 horses presented IgM against WNV 18 affected horses died 2 non-fatal human cases were confirmed	Garcia-Bocanegra et al., 2012
2010	Morocco	Disease reported in 17 horses 8 fatalities confirmed	Benjelloun et al., 2017
2011	Greece	31 cases of WNV neuroinvasive disease were reported 17 of these cases were reported in regions that were not affected in 2010	Danis et al., 2011a
2011	Australia	At least 1000 horses were affected A fatality rate of 10-15% has been confirmed Linked to NSW2011 Kunjin strain	Frost et al., 2012

Table 1.2 cont: A table showing notable WNV outbreaks since its first isolation in 1937

Year	Location	Description	Reference
2012	USA	Largest state-wide outbreak in Texas 1868 human cases reported 89 fatalities	Chung et al., 2013
2012	Italy	56 confirmed human cases 25 cases had neuroinvasive symptoms, while 17 cases of West Nile fever were reported	Barzon et al., 2013
2012	Tunisia	7 positive WNV cases confirmed Determined that 2 lineages were circulating	Monastiri et al., 2018
2012	Serbia	58 cases were confirmed 9 patients died >60 years of age were associated with infection	Popovic et al., 2013
2014	USA	Largest outbreak to date in Harris County 139 human cases reported 2 fatalities 1286 positive mosquito pools	Martinez et al., 2017
2014	South Africa	23 confirmed WNV positive cases in horses Resulted in 5 fatalities 91% of samples had neurological signs	Venter, 2017
2015	Israel	149 WNV positive cases in humans from 88 different localities Lineage I was circulating	Lustig et al., 2017
2015	Pakistan	First report of human cases in this country 105 patients tested positive for IgM antibodies against WNV	Khan et al., 2018
2016	Romania	93 neurological cases recorded New lineage 2 strain co-circulating with previously endemized lineage 2 virus (Volgograd 2007-like strain)	Cotar et al., 2018

Table 1.2 cont: A table showing notable WNV outbreaks since its first isolation in 1937

Year	Location	Description	Reference
2017	Greece	45 confirmed human WNV cases 4 deaths in people >70 years of age 39 cases were reported in regions never identified before	Mavrouli et al., 2019
2017	South Africa	54 positive cases in horses 39% mortality rate Cases mostly occurred in young, unvaccinated horses	Bertram et al., 2020
2018	Italy	149 equine cases reported 327 human cases 13 fatalities	Riccardo et al., 2020
2018	Czech Republic	WNV lineage 2 was detected in 12 captive and 5 wild goshawks 2 wild sparrowhawks tested positive 3 other captive birds of prey died	Hubalek et al., 2019
2018	USA	2647 WNV cases confirmed 1658 cases were neuro-invasive 167 deaths reported	CDC, 2018
2019	Germany	76 WNV cases in birds 36 positive cases in horses 5 human cases reported Extraordinary high temperatures triggered outbreak	Ziegler et al., 2020
2020	Israel	17 human cases reported	Bakonyi and Haussig, 2020
2020	Spain	77 human cases of WNV 137 documented equine cases	Bakonyi and Haussig, 2020

1.7.2 Wesselsbron virus

Wesselsbron virus results in a high mortality rate of up to 27% in newborn lambs and the symptoms are usually present for 72 hours (Weyer et al., 2013). Fever, anorexia, general weakness, listlessness and increased respiratory rate are typically observed in newborn lambs and goat kids, while adult livestock and cattle show mild, nonfatal febrile illness, with abortions or congenital malformations during pregnancy as the most extreme cases (Coetzer et al., 1978).

Human cases reported have shown the sudden onset of non-fatal influenza-like symptoms including fever, rashes, rigors, myalgia, as well as tachycardia (Jupp, 2014). The acute phase is typically one to three days (Weyer et al., 2013). No fatal human

cases have been reported to date, but the most severe case of WSLB recorded was when a laboratory worker got infected with the virus through splashing of the sample in his eye and he showed symptoms of encephalitis, dementia, and temporary hearing loss (Heymann et al., 1958 Notable outbreaks of WSLB since its first isolation can be found in Table 1.3.

Table 1.3: A table showing notable WSLB outbreaks since its first isolation in 1955

Year	Location	Description	Reference
1955-1957	South Africa	Eight field workers get infected with WSLB Seroconversion on all patients Virus only isolated from two cases	Smithburn, 1957
1959	Uganda	Laboratory-acquired infection after splash in the eye	Weinbren, 1959
1960	South Africa	Isolation from Cape short-eared gerbil	Diagne et al., 2017
1965	Senegal	Human infection acquired through laboratory work	Swanepoel, 1989
1966	Thailand	Only case of WSLB outside the African continent No further investigation	Gould et al., 1967
1969	USA	Laboratory-acquired infection Possible aerosol transmission noted Live virus isolated from throat swab	Justines and Shope, 1969
1972	Nigeria	Patient was exposed to mosquito suspensions prepared for virus isolation and challenge virus used for neutralization assays	Tomori et al., 1981
1972-1976	South Africa	Four human infections reported Two were laboratory workers, the other two circumstances unknown	Swanepoel, 1989

Table 1.3 cont: A table showing notable WSLB outbreaks since its first isolation in 1955

Year	Location	Description	Reference
1981-1983	Central African Republic	Nine cases including one laboratory-acquired infection	Swanepoel, 1989
1997	South Africa	Serological evidence found in wild ruminants including buffalo, zebras, and wildebeest	Barnard, 1997
2008	South Africa	Two equine cases positive for WSLB Severe neurological signs (ataxia and paresis)	Human, 2008
2013	Senegal	Two human cases reportedFirst report in black rats	Diagne et al., 2017

1.8 Diagnostic tools to detect WNV and WSLB

1.8.1 Background

To diagnose WNV or WSLB, well-established diagnostic tools are required in the laboratory to confirm a case of WNV or WSLB infection (McVey et al., 2015). Molecular and serological tools are used together, for accurate detection of infection. Real-time RT-PCR assays are used to detect viral RNA in serum or cerebrospinal fluid (CSF) samples (Sambri et al., 2013). The detection of the WNV or WSLB genome in the samples during the acute stage, is considered a confirmed positive sample (McVey et al., 2015). Due to the short viraemia of flaviviruses, serological tools (Figure 1.10) are used to complement the use of molecular assays, like PCRs (Kuno, 2003). The detection of specific IgM immune response in the serum or cerebrospinal fluid (CSF) sample, can be used as a reliable diagnostic indicator for acute infection and confirmed through IgG seroconversion (Sambri et al., 2013).

1.8.2 Molecular tools

The use of quantitative, nucleic-acid based techniques like real-time polymerase chain reaction (RT-PCR) have the advantages of being sensitive, specific, and rapid for RNA detection of viruses such as WNV and WSLB (Vazquez et al., 2016). The drawbacks of using the PCR techniques are that cases can be missed due to the short viraemia

phase exhibited by viruses like the flaviviruses, as well as the possibility of acquiring mutations in the PCR primer binding sites of new strains, rendering them undetectable (Lustig et al., 2018). Therefore, it is essential for PCR methods to be constantly updated to ensure high sensitivity and suitability to detect WNV and WSLB. A panflavi real-time RT-PCR has been published and is a rapid, broad-range flavivirus-specific and highly sensitive assay, making it a valuable tool for rapid detection of flaviviruses in livestock samples, epidemiological studies, or as useful complement to single flavivirus-specific assays for clinical diagnosis (Patel, 2013). Sensitive fluorescent probe-based RT-qPCR and reverse-transcription-recombinase polymerase amplification (RT-RPA) assays have been developed and evaluated for rapid and specific detection of WSLB are suitable for use in routine laboratory diagnosis of WSLB infection (Figure 1.8) in both humans and animals and for field diagnosis in limited-resource settings during entomological or veterinary surveillance (Faye, 2022).

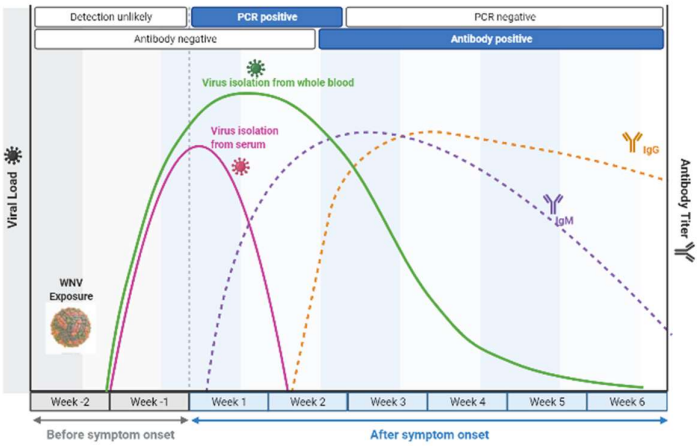

Figure 1.8: Theoretical depiction of WNV presence in body fluids and WNV immune response. The phases of WNV detection period in serum and whole blood as well as the IgM and IgG immune response to WNV infection are presented with respect to the day of illness. Adapted from (Lustig et al., 2018).

1.8.3 Serological tools

A variety of serological tools can be used to test for flaviviral antibodies and include virus neutralisation tests (VNT), the hemagglutination-inhibiting test (HA), enzyme-linked immunosorbent assay (ELISA) and the immunofluorescence assay (IFA) (Kuno, 2003). It is important to note that seropositive tests should be interpreted with care, due to the high degree of cross-reactivity of flaviviruses (Sotelo et al., 2011; Beck et al., 2017). Cross-reactivity can be due to protein similarity and/or low antibody response to flaviviruses (Endale, 2021). The biggest problem is the E protein, containing highly

conserved parts in the fusion loop, which is recognised by most of the cross-reacting antibodies (Crill and Chang, 2004). To overcome this lack of specificity, a plaque reduction neutralisation technique is performed under biosafety level 3 (BSL3) conditions, providing the highest specificity (Sambri et al., 2013). Immunofluorescence assays (IFA) and ELISAs can be used to detect IgM and IgG antibodies (Abs), after 4 and 8 days respectively (Kitai et al., 2007; Busch et al., 2008). These assays can be used to monitor WNV and WSLB activity and provide high throughput diagnostic and surveillance techniques (Beck et al., 2017).

Enzyme immunoassays make use of antigens attached to one of the reactants in an immunoassay to allow quantification through the development of color after the addition of a suitable substrate/chromogen (Crowther, 2002). The key to all ELISA systems is the detection of antigens by antibodies, which are proteins that are produced in all animals and humans as a response to antigenic stimuli (Crowther, 2002). Enzyme linked immunosorbent assay uses the basic concept of an antigen and antibody binding to each other and allowing detection of proteins, peptides, hormones, or antibodies (Figure 1.9) (Gan and Patel, 2013). The principle of an ELISA is the immobilisation of an antigen to a microtiter plate and is which then reacts to a specific antibody in the sample (Crowther, 2002; Gan and Patel, 2013). Next, a second antibody with a marker is added and a positive reaction is detected by the marker changing colour when an appropriate substrate is added (Crowther, 2002). If there are no antibodies in the sample, the second antibody will not be able to bind and there will be no colour change (Crowther, 2002). The second antibody is specific to the host species fragment crystallization (Fc) region and is, therefore, species specific (Crowther, 2002).

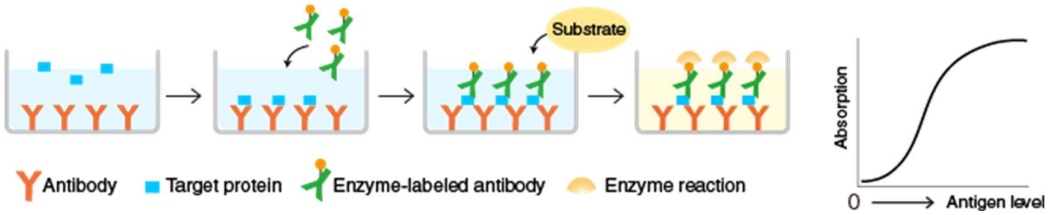

Figure 1.9: Basic ELISA principle. Enzyme linked immunosorbent assays work on the principle that specific antibodies bind to target antigens and detect the presence and quantity of antibodies binding. Adapted from (Crowther, 2002).

The advantages of an ELISA are its simplicity, high throughput, high sensitivity, low cost, safety, and acceptability as a diagnostic tool in various fields (Crowther, 2002). There are limitations like the need for specific antigens and antibodies, as well as non-specific binding resulting in false positives (Gan and Patel,2013).

When developing a diagnostic test, precise and optimal conditions are required for all steps of the protocol. Before routine usage in diagnostics, the newly developed or modified assay must be proven to be accurate, precise, and reproducible (Rajna and Irena, 2020). To measure the values obtained with the test, it is necessary to standardise the test, thus optimisation, validation, and standardisation of the ELISAs are important and necessary for accurate detection of infection (Rajna and Irena, 2020).

1.9 Treatment & Prevention for WNV and WSLB

There is no specific treatment available for WNV and it depends on symptom management (Hayes et al., 2005). Horses can be given intravenous fluids and supplements to prevent dehydration, where as a sling can be used to help horses who are struggling to stand, or care can be provided on the ground when safe (Talk, 2020). Vaccines for WNV are available for equines and provide successful immunity against lineage I and II, while several promising human WNV vaccine candidates have undergone successful early phase clinical trials (Iyer and Kousoulas, 2013). These vaccines did not show any adverse effects or safety concerns but moving on to the final stage of development is difficult, since the target population is the elderly with weakened immune systems, most infections are asymptomatic and the effect of vaccination in a population cannot be determined (Ulbert, 2019). Annual vaccination is recommended for horses in endemic areas, especially pregnant mares in their third trimester or foals over four months (Iyer and Kousoulas, 2013). The most efficient way to control these pathogens would be prevention and surveillance (Peterson and Marfin, 2007; Iyer and Kousoulas, 2013). The number of vector mosquitoes must be reduced and bites by vector mosquitoes must be prevented (Peterson and Marfin, 2007). Insecticides are used to control the number of vectors in the USA, while repellents such as N, N- diethyl-meta-toluamide (DEET) are recommended for use on horses and humans in summer (Sampathkumar, 2003). Improved water quality and surface draining, as well as avoiding the occurrence of water pooling, can decrease the availability of mosquitohabitats (McVey et al., 2015).

There is no specific treatment for WSLB, and it remains supportive (Hayes et al., 2005). Freeze-dried, live attenuated WSLB vaccines have been developed for sheep and goats by Onderstepoort Biological Products (OBP), with therecommendations that lambs from immune animals should not be inoculated before they are six months old because maternal antibodies may block the vaccine response,as well as no vaccination of pregnant animals as the virus can affect the foetus (OBP, 2021).

To prevent WSLB infection in animals, the moving of pregnant and neonatal small ruminants into endemic areas could be efficient (CFSPH, 2017). Vector control is also theoretically possible, but not practical for protecting small ruminant flocks. Individuals who handle WSLB or contaminated tissues should wear protective clothing like gloves, to prevent contact with the virus (Hardcastle, 2020). Mosquito bite prevention measures like repellents and mosquito netting can be useful (CFSPH, 2017). Since WSLB often occur simultaneously as RVF, the RVF preparedness activities like early response and control techniques are crucial (Hardcastle et al., 2020). Making use of existing forecasting tools like NASA's Rift Valley Fever Monitor can aid in identifying climatic patterns providing warnings well in advance (Hardcastle et al., 2020).

1.10 Syndromic surveillance of West Nile virus and Wesselsbron virus

1.10.1 Background on arbovirus surveillance

Emphasis has recently been placed on the importance of a global effective zoonotic surveillance system for preventing global outbreaks and detect emerging and reemerging arboviruses (Tajudeen, 2022). It can be used to demonstrate the health status of a population, the history of the disease, detecting epidemics, evaluating control and prevention measures, and monitoring changes in infectious agents (Janković, 2008). To be functional, long-term,and sustainable, funding is required to ensure that the infrastructure, laboratory technology and manpower is up to standard (Bird and Mazet, 2018).

1.10.2 One Health

One Health is an integrated, unifying approach that aims to sustainably balance and optimise the health of people, animals, and ecosystems, as seen in Figure 1.10 (One Health High-Level Expert, 2022). It recognises that the health of humans, domestic and wild animals, plants, and the wider environment (including ecosystems) are closely linked and interdependent (One Health High-Level Expert, 2022). One Health

is a very promising surveillance tool and can control vector-borne diseases, like arboviruses whose life cycle involves multiple hosts, establishing itself as a surveillance system making use of all the various sectors (Amato et al., 2020). Outbreaks in animals can predict human outbreaks, as well as vector abundance influencing infection rates (MacIntyre, 2023).

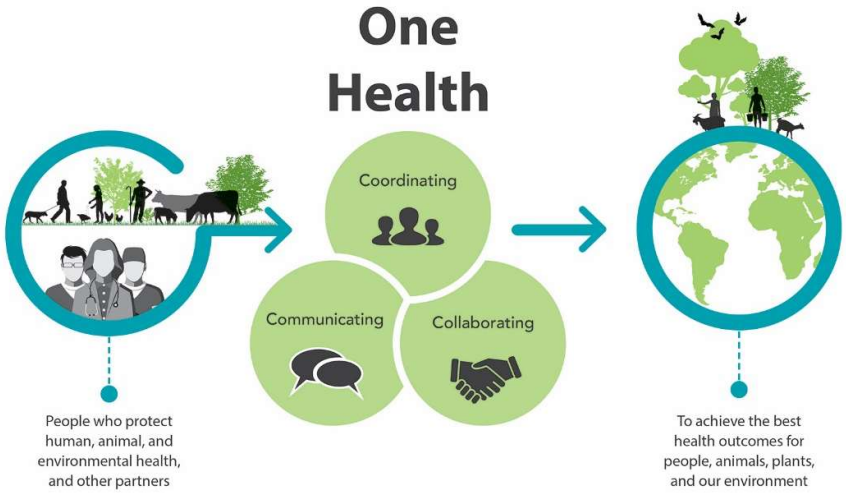

Figure 1.10: The One Health basics showing the relationship between humans, animals and the environment. Adapted from CDC (2021).

1.10.3 Importance of surveillance

West Nile virus, as well as WSLB, has the possibility to emerge globally, due to the various mosquito vectors and possible vertebrate hosts, and this can result in scattered outbreaks (Gubler, 2007; Smith, 2017). Genetic modifications that increase interaction with the host factors can also increase the incidence of WNV and WSLB (Hayes et al., 2005). Both viruses are a big threat to humans, birds, equines, and livestock and are often deemed unimportant due to the lack of monitoring of the virus (Diagne et al., 2017). Laboratory diagnostics, epidemiology and vector control improvement are critical to implementing effective control and prevention strategies against zoonotic viruses (Gubler, 2002). Lack of these strategies will result in other potential emergingvector-borne viral diseases spreading at a very fast pace should the opportunity arise (Gubler, 2007). The life cycle and impact on the public health of the virus must be investigated more closely, to ensure that the distribution of WSLB and WNV are not underestimated (Steyn et al., 2019). Clinical WNV disease has been reported in several non-equine species like birds, crocodiles, bats, wolves, cats, and dogs, apartfrom cattle and sheep (Steyn et al., 2019). Wildlife species in Africa are also susceptible and the role they play in amplifying WNV is unknown, emphasising

the need for surveillance (Steyn et al., 2019). With regards to WSLB, export testing requires negative serological tests according to World Organization for Animal Health (WOAH) guidelines, but no commercial test is available (WOAH, 2022).

11. Justification for research project

The ZARV research group has been very active in the surveillance of arboviruses, especially WNV over the last couple of years, mainly through molecular screening. Animals including livestock, wildlife, avian, domestic, and equine species are all affected, as well as humans. The arbovirus season in South Africa is between January and June, so having sufficient tools in place for detection is very important. The development of in-house serological tools using recombinant antigen to detect acute cases and to determine the seroprevalence in different species assisted in the detection and defining the incidence of cases as well as surveillance of the viruses across South Africa.

12.Aim of the project

The aim of this project is to establish molecular and serological assays that can be used as screening tools for West Nile and Wesselsbron virus infection in humans, cattle and horses and validate these by investigating the incidence of cases over 2 years in South Africa.

13. Objectives

1. To identify new West Nile and Wesselsbron virus cases amongst neurological animals in 2021-2022 making use of real-time PCR, culture and sequencing of acute infections as part of the ZARV surveillance program. A follow up serum sample will be requested to obtain IgM positive sera for use in ELISA validation.
2. To screen WNV IgM positive horse and human cases previously detected with a commercial ELISA with serum neutralization tests for WNV and Wesselsbron to identify virus specific sera that can be used to validate a new inhouse ELISA for each virus.
3. To screen cattle sera from animals with neurological signs for Wesselsbron and WNV using neutralization assays for ELISA validation.
4. To express the cloned baculovirus WNV NS1 protein in insect cells for use in establishment of serological assays.

5. To test the baculovirus expressed NS1 protein for WNV and Wesselsbron virus for activity against known positive sera, as well as generate more NS1 protein for future use.
6. To develop an IgM ELISA and validate these assays against known positive horse, cattle and human sera.
7. To screen a selection of horse and cattle sera from neurological cases in South Africa to determine the incidence of WNV vs Wesselsbron virus in these two species.
8. To develop an epitope blocking ELISA and validate it against known IgG positive sera from wildlife, horses, and cattle for WNV and WSLB as a species independent IgG assay.
9. To screen human samples from The African Network for improved Diagnostics, Epidemiology and Management of Common Infectious Agents (ANDEMIA) countries using the newly developed IgM assay for Wesselsbron Virus.

Chapter 2 – Validation of a flavivirus and specific real-time one-step reverse transcriptase polymerase chain reaction to detect West Nile and Wesselsbron virus infections

2.1 Introduction

2.1.1 Background

In the case of suspected flavivirus infection, as with many viral etiologies the diagnostic method usually performed is some form of reverse transcriptase polymerase chain reaction (RT-PCR) assay (Sambri et al., 2013). This method is performed to detect viral ribonucleic acid (RNA) from a clinical sample. One of the biggest breakthroughs in polymerase chain reaction (PCR), was the introduction of monitoring deoxyribonucleic acid (DNA) amplification in real-time, by monitoring fluorescence (Kralik and Ricchi, 2017). After each cycle of PCR, the fluorescence is measured and its intensity indicates the number of DNA amplicons in the sample at the current moment (Kralik and Ricchi, 2017). To visualise the amplified DNA fragments, non-specific fluorescent DNA dyes or fluorescently labelled oligonucleotide probes can be used (Holland et al.,1991). The viraemic period of flaviviruses are very short, thus if viral RNA is not detected in the plasma or cerebrospinal fluid (CSF) sample, a serological assay, like an enzyme linked immunosorbent assay (ELISA) for example, can be performed to detect specific immunoglobulin M (IgM) antibodies, which indicate an early stage of an acute infection (McVey et al., 2015). Polymerase chain reaction (PCR) provides a short timeframe in which it is sensitive enough to serve as a diagnostic tool, since the viraemia rapidly decreases after 5 days of symptom onset (Figure 2.1) (Sampathkumar, 2003).Within the first two weeks after symptom onset, serological tools may play a role in detection by testing for IgM and immunoglobulin G (IgG) antibodies respectively (Sampathkumar, 2003).

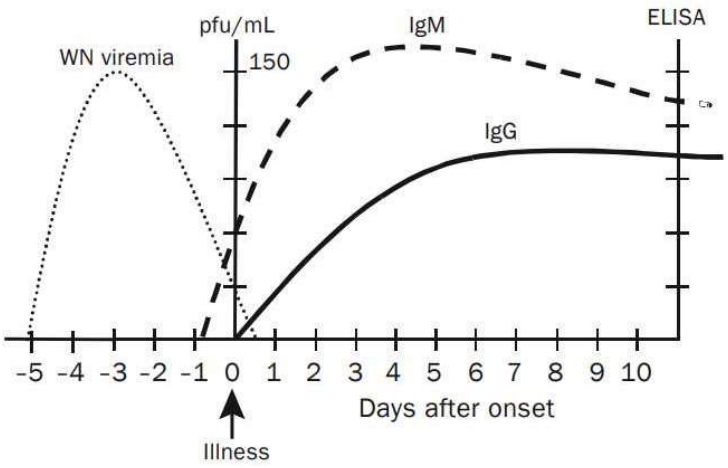

Figure 2.1: Graph of WNV flavivirus viraemia. Duration of WNV viremia, the appearance of antibodies following the onset of illness and the appropriate diagnostic test for each stage. Adapted from Sampathkumar, 2003.

The principle of the PCR is based on the use of DNA polymerase replicating DNA sequences in vitro (Karim, 2019). Billions of copies of the DNA fragment of interest from the extracted sample, can be generated (Karim, 2019). Amplification is based on the replication of a double-stranded DNA template and is broken down into three phases – a denaturation phase,a hybridisation phase with primers and an elongation phase, with each product serving as a template for the following step (Karim, 2019). Reverse transcription quantitative PCR (RT-qPCR), as used by the Zoonotic arbo- and respiratory virus (ZARV) laboratory, is used when the starting material is RNA (Kralik and Ricchi, 2017). In this method, RNA is first transcribed into complimentary DNA (cDNA) by reverse transcriptase from total RNA or messenger RNA.

A study by Lanciotti et al. (2002) showed that nucleic acids in a sample using real-time RT-qPCR could be detected in 57% of CSF samples and only 14% of serum samples (Lanciotti, 2002). Since then, several improvements have been made to real-time RT-PCR assays to continuously increase the sensitivity and specificity of these assays as described below.

Nucleic acid-based techniques, like real time RT-qPCR are advantageous due to its high sensitivity, specificity, and the rapid detection of RNA in biological specimens to confirm acute infection (Kralik, 2017). However, there are also disadvantages, namely the fact that new and emerging flavivirus strains may acquire mutations in the PCR

primer binding sites, which will render them undetectable using the current assay (Sambri et al., 2013). Extracted RNA can be tested on the flavivirus nested real-time RT-PCR, with WNV specific probes which was the method used for flavivirus diagnostics in the ZARV program over the past decade and was developed by a ZARV member (Zaayman, 2009). This test provides a qualitative answer making use of melting temperatures and incorporate WNV specific probes for rapid identification of WNV positive cases followed by gel electrophoresis to identify other flaviviruses. The principle of hybridisation probes is based on fluorescence resonance energy transfer (FRET). Two sequence-specific oligonucleotide probes, labelled with different dyes (donor and acceptor), are added to the reaction mix in addition to PCR primers. HybProbe probes hybridize to the target sequences on the amplified DNA fragment during the annealing phase in a head-to-tail arrangement, thereby bringing the two dyes into close proximity. The donor dye (fluorescein) is excited by the blue light LED source and the energy emitted by the donor dye excites the acceptor dye attached to the second HybProbe probe, which then emits fluorescent light at a different wavelength. The amount of fluorescence is directly proportional to the amount of target DNA generated during the PCR process (Zaayman, 2009). The technology is however expensive and the real-time PCR only incorporated WNV specific probes. The LightCycler 2.0® (Roche Applied Science, Mannheim, Germany) that is used for the nested real-time RT-PCR is no longer available for purchase, which makes servicing the instrument very difficult, as well as purchase of consumables, yielding it out of date. Therefore, it is essential to ensure that current PCR methods are constantly updated with regards to sensitivity to ensure that the PCR method is suitable for detection. A panflavi real-time RT-PCR has been published and is a rapid, broad-range flavivirus-specific and highly sensitive assay, making it a valuable tool for rapid detection of flaviviruses (Patel, 2013).

Making use of a nested real-time RT-PCR to detect the presence of all flaviviruses, reduces the chance of non-specific binding, which would yield a false result on conventional PCR (Haija, 2017). Another big advantage of real-time PCR over conventional PCR is the high sensitivity and specificity, as well as amplifying genes that are present in low abundance (Haija, 2017). There are definitely drawbacks with regards to a nested RT-PCR and it includes the possibility of contamination (Haija, 2017).

The hydrolysis probe WNV assay, developed and published by a previous ZARV member (Zaayman et al 2009), had been further improved in-house by addition of WSLB probes (van Niekerk, Unpublished). This PCR was chosen as reference to evaluate and optimise a new specific TaqMan one step real-time RT-PCR for the detection of Wesselsbron virus (WSLB), using primers and probes designed by Dr Marthi Pretorius that was previously in the group.

Briefly, the principle of the TaqMan one step real-time RT-PCR is based on a single probe containing two labels: a fluorescent reporter dye and a fluorescentquencher (Kralik and Ricchi, 2017). While the probe is intact, the quencher is close tothe reporter dye and suppresses the reporter fluorescence via fluorescence resonance energy transfer (FRET) (Zaayman, 2009; LifeScience, 2021). When the probe is hybridised to the target sequence, the 5'-nuclease activity of the polymerase cleaves the hydrolysis probe, separating the reporter and quencher (Kralik, 2017). With an increasing amount of target sequence during PCR, more probe is cleaved, and the fluorescence signal of the unquenched reporter dye increases (Kralik, 2017). Molecular assays are available for flaviviruses but requires sequencing of positive bands to differentiate between individual viruses.

Wesselsbron virus was first reported in 1955 in the Wesselsbron area in the Orange Free State of South Africa (SA), where substantial mortality in newborn lambs and abortions in full-term pregnant ewes occurred (Weiss et al., 1956). In a 2014 study, WSLB virus nucleic acids were detected in two humans who were suspected of being infected with Rift Valley Fever (RVF) virus during a RVF outbreak in South Africa (Burt et al., 2014). Humans and livestock were affected during the outbreak of 2010 and 2011 (Weyer, 2013). Partial nucleic acid sequences were obtained from patients that was included in a genetic analysis, together with sequence data from GenBank (Burt et al.,2014).

Analysis of the sequence data resulted in the identification of two clades of WSLB circulating (Diagne, 2017). Clade I isolate were collected from South Africa, Kenya and Zimbabwe, while clade II includes isolates from KwaZulu Natal, South Africa (Figure 2.2) (Burt et al., 2014, Diagne et al., 2017). The diversity in the two clades was almost

1%, while inter-clade diversity was 6% in the sequenced nonstructural protein 5 (NS5) region and 8% in the E protein region (Diagne et al., 2017). The nucleotide changes were mostly synonymous with an average of 0.5% and maximum of 1% amino acid difference between the isolates (Diagne, 2017). Even though diversity between the clades have been noted, no geographical or spatial correlation has been observed (Diagne et al., 2017).

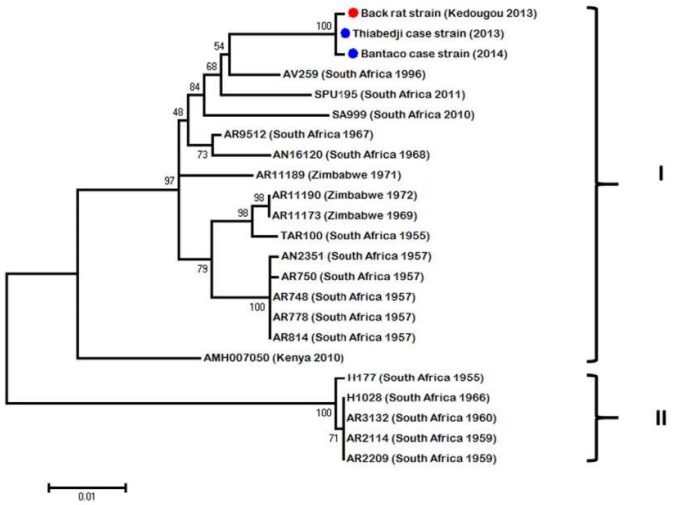

Figure 2.2: Maximum likelihood tree of the sequenced NS5 region of WSLB strains obtained in Senegal and South Africa since 1956. Adapted from Diagne et al., 2017.

This report describes the validation of both a nested real-time RT-PCR using FRET probes for WNV and WSLB virus (Modification of Zaayman et al 2009) and a one-step real-time TAC RT-PCR to detect WSLB (using Dr Marthi Pretorius' primer and probe sets), as well as provides a comparison of the sensitivity and specificity of the two assays. This will allow for increased sensitivity in surveillance and epidemiological studies.

2.2 Materials and Methods

2.2.1 Virus strains and clinical specimens

All viral isolates used in this study were obtained from the National Institute for Communicable Diseases (NICD) and Centers for Disease Control and Prevention (CDC) collections (Table 2.1). Clinical specimens, whole blood, or tissue were submitted through the South African veterinarian network to ZARV arbovirus surveillance program for testing of a range of arboviruses including flaviviruses between 2008 and 2022. Three WSLB strains were used to determine sensitivity and

specificity – AR16210, AV259 and H177. These strains have all been isolated in South Africa and the cultures are available in the ZARV biobank (Table 2.1). In order to measure sensitivity, several different cultured isolates representing different stages of passages and thus different concentrations were used. In order to measure specificity, RNA extracted from other arboviruses, Shuni virus (SHUV), Sindbis virus (SINV), WNV and Middelburg virus (MIDV), that are used in the lab, were ran on the WSLB one-step real time RT-PCR as a blind panel to determine specificity of the WSLB assay. Particularly important was to determine that WNV could not be detected as it is also a flavivirus.

Table 2.1: WSLB virus isolation strains. A table showing the WSLB virus strains used in this study and where they were isolated from.

Virus strain	Location	Date isolated	Host isolated from	Received as isolate
H177	Mkuze, KwaZulu-Natal	7 March 1974	Human	Vero
AR16210	Graaff-Reinet, Eastern Cape	9 August 1989	Sheep	Vero
AV259	Bultfontein, Free State	4 April 1996	Human	Mouse brain

2.2.2 Primer and probe used for the FRET nested real-time RT-PCR

Genus specific primers (FU1 and 9317) were used in the first round of the nested real-time RT-PCR and was designed using Primer 3. For the second round of real-time RT-PCR, primers FS778 and CFD2 were used (Scaramozzino et al., 2001). A published article by a previous ZARV member, the WNV probes were designed by multiple sequence alignments of the NS5 gene on Clustal X (version 1.83) to identify optimal probe binding (Zaayman et al., 2009). The WSLB specific probes were subsequently designed by Stephanie van Niekerk (unpublished). Fluorescence resonance energy transfer hybridisation probe sets were designed using the LightCycler 2.0®probe design software package (Roche Applied Science, Mannheim, Germany) within the NS5 region and showed different melting curves to distinguish between WNV and WSLB (Table 2.2).

Table 2.2: Flavivirus nested RT-PCR primers with WNV and WSLB specific probes. A table showing the primers and probes sequences designed for the first and second round of the nested flavivirus RT-PCR

Primer name	Orientation	Sequence	Reference
First round RT-PCR			
FU1	Sense	5'-TACAACATGATGGGAAAGAGAGAGAA-3'	Kuno et al., 1998
9317	Anti-sense	5'-BBGTGATKCKHGTGTCC-3'	Zaayman et al., 2009
Second round RT-PCR			
FS778	Sense	5'AARGGHAGYMCDGCHATHTGGT3'	Scaramozzino et al., 2001
CFD2	Anti-sense	5' GTGTCCCAGCCGGCGGTGTCATCAGC 3'	Kuno et al., 1998
Probe name	**Channel**	**Sequence**	**Reference**
WN_9167S	640	5'AAGACCACTGGCTTGGAAGAAAG-6-Fam3'	Zaayman et al., 2009
WN_9191A	640	5': Atto 620 ACTCAGGAGGAGGAGTCGAGGGCTTPhosphate 3'	Zaayman et al., 2009
WSLB_1	720	5' AAGACCACTGGGTGGCCCGAGAG-6-Fam 3'	van Niekerk, Unpublished
WSLB_2	720	5' Texas Red ACTCAGGGGGAGGGGTGGAAGGAAC-Phosphate 3'	van Niekerk, Unpublished

2.2.3 Primer and probe design for WSLB TaqMan one step real-time RT-PCR

A consensus sequence of multiple alignments of WSLB sequences were generated, to ensure that the site being amplified is conserved. Primers and probes were designed using Primer Express 3 by a previous ZARV member, Dr Marthi Pretorius. Both primers and TaqMan probe were designed based on the E protein of WSLB (Table 2.3). The size of the amplicon was determined to be 80 bp.

Table 2.3: Table of the primer and probe sequences for the WSLB TaqMan RT-PCR. A table showing the sequence,orientation, and position in the genome of the E gene that is amplified by the WSLB one step real-time RT-PCR.

Primer name	Orientation	Sequence	Position
WSLB_E422 F	Sense	5'-ACTGGAGCTCCGTGCAGAAT-3'	422-441
WSLB_E478 R	Anti-sense	5'-TTCTGTTCCCGCCATGGA-3'	478-461
WSLB_E_P4 43	Probe	5'-FAM-CCAGTGATTGCAGCAGA-TAMRA-3'	443-459

2.2.4 Cloned plasmid control

The TAC assay detects multiple pathogens and requires a cloned plasmid control (CPC) for both DNA and RNA targets in a multiple-pathogen-detection technology (Kodani, 2012). The design includes a series of genomic regions cloned into multiple plasmids as a multiplex control and can be used to monitor reagent quality, amplification efficiency and inhibition (Kodani, 2012). For CPC1, designed by Dr Marthi Pretorius, used as a control in the validation process, a forward primer sequence, followed by a probe sequence and the reverse complement of the forward sequence were combined and the final construct inserted into a plasmid for the purpose of developing a TaqMan array card as part of a larger project carried out in the ZARV programme (Figure 2.3).

CPC1 sequence:

TAATACGACTCACTATAGGGAGACCTGTGTGAGCTGACAAACTTAGTCCTGGTTCTTAGACATCGAGATCTCGTGCGGC
TGTCAATATGCTAAAACGCACTGGAGCTCCGTGCAGAATCCAGTGATTGCAGCAGATCCATGGCGGGAACAGAATACAA
CATGATGGGGAAAAGAGAAAATACAACATGATGGGAAAACGCGAAAATGGTCATGTGGCTGGGAGCTTTCTGGAATTTG
AAGCCCTGGGTTTGACGATACAGCAGGCTGGGACACAAGTGCGAGGTGGCGACTTCACGCACTCATCGCTTTGGAGG
CACTCTGGTGGGGTTCCTACCACAGCGACGATTTGGACATAGGCAGCGCATGATACTGGTGCTCGGAAAACATCACTC
CCTGCTGGACTTGATAGAAGGTACGCGCTTCAAGTTCGGCGGGTATGTTCCTAACTCTGTTCGTCAAGCAGGGAGGCC
AGGACAGTCCAGCGGCAGGAGCAATACATACTGGCTCAAAGAAAAAGGGGCCCGCTGCCCAACACAAGAGCCTACCTT
GACAAGCAGTCAGACACTCAAATGTCTGCAAAAGAACGTTAGTGGGGCTCCAACACTCGCAAGATGTTGGCACGCATTA
CGCGCTATGCAGCCTATTAATCCGCCGATAGCGGCTAGAGCCCTTTCTAAGAGCATGTGTTACTGCAGCTACCATGGCT
CCTCAAGTTCATGTCAACGCACTCCCACCCTACGCTGCTCCACAGAAACGCCCGACCCGGGCTATTGGATTACAGCGA
GATCAGCGCCGTAACCAGCTTCACGCCCTCCGATTCTACTGGCAGACGACGGAACCTCAATTCTGATGACGAGGATTA
CTTCTCCGGGGCTGTCTATACTCGAATCATGCTGGTCTCTGCAGTTATCACCATCGACAGCTCCCGACACTGCCGAGGA
TTGAAACTAGAAGATGGGCTAAGTACGTAGCTTGCTTTTGGATCATTTGGGCAAGACAAATAGAAGCAGGACTAGATGT
ATGAAAAGGCAAGGAACTCTTCTATAGTGTCACCTAAAT

Figure 2.3: CPC1 sequence used as a control in the one-step real-time RT-PCR showing the WSLB forward primer (red), WSLB probe (blue) and WSLB reverse primer (green).

2.2.5 Virus isolates and RNA extraction

For the validation of the one-step real-time RT-PCR, eight WSLB culture isolates at different passages were used from strains A259, AR16210 and H177. These isolates were extracted using the QIAamp® Viral RNA Mini Kit (Qiagen, Valencia, USA) based on manufacturer's instructions. Briefly, 140 µL of virus culture was added into a labelled 1.5 mL microcentrifuge tube using a pipette. Next 560 µL AVL-Carrier RNA buffer was added to each 1.5 mL microcentrifuge tube, vortexed and incubated for 10 minutes at room temperature (20-22°C). Next, 560 µL of 96%-100% ethanol was added to each 1.5 mL microcentrifugetube and vortexed well. The QIAmp® spin columns were marked and combined with collection tubes. Subsequently 630 µL of

the sample mix were added to the corresponding spin column and centrifuged for 1 minute. All centrifugation steps were performed at 6000x*g*. The flow through was discarded and the spin column placed in a new collection tube. The previous step was repeated. Next 500 µL AW1 buffer was added,and the tubes centrifuged for 1 minute. The flow through was discarded and the spin column placed in a new collection tube. A volume of 500 µL AW2 buffer was added, and the tubes centrifuged for 3 minutes. The flow through was discarded and the tubes centrifuged for another 1 minute to eliminate any possible carry-over of the wash buffers. The collection tubes were discarded, and the spin column placed in labelled 1.5 mL microcentrifuge tubes. RNA was eluted by adding 40 µl elution buffer to the spin columns membrane and centrifuged for 1 minute. This step was repeated.

2.3 West Nile virus and Wesselsbron virus real-time reverse transcription polymerase chain reactions

2.3.1 Flavivirus nested real-time RT-PCR (First round PCR)

The published flavivirus nested real-time PCR with WNV (Zaayman et al 2009) and WSLB (van Niekerk, Unpublished) specific FRET probes were validated for rapid detection of both viruses. The first-round PCR is designed to detect all known flaviviruses. The FU1 and 9317 primers refer to Table 2.1, was used in the first round with. The PCR reaction contained 0.5 µL of each primer (20 pmol), 12.5 µL of Reverse Transcription (RT) buffer, 1 µL of SuperScript™ III RT/Platinum™ Taq Mix enzyme (Thermo Fisher Scientific, California, USA) (Kuno et al., 1998), 0.5 µL of nuclease-free water (Ambion, Thermo Fisher Scientific, California, USA) and 10 µL of template RNA. The PCR was cycled on a thermocycler (Applied Biosystems, Thermo Fisher Scientific, California, USA) at 50°C for 30 minutes, 94°C for 2 minutes, (94°C for 15 seconds, 55°C for 30 seconds, 68°C for 1 minute) x 35 cycles, with a final elongation step of 68°C for 5 minutes. A non-template control (NTC) was included to serve as a general control for extraneous nucleic acid contamination, as well as WNV and WSLB positive cultures as positive controls.

2.3.2 Probe-utilization PCR to detect the presence of WNV and WSLB (Second round PCR)

Specific probes for WNV and WSLB based on the conserved region of the NS5 gene was used to differentiate between lineage 1 and 2 of WNV and WSLB. The LightCycler® FastStart DNA MasterPLUS HybProbe (Roche Applied Science, Mannheim, Germany) was performed according to the manufacturer's instruction. First

0.5 µM of each primer (FS778 and CFD2) was added to 0.2 µM of the WNV and WSLB probes (WNV 9177S; WNV 9021A; WSLB 1 and WSLB 2), 2 µL of the first-round PCR product, 4 µL master mix, and 11.2 µL of nuclease-free H_2O for a final volume of 20 µL. Real-time PCR was carried out in a LightCycler 1.5 instrument (Roche Applied Science, Mannheim, Germany). Cycling commenced at 95ºC for 10 minutes, followed by 45 cycles of 92ºC for 10 s, 50ºC for 8 s, and 72ºC for 8 s and finally melting curve analysis between 30 and 95ºC, carried out at a temperature ramp rate of 0.1ºC/s. A product of approximately 200 bp was visualised by agarose gel electrophoresis (Zaayman et al., 2009). For analysis of the melting curves, the fluorescent channels were set to 705/530 for both WNV and WSLB. Lineage 2 WNV has a melting temperature of between 47°C and 49°C and Lineage 1 WNV has a melting temperature of between 52°C and 54°C. WSLB has a melting temperature of between 56°C to 58°C and a second peak of between 66°C to 68°C. Any specimen outside these ranges were repeated and further investigated.

2.3.3 One-step WSLB TaqMan real-time RT-PCR

To determine the presence of WSLB in a sample, a one-step real-time TaqMan RT-PCR was optimised and evaluted. The TaqMan assay was designed by Dr Marthi Pretorius as part of a series of reactions designed for an arbovirus TaqMan array card (TAC). The primers, WSLB_E422F, WSLB_E478R and probe, WSLB_E_P443, were used in the reaction (Table 2.1). For each reaction, 0.25 µL of both the WSLB_E422F (50 µM) and WSLB_E478R (50 µM) were added to MicroAmp™ Optical 8-Tube Strips (Applied Biosystems, Thermo Fisher Scientific, California, USA), together with 0.5 µL WSLB__E_P443 (20 µM). A total of 12.5 µL of the 2x Ag-Path reaction mix (Applied Biosystems, ThermoFisher Scientific, California, USA) was added to 1 µL of the 25x Ag-Path enzyme mix (Applied Biosystems, ThermoFisher Scientific, California, USA). Approximately 0.5 µL of nuclease-free H_2O was added to a final volume of 15 µL. Finally, 10 µL RNA of the respective sample was added to the master mix. Cycling commenced on the ViiA 7 Real-Time PCR System (Applied Biosystems, ThermoFisher Scientific, California, USA) at 50°C for 30 minutes, followed by 94°C for 2 minutes and 40 cycles of 94°C for 15 s and 58°C for 1 minute.

2.4 Agarose gel electrophoresis

The PCR reaction mixtures from the nested PCR were analysed on a horizontal 2% (w/v) agarose gel made up of 3 grams (g) agarose powder (SeaKem, Lonza, Basel,

Switzerland) and 150 mLof 1xTris-acetate-EDTA (20 mM acetic acid, 100 mM EDTA, 40 mM Tris at pH 8.0) (TAE) buffer (ThermoFisher Scientific, California, USA). The PCR products were electrophoresed at 120 volts (V) in 1xTAE buffer for 35-45 minutes. To allow for visualisation of the amplified PCR products on the BioRad Molecular Imager® Gel DOC™ X+ transilluminator (BioRad, California, USA), 5 µL/100 mL of SmartGlow™ DNA Stain (Accuris Life Science Reagents, New Jersey, USA), was added to the agarose gel. A 100bp DNA molecular marker (DNA molecular marker XIV, Roche, Mannheim, Germany) was included on the agarose gel to determine the size of the DNA amplicons, as well as the concentration.

2.5 Comparison of sensitivity and specificity

To ensure the WSLB TaqMan RT-PCR performed as well as the HybProbe nested PCR, a series of experiments were performed. The sensitivity of the WSLB TaqMan RT-PCR compared to the HybProbe nested PCR was determined by using a 10-fold serial dilution series of titrated WSLB cultures that was tested through singular reactions. A standard curve for the WSLB TaqMan RT-PCR was generated from the dilution series, by plotting the tissue culture infection dose ($TCID_{50}$) U/mL of the WSLB AR259 control against the corresponding cycle threshold (Ct) value, to determine the efficiency, sensitivity, and reproducibility of this assay. As the two PCRs employ different fluorescent chemistry, comparison of Ct values, and thus standard curves, was not possible. Rather a detected vs not detected approach was employed. The specificity was tested using arbovirus controls that we use in the ZARV lab and includes WNV, WSLB, Middelburg virus (MIDV) and Sindbis viruses (SINV) (Alphavirus), and Shuni virus (SHUV) (Orthobunyavirus). To determine the sensitivity of the WSLB one-step RT-PCR compared to the nested RT-PCR, a dilution series of a titrated WSLB strain, H177 P3, was used to determine the limit of detection. A dilution series of cloned plasmid control 1,(CPC1), which contains the WSLB E-gene specific primers and probes cloned in sequence after each other in a single plasmid was used for the TaqMan PCR as described in (Kodani, 2012), to monitor the sensitivity of the PCR reaction, amplification efficiency, and inhibition, as well as a WSLB specific plasmid for the nested HybProbe PCR that contains the NS5 region specific for the flavivirus PCR (Zaayman et al 2009).

2.6 Results
2.6.1 Specificity

A one-step real time RT-PCR was optimised targeting the E protein to a size of 80 bp and compared to a HybProbe nested flavivirus PCR targeting the NS5 gene with a size of 240 bp. The RNA extracted from the eight WSLB culture isolates namely AR16210 P1, AR16210 P3-P4, AR16210, AR16210 P4, AR16210 P3, A259 P4, H177 P2 and H177 P3, were amplified successfully with the one-step WSLB TaqMan real-time RT-PCR. The higher passages of the cultures had higher concentration of the virus, and lower Ct values than the lower passages (Figure 2.3). Lower Ct values indicate high RNA concentrations. In figure 2.4, the amplification plot of the eight extracted WSLB culture isolates can be seen, as well as their Ct-values, with figure 2.5 showing the results of the agarose gel electrophoresis image.

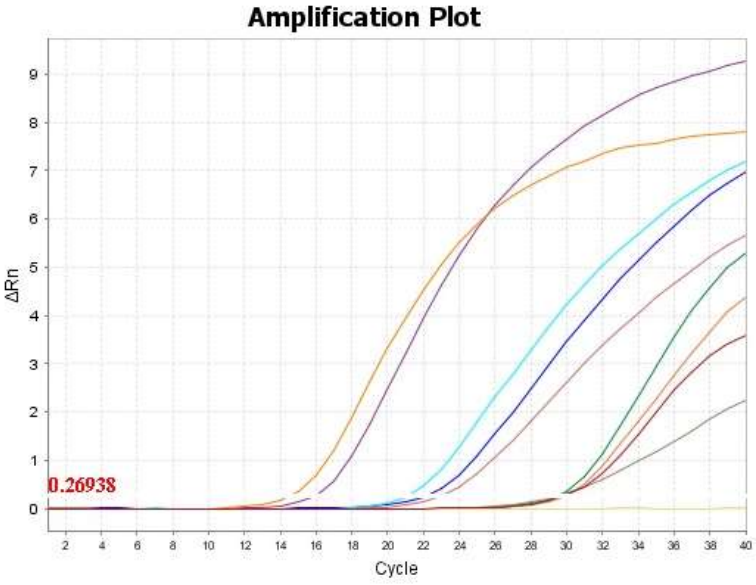

	Strain	Passage	CT-value
	WSLB AR16210	P1	29.88
	WSLB AV259	P4	22.19
	WSLB AR16210	P3-P4	29.57
	WSLB AR16210	P0	14.56
	WSLB H177	P2	29.51
	WSLB AR16210	P4	29.94
	WSLB H177	P3	15.93
	WSLB AR16210	P3	23.04
	WSLB Pos (AV259)	P3	21.12
	NTC	n/a	Undetermined

Figure 2.4: Amplification plot of the eight extracted WSLB cultures on the WSLB TaqMan RT-PCR. Ct-values were detected for all eight WSLB cultures, with lower Ct values representing higher viral load. The WSLB control came up and the non-template control (NTC) was undetected.

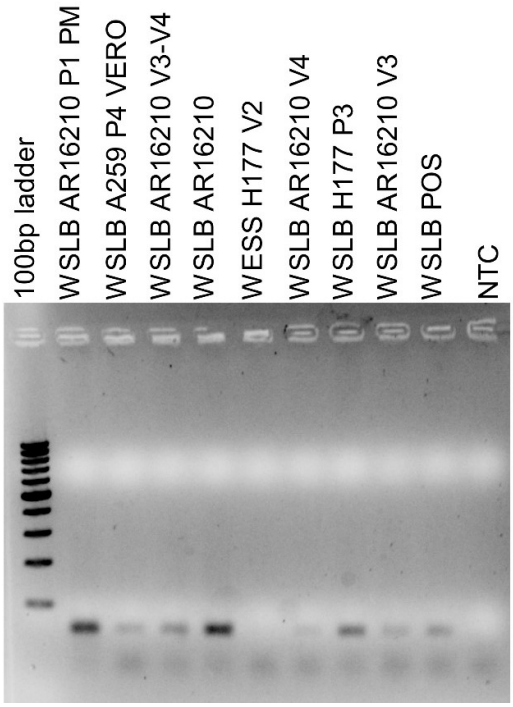

Figure 2.5: Gel image of the eight extracted WSLB cultures on the WSLB TaqMan RT-PCR. The bands formed were approximately 80 bp with very faint bands visible.

For the nested flavivirus real-time RT-PCR, RNA from five samples namely WSLB OBP Vaccine, passage 1 and passage 3 from WSLB NICD passage 3 and the A259 strain passage 4, were extracted and tested using the nested HybProbe RT-PCR. The virus strains were amplified on the LightCycler® and had two distinct melting peaks (Figure 2.6). The melting temperatures were between 44-49°C and 58-63°C respectively. Fluorescence of 0.09 was achieved. Figure 2.6 shows the results for the nested HybProbe RT-PCR on the different WSLB strains. To determine the sensitivity of the assays, serial dilutions of the NS5 gene fragment cloned in a plasmid was used.

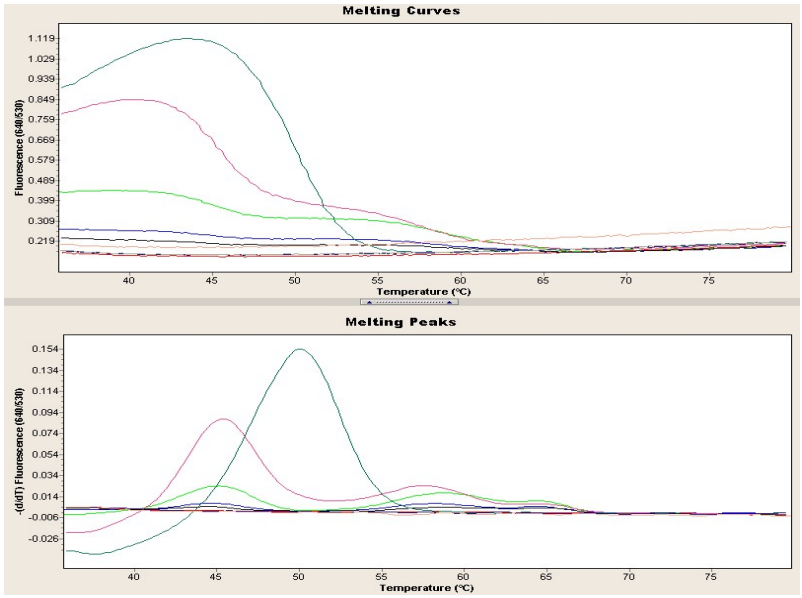

Color	Pos	Name	Tm1	Tm2
	1	WSLB 1 OBP VACC	44.68	60.01
	2	WSLB 2 NICD P1	44.93	59.79
	3	WSLB 3 OBP P3	43.41	61.17
	4	WSLB 4 NICD P3	44.48	63.11
	5	WSLB 5 A259 P4	45.42	58.12
	6	WNV POS	49.99	
	7	NEG EXT		
	8	NTC 1		
	9	NTC 2		

Figure 2.6: The specificity of the light cycler on WSLB cultures. Melting curve of the five extracted WSLB cultures on the LightCycler nested real-time RT-PCR. Melting peaks between 44-49°C and 58-63°C respectively were obtained, as well as fluorescence of 0.09.

With regards to measuring specificity of the WSLB assay, a blind panel was performed including other arboviruses present in SA. Table 2.4 shows the Ct values obtained for the blind panel. Only Unknown 4 had a curve, which was the WSLB sample, while all other samples, as well as the NTC were not amplified. With WNV being the other endemic flavivirus in South Africa, the fact that it was not amplified, indicates that there is no cross-reactivity with this assay and false positives not likely to be obtained.

Table 2.4: Arbovirus controls ran on the WSLB TaqMan RT-PCR. Five unknown samples were ran on the WSLB TaqMan RT-PCR and the virus as well as Ct value is shown in the table.

Sample ID	Virus (unblinded)	Ct value
Unknown 1	SHUV	Undetermined
Unknown 2	WNV	Undetermined
Unknown 3	SINV	Undetermined
Unknown 4	WSLB	20.024
Unknown 5	MIDV	Undetermined

2.6.2 Sensitivity

The limit of detection for the WSLB TaqMan one-step RT-PCR was determined to be the 10^{-8} dilution of CPC1, which had an original concentration of 24 ng/µL, as measured using the Nanodrop. Using Science Primer (https://scienceprimer.com/copy-number-calculator-for-realtime-pcr), the limit of detection was determined to be $2.068x10^3$ plasmid copies/µL. Figure 2.8 shows the amplification plot of the CPC1 dilution series on the one-step WSLB TaqMan RT-PCR. The same experiment was repeated using a dilution series of the H177 P3 culture extract and the detection limit was determined to be 10^{-6} $TCID_{50}$ U/mL, which had an original viral titre of $10^{-8.667}$ $TCID_{50}$ U/mL, thus the limit of detection was determined to be $10^{-2.667}$ viral genome copies/mL. Figure 2.9 shows the amplification plot of the H177 P3 dilution series on the WSLB TaqMan one-step RT-PCR. A WSLB positive control, AV259 P4, was included as a control for the assay.

A standard curve for WSLB TaqMan RT-PCR dilution series is shown in Figure 2.7. The efficiency of the PCR, calculated from the slope of the standard curve, was 93.43% (slope = -3.49). The correlation coefficient (R^2) estimates how good the data

points fit the trendline and was calculated as 0.81 for the WSLB one-step real-time RT-PCR. The y-intercept of the standard curve indicating the number of cycles required to reliably detect the lowest dilution of the CPC plasmid control (10^{-1}) at 11.91 cycles (as also shown in Figure 2.8 in the dilution series) up to the highest dilution (at 10^{-8}) for the WSLB one-step real-time RT-PCR.

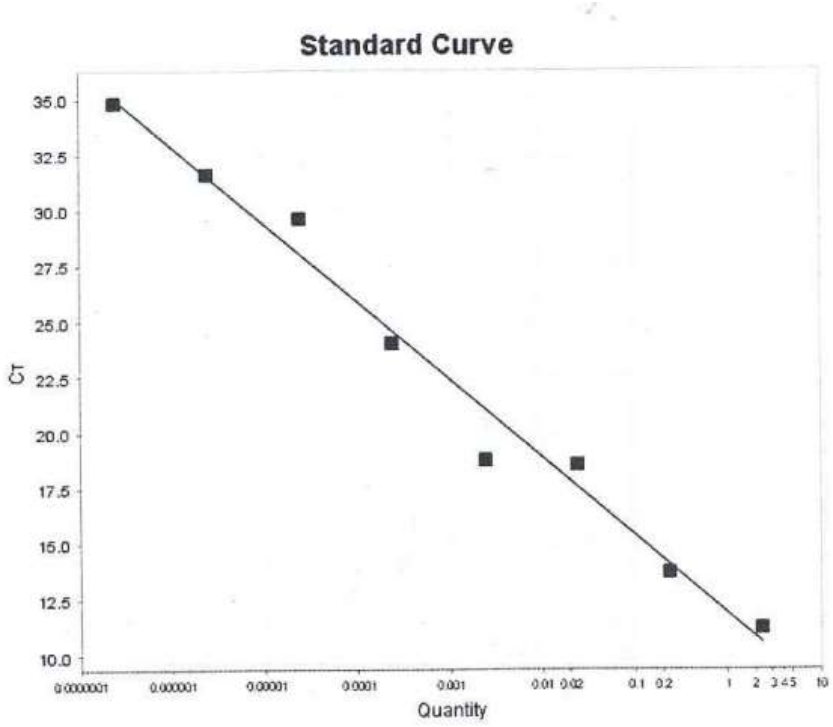

Strain	CT-value	Copy number
CPC1 10^{-1}	11.22	2.068
CPC1 10^{-2}	13.73	0.02
CPC1 10^{-3}	18.58	0.01
CPC1 10^{-4}	18.74	0.001
CPC1 10^{-5}	24.03	0.0001
CPC1 10^{-6}	29.66	0.00001
CPC1 10^{-7}	31.62	0.000001
CPC1 10^{-8}	34.62	0.0000001

Figure 2.7: The standard curve of the WSLB one-step RT-PCR. The curve was generated from a serial dilution of the CPC control that was tested through singular reactions. The slope of the curve was -3.49 which translates to a reaction efficiency of 93.43%, the y-intercept was 11.91, the correlation coefficient (R^2 = 0.981) represents a highly linear reaction with a minimal error (error = 0.198).

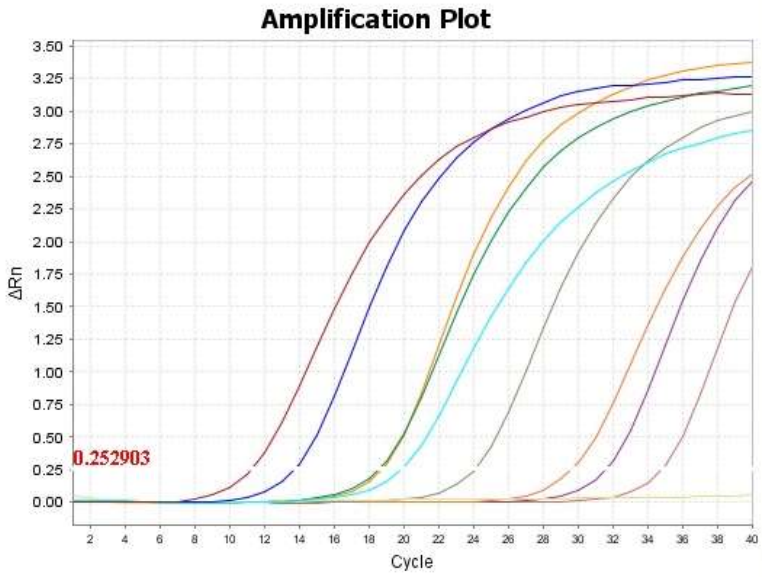

	Strain	CT-value
	CPC1 10^{-1}	11.22
	CPC1 10^{-2}	13.73
	CPC1 10^{-3}	18.58
	CPC1 10^{-4}	18.74
	CPC1 10^{-5}	24.03
	CPC1 10^{-6}	29.66
	CPC1 10^{-7}	31.62
	CPC1 10^{-8}	34.62
	WSLB Pos Control	19.9
	NTC	Undetermined

Figure 2.8: Amplification plot of the CPC1 dilution series on the one-step WSLB TaqMan RT-PCR. Ct-values were detected for the CPC1 dilutions from 10^{-1}, which had a Ct-value of 11.22, up to the 10^{-8} dilution with a Ct-value of 34.82. As the dilution increased, the Ct-value decreased.

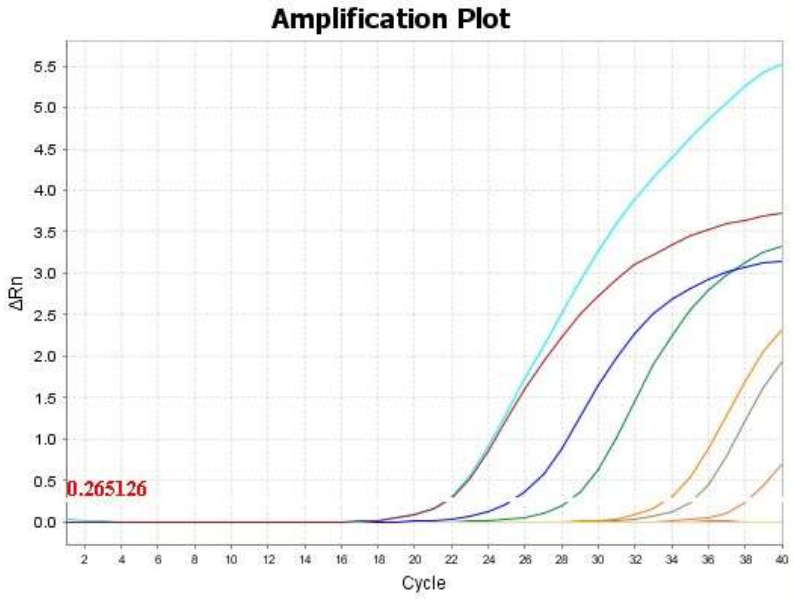

	Strain	CT-value
	WSLB H177 10^{-1}	21.83
	WSLB H177 10^{-2}	25.43
	WSLB H177 10^{-3}	28.52
	WSLB H177 10^{-4}	33.76
	WSLB H177 10^{-5}	35.13
	WSLB H177 10^{-6}	38.18
	WSLB H177 10^{-7}	Undetermined
	WSLB H177 10^{-8}	Undetermined
	WSLB Pos Control	21.71
	NTC	Undetermined

Figure 2.9: Amplification plot of the WSLB virus culture dilution series on the one-step WSLB TaqMan RT-PCR. CT-values were detected for the WSLB H177 dilutions from 10^{-1}, which had a CT-value of 21.83, up to the 10^{-6} dilution with a CT-value of 38.18. As the dilution increased, the CT-value decreased.

The concentration of the WSLB plasmid 2 control containing the NS5 gene fragment cloned into a plasmid, designed in the ZARV lab, used to determine the limit of detection for the HybProbe nested PCR, was 28.8 ng/µL. The detection limit was determined to be 5.509 x10^{-2} copy numbers/µLof the plasmid 2 control, which was detected on the nested HybProbe PCR as seen in Figure 2.10.

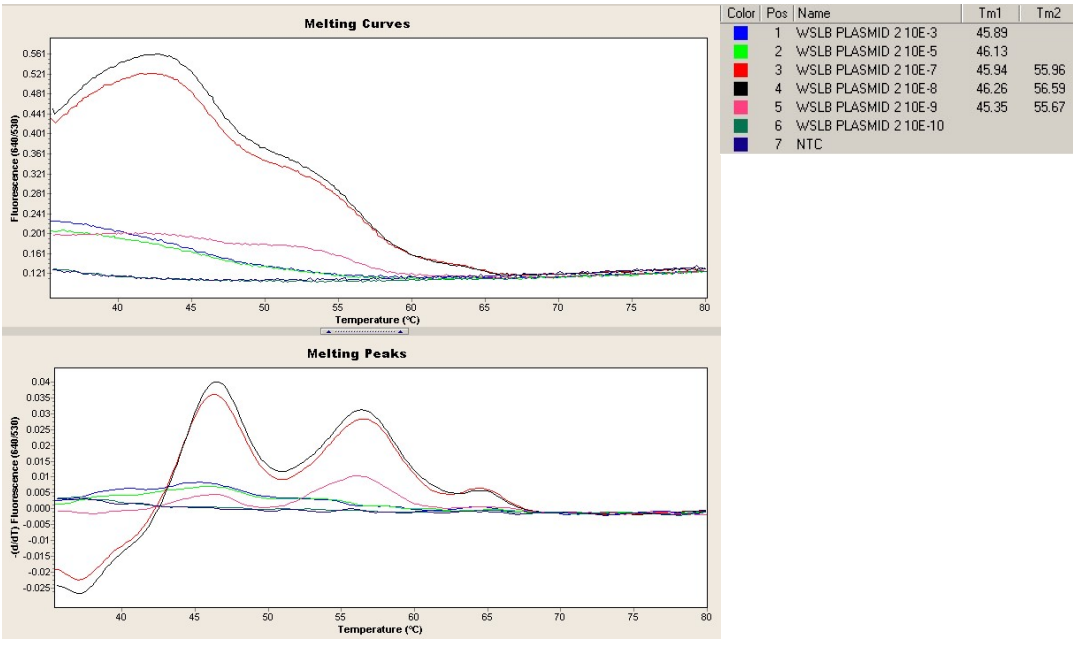

Figure 2.10: The sensitivity of the LightCycler on WSLB cultures. Melting curve of the dilutions of the plasmid control on the LightCycler nested real-time RT-PCR. Melting peaks between 44-49°C and 58-63°C respectively were obtained, as well as fluorescence of 0.04.

Extracted RNA from previously positive WSLB cases were unavailable to show detection using the WSLB TaqMan, however two positive cases were detected and confirmed with the flavivirus real-time PCR that could be confirmed with this assay in Chapter 4.

2.7 Discussion

In this study, validation of a one-step WSLB real-time RT-PCR is described compared to an established nested HybProbe flavivirus PCR, which has applications in diagnostics, as well as epidemiology and surveillance programs. With WSLB being a neglected arbovirus in South Africa, it is important to ensure that there are molecular diagnostic tools in place to correctly detect any infections, thus providing a better understanding of the incidence of the virus.

The E region of the genome was selected as the target for the assays, due to its high level of conservation. Making use of a one-step real time RT-PCR, has the advantage of being a rapid, sensitive approach, excluding the need for pre-PCR cDNA synthesis and even post-PCR gel electrophoresis. By limiting the handling of the samples, this also reduces the risk of contamination. Another advantage of the one-step real-time RT-PCR is the fact that it is quantitative, where a lower Ct value indicates higher viral load. A drawback of the one-step real time RT-PCR is the small product size of only, 80 bp that can be visualized on the agarose gel, which are too small for sequencing and phylogenetic analysis.

The results obtained from the one-step real time RT-PCR showed that three different virus strain cultures at various passages could be detected using a real time PCR platform. The limit of detection using virus culture H177 was determined to be a titre of $10^{-2.667}$ viral genome copies/mL while the limit of detection making use of CPC1, was determined to be 2.068×10^{3} plasmid copies/µL. The established WSLB RT-PCR by Faye et al., 2022, had a limit of detection of 100 pfu/mL. Comparing this to the WSLB TaqMan RT-PCR, the assay showed good comparison and indicated excellent diagnostic performances, which indicates that it is sensitive and specific. There was no cross-reactivity with other arboviruses including WNV. The HybProbe nested PCR was determined to have a sensitivity of 5.509×10^{-2} copy numbers/µL. The correlation coefficient (R^2) defines how well the data fit the standard curve, and therefor reflects the linearity of the standard curve. The one-step real-time WSLB PCR was deemed

highly linear, with R^2=0.981, which is close to the maximum value attainable. The reaction efficiency, which in turn corresponds to the slope of the standard curve, details the percentage of RNA converted into complementary deoxyribonucleic acid (cDNA), with anything greater than 90.00% is deemed efficient. Therefore, the WSLB TaqMan one-step RT-PCR is highly efficient (93.43%).

The sensitivity and specificity of the one-step WSLB real-time RT-PCR is equally as good as that of the LightCycler HybProbe assay. The one-step real time RT-PCR is a less time consuming and cost-effective assay compared to the nested HybProbe PCR assay. The ViiA7 machine (Applied Biosystems, ThermoFisher Scientific, Massachusetts, USA) can process 96 reactions in a single run, as opposed to 32 reactions on the LightCycler, therefore the pan-flavivirus TaqMan PCR has a higher throughput and can increase turnaround time. The use of relatively cheap plastic PCR tubes or plates is a lesser health and safety risk compared to the expensive glass capillaries utilised by the LightCycler machine and the running cost of a single one-step PCR is much less than that of a nested PCR. Therefore, the WSLB one-step RT-PCR was successfully validated to be a highly efficient and sensitive confirmation tool for WSLB in animals.

A limitation of the study is that there are not many positive WSLB clinical samples available for validation, which is why plasmids and virus cultures were relied on to determine sensitivity and specificity. The assay was used in chapter 5 to confirm WSLB virus cases that was detected by a flavivirus PCR assay. At the end of this project Faye et al. (2022), also described a sensitive fluorescent probe-based RT-qPCR and a real time reverse-transcription polymerase amplification (RT-RPA) were developed and evaluated for rapid and sensitive detection of WSLB. Both of these assays were a one-step assay with a sensitivity and specify of 100% each (Faye et al., 2022). The in-house assay described in my study was however used to confirm positive WSLB cases going forward.

2.8 Conclusion

Annually, a high percentage of neurological disease in animals go undiagnosed due to the substantial number of potential pathogens, which are excluded from routine diagnostics. The one-step real time WSLB RT-PCR is sensitive enough to be used on the TaqMan array card and as a confirmatory assay for WSLB detected through flavivirus

genus PCRs and will aid in potentially identifying WSLB infections in undiagnosed cases of neurological disease, which will result in a better understanding of its incidence in South Africa.

Chapter 3 – WNV infections in humans from 2021 to 2022 in South Africa

3.1 Introduction

3.1.1 West Nile virus in humans

West Nile virus (WNV) is a vector-borne flavivirus that is endemic to South Africa and a continuous global concern, yet understudied in hospitalised patients (Zaayman, 2012). Humans are dead-end hosts in the WNV transmission cycle, since they typically do not have a viremia sufficient enough to infect feeding mosquitoes (Beasly, 2011). Humans are able to clear WNV infection, with 80% being asymptomatic, while 20% of humans present with clinical symptoms and in 1% leading to neuro-invasive syndrome, with a fatality rate of less than 10% (Zouet al., 2010).

Disease manifestations reported include symptoms ranging from fever and myalgia to meningoencephalitis and death (Colpitts et al., 2012). Encephalitis is not common and only occurs in a small percentage of infected people (Li, 2003). West Nile Fever (WNF) is characterised by an abrupt onset of febrile illness consisting of clinical signs, such as headache, malaise, skin rashes, fever, myalgia, and/or joint pain (Schwarz, 2023). West Nile Encephalitis (WNE) presents as a spectrum, from mild short-term confusion and disorientation to severe changes in cognition and sensorium (Schwarz, 2023). Seizures can occur but are not as common (Schwarz, 2023). Meningitis without changes in mental state also occurs and is characterised by fever, headache, and stiff neck, while acute flaccid paralysis (AFP) is primarily characterised by the acute onset of flaccid paralysis that is usually asymmetrical with a general loss of spinal reflexes without sensory disruption (Schwarz, 2023). The initial clinical phase is associated with depression, alteration of mental status, lethargy, and personality change (Habarugira et al., 2020). Other symptoms include headache, malaise, a high fever above 38°C, myalgia, chills, vomiting, a rash predominant over the torso and eye pain (Zou et al., 2010).

Age seems to affect risk for more severe infections, with older people being more susceptible to infection due to a weaker immune response, with case fatality rates of approximately 10% in neurological cases (Peterson and Marfin, 2002; McVey et al., 2015). Higher fatality rates have been reported in infected infants and immunocompromised patients, with risk factors including homelessness, being prone to cardiovascular disease or chronic renal disease, hepatitis C infection and immunosuppression (Granwehr et al., 2004; Murray,2006).

Two out of the nine confirmed lineages, lineage 1 and 2, are associated with the majority of outbreaks (Sule, 2018). The United States (US) Stats as of January 10, 2023, a total of 1035 cases of WNV disease in people have been reported to the Center for Disease Control (CDC). Of these, 737 (71%) were classified as neuroinvasive disease (such as meningitis or encephalitis) and 298 (29%) were classified as non-neuroinvasive disease (CDC, 2023). Since the beginning of the 2022 transmission season and as of 23 November 2022, European countries have reported 965 human cases of WNV infection in humans, with 73 deaths (ECDC, 2022). The recent outbreaks have confirmed that both lineage 1 and lineage 2 is of public health concern (CDC, 2023).

3.1.2 Human West Nile virus cases in South Africa

West Nile virus outbreaks in the human population before the early 1990s were sporadic and neurological infections very uncommon (Sejvar, 2008). The first well-established link between WNV and neurological disease in humans was identified in Israel in 1957 following an outbreak in a nursing home, where one-third of the infected patients presented with encephalitis (Weinberger, 2001). A study done by Zaayman and Venter (2012), proposed that WNV is missed as a cause of neurological infections in humans in South Africa. In the study, 206 patient samples collected between September 2008 and May 2009 through the Tshwane Academic Division, National Health Laboratory Service Virology laboratory from public sector hospitals in Tshwane, with clinical symptoms consistent with WNV infection, including fever, headache, rash, and other neurological signs, were screened using neutralisation assays, real-time reverse transcriptase polymerase chain reaction (RT-PCR) and an immunoglobulin M (IgM) enzyme linked immunosorbent assay (ELISA) (Zaayman and Venter, 2012). The authors reported that neutralising antibodies to WNV were present in 40/206 (19.42%) of serum samples, while 4/15 (26.67%) cerebrospinal fluid (CSF) samples suggesting a possible WNV infection (Zaayman and Venter, 2012). Although IgM antibodies could not be investigated due to limited sample volume, the study suggested that WNV may be overlooked in South Africa, and clinical awareness, proper surveillance and efficient diagnostic methods are required to understand the true burden of the disease (Zaayman and Venter, 2012). Despite being endemic in South Africa, only 5-15 human WNV cases are reported annually, although this is likely an underestimate due to the clinical awareness of the disease potential (Burt, 2002).

3.1.3 Diagnostic methods used to detect West Nile virus in patients

Early WNV infection can be diagnosed by detecting viral RNA using quantitative RT-

PCR (Lustig et al., 2018). Samples used for testing includes serum, plasma, and CSF but has limitations due to low levels of viraemia, as well as a short window for detection (Lustig et al., 2016). Currently there are various serological assays available, where detection of IgM antibodies or serum neutralisation test indicates infection (McVey et al., 2015). The ELISA kits are not guaranteed to be free from cross-reactivity (Llorente et al., 2019). The plaque reduction neutralisation test (PRNT) is regarded as the gold standard test, due to the cross-reactivity between flaviviruses using an ELISA but does not differentiate between IgM and IgG antibodies and is therefore used as confirmation of either (Llorente et al., 2019). Neutralisation assays make use of titrating neutralising antibodies for a specific flavivirus and getting a positive result, is considered proof of specificity (Endale et al., 2021). Flaviviruses in the same sero-complex, like WNV and Usutu virus (USUV), are most likely to exhibit cross-reactivitythan flaviviruses from different sero-complexes like WNV/USUV and Bagaza virus (BAGV) or Wesselsbron virus (WSLB) (Calisher et al., 1989).

3.1.4 African Network for improved Diagnostics, Epidemiology and Management of Common Infectious Agents

The African Network for improved Diagnostics, Epidemiology and Management of Common Infectious Agents (ANDEMIA) was a prospective research study aimed at enrolling cases of acute febrile disease of unknown cause in sub-Saharan Africa between August 2018-December 2021 (Schubert et al., 2022). In this study, patients matching an acute febrile and neurological disease case definition were enrolled from two sentinel surveillance sites and primarily screened using a molecular diagnostic tool targeting 30 pathogens associated with febrile and neurological disease including WNV (Venter and Swanepoel, 2010). Data on the burden of disease to these arboviruses in the ANDEMIA countries are limited.

In South Africa, the risk factors for WNV infection and the burden of disease, have not yet been investigated in hospitalised patients that are experiencing acute fever of unknown cause with or without neurological signs. To address this gap, the association of WNV with neurological disease using molecular and IgM serodiagnosis with neutralisation tests for confirmation, were investigated.

3.2 Materials and Methods:

3.2.1 Ethics Approval

To conduct this study, ethics approval was granted by the University of Pretoria, Faculty of Health Sciences Research Ethics Committee Protocols - 100/2017 and

101/2017 for the ANDEMIA study, 181/2021 for MSc project ethics approval. Hospital approvals were obtained from Kalafong Hospital (KPTH 33/2017) and the Department of Health, Mpumalanga province.

3.2.2 Study Design

Three hospitals were selected as sentinel sites for the surveillance of acute febrile disease of unknown cause (AFDUC), as part of ANDEMIA. The hospitals included Kalafong hospital in the Gauteng province and Matikwana and Mapulaneng hospitals in Mpumalanga, South Africa. Information on the patient's age, sex, area of residence, symptom onset, medical history, pre-existing conditions, reason for hospitalisation, clinical signs, and socio-economic data was collected by surveillance officers using a standardised case investigation form. Informed consent was obtained from the patients, with a legal guardian providing consent if the patient was underaged. The objectives of the surveillance study, benefits of participation and potential risks were communicated to all patients. The information was stored on an online database and remained confidential.

Figure 3.1: Map showing sentinel sites. The map of South Africa shows the coordinates of the three sentinel sites that were part of the ANDEMIA study. Kalafong hospital is in Gauteng, while Mapulaneng and Matikwana hospitals are in the Mpumalanga province, South Africa. Map was made using Arcgis.

3.2.3 Sample collection

Specimens, including serum, whole blood and CSF, were collected from patients that fit the case definition of AFDUC and submitted in EDTA tubes (Schubert et al., 2021). CSF samples were only taken as part of the standard of care. The case definition for AFDUC states that a patient should:

- Have a fever (≥38°C) or have history of fever in the last 10 days
- Present with acute neurological signs or symptoms, including headache, meningitis, encephalitis, acute flaccid paralysis, recent onset of Guillain-Barré syndrome, central or peripheral neurological dysfunction, signs of arthralgia and rash
- Have a negative malaria test

Whole blood (EDTA) samples were used for molecular testing, while red blood cells were separated from plasma by centrifugation and used for serological assays, in the case where a serum sample could not be obtained. All samples were aliquoted into 1.5 mL microcentrifuge tubes and stored at -70°C until testing. Samples submitted to ZARV were assigned an additional sample number, Zoonotic Research Unit ANDEMIA (ZRUA), for the purpose of in-house record keeping. Samples submitted between January and June in 2021 and 2022 were used for the purpose of this study. Limited samples were available for 2022, due to the study coming to an end. The arbovirus season refers to the late summer to autumn months (January to May) when mosquito populations reach their peak (Cornel, 2018). The seasonality also correlates with previous published reports of WNV in wildlife and horses in South Africa (Venter, 2017; Steyn, 2019).

3.2.4 Molecular testing (LCD Array)

Ribonucleic acid from clinical specimens submitted between January 2021 and April 2022 was extracted according to manufacturer's instructions, using the QIAmp Viral RNA Kit (Qiagen, Hilden, Germany). A multiplex PCR-based macro-array assay was developed in the ZARV lab and produced at Chipron GmBH (Chipron GmBH, Berlin, Germany), to use as a differential diagnostic tool to simultaneously screen for 30 pathogens responsible for acute febrile and nervous system infections, causing disease in southern Africa, including WNV and other flaviviruses (Venter et al., 2014). The primer sequences are listed in Appendix Table A2. Briefly, complementary deoxyribonucleic acid (cDNA) synthesis was performed with the Expand Reverse Transcriptase (Roche, Mannheim, Germany) in a 20 µL reaction containing 10 µL template nucleic acid. Subsequently, two PCR reactions were performed per sample, using a mix of 30 primer sets that were labelled with biotin, using the Qiagen Multiplex PCR kit (Qiagen, Valencia, California, USA) containing 5 µL cDNA in a 25 µL reaction. The PCR products were denatured and hybridised to the custom printed microarray surface (chip) that was coated with target probes directed against each pathogen. Streptavidin-conjugated labelled enzyme (Chipron GmBH, Berlin, Germany) and

substrate was added to each well. A positive reaction was identified by colourimetric detection on the Chipron slide reader and the LCD SlideReader V12 software package (Chipron, GmBH, Berlin, Germany).

3.2.5 Serological testing (WNV IgM Euroimmun ELISA kit)

A commercial WNV IgM ELISA kit available for testing human samples (Euroimmun, Lübeck, Schleswig-Holstein, Germany) was used to screen for IgM antibodies in serum, plasma, and CSF samples. The ELISA was performed according to manufacturer's instructions. In short, patient samples were diluted 1:101 with sample buffer, vortexedand incubated for 10 minutes at room temperature (20°C to 22°C). Subsequently, 100 µL of the provided calibrator, positive and negative controls, as well as the diluted patient samples were added to the microplate wells according to the protocol. The plate was added to a humidified chamber, which consists of a Tupperware container with moist tissue paper, and incubated for 1 hour at 37°C. Following the incubation step, the plate was washed three times using 300 µL of wash buffer per well and the plate tapped on absorbent paper to remove any residual wash buffer. A total of 100 µL enzyme conjugate (peroxidase-labelled anti-human IgM) was added to each well and the plate incubated for 30 minutes at room temperature. The washing step was repeated. Next 100 µL of the substrate solution was added into each of the wells and incubated for 15 minutes at room temperature in a dark room. To stop the reaction, 100 µL of stop solution was added into each well. The plate was measured at a wavelength of 450 nanometre (nm) using a Mindray MR-96A microplate reader (Mindray, Hong Kong, China). The OD value of the calibrator defines the cut-off value for non-infected persons and was used in the following calculation: OD of test sera/OD of the calibrator. A ratio of ≥ 1.1 was considered positive and < 0.8 was considered negative. Values in-between 0.8 and 1.1 were deemed borderline. All positive and borderline samples were subjected to neutralisation assays to confirm the presence of WNV neutralising antibodies.

3.2.6 Virus culture and titration

A positive WNV culture was titrated for use in neutralisation assays. The culture was maintained in Vero cells, containing Eagle's Minimum Essential Media (EMEM) (Lonza, Basel, Switzerland), supplemented with 10% foetal calf serum (FCS) (Invitrogen, Carlsbad, CA), glutamine (Gibco, Thermo Fisher Scientific, California, USA) and Mycozap (Gibco, Thermo Fisher Scientific, California, USA). Viral infections are allowed to proceed until a cytopathic effect (CPE) of 80% became apparent, after which the virus was harvested and stored at -80°C until further use.

For viral titration, a cell culture flask was trypsinised and cells were diluted to $8x10^5$ cells/mL in MEM containing 5% FCS. A volume of 25 µL of the cell suspension was dispersed into each well of the 96 well plate. Next 200 µL of 10% EMEM was added to each well andthe plate incubated in a humidity chamber overnight at 37°C. Ten-fold serial dilutionswere made from 10^{-1} to 10^{-9} using 100 µL sample and 900 µL of serum free EMEM. The plate was washed three times with phosphate buffered saline (PBS). Next 100 µL of each dilution was added to six wells of the microtiter plate starting from the highest dilution to the lowest. The plate was covered in a humidity chamber and kept in the carbon dioxide (CO_2) incubator (Series 2000, Scientific Engineering, Johannesburg, South Africa) at 37°C for one hour. A volume of 100 µL of cell culture media containing 2% FCS was added to each well. Cells were inspected daily for the presence of CPE. Viral titre was calculated using the formula tissue culture infectious dose ($TCID_{50}$)= - (x0 - d/2 + d $\sum$ r/n). Whereby:

x0 = the highest dilution (lowest concentration) at which all replicates are dead
d = the dilution factor

n = the number of replicates

r = the sum of everything dead at the lowest concentration and every well thereafter.

3.2.7 Neutralisation assays

A micro-virus-neutralisation test (micro-VNT) was used to determine the neutralising antibody titres in serum samples, as previously described (Figuerola et al., 2007). Serum samples were heat-inactivated at 56°C for 30 minutes before analysis using a heating block (Thermo Fisher Scientific, California, USA). Dilutions of test sera were performed using serum-free minimal essential media (MEM) that weresupplemented with antibiotics (100 U penicillin/mL and 100 mg streptomycin/mL) (Gibco, Thermo Fisher Scientific, California, USA). A 100 $TCID_{50}$ U/mL of WNV was prepared in cell culture media containing 2% FCS (Gibco, Thermo Fisher Scientific, California, USA), and 100 µL of this was dispensed into columns 1,2,3,5,6,7 of the 96-well plate (Nunc-Immuno, Sigma Aldrich, Missouri, USA), leaving the last two columns free for back titration. The back titration was prepared by transferring 100 µL of each dilution in quadruplicate so that 100 $TCID_{50}$, 10 $TCID_{50}$, 1 $TCID_{50}$, and 0 $TCID_{50}$ occur in the last two columns. Finally, 100 µL of each 2-fold duplicate dilutions of sera were dispensed into the appropriate wells. The plate was incubated (Series 2000, ScientificEngineering, Johannesburg, South Africa) at 37ºC for 45 minutes. A cell culture flask containing a confluent monolayer of Vero cells with a cell concentration of $8x10^5$ cells/mL was

trypsinized (Merck, New Jersey, USA), and 25 µL of cells was dispensedinto all wells of the 96- well plate (Nunc-Immuno, Sigma Aldrich, Missouri, USA). The plates were incubated for 6 to 7 days at 37°C until a cytopathic effect (CPE) was seen in the control wells, which were at the back of the plate. Virus-neutralisation positive samples were those inhibiting CPE at 1:8 or higher dilutions. Neutralizing serum titre was regarded as the highest value of the reciprocal serum dilution where there is no CPE present (Sotelo et al., 2011). All samples that tested positive on the WNV IgM commercial ELISA, but negative with the WNV neutralisation assay, were subjected to screening for WSLB, Usutu virus (USUV), Bagaza virus (BAGV) and Banzi virus (BANV) neutralization assays to determine whether there was any cross-reactivity (Table 3.1).

Table 3.1: A table showing the flaviviruses used in neutralisation assays for samples that were positive on the WNV IgM ELISA, but negative with WNV neutralisation assays.

Virus	ZARV ID	Accession number	Reference
Bagaza virus	ZRU349/17/3 P5	MN329586	Steyn et al, 2019
Banzi virus	LAP13MP25	OL411961.1	MacIntyre et al, 2023
Usutu virus	SAAr 1776 P7 V2	AY453412	Bakonyi et al, 2004
Wesselsbron virus	AR259 P4	JN226796.1	Human, 2011

3.2.8 Data analysis

Data analysis was carried out in EpiInfo™ (version 7.2.4.0) using Fisher's exact test with a 95% confidence interval (CI) and odd ratios (OR). Risk factors associated with a WNV infection were calculated based on patient demographic and clinical features using a univariate analysis. Median age is used as an indicator, due to the data not being normally distributed. A p value < 0.05 was considered as significant. All data were reported using tables and graphs.

3.3 Results:

By combining molecular (meningo-fever chip) and serological (IgM) testing, patients with acute WNV infection could be identified from ANDEMIA samples. The use of a combined approach is useful due to the short viraemia of flaviviruses, therefore, serological testing with the commercial WNV IgM ELISA kit was used in conjunction to ensure that no cases were missed. All positive cases were confirmed by serum neutralisation assays to rule out cross-reactions.

Between January 2021 and April 2022, a total of 432 samples from 325 patients presenting with symptoms that matched the case definition, were submitted (Table 3.2). Only the 183 serum samples submitted during the arbovirus season (Table 3.3), January to June in South Africa, were relevant to this study and included in IgM testing; however, all samples throughout the year were screened with molecular testing for routine testing for WNV and other pathogens, as part of the bigger ANDEMIA study.

A total of 216 samples submitted through 2021 and beginning months of 2022, were tested using the fever chip, with one sample testing positive for WNV on nucleic acids using the ChIP (Table 3.3). This case could not be confirmed using additional molecular assays. For the WNV IgM antibody testing, 143/183 (78.1%) samples were subjected to testing (Table 3.3). This is due to the fact that some samples were depleted after performing the nucleic acid extraction for the ChIP assay. Of these, 16/143 (11.2%) tested positive using the commercial ELISA kit. To note, an additional 10/143 (6.9%) samples came up as borderline on the kit, meaning that it could not be determined whether they are positive or negative.To rule out any cross-reactivity and in order to confirm that WNV was responsible for the ELISA results due to flavivirus cross-reactivity, positive and borderline cases were subjected to a virus neutralisation assay using a cultured WNV isolate at a standard concentration. Regarding the borderline samples, 5/8 tested positive for WNV neutralising antibodies with the neutralisation assays. These assays resulted in 13/26 (50%) samples having WNV neutralising antibodies. Overall, 13/143 samples were positive for WNV, and this resulted in an overall IgM incidence of 10.3% for January to June in 2021 and 2.4% for 2022 in South Africa. One CSF specimen (ZRUA1525/21) tested positive for WNV IgM antibodies and was confirmed with neutralisation assays, the other positive samples were plasma, 7/13 (53.9%) and serum, 5/13 (38.4%). In Gauteng, 2/8 (25%) specimens tested positive for neutralising antibodies, compared to 11/18 (61.1%) in Mpumalanga. Samples that tested positive on the WNV IgM ELISA, but negative with WNV neutralisation assays, were subjected to neutralisation assays against WSLB, USUV, BAGV and BUNV, but all samples were negative for these viruses.

Table 3.2: Table summarising the sample submission for 2021 and 2022. The table summarises the total amount of samples submitted between January and December from Gauteng and Mpumalanga, as well as what types of samples were submitted (plasma, serum or CSF).

	Gauteng		Mpumalanga		Total
Collection year	2021	2022	2021	2022	
Patients enrolled from January to December (n=x)	212 (65.2%)	21 (6.5%)	72 (22.2%)	20 (6.2%)	325
Sample type					
Whole blood	166 (61.5%)	15 (5.6%)	69 (25.6%)	20 (7.4%)	270
CSF	8 (33.3%)	1 (4.2%)	5 (20.8%)	10 (41.7%)	24
Serum	97 (70.3%)	8 (6.8%)	29 (21.0%)	4 (2.9%)	138
Total specimens submitted	271 (62.7%)	24 (5.6%)	103 (23.8%)	34 (7.9%)	432

Table 3.3: Table summarising the results of testing. The table summarises the samples enrolled in the arbovirus season, January to June, and what their results were when tested with the LCD assay, WNV IgM commercial ELISA kit, as well as neutralisation assay.

	Gauteng		Mpumalanga		Total
	2021	2022	2021	2022	
Enrolled Jan-June (%)	109	21	33	20	183
ChIP tested	134	22	39	21	216
Positive (%)	0 (0)	0 (0)	1 (2.6)	0 (0)	1 (0.5)
Negative (%)	134 (100)	22 (100)	38 (97.4)	21 (100)	215 (99.5)
IgM tested	74	9	42	16	143
Positive (%)	6 (8.1)	0 (0)	8 (19.1)	2 (12.5)	16 (11.2)
Negative (%)	66 (89.2)	9 (100)	27 (64.3)	13 (81.3)	115 (80.4)
Bordeline (%)	2 (2.7)	0 (0)	7 (16.7)	1 (6.3)	10 (8.4)
Micro-neutralization assay	8	0	15	3	26
Positive (%)	2 (25)	0 (0)	10 (66.7)	1 (33.3)	13 (50)
Negative (%)	6 (75)	0 (0)	5 (33.3)	2 (66.7)	13 (50)

The majority of samples received were from females, 78/143 (54.6%) compared to males (44.0%) (Table 3.4). In terms of age range, 71/143 (49.7%) were from patients between the ages of 0-5 years, whereas the least number of specimens were received from patients aged 50+ years,7/143 (4.9%) (Table 3.4).

The highest proportion of WNV IgM positivity was detected in patients aged 50+ years old, with 2/7 (28.6%) having WNV antibodies, with the lowest proportion of WNV IgM positivity detected in patients aged 6-20 years, with 1/23 (4.4%) testing positive (Table 3.4). However, the number of positive cases identified in these age groups were very low. Due to varied sample size, it could not be concluded whether there was an association between age and WNV positivity. Generally, WNV infection (as determined by the presence of IgM antibodies), were found in more males 8/63 (12.7%) than in females 5/78 (6.4%). There was a higher incidence of cases in Mpumalanga, with 11/13 (84.6%) positive cases recorded at either Matikwana or

Mapulaneng hospital (Table 3.3), compared to 2/13 (15.4%) positive cases in Gauteng. There was 12/116 (10.3%) positive cases in 2021, with only 1/41 (2.4%) positive case in 2022 (Table 3.3), which could be due to the study coming to an end in April 2022 and less samples being submitted.

Table 3.4: Table summarising the demographics for samples submitted. The table summarises demographic characteristics of the study group (January to June 2021 and 2022, n=143) subjected to serological testing.

Demographics	WNV positive (N=13)	WNV negative (N=128)	Odds ratio [CI]	p-value
Sex (%)				
Male (n=63)	8 (12.7)	55 (87.3)	2.12 [0.65;6.84]	0.161
Female (n=78)	5 (6.4)	73 (93.6)	0.47 [0.14;1.51]	0.161
Age (%)				
0-5 (n=71)	4 (5.6)	67 (94.4)	0.4 [0.11;1.38]	0.116
6-20 (n=23)	1 (4.3)	22 (95.7)	0.4 [0.04;3.24]	0.336
21-49 (n=40)	6 (15)	34 (85)	2.36 [0.74;7.55]	0.122
50+ (n=7)	2 (28.6)	5 (71.4)	4.47 [0.77;25.79]	0.126
HIV Status (%)				
Positive (n=32)	3 (9.4)	29 (91.6)	1.04 [0.26;4.04]	0.591
Negative (n=91)	4 (4.4)	87 (95.6)	0.21 [0.06;0.75]	0.012
Unknown (n=20)	6 (30)	14 (70)	7.10 [2.08;24.13]	0.003
Job type (%)				
Inside/Office (n=10)	0 (0)	10 (100)	0 [undefined]	0.179
Labourer (n=4)	1 (25)	3 (75)	2.16 [0.19;24.38]	0.471
Unemployed (n=35)	6 (17.1)	29 (92.9)	2.68 [0.29;24.66]	0.343

Peaks in positivity rate were noted in January (13.3%) and June (25%), as seen in Figure 3.2. In January, the most positive cases were detected 8/13 (61.5%), compared to the other months.

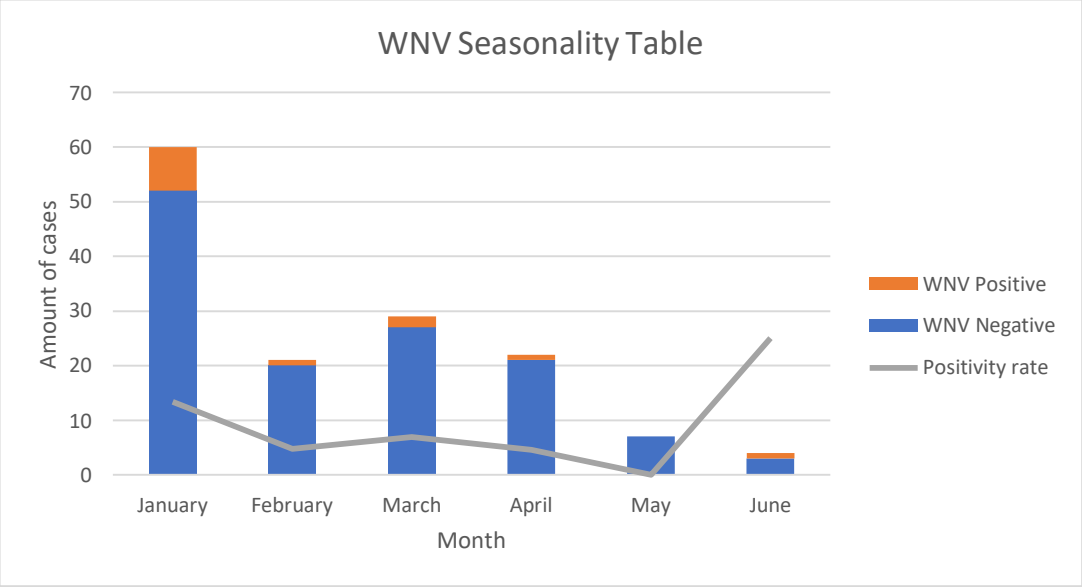

Figure 3.2: Graph showing the seasonality of WNV infection in South Africa. The graph shows the total amount of samples that tested negative (blue) and positive (orange) in the arbovirus season, January to June, as well as the positivity rate, indicated by the grey line.

To determine what symptoms were associated with WNV infection, the positive and negative samples, determined by the WNV IgM antibody outcome and confirmed with neutralisation assays, were compared. There was a statistically significant (p value < 0.05) association with headache (OR=4.3) and meningitis (OR=4.9). There was a weak association between rash, myalgia, fever, vomiting, fatigue, and drowsiness (Table 3.4). Human immunodeficiency virus (HIV) status did not affect the outcome of WNV infection (Table 3.3). Overall, 10/13 (68.5%) of patients that tested positive for WNV recovered fully at the time of the one-month follow-up, compared to 3/13 (31.5%) that are alive, but characterised as not doing well (Table 3.4). The patients presenting with more severe neurological symptoms including encephalitis, seizures, acute flaccid paralysis and meningitis, had a slower recovery. No fatalities were reported.

Table 3.5: Table summarising the symptoms reported. The table summarises the symptoms reported for the study group subjected to serological testing (n=143).

Symptoms experienced		WNV positive (N=13)	WNV negative (N=128)	Odds ratio [95% CI]	p-value
Febrile symptoms	Fever (≥38°C) (n=61)	2 (3.3%)	59 (96.7%)	0.2 [0.04;0.95]	0.024
	Chills (n=20)	2 (10%)	18 (90%)	1.13 [0.23;5.53]	0.57
Dermatological symptoms	Rash (n=10)	0 (0%)	10 (100%)	0 [undefined]	0.37
Neurological symptoms	Headache (n=54)	9 (16.7%)	45 (83.3%)	4.25 [1.24;14.56]	0.016
	Seizures (n=36)	1 (2.8%)	35 (97.2%)	0.22 [0.03;1.80]	0.11
	Convulsions (n=33)	3 (9.1%)	30 (89.9%)	1 [0.25;3.86]	0.62
	Myalgia (n=11)	0 (0%)	11 (100%)	0 [undefined]	0.336
	Fatigue (n=74)	3 (4.1%)	71 (95.9%)	0.24 [0.06;0.94]	0.028
	Drowsiness (n=1)	0 (0%)	1 (100%)	0 [undefined]	0.909
	Meningitis (n=50)	9 (18%)	41 (82%)	4.88 [1.42;16.78]	0.01
	Swollen lymph nodes (n=1)	0 (0%)	1 (100%)	0 [undefined]	0.454
	Sepsis (n=5)	0 (0%)	5 (100%)	0 [undefined]	0.308
	Arthralgia (n=9)	0 (0%)	9 (100%)	0 [undefined]	0.206
	Lethargic (n=7)	1 (14.3%)	6 (85.7%)	1.72 [0.19;15.51]	0.495
	Acute flaccid paralysis (n=18)	2 (11.1%)	16 (88.9%)	1.29 [0.26;6.38]	0.509
Gastrointestinal symptoms	Vomiting (n=26)	1 (3.8%)	25 (96.2%)	0.35 [0.04;2.82]	0.27
One month follow-up	Alive, not well (n=12)	3 (25%)	9 (75%)	4 [0.931;17.176]	0.047
	Fully recovered (n=98)	10 (10.2%)	88 (89.8%)	1.55 [0.405;5.945]	0.276
	Dead (n=5)	0 (0%)	5 (100%)	0 [undefined]	0.308

3.4 Discussion

Despite originating in Africa, limited data exist around the burden of WNV disease in humans on the African continent. Currently, no studies determining the demographic and socioeconomic risk factors for WNV infection in South Africa exist, nor a study examining a large group of hospitalised patients experiencing acute fever of unknown cause with or without neurological signs. In this study, specimens from hospitalised patients presenting with febrile disease, including neurological symptoms were collected from three sentinel sites in Mpumalanga and Gauteng during the arbovirus season in 2021 and a part of 2022. Detection of arboviruses using molecular assays, like RT-PCR, is possible; however, the viraemic period of flaviviruses specifically leaves a small window for detection (McVey et al., 2015). By combining molecular and serological assays, a better understanding of the incidence of WNV specifically could be obtained for January to June 2021-2022 in Mpumalanga and Gauteng, South Africa. One patient tested positive for WNV RNA using the meningo-chip but could not be confirmed with sequence information. Commercial ELISA testing; however, detected WNV specific IgM antibodies in several samples. This correlates with previously published research indicating that the end of viraemia coincides with the first appearance of IgM antibodies (Lustig et al., 2018). Molecular testing through PCR may be a suitable diagnostic tool during early infection, but after seroconversion has taken place, serological testing is more likely to correctly identify cases (Lustig, 2018). The WNV IgM positive samples were confirmed with neutralisation assays, which are seen as the gold standard, and ruled out any cross-reactivity between other flaviviruses. Based on the results obtained in this study, a positivity rate of 2.4 to 10.3% for WNV in 2021-2022 was determined from the three study sites. This suggest WNV contribute significantly (p value < 0.05) to AFDUC cases with neurological signs in hospitals in South Africa. It also suggests that 5-15 cases that are confirmed annually by the NICD is a significant underestimation of the true burden of disease in the country (Burt et al., 2002; Sule et al., 2018; Venter, 2018).

The discrepancy between the WNV IgM positive cases and the WNV positive neutralising antibody test could be explained by weak neutralisation of the samples or cross-reactivity. The samples that tested positive on the commercial kit, but negative with the neutralisation assay was subjected to neutralisation assays with other endemic flaviviruses, including WSLB, USUV, BANV, and BAGV, to rule out any cross-reactivity. None of the samples had neutralising antibodies against these viruses, which suggests either other flaviviruses are present or cross reaction to other viruses or the discrepancy is due to weak neutralisation of the antibodies that are present or that the neutralisation assay lacks sensitivity.

There were a lot more sample submissions in 2021 (87% of total) than in 2022 (13%),due to the ANDEMIA project coming to an end in April 2022. Even though a full report for 2022 could not be provided, it is still important to include the data for a better understanding of the incidence of WNV in South Africa. The positivity rate fluctuated between January and June (the arbovirus season), with January being statistically significantly (p value < 0.05) associated with WNV infection (61.5%) in both 2021 and 2022. Arbovirus seasons can differ drastically from year to year. A fellow ZARV member, Miss Caitin MacIntyre, did the surveillance for the first few years of the study (2018-2020), where she determined that March had the highest positivity rate for WNV infection in humans (MacIntyre, 2022). There is thus a correlation with the peak positivity in January compared to March, indicating the summer months are a higher risk for WNV infection. Seasonality of WNV infection in horses has also been studied and showed that the summer months (December to March) does have the highest WNV positivity (Venter, 2017). It has been noted that WNV incidence is seasonal and linked with warmer, temperate zones, with transmission increasing after heavy spring and summer rainfall (Gubler, 2007; Jupp, 2014). The majority of patients were enrolled in Gauteng, 233/325 (71.7%), over Mpumalanga, 92/325 (28.3%) (Table 3.1). A higher positivity rate was seen in Mpumalanga, 11/83 (13.3%) compared to Gauteng, 2/88 (2.3%) (Table 3.2). A possible explanation for the higher positivity rate in Mpumalanga, is that it is a more rural province with many patients having outdoor lifestyles, working on farms or in construction, bringing them into close contact with mosquito vectors, as well as a warmer climate resulting in a more favourable mosquito breeding site. Interestingly enough, more equine cases are identified in Gauteng, so it could suggest that the lifestyle of people living in more rural areas puts them at a higher risk for infection. The highest number of WNV infections, was seen in patients who are young adults (21-49), 6/13 (46.2%), followed by individuals between 1-5 years old, 4/13 (30.8%). This could be explained by young adults spending more time outside and working, which could bring them into close proximity to mosquito vectors, and young children being susceptible due to their weaker immune system. No linear trend was observed regarding age and susceptibility to WNV infection. For the years 2018-2020, the median age of patients were 4 years old, while the median age of patients for 2021-2022 were 5 years old.

The majority of samples submitted were plasma or serum samples, due to the invasive nature of CSF sampling. One CSF specimen (ZRUA1525/21) tested positive for WNV IgM antibodies and was confirmed with neutralisation assays, the other positive samples were plasma, 7/13 (53.9%) and serum, 5/13 (38.4%). In the early stages of acute WNV infection, IgM antibodies may be detectable in CSF, before it becomes detectable in serum

(Bakos et al., 2022).

In humans that develop symptoms, WNV is historically characterised by acute onset of fever, headache, malaise, gastrointestinal symptoms like vomiting and diarrhoea, and a rash (Hayes et al., 2005). In this study, the most observed symptom associated with WNV infection was headache, and meningitis.Less common symptoms reported was convulsions, and fatigue, With regards to HIV status of the patients, patients that tested positive were HIV positive, and not statistically significantly (p value > 0.05) associated with WNV infection. No fatalities were reported.

A big limitation of the study is the fact that there was such a significant difference in samples submitted in 2021 compared to 2022 due to the end of the study, which resulted in a small sample size for 2022. The small sample size could make it difficult to determine if a particular outcome is a true finding or not for 2022. These samples were therefore mainly used in combination with the 2021 cases to analyse the clinical presentations and disease association with other patient demographics. In some instances, especially when the patient was very young, a small volume of plasma, serum or CSF was available for testing, due to the invasiveness of obtaining the sample and could thus not be tested with the WNV IgM ELISA since molecular testing had preference. It has been reported that WNV IgM antibodies could persist for as long as three years post infection (Papa et al., 2015). With a follow-up sample, a rise in antibody titre would further confirm an acute infection, so any IgM positive result in patients should also be correlated with the clinical relevance of cases to determine if these are acute infections.

3.5 Conclusion

West Nile virus contributed to AFDUC cases in hospitalised patients between January and June in South Africa over 2021 and 2022. The association with neurological signs reported in this study, confirms the importance of WNV surveillance as well as the underestimation of cases. This study also underlines the value of IgM serology in diagnosing acute cases for arboviruses. Medical health practitioners need to be aware and familiar with zoonotic infections and how they present. Without proper treatment, a cure or WNV vaccines for prevention, vector control is the only way to limit infection.

Chapter 4 – Surveillance of West Nile Virus and Wesselsbron virus in animals with neurological signs in South Africa 2021-2022

4.1 Introduction

4.1.1 West Nile virus in horses

West Nile virus (WNV) continually circulates among mosquitoes and birds and infection has been reported in wild and domestic animals, including birds, reptiles, and mammals (McVey et al., 2015). West Nile virus is also associated with febrile disease, meningoencephalitis and even death in humans and horses (Steyn et al., 2019). Thedisease is maintained in a bird-mosquito-bird transmission cycle (McVey, 2015). Passeriformes are the most important order of avian hosts for WNV, and include northern cardinals, pigeons and house finches (Komar, 2001). Birds develop sufficient viraemia to infect mosquitoes, but not all birds present with symptoms (Petersen et al., 2013). There are several avian species in South Africa that do not develop clinical illness or mortality, possibly due to genetic resistance to WNV, and therefore can replicate the virus at extremely high levels (Jupp, 2001).

Horses are the most affected domestic animal, with 80% of infected horses being asymptomatic (Sule et al., 2018). With regards to the 20% developing symptoms, up to 90% of cases present with neurological signs and the disease has a mortality rate of 30% (Sule et al., 2018). Neurological signs include ataxia, paresis, or paralysis of the limbs, usually affecting the hind legs, recumbency, as well as tremors in the face and neck muscles (Castillo-Olivares and Wood, 2004). Treatment guidelines for horses presenting with clinical symptoms are based on symptom management – reducing central nervous system (CNS) inflammation, preventing self-inflicted injuries, and providing the necessary fluid and nutritional care (Long et al., 2002). West Nile virus has also been reported in several non-equine species including birds,crocodiles, wolves, cats, dogs, cattle, and sheep (Gould and Fikrig, 2004).

4.1.2 West Nile virus in animals in South Africa

Several studies have been done by the Zoonotic arbo- and respiratory virus (ZARV) research group, which investigated the seroprevalence of WNV in horses and non-equine animals in South Africa (Venter et al, 2017). The first study by Venter et al. (2017), investigated animals presenting with neurological symptoms between 2008-2015. West Nile virus was detected in 79/1069 (7.3%) of horses, 1/206 (0.5%) of wildlife and 2/132 (1.5%) of livestock (Venter et al., 2017). Co-infections with Middelburg virus (MIDV), African horse sickness virus (AHSV), Equine Encephalitis (EEV), Sindbis virus

(SINV) and Shuni virus (SHUV) were reported (Venter et al., 2017). Building onthis study, a paper was published by Bertram et al. (2020) that reported on WNV in horses between 2016-2017 in South Africa. In 2016, six positive WNV cases were reported, while 48 positive cases were reported in 2017 (Bertram et al., 2020). The increase in cases in 2017 was said to be due to optimal conditions for vector breeding, including high rainfall and very high temperatures recorded in South Africa (Bertram et al., 2020). Steyn et al. (2019) did a study in wildlife and non-equine animals between 2010-2018 to determine the incidence of WNV in South Africa during that time. A 1.8% (11/608) positivity rate was reported in animals including cattle (*Bos taurus*), buffalo (*Syncerus caffer*), a dog (*Canis lupus familiaris*), exotic fallow deer (*Dama dama*), giraffes (*Giraffa camelopardalis*), goats (*Capra aegogarus hircus*), a lion (*Panthera leo*), a sheep (*Ovis aries*) and roan antelope (*Hoppotragus equinus*) although it was much higher in individual species and only investigated by real-time reverse transcriptase polymerase chain reaction (RT-PCR) (Steyn et al., 2019). The data generated by these studies suggest that severe disease and neurological signs occur in horses, as well as other species, and these signs can be used for surveillance to help predict WNV outbreaks and predict spillover to human populations.

4.1.3 Wesselsbron virus in animals

Wesselsbron virus (WSLB) is an endemic flavivirus and is transmitted by *Aedes* mosquitoes to several species, including occasional spillover to humans (Weiss et al., 1956). The disease is therefore associated with heavy rainfall and flooding, and cases may be concurrent with and resemble RVF, resulting in cases being missed (Swanepoel, 1989).

Wesselsbron virus was first isolated from a decomposed lamb in the Wesselsbron district, South Africa in 1955 (Weiss et al., 1956). Since then, WSLB cases were reported throughout the African continent, where it infects a wide range of animals including sheep, goats, cattle, camels, and horses (Swanepoel, 1989). Sheep seems to be the most susceptible to WSLB infection with disease manifesting in adult sheep as asymptomatic or mild to moderate fever (Oymans et al., 2020). In newborn lambs, disease is more severe and can be fatal, while infected pregnant ewes can result in abortion or congenital malformations (Coetzer et al., 1978). Abortions and malformations are not common in goats and calves (Coetzer et al., 1978).

4.1.4 Wesselsbron virus in animals in South Africa

Looking at WSLB cases in South Africa after the first isolation in 1954, an isolation was made from a Cape short-eared gerbil (*Desmodillus auricularis)* in Southern Africa in 1960 (Kokernot et al., 1958; Diagne et al., 2017). Between 1993-1995, serum

samples were collected from free-living wild animals in South Africa and a study performed testing forWSLB antibodies (Barnard, 1997). Serological evidence was found in 15 species, including buffalo, zebras, and wildebeest (Barnard, 1997). The ZARV research group reported two WSLB cases in horses presenting with neurological disease, one case being fatal, in 2010 (Human, 2008). One case was from Pretoria West/Hartbeespoort area and the other from Stellenbosch in the Western Cape (Human, 2008). Surveillance of WSLB has been neglected over the last few decades and its importance unknown.

4.1.5 Diagnostic methods

Diagnostic methods for WNV and WSLB infection include detection of viral RNA using quantitative real-time RT-PCR (Lustig et al., 2016). Samples used for real-time RT-PCR includes RNA extracted from tissue samples, as well as whole blood (Lustiget al., 2016). Due to the short viraemic period of flaviviruses, cases can go undetected, which is why the combination of serological assays with molecular assays, is the optimal diagnostic method (McVey et al., 2015). There are commercial ELISA kits available for WNV, but not for WSLB. Due to the cross-reactivity of flaviviruses, the plaque reduction neutralisation test (PRNT) is seen as the gold standard and should be used to confirm serological results (Llorente et al., 2019). More about the cross-reactivity of flaviviruses and plaque reduction neutralization tests (PRNTs) can be found in Chapter 3 of this dissertation.

4.2 Materials and Methods

4.2.1 Ethics Approval

To conduct this study, ethics approval was granted by the University of Pretoria Animal Ethics Committee and the Faculty of Veterinary Sciences Research Ethics Committee - 181/2021 for MSc project ethics approval. The Department of Agriculture, Land Reform and Rural Development (DALRRD) approval had been obtained for testing of Centre for Viral Zoonosis (CVZ) samples under Section 20 approval. Annual reports of the cases detected by the CVZ were submitted to DALRRD. Veterinarians and owners involved gave consent to testing for arboviruses and were informed that any positive cases would be used for further analysis and research. Submission forms were completed by the veterinarians listing all symptoms and demographic details regarding the sample.

4.2.2 Sample Collection

Samples including central nervous system (CNS) tissue, visceral organs and ethylenediaminetetraacetic acid (EDTA) blood specimens from animals presentingwith neurological, febrile and/or respiratory signs or sudden unexpected

death (SUD), were submitted to the ZARV group at the CVZ, University of Pretoria (UP). This formed part of countrywide passive surveillance program for the detection of zoonotic arboviruses in animals. All samples were aliquoted into 1.5 mL microcentrifuge tubes and stored at -70°C until testing. Samples submitted to ZARV were assigned a Zoonotic Research Unit number (ZRU), for the purpose of in-house record keeping. In total, 338 samples were submitted between January 2021 and December 2022 from animals including horses,wildlife, and domestic animal species.

4.2.3 RNA Extraction

Animal blood were extracted using the Qiagen RNA Viral Mini Kit (Qiagen, Valencia, CA, USA) according to the manufacturer's instructions and eluting the RNA twice with a volume of 40 µL AVE buffer. All tissue specimens were processed separately regardless of being from thesame animal. The RNA extraction for all specimens were performed under biosafety level 3 (BSL3) conditions. Pieces of sample, approximately 30 mg, were randomly cut from differentparts of the individual organs and placed in lysis buffer with sterile glass beads (Merck, Kenilworth, New Jersey, USA). Samples were homogenised using the TissueLyzer™ (Qiagen, Valencia, CA, USA) for 3 minutes at 3000x*g*. Homogenised samples were then centrifuged for 10 minutes at 3000x*g* to collect debris. Ribonucleic acid (RNA) from tissue samples were extracted using the RNeasy kit (Qiagen, Valencia, CA, USA). Extraction was completed according to manufacturer's instructions and RNA eluted using a double elution of 40 µL of nuclease-free water.

4.2.4 Pan-flavi Real-time RT-Polymerase Chain Reaction

To test for flaviviruses, all specimens were subjected to nested pan-flavi real-time RT-PCR targeting the flavivirus genus (Refer to Table 2.2). Briefly, FU1 and 9317 primers was used in the SuperScript III with Platinum Taq RT- PCR kit (ThermoFisher Scientific, California, USA). The PCR reaction contained 0.5 µL of each primer (20 pmol), 12.5 µL of reverse transcription (RT) buffer, 1 µL of SuperScript™ RT/Platinum Taq™ mix enzyme, 0.5 µL nuclease free water (Ambion, ThermoFisher Scientific, California, USA) and 10 µL of template RNA. The first round of the PCR was cycled on a thermocycler (Applied Biosystems, ThermoFisher, Scientific, California, USA) at 50°C for 30 minutes, 94°C for 2 minutes, 35 cycles of 94°C for 15 seconds, 55°C for 30 seconds, 68°C for 1 minute, with a final elongation step of 68°C for 5 minutes.

For the second round of the pan-flavi PCR, each reaction is made up of 0.25 µL Flavi All S primer (40 µM), 0.25 µL Flavi All S2 primer (40 µM), 0.25 µL Flavi All AS4 primer (40 µM), 0.6 µL Flavi All Probe 3 mix (12 nM each) (Table 4.1), 12.5 µL Ag-Path reaction mix, 1 µL of Ag-Path enzyme mix, as well as 2 µL of the first-round product.

The reaction is run on the QuantStudio 3 Real-Time PCR System (ThermoFisher, Scientific, California, USA) at 50°C for 30 minutes, 95°C for 2 minutes, followed by 45 cycles of 95°C for 15 seconds and 58°C for 1 minute A non-template control (NTC) was included to serve as a negative control, as well as two positive controls, WNV and WSLB cultures. Samples that came up as positive on the panflavi real-time PCR were subjected to screening with the WSLB specific RT-PCR, described in Chapter 2, as confirmation assay.

Table 4.1: Pan-flavivirus RT-PCR primers and probes. A table showing the primer and probe sequences designed for the second round of the nested flavivirus RT-PCR

Target virus	Target gene	Assay	Primer/Probe name	Orientation	Primer/Probe sequence (5'-3')	Fragment size (nt)
Flavivirus	NS5	Pan-flavivirus real-time RT-PCR	Flavi All S	Sense	TACAACATGATGGGGAARAG AGARAA	243
			Flavi All S2	Sense	TACAACATGATGGGMAAACG YGARAA	
			Flavi All AS4	Antisense	GTGTCCCAGCCNGCKGTRTC RTC	
			Flavi All Probe 3 mix	Sense	FAM-TG+gTWYATGT+gGYTNG+gR GC-BBQ	
					FAM-CCGTGCCATATGGTATATGT GCTGGGAGC-BBQ	
					FAM-TTTCTGGAATTTGAAGCCCTG GGTTT-BBQ	

Degenerate bases: R = (A/G), W = (A/T), K = (T/G), Y = (C/T), N = (A/G/T/C). Locked nucleic acid bases are written as '+ G'. FAM: Fluorescein amidite

4.2.5 Agarose Gel Electrophoresis

The PCR reaction mixtures were analysed on a horizontal 2% (w/v) agarose gel made up of 3 grams (g) agarose powder (SeaKem, Lonza, Basel, Switzerland) and 150 mL of 1xTAE buffer (20 mM acetic acid, 100 mM EDTA, 40 mM Tris at pH 8.0) (Thermo Fisher Scientific, California, USA). Despite being able to confirm positive flaviviruses by real-time PCR alone, the products are analysed by gelelectrophoresis in order to detect any other flaviviruses missed by the panflavi probesand to use all PCR positive products for sequencing and phylogenetic analysis. The PCR products were electrophoresed at 120 volts (V) in 1xTAE buffer for 35-45 minutes. To allow for visualisation of the amplified PCR products on the BioRad Molecular Imager® Gel DOC™ X+ transilluminator (BioRad, California, USA), 0.5 µg/mL of SmartGlow™ DNA Strain was added to the agarose gel. A 100 bp DNA molecular marker (DNA molecular marker XIV, Roche, Mannheim, Germany) was included on the agarose gel to determine the size of the DNA amplicons, as well as the concentration. The gel was viewed using a BioRad Molecular Imager® Gel DOC™ X+ transilluminator

(BioRad, California, USA).

4.2.6 Sanger Sequencing and phylogenetic analysis

Amplicons of the correct size were purified using the Zymoclean Gel DNA Recovery Kit (Zymo Research, California, USA) and submitted for sanger sequencing. Briefly, gel slices were dissolved in 400 µL of agarose binding buffer at 55°C for 10-15 minutes, until completely dissolved. The DNA was eluted following a series of spin and wash steps by adding between 6-15 µL of elution buffer. Sanger sequencing was outsourced to Inqaba Biotech™. Sequencing files received from Inqaba were edited using CLC main workbench version 8.0.1 (CLC Bio, Aarhus, Denmark, available from hhtps://www.qiagenbioinformatics.com). Multiple sequence alignments were done using Multiple Alignment using Fast Fourier Transform (MAFFT) (v7) (http://mafft.cbrc.jp/alignment/server/index.html) and Molecular Evolutionary Genetics Analysis (MEGA) software 6.06 was used to assemble concatenated sequences. Reference sequences from the flavivirus genus were selected based on the gene segment and downloaded from GenBank. The maximum likelihood tree was constructed using MEGA-X using 1000 bootstrap replicates. The number of nucleotide differences between sequences of each virus was determined using pairwise distance analysis with 1000 bootstrap replicates.

4.2.7 Serological testing (WNV IgM InBios Equine ELISA)

A commercial WNV IgM ELISA kit is available for equines (InBios, Seattle, Washington, USA) and was used to screen for IgM antibodies making use of plasma or serum samples. The ELISA was performed based on manufacturer's instructions with a positive and negative control provided in the kit. Briefly, test sera and controls were diluted 1:100 using the provided sample dilution buffer, using at least 4 µL of the unknown serum samples and controls. Next 50 µL of the diluted sera and controls were added in duplicate to the wells. The plate was incubated at 37°C for 1 hour in a non-humidified chamber. Following the incubation, the plate was washed six times with an automatic plate washer using 300 µL of the 1X wash buffer per well. Subsequently, 50 µL of ready to use West Nile recombinant antigen (WNRA) was added to duplicate 1 of the respective sera, while 50 µL of normal cell antigen (NCA) was added to duplicate 2 of the respective sera. The plate was incubated for 16-20 hours at 2-8°C. After the incubation, the wash step was repeated. Next, 50 µL of ready to use enzyme conjugate-horse radish peroxidase (HRP) was added to all wells. The plate was incubated for 1 hour at 37°C in a non-humidified chamber (Series 2000, Scientific Engineering, Johannesburg, South Africa). The wash step was repeated.

After the wash step, 150 µL of EnWash solution was added to all wells and the plate incubated for 5 minutes at room temperature (20-22°C). The wash step was repeated. Next, 75 µL of liquid 3,3',5,5'- tetramethylbenzidine (TMB) substrate was added to all wells and the plate incubatedat room temperature in darkness for 10 minutes. Lastly, 50 µL of stop solution was added to the plate and incubated at room temperature for 1 minute. The optical density(OD) values were read at 450 nm using the Mindray MR-96A microplate reader (Mindray, Hong Kong, China). To compute the WNRA/NCA ratio, immune status ratio (ISR), the OD value for duplicate 1 with WNRA was divided by the OD value for duplicate 2 with NCA. Specimens with an ISR of ≥ 3 were considered positive, and those with an ISR of ≤ 2 were considered negative as defined by the kit. Specimens with an ISR of < 3.0 but > 2.0 were considered borderline but possible positives.

4.2.8 Neutralisation assay

All equine samples that were tested with the WNV IgM InBios commercial ELISA, were subjected to neutralisation assays to confirm presence/lack of of WNV neutralising antibodies. This was done as described in chapter 3 (see virus culture, virus titration and neutralisation assays) to ensure that true positives are used in the analyses. Since no IgM ELISA was available for WSLB virus we screened 50% of horses submitted in 2022 during the arbovirus season with serum neutralization assays to determine if more cases may have occurred. In total, 5 specimens were selected from each month from all provinces in South Africa, resulting in 30 samples subjected to neutralisation assays.

Livestock samples from animals with neurological signs that tested negative by flavivirus RT-PCR, submitted to the ZARV group between 2012-2022 were subjected to screening with neutralization assays to determine whether any of these samples had neutralizing antibodies against WSLB. Briefly, all plasma or serum samples were confirmed using a WSLB specific virus neutralization test with 10^5 TCID50U/mL of WSLB culture (AV259, accession number JN226796, passage 4) as previously described (Swanepoel, 1976). Samples were read at dilutions of 1:8-1:32.

4.2.9 Data analysis

Data analysis was carried out in EpiInfo™ (version 7.2.4.0) using Fisher's exact test with a 95% confidence interval (CI) and odd ratios (ORs). All data were reported using tables and graphs. A p value of < 0.05 is regarded as significant.

4.3 Results

Between 2021 and 2022, 338 samples (197 from 2021 and 141 from 2022) from animals showing clinical signs were submitted to the ZARV group from veterinarians all over the country. These samples were taken from equines, 231/338 (68.3%) and wildlife, avian, livestock and domestic animals 107/338 (31.7%) (Table 4.2). The majority of the samples submitted were whole blood, 244/347 (70.3%), while visceral organs, 103/347 (29.7%) were received from animals that were either found dead or euthanised (Table 4.2).

Table 4.2: Table summarising the sample submission for 2021 and 2022. The table summarises the total amount of samples submitted between January and December from all over South Africa, as well as what types of samples they were (whole blood or visceral organs).

	Equines		Non-equines		Total
Collection year	2021	2022	2021	2022	
Samples submitted between January to December (n=x)	120 (51.9%)	111 (48.1%)	77 (72.0%)	30 (28.0%)	338
Sample type					
Whole blood	106* (85.5%)	99 (84.6%)	32 (43.2%)	7 (21.9%)	244 (70.3%)
Visceral organs	18 (14.5%)	18 (15.4%)	42 (56.8%)	25 (78.1%)	103 (29.7%)
Total specimens submitted	124	117	74	32	347

**Percentage in brackets refers to sample type/total specimens submitted*

The majority of the samples submitted came from the Gauteng province in South Africa, followed by the Western Cape and KwaZulu-Natal (Figure 4.1). The highest positivity rate for flaviviruses, WNV and WSLB, was observed in KwaZulu-Natal, 6/56 (10.7%),with Gauteng having the second highest number of positive cases, 6/103 (5.8%) and the Western Cape, 1/72 (1.4%) (Figure 4.1).

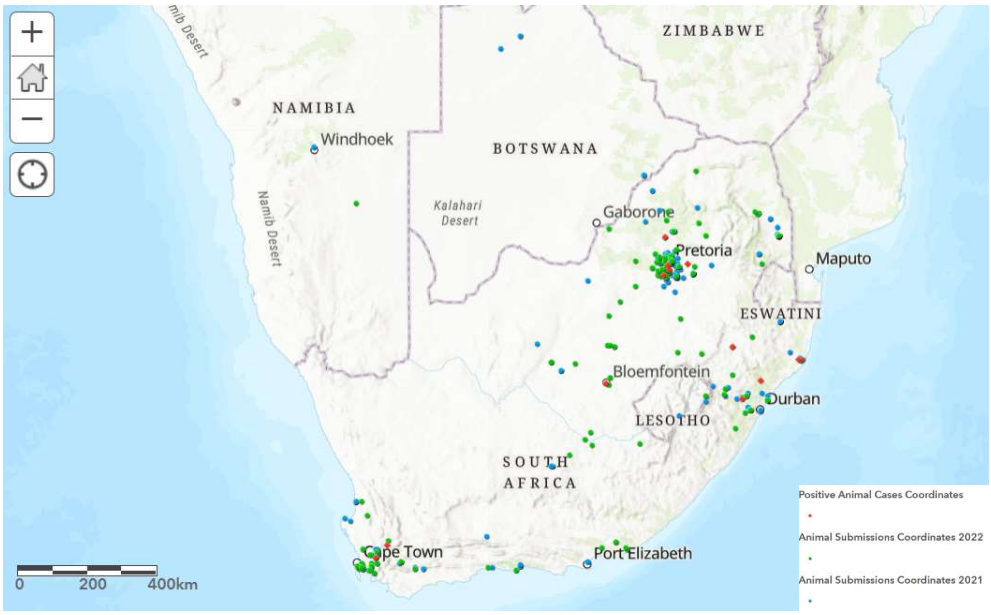

Figure 4.1: Map showing sample submission. The map of South Africa shows the coordinates of the sample submissions for 2021 (green) and 2022 (blue). Samples that tested positive for WNV or WSLB are indicated in red. Map was created using Arcgis.

4.3.1 Flavivirus RT-PCR results in non-equines

The majority of non-equine samples were submitted in 2021, 77/107 (72.0%), with only 30/107 (28.0%) samples were submitted in 2022 (Table 4.3). No RT-PCR positive WNV were detected in these samples, with one avian sample testing positive for WSLB in March 2022.

Table 4.3: Table summarising the results of testing for non-equine and equine samples. The table summarises the samples enrolled in 2021-2022, and what their results were when tested with the pan-flavi real time RT-PCR.

Real-time RT-PCR results	2021		2022	
	Non-equines	Equines	Non-equines	Equines
Total samples submitted	77	120	30	111
West Nile Virus				
Positive	0 (0%)	0 (0%)	0 (0%)	1 (0.9%)
Negative	77 (100%)	120 (0%)	30 (100%)	110 (99.1%)
Wesselsbron virus				
Positive	0 (0%)	0 (0%)	1 (3.33%)	1 (0.9%)
Negative	77 (100%)	120 (100%)	29 (96.67%)	110 (99.1%)

The main clinical signs reported for the specimens submitted, was neurological, reporting signs like ataxia, paresis and recumbency, with majority of the animals euthanised due to severe disease. The only flavivirus positive case detected using real-time RT-PCR in the non-equine group, was from an avian sample. The sample of a female toucan was submitted from Bromhof, Johannesburg and reported signs like ataxia, head tilt and seizures. The toucan was euthanised, and a brain sample submitted for testing. No co-infection was reported. We did not investigate the association between positivity and disease as there were too few cases.

The clinical signs that were reported for all equine submissions were mostly neurological signs including ataxia, paresis, seizures, icterus and recumbency. The WNV positive horse (ZRU175/22) was a pregnant mare, specifically a Boerperd, from the Onderstepoort area, Gauteng. During labour, the mare had a prolapsed distal colon through the rectum and had to be euthanised. The foal was cut out, but grossly deformed with arthrogryposis and suspected spina bifida and ultimately had to be euthanised as well. Specimens for the foal was not submitted for testing. The WSLB positive horse (ZRU091/22) was a thoroughbred stallion from Dundee, KwaZulu-Natal. The horse had a fever of 38°C and presented with signs like ataxia, anorexia, mild icterus, unilateral blindness, head was shaking, twitching and was uncoordinated when trying to move. The horse was treated symptomatically with vitamin B1 and D, as well as Depomycin and corticosteroids, which resulted in the horse surviving. A follow-up sample was sent two weeks later; the horse was still alive, but no update on its condition has been received.

4.3.2 Phylogenetic analysis of the WNV and WSLB positive cases

Sanger sequencing was successful on the PCR products of the three cases that tested positive by real-time RT-PCR. For the two WSLB cases, a 240 bp sequence read was obtained for each sample, whilst for the WNV case, only a 100 bp sequence read could be obtained, even after a nested PCR was performed. Two separate trees were constructed for the WSLB and WNV cases. Figure 4.2 shows the WNV phylogenetic tree and table 4.4 shows the p-distance values, while Figure 4.3 shows the WSLB phylogenetic tree and table 4.5 shows the p-distance values.

Figure 4.2: Evolutionary analysis by maximum likelihood method for the WNV positive sample. The maximum likelihood tree was constructed using Mega X. The bar scale indicates 0.05 nucleotide substitutions per site. Estimates were based on bootstrap values carried out with 1000 replicates. Only values of >50 are shown. West Nile virus strains from lineage 1 and lineage 2 were identified and obtained from GenBank. There were a total of 100 positions in the final dataset.

Table 4.4: Estimates of evolutionary divergence between sequences. P-distances between pairs of sequences are shown. Analyses were conducted using the Kimura 2-parameter model. This analysis involved 16 nucleotide sequences. There was a total of 100 nucleotides in the final dataset. Evolutionary analyses were conducted in MEGA X

	% Similarity
	ZRU175_22
NC_009942_1_West_Nile_virus_lineage_1_complete_genome	68.17
EU249803_1_West_Nile_virus_strain_68856_complete_genome	65.95
KT163243_1_West_Nile_virus_isolate_68856-ICDC-4_complete_genome	65.95
EF429197_1_West_Nile_virus_SPU116/89_complete_genome	94.35
KF179639_1_West_Nile_virus_strain_Greece/2012/Kavala/39_1_complete_genome	91.07
KM203861_1_West_Nile_virus_strain_Cz_13-329_complete_genome	91.10
KM659876_1_West_Nile_virus_strain_BD-AUT_complete_genome	91.91
KF647248_1_West_Nile_virus_strain_Italy/2013/Rovigo/34_1_complete_genome	92.72
KP789954_1_West_Nile_virus_strain_Italy/2014/Cremona2_complete_genome	92.72
KM203860_1_West_Nile_virus_strain_Cz_13-104_complete_genome	92.72
KP789956_1_West_Nile_virus_strain_Italy/2014/Verona/35_2_complete_genome	92.72
KX375812_1_West_Nile_virus_isolate_Novi_Sad_24/2013_polyprotein_gene_complete_cds	92.72
KM203863_1_West_Nile_virus_strain_Cz_13-502_complete_genome	92.72
KT207792_1_West_Nile_virus_isolate_1270/14_complete_genome	92.72
OM037672_1_West_Nile_virus_isolate_Spain/2020/Northern_goshawk/AC923_complete_genome	92.72
HQ537483_1_West_Nile_virus_isolate_Nea_Santa-Greece-2010_complete_genome	92.72
KP789958_1_West_Nile_virus_strain_Italy/2014/Pavia5_complete_genome	91.90
NC_001563_2_West_Nile_virus_lineage_2_complete_genome	93.51
EF429199_1_West_Nile_virus_SA381/00_complete_genome	91.73
KT207791_1_West_Nile_virus_isolate_792/14_complete_genome	90.14
EF429200_1_West_Nile_virus_H442_complete_genome	91.85
KM052152_1_West_Nile_virus_isolate_349/77_polyprotein_gene_complete_cds	91.85
EF429198_1_West_Nile_virus_SA93/01_complete_genome	91.63
JN393308_1_West_Nile_virus_strain_HS101_08_complete_genome	95.99
M18370_1_Japanese_encephalitis_virus_strain_JaOArS982_complete_genome	51.48
JN226796_1_Wesselsbron_virus_from_South_Africa_complete_genome	50.94

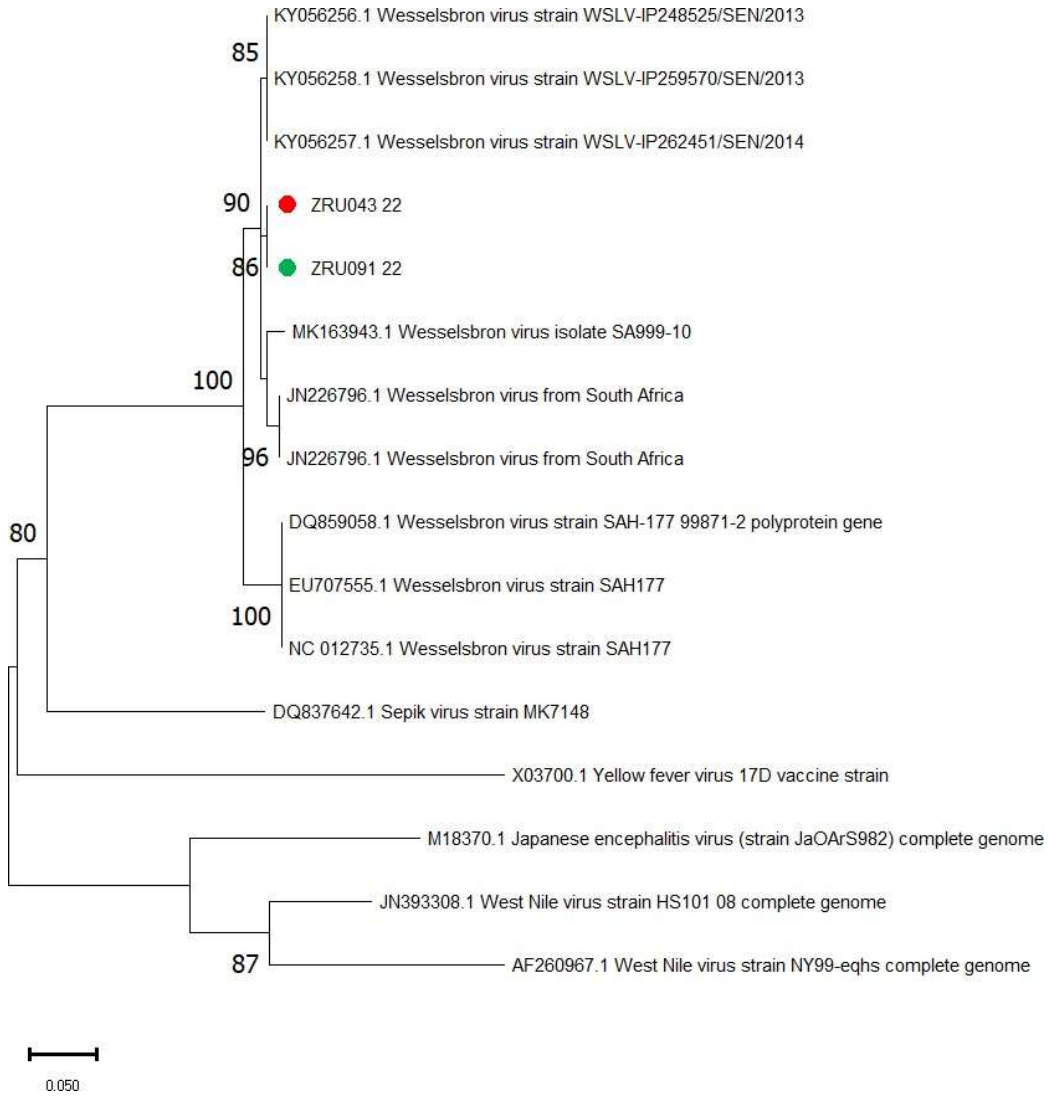

Figure 4.3: Evolutionary analysis by maximum likelihood method for the WSLB positive samples. The evolutionary history was inferred by using the maximum likelihood method and Kimura 2-parameter model. The tree with the highest log likelihood (-1143.33) is shown. The percentage of trees in which the associated taxa clustered together is shown next to the branches. Initial tree(s) for the heuristic search were obtained automatically by applying Neighbour-Join and BioNJ algorithms to a matrix of pairwise distances estimated using the maximum composite likelihood (MCL) approach, and then selecting the topology with superior log likelihood value. The rate variation model allowed for some sites to be evolutionarily invariable ([+*I*], 26.2% sites). The tree is drawn to scale, with branch lengths measured in the number of substitutions per site. This analysis involved 16 nucleotide sequences. There were a total of 221 positions in the final dataset. Evolutionary analyses were conducted in MEGA X.

Table 4.5: Estimates of Evolutionary Divergence between Sequences. The number of base substitutions per site from between sequences are shown. Analyses were conducted using the Maximum Composite Likelihood model. This analysis involved 16 nucleotide sequences. Codon positions included were 1st+2nd+3rd+Noncoding. All ambiguous positions were removed for each sequence pair (pairwise deletion option). There was a total of 221 positions in the final dataset. Evolutionary analyses were conducted in MEGA X.

	Similarity (%)	
	ZRU043_22	**ZRU091_22**
JN226796.1_Wesselsbron_virus_from_South_Africa_complete_genome	99,25	99,25
KY056256.1_Wesselsbron_virus_strain_WSLV-IP248525/SEN/2013_complete_genome	99,63	99,63
KY056258.1_Wesselsbron_virus_strain_WSLV-IP259570/SEN/2013_complete_genome	99,63	99,63
KY056257.1_Wesselsbron_virus_strain_WSLV-IP262451/SEN/2014_complete_genome	99,63	99,63
MK163943.1_Wesselsbron_virus_isolate_SA999-10_complete_genome	99,06	99,06
DQ859058.1_Wesselsbron_virus_strain_SAH-177_99871-2_polyprotein_gene_complete_cds	98,11	98,11
EU707555.1_Wesselsbron_virus_strain_SAH177_complete_genome	98,11	98,11
DQ837642.1_Sepik_virus_strain_MK7148_complete_genome	89,12	89,12
X03700.1_Yellow_fever_virus_complete_genome_17D_vaccine_strain	84,97	84,97
M18370.1_Japanese_encephalitis_virus_(strain_JaOArS982)_complete_genome	86,6	86,6
JN393308.1_West_Nile_virus_strain_HS101_08_complete_genome	87,55	87,55
AF260967.1_West_Nile_virus_strain_NY99-eqhs_complete_genome	84,18	84,18

Phylogenetic analysis of the partial NS5 gene for WNV (nucleotides (nt) = 100) clustered the positive WNV equine case (ZRU175/22) to previously identified lineage 2 strains identified in animals and humans. The identified lineage 2 strain in the equine sample (ZRU175/22) shows a nucleotide similarity of between 95.99% to the South African lineage 2 strain, HS101/08, isolated from the brain of a fatal encephalitic horse in Gauteng (Table 4.4).

With regards to the two WSLB samples, phylogenetic analysis of the NS5 gene (nt =221) clustered the positive cases (ZRU043/22 and ZRU091/22) between South African strain and the WSLV-IP248525/SEN/2013 strain from Senegal, with a similarity of 99.25% and 99.63% respectively (Table 4.5). The two samples were also confirmed with the TaqMan WSLB specific real-time RT-PCR, described in Chapter 2.

4.3.3 Investigation of WNV and WSLB in livestock through neutralisation assays

With regards to serological testing of non-equine specimens, neutralisation assays were performed on livestock samples from 2012-2022 to determine whether these samples have neutralising antibodies against WNV or WSLB to use in the validation of bovine IgM ELISAs in a later chapter. A total of 139 livestock samples from animals presenting with neurological signs were submitted over the last ten years, with 29/139 being plasma samples. Only 23/29 plasma samples were available for screening and the results can be seen in Appendix Table A4. For WNV, 7/139 (5.04%) livestock samples had neutralising antibodies against WNV, while 7/139 (5.04%) livestock samples had neutralising antibodies against WSLB. There were two samples that tested positive for WNV/WSLB neutralising antibodies. The WSLB positive samples had low neutralising ability, which could be due to a previous infection or vaccination.

With regards to the livestock samples that had WNV neutralising antibodies, clinical signs like fever, ataxia, recumbency and nasal discharge was reported, while samples positive for WSLB neutralising antibodies reported signs like recumbency, seizures, abortions in ovines, and anaemia. There were two samples that had neutralizing antibodies for both WNV and WSLB. The one sample (ZRU109/22) was an ovine sample that presented with clinical signs including recumbency and an abortion. The other sample (ZRU181/12/1) was a bovine, specifically a Bonsmara cow, that had fever and nasal discharge.

4.3.4 Serological results (IgM and neutralisation positive cases in horses)

In 2021, 77/120 (64.2%) equine samples submitted were tested with the kit with 10/77 (13.0%) testing positive for WNV IgM antibodies and 9/10 (90%) of the positives confirmed with neutralisation assays (Table 4.6). In 2022, 89/111 (80.2%) of the equine samples submitted were tested with the commercial kit. In total only 2/89 (2.5%) tested positive for WNV IgM antibodies and only 1/2 (50%) positive was confirmed with neutralisation assays (Table 4.6). Over the two years, 10/166 samples subjected to serological testing, were positive for WNV IgM antibodies. A positivity rate of 11.7% (9/77) was obtained for 2021 and 1.1% (1/89) for 2022.

With the positive real-time RT-PCR WSLB case detected in an equine in 2022, it was decided to perform neutralisation assays on the equine samples submitted during the arbovirus season (January to June) in 2022 to determine if any other equine samples have been missed. In total, there were 60 equine specimens submitted between January to June in 2022, but five specimens from each month were selected across all provinces in South Africa. Thus, 30/60 equine specimens were screened with neutralisation assays, with 0/30 (0%) having neutralising antibodies against WSLB.

Table 4.6: Table summarising the results of serological testing. The table summarises the equine samples enrolled in 2021-2022 and what their results were when tested with the WNV IgM commercial ELISA kit, as well as neutralisation assay.

	Equines	
	2021	2022
Total samples submitted	120	111
WNV IgM tested	77 (64.2%)	89 (80.2%)
Positive (%)	10 (13.0%)	2 (2.5%)
Negative (%)	67 (87.0%)	86 (96.6%)
Bordeline (%)	0	1 (1.1%)
Micro-neutralization assay	10	2
Positive (%)	9 (90%)	1 (50%)
Negative (%)	1 (10%)	1 (50%)

4.3.5 Seasonality of WNV and WSLB in animals

There were two WSLB positive cases in 2022. The last reported cases of WSLB in this surveillance program was detected in horses in 2010 suggesting that it is relative rare relative to WNV. The toucan tested positive in March, 1/70 (1.4%) and the horse from KwaZulu-Natal tested positive in May 2022, 1/58 (1.7%). There were no positive cases in 2021 (Figure 4.4).

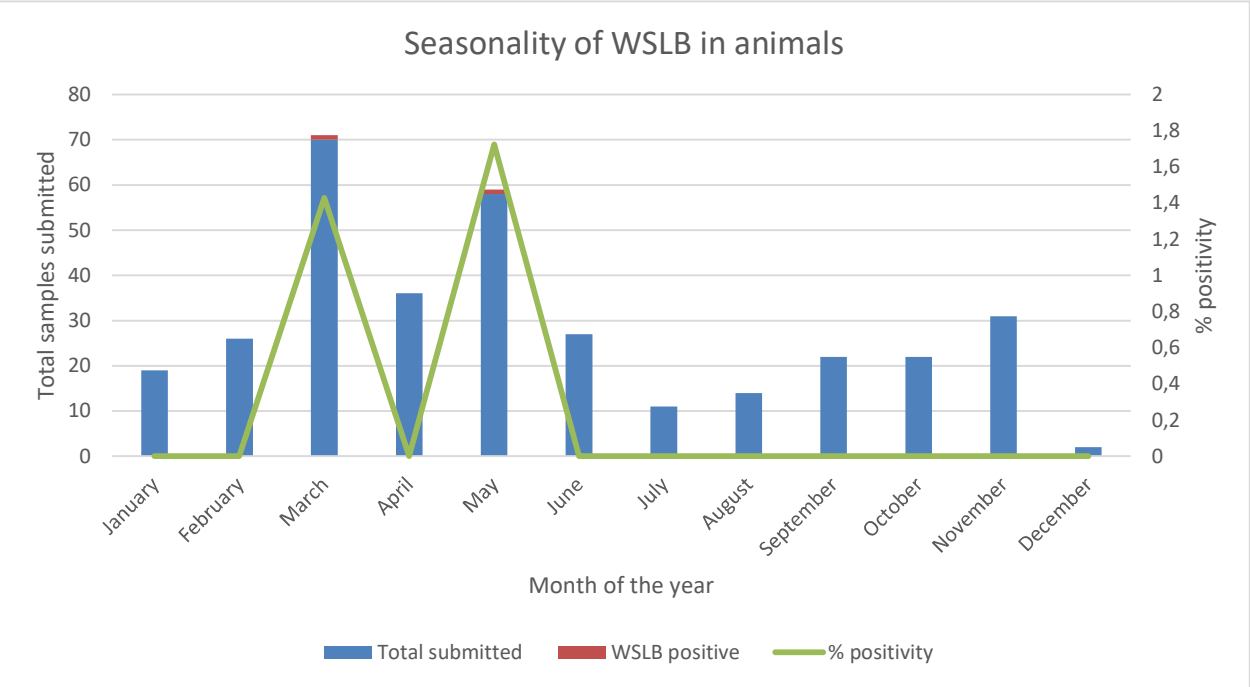

Figure 4.4: Graph showing the seasonality of WSLB infection in South Africa in animals using RT-PCR testing. The graph shows the total amount of specimens submitted that tested negative (blue) and positive (red) for WSLB in 2021-2022, as well as the positivity rate, indicated by the green line.

Looking at the seasonality of the WNV molecular and serology cases, peak positivity rates were observed in January (12.5%) and September (20%), as seen in Figure 4.5. March reported the highest number of positive cases, 3/32 over the surveillance period, compared to the other months. Positive cases were identified in months outside of the arbovirus season, indicating that WNV infections fluctuates depending on the rainfall and temperature. In 2021, there were ten positive cases compared to the two positive cases in 2022, resulting in a higher incidence of WNV in 2021 by nearly 80%.

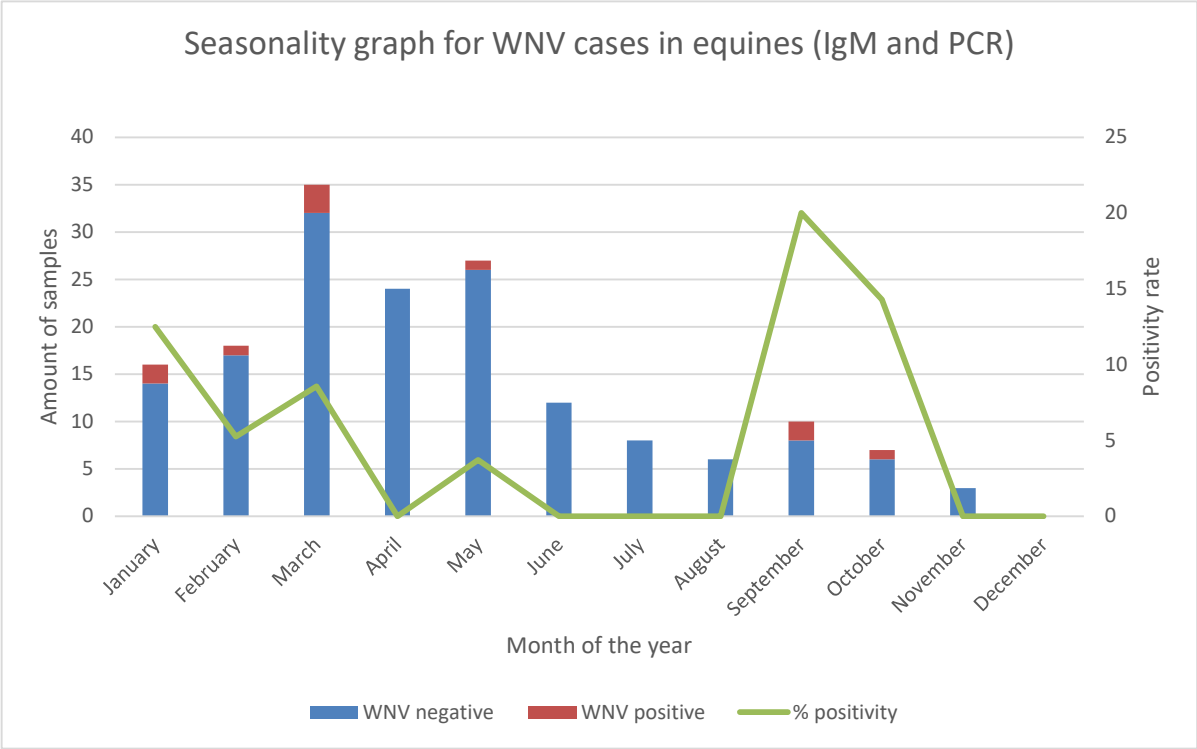

Figure 4.5: Graph showing the seasonality of WNV infection in South Africa in equines using RT-PCR and serological testing. The graph shows the total amount of equine samples that tested negative (blue) and positive (red) in 2021-2022, as well as the positivity rate, indicated by the green line.

4.3.6 Clinical analysis of WNV positive cases

Only samples that tested WNV IgM positive and confirmed via neutralisation assay are considered true positives. Looking at the clinical signs recorded, 7/10 (70%) of WNV positive horses were febrile, while 100% displayed neurological signs and no fatalities reported (Table 4.8). West Nile virus positive associated signs included ataxia (OR=3.704), blindness (OR=3.356) and seizures (OR=17.222) reported in two horses (Table 4.8). However, due to the low number of positive cases identified, none of the associations were statistically significant. Overall, neurological signs are a strong predictor of WNV positivity, while fever is a weak predictor. With regards to the vaccination status of the equine samples submitted, 10/10 (100%) of WNV positive horses were unvaccinated (Table 4.7). Only 17/166 (10.2%) of the total samples received were vaccinated with all 17/17 (100%) testing negative for WNV IgM antibodies (Table 4.7).

Table 4.7: Table summarising the vaccination status of equines subjected to serological testing. The table summarises the equine samples enrolled in 2021-2022 and what their vaccination status and WNV IgM ELISA outcome was.

Vaccination status	WNV positive (N=10)	WNV negative (N=156)	Odds ratio [% CI]	p-value
Vaccinated (n=17)	0 (0%)	17 (10.89%)	0 [Undefined]	0.164
Unvaccinated (n=139)	10 (100%)	129 (82.69%)	Undefined	0.080
Unknown (n=10)	0 (0%)	10 (6.42%)	0 [Undefined]	0.263

Table 4.8: Table summarising the clinical signs reported for the equine samples subjected to serological testing. The table summarises the symptoms reported for the equine samples subjected to testing with the commercial WNV IgM Equine ELISA kit (n=166).

Clinical Sign		WNV positive (N=10)	WNV negative (N=156)	Odds Ratio [95% CI]	p-value
Main sign	Fever (n=90)	7 (70%)	148 (94.9%)	2.05 [0.511; 8.228]	0.163
	Neurological signs (n=118)	10 (100%)	146 (93.6%)	Undefined	0.015
Signs reported	Ataxia (n=89)	8 (80%)	148 (94.9%)	3.704 [0.762; 17.999]	0.047
	Paralysis (n=12)	1 (10%)	155 (99.4%)	1.465 [0.169; 12.637]	0.347
	Hind leg paralysis (n=13)	1 (10%)	155 (99.4%)	1.333 [0.156; 11.427]	0.373
	Paresis (n=12)	1 (10%)	155 (99.4%)	1.464 [-0.169; 12.637]	0.347
	Tongue paralysis (n=4)	0 (0%)	156 (100%)	0 [Undefined]	0.389
	Recumbency (n=22)	1 (1%)	155 (99.4%)	0.714 [0.086; 5.930]	0.419
	Dyspnoea (n=7)	0 (0%)	156 (100%)	0 [Undefined]	0.321
	Haemorrhage (n=5)	0 (0%	156 (100%)	0 [Undefined]	0.365
	Blindness (n=6)	1 (10%)	155 (99.4%)	3.356 [0.354; 31.835]	0.179
	Icterus (n=26)	2 (20%)	154 (98.7%)	1.375 [0.275; 6.874]	0.338
	Seizure (n=2)	1 (10%)	155 (99.4%)	17.222 [0.994; 298.379]	0.060
Outcome	Alive (n=151)	10 (100%)	146 (93.6%)	Undefined	0.189
	Euthanized (n=15)	0 (0%)	156 (100%)	0 [Undefined]	0.189

4.4 Discussion

In the study, 338 samples received from animals presenting with febrile and/or neurological signs were submitted through the veterinary network in South Africa over the 2021-2022 period. All samples submitted were tested for flaviviruses using a genus specific PCR, which detected two flaviviruses of interest, WNV and WSLB. Due to the short viraemic period of flaviviruses, a combination of molecular and a commercial serological assay was used to test for WNV to ensure that no cases go undetected. To determine if WNV and WSLB infections may contribute to neurological cases in livestock we also screened these animals by VNT. Livestock specimens submitted to the ZARV group between 2012-2022 were screened with neutralisation assays against WNV and WSLB to determine if any of these specimens had antibodies against these flaviviruses to obtain a pool of positive and negative cattle sera for validation of a bovine ELISA in a later chapter. With regards to the livestock samples that had WNV neutralising antibodies, clinical signs like fever, ataxia, recumbency and nasal discharge was reported, while samples positive for WSLB neutralising antibodies reported signs like recumbency, seizures, abortions in ovines, and anaemia.

Unfortunately, a commercial WSLB ELISA assay is not available for equines. Equine samples submitted during the arbovirus season in 2022 were subjected to neutralisation assays to determine whether any have neutralising antibodies against WSLB. In total, 30/60 specimens submitted during the January to June period were subjected for testing, with no samples having neutralising antibodies against WSLB. All positive WNV IgM results were confirmed with neutralisation assays, to rule out cross reactivity to other flaviviruses and confirm the presence of neutralising antibodies.

There were more samples submitted in 2021 (197/338) than in 2022 (141/338). The majority of the sample submissions were from the Gauteng province, 103/338 (30.5%) in South Africa. For KwaZulu-Natal, 56/338 (16.6%) samples were submitted with 6/56 (10.7%) tested positive for WNV. KwaZulu-Natal has a warmer, temperate climate, which provides the ideal conditions for mosquito breeding sites, resulting in higher risk of virus transmission (Gbenga et al., 2016). The type of samples submitted were mostly whole blood (70.3%) and tissue samples (29.7%), which included brain, spleen, liver, and lung from equines, livestock, and domestic animals. Only plasma or serum specimens can be subjected to serological testing.

Two WSLB positive cases were detected by PCR, a horse, and a toucan from a private birdpark in Johannesburg. The toucan presented with ataxia, head tilt and seizures and

was euthanised, while the equine recovered from signs reported like ataxia, head shaking, twitching, uncoordinated and reluctance to move. To our knowledge it is the first time that WSLB was described in birds with neurological signs in South Africa. The toucan was an exotic bird to South Africa and could potentially be more sensitive to neurological signs that endemic birds. The NS5 region of the virus was sequenced, and a phylogenetic tree constructed to determine the virus strain of these infections. The toucan and equine sample clustered together with no nucleotide differences across the 240 bp region sequences. This formed a monophyletic group with sister groups with good agreement formed by other strains isolated from South Africa and Senegal. Similarity between the two new sequences was 99.25% with the South African 999 strain (NICD, 2018) and 99.63% with the Senegal isolate (WSLV-IP248525/SEN/2013). This is therefore suggestive of the emergence of a unique WSLB isolate in 2022 in South Africa. However, it is important to note that only 260 bp were sequenced and thus sequencing of the full genome would provide more information on the strain and should be followed up on. This raised the question if cases are missed due to low vireamia similar to WNV. To address this, we screened horses and cattle samples by VTN. For equines, 0/30 (0%) had neutralising antibodies against WSLB, while 7/139 (5.0%) of livestock samples had neutralising antibodies against WSLB. These samples will be used in the next chapters to set up a WSLB IgM ELISA.

During the two-year surveillance period, 1/231 (0.4%) equine samples received, tested positive for WNV with real-time RT-PCR, with 12/166 equine samples subjected to testing with the commercial WNV IgM ELISA testing positive for WNV, but only 10/12 confirmed as positive with the virus neutralisation assay, resulting in a positivity rate of 11.7% for 2021 and 1.1% for 2022. The PCR positive case did not have IgM neutralising antibodies. This correlates with previous studies published reporting 5-20 positive WNV cases in South Africa, annually in horses, with an average of 3-11% positivity per year (Venter et al., 2017). There is not a big difference between the number of positive samples obtained through using the commercial serological assay and confirmed with neutralisation assay (10/12, 83.3%), which could indicate a highly sensitive and specific ELISA test from InBios. The two samples that did not have neutralising antibodies against WNV, could be due to low levels of neutralising antibodies or cross-reactivity with other flaviviruses on the ELISA.

The majority of equine samples submitted presented with neurological signs or were euthanised, resulting in a small number of positive samples, which could create a bias in the study. Using serological testing, 10/166 positive cases were confirmed from plasma

samples, while the positive molecular case (ZRU175/22) came from lung, brain and spleen tissue submitted, with the brain specimen testing positive. Due to only receiving tissue samples, serology could not be performed on ZRU175/22. Sequencing the NS5 region of the WNV positive RT-PCR sample, only a short region (100 bp) could be amplified, and the sample clustered with the WNV HS101/08 strain. The nucleotide group mean distance for the positive equine sample (ZRU175/22) was 95.99% with the WNV HS101/08 South African strain.

The clinical signs generally reported in positive WNV horses, include fever, hind leg paralysis, muscle fasciculation, staggering, weakness and difficulty eating or drinking. In this study, the most observed symptom associated with WNV infection was ataxia, 8/10 (80%), and icterus, 2/10 (20%), with paralysis, paresis, recumbency, blindness and seizures being reported in 1/10 horses (10%) each. Ataxia has a positive association with WNV infection [OR = 3.704; (%CI 0.762-17.999), p value 0.047]. All the positive WNV cases were unvaccinated. Only 17/166,(10.2%) samples were vaccinated against WNV, which is very low.

A limitation of the study is the fact that the sample size was not very large, nevertheless a positivity rate of 11.7% for 2021 and 1.1% for 2022 suggests that WNV contribute significantly to neurological cases. This is reliant on the number of samples submitted through the veterinary network and the fact that serology can only be done on plasma or serum samples, suggesting that some cases could be missed. There was also a significant difference in samples submitted in 2021 compared to 2022. A follow-up sample was provided for the positive WSLB equine sample, but no other follow-up sample for the WNV positive horses were received. While IgM suggests a recent infection it should be evaluated in combination with the clinical presentation in animals. All WNV IgM positive cases that were confirmed here with VTNs also had neurological signs, which would be acceptable as a positive diagnosis. Measuring a rise in IgG antibody titres may be used as an alternative in the absence of IgM assays for WSLB; however, the researcher was unable to confirm VTN in the WSLB RT-PCR positive case. The IgM positive cases for WNV are therefore the only confirmed acute infections other than the PCR positive cases.

4.5 Conclusion

The importance of flaviviruses, specifically WNV in neurological cases in horses, was established in this and previous studies but is likely still underestimated in South Africa. The low level of vaccination suggests that horse owners are still not aware of the risk

of severe neurological WNV infection in horses. The incidence of WSLB remains unknown but this study suggest that it may also result in neurological infections in exotic birds, apart from equine species previously reported on. The use of both molecular and serological assays is; however, needed to ensure that no cases go undetected. The last reported case of WSLB in this surveillance programme was detected in 2008. Detection of neutralising antibodies to WNV and WSLB in livestock with neurological signs suggest WNV may also be missed in other species. Immunoglobulin M (IgM) assays or paired serum is required to resolve this. Continued surveillance is required to determine the incidence of these viruses and raise awareness amongst veterinarians and animal owners of the risks of WSLB and WNV in the country and to take the necessary precautions to prevent infection in animals.

Chapter 5 – Baculovirus expression system to generate recombinant NS1 proteins for WNV and WSLB

5.1 Introduction

Recombinant proteins are proteins encoded by recombinant DNA that has been cloned in an expression vector that supports expression of the gene and translation of messenger RNA (mRNA) (Palomares et al., 2004). Modification of the gene by recombinant DNA technology can lead to expression of a mutant protein (Palomares et al., 2004). Recombinant protein is a manipulated form of native protein, which is generated in various ways to increase production of proteins, modify gene sequences, and manufacture useful commercial products (Spencer et al., 2007).

In the last three decades, the baculovirus expression vector system (BEV) has evolved to one of the most widely used eukaryotic systems for heterologous protein expression including approved vaccines and therapies (Scholz and Suppmann, 2017). Despite the significant improvements introduced during the past years, the BEV system still has major drawbacks, primarily the time required to generate recombinant virus and virus instability for certain target proteins (Scholz and Suppmann, 2017).

Briefly, a recombinant baculovirus is constructed comprising of the desired gene of interest cloned into a transfer plasmid, typically behind the strong promoter to drive protein expression to high levels in insect cells (Felberbaum, 2015). Insect cells are then co-transfected with a mixture of the transfervector plasmid and parental linear DNA, to undergo homologous recombination to generate de novo recombinant baculoviruses (Felberbaum, 2015). These baculoviruses are passaged through multiple rounds of insect cell infection to generate high titre stock that can be utilised for protein production (Felberbaum, 2015). Protein production averages 3 to 5 weeks and yields highly pure, biologically active products (Felberbaum, 2015).

This report describes the expression and purification of recombinant WNV and WSLB NS1 proteins using the baculovirus expression system to use in downstream applications. Our partners at Wageningen University had expressed and purified NS1 proteins for us and supplied it for the use in enzyme linked immunosorbent assay (ELISA) development described in Chapter 6 and 7. The Bacmid plasmids were provided by WUR to allow for in-house protein production in the future. The aim of this chapter was to determine the feasibility of producing this locally in future.

5.6 Materials and Methods

5.2.1 Expressed NS1 plasmids

Our partners at Wageningen University & Research (WUR) expressed the WNV and WSLB NS1 plasmids and exported it for us to use in the expression of the recombinant WNV and WSLB NS1 proteins.

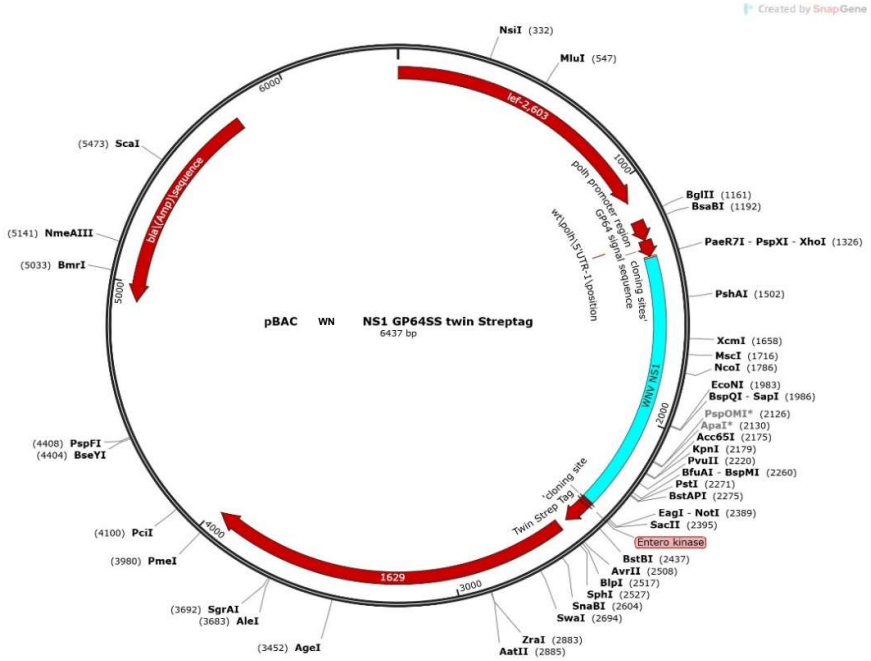

Figure 5.1: pBAC WNV NS1GP64SS Streptag plasmid. A plasmid showing the pBAC plasmid with the WNV NS1 cloned used for baculovirus expression.

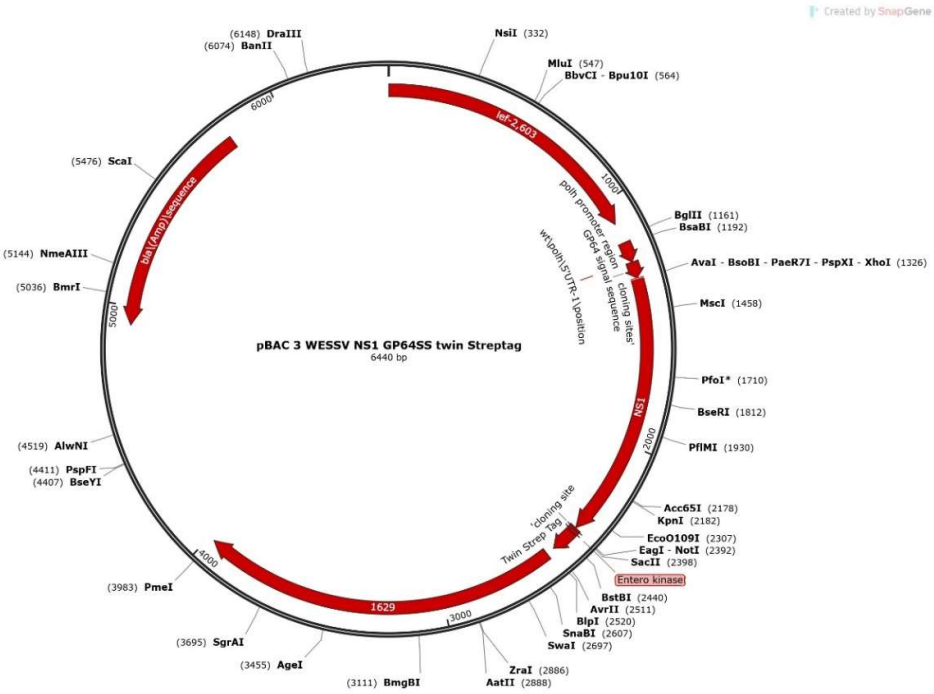

Figure 5.2: pBAC WSLB NS1GP64SS Streptag plasmid. A plasmid showing the pBAC plasmid with the WSLB NS1 cloned used for baculovirus expression.

5.2.2 Cell culture

Clonal isolates from *Spodoptera frugiperda* IPLB-Sf21-AE (Sf9) cells were used as the host for the baculovirus transfer vector. Insect cells were maintained in a T75 flask using 10 mL TC-100 insect culturing media (Gibco, Thermo Fisher Scientific, California, USA), 10% heat-inactivated foetal calf serum (FCS) (Gibco, Thermo Fisher Scientific, California, USA), and 100 µL antibiotic-antimycotic, MycoZap CL-Plus (Lonza, Basel, Switzerland) to prevent contamination (ThermoFisher, Massachusetts, USA). The optimal temperature range to grow the insect cells are 27°C to 28°C, with no CO_2 required in the incubator (Esco LifeSciences, Singapore).

5.2.3Transfecting the Sf9 insect cells

Approximately 1 hour prior to transfection, cells were plated in 2 mL complete growth medium per well in a 6-well plate (NEST Biotechnology, Jiangsu, China). The cell monolayer was even and sub-confluent. For the Sf9 cells, $1x10^6$ cells/dish in 2 mL volume of medium was used. One well was set up as an untransfected control. The cells were incubated at room temperature (20-22°C) for 1 hour. The TransIT®-Insect Reagent (MirusBio, Wisconsin, USA) was warmed to room temperature and vortexed gently before use. A total volume of 100 µL of serum-free insect culture media, Grace Basal Medium (Thermo Fisher Scientific, Massachusetts, USA, was placed in a sterile tube. Next 500 ng (1 µL of 500 ng/µL stock) transfer vector or control DNA was added to the tube. Subsequently, 100 ng (5 µL of 20 ng/µL stock DNA) of flashBAC™ (MirusBio, Wisconsin, USA) was added to the same tube. Pipettes were used to gently mix. Lastly 1.2 µL TransIT®- Insect Reagent was added to the diluted DNA mixture and gently pipetted to mix. The mixture was incubated at room temperature for 15-20 minutes to allow for complexes to form. A volume of 1 mL of culture medium was removed from each well of cells using a sterile pipette to ensure that the monolayer was not disturbed (1 mL left in the dish). The TransIT®-Insect Reagent:DNA complexes were added in a drop-wise manner to different areas of the wells. The culture vessel was gently rocked back-and-forth and from side-to-side to evenly distribute the TransIT®-Insect Reagent:DNA complexes. The cells were incubated overnight at 28°C in the CO_2 free incubator (Esco LifeSciences, Singapore).

The following day, 1 mL of complete insect culture medium was added to each well for a total of 2 mL medium per well. The cultures were incubated at 28°C for four more days in the CO_2 free incubator (Esco LifeSciences, Singapore). The cells were observed for any signs of infection. At 5 days post-infection, 2 mL of culture medium containing the recombinant virus, were added to a sterile tube and centrifuged at 300

x*g* for 5 minutes to remove cell debris. The supernatant was transferred to a new sterile tube and stored at 4°C, protected from light. Optimisation of the baculovirus transfection included DNA concentration, Sf9 cell viability and transfection incubation time.

5.2.4 Harvesting and amplifying the baculovirus

The virus was harvested by centrifuging the 2 mL insect culture medium at 1000x*g* at 4°C for 15 minutes. The supernatant was added to a sterile tube and the recombinant virus (P1) stored at 4°C. After infection, 2 mL of the media containing the virus was collected from each well and centrifuged. The supernatant is the P2 viral stock. This process can be repeated until the desired viral titre is achieved. The virus was harvested at different days after infection, until the optimal harvest time was determined.

5.2.5 PCR confirmation of establishment of recombinant baculoviruses

A conventional PCR was developed to test if the recombinant gene could be detected following the transfection and each subsequent baculovirus infection on DNA extracted from the cells and supernatant. To detect the WSLB NS1 gene insert, 20 pmol of the primers, W2845F and W4039R designed by a previous ZARV member, Miss Stacey Human (Human, 2011), were added to 2x Reaction Mix SuperScript (ThermoFisher, Massachusetts, USA) and SuperScript™ III RT/Platinum™ Taq Mix (ThermoFisher, Massachusetts, USA). The cycling conditions include 50°C for 30 minutes, 94°C for 2 minutes, 40 cycles of 94°C for 15 sec, 61°C for 30 seconds and 68°C for 5 minutes, with a final elongation step of 68°C for 5 minutes. The products were ran on an agarose gel (Refer to chapter 2) and an amplicon size of 573 bp was expected. The same approach was used to detect WNV NS1 in the expressed baculoviruses. Primers, WNVUS1_10_Left_2 and WNVUS1_10_Right (20 pmol) (Sikkema, 2020), was added to 2x Reaction Mix SuperScript (ThermoFisher, Massachusetts, USA) and SuperScript™ III RT/Platinum™ Taq Mix (ThermoFisher, Massachusetts, USA) (Table 5.1). The cycling conditions include 50°C for 30 minutes, 94°C for 2 minutes, 40 cycles of 94°C for 15 sec, 60°C for 30 seconds and 68°C for 5 minutes, with a final elongation step of 68°C for 5 minutes. The products were ran on an agarose gel and an amplicon size of 465 bp was expected.

Table 5.1: WNV and WSLB NS1 primers. A table showing the WNV and WSLB NS1 forward and reverse primer sequences used to check expression.

Target	Primer name	Orientation	Sequence
WNV NS1	WNVUS1_10_LEFT_2	Sense	5'-AGACTCGAGCACCAAATGTGGG-3'
	WNVUS1_10_RIGHT	Anti-sense	5'-GAACGCCCTTCAAGCTTCC-3'
WSLB NS1	WSLB NS1 F	Sense	5'-GCTTCCAAAGGAGATGTTGA-3'
	WSLB NS1 R	Anti-sense	5'-TGGTTGAGACGCTGTCAGTC-3'

5.2.6 Protein purification

The Strep-tag purification system (IBA LifeScience, Goettinger, Germany) was used to purify the proteins from the collected supernatants. The pH of the supernatants was checked with pH strips (Sigma Aldrich, Missouri, USA) and had to be around 7.5. If the pH was too low, it was increased using 10x buffer W (wash buffer). Next, 15 µL of avidine, provided with the purification kit, was added to each 50 mL falcon tube (NEST Biotechnology, Jiangsu, China) to block free biotin in the supernatant and the tubes incubated (Series 2000, Scientific Engineering, Johannesburg, South Africa) for one hour at 37°C until they became cloudy. The tubes were then centrifuged for 30 minutes at maximum speed and the supernatant stored in new tubes. The purification was performed based on the IBA Short Protocol StrepTactin Purification (IBA LifeSciences, Goettinger, Germany). In short, the 1 mL columns were placed into 15 mL falcon tubes (ThermoFisher, Massachusetts, USA). The supernatants were added to the column and allowed to run through. The column was washed five times with 1 column volume (CV) of 1x buffer W. One column volume refers to 1 mL. For elution, 500 µL of 1x buffer E (elution buffer) were added to the columns and repeated six times. Each fraction was collected in a separate 1.5 mL microcentrifuge tube. The column was washed three times with 5 CV of 1x buffer R (regeneration buffer) and finally buffer R was removed by adding 2x 4CV of 1x buffer W. All eluted fractions were measured with the Nanodrop to measure the concentration of the proteins eluted (ThermoFisher, Massachusetts, USA).

5.2.7 Sodium dodecyl-sulfate polyacrylamide gel electrophoresis (SDS-PAGE)

First, 15 µL of 1xTris-glycerine sodium dodecyl-sulfate polyacrylamide gel electrophoresis (SDS) sample buffer (2x) (Life Technologies, California, USA) and 15 µL of the virus stock was added to a 0.2 µL microcentrifuge tube. The tube was placed in a heating block at 98°C for 10 minutes to denature the protein. The XCell Sure Lock 10% precast gel (ThermoFisher, Massachusetts, USA) was placed in the gel tank filled with 1x NuPage running buffer (ThermoFisher, Massachusetts, USA). A total volume of 15 µL of Novex

Sharp Prestain Protein Standards ladder (ThermoFisher, Massachusetts, USA) was loaded into the first well of the gel. Next 30 µL of the denatured protein purified with the kit, was added to the respective wells. The SDS-PAGE ran at 200 V for 45 minutes. The gel was carefully removed from the cast using a spatula and placed into a container containing GelCode blue stain (ThermoFisher, Massachusetts, USA) to immerse the gel in. The container was placed on a shaker overnight and destained with distilled water the following day. The gel was viewed using a BioRad Molecular Imager® Gel DOC™ X+ transilluminator (BioRad, California, USA).

5.2.8 Expressed antigen test with ELISA

To coat the MaxiSorp medium-affinity ELISA plate (Thermo Fisher, Massachusetts, USA), 100 µL of the in-house expressed NS1 WNV and WSLB antigen and purified controls provided by Wageningen University & Research (WUR) (Netherlands) was added to each well at a concentration of 2 µL/mL and incubated overnight at 4°C in the fridge. The following day, the plate was washed six times with 300 µL 0.1% Tween (Sigma Aldrich, Missouri, USA) using an automatic plate washer (Mindray MW-12A, Vacutec, South Africa). Next 200 µL of 10% skim milk (SPAR, Pretoria, South Africa) was added to each well for the blocking step and the plate incubated (Series 2000, Scientific Engineering, Johannesburg, South Africa) for 1 hour at 37°C. The washing step was repeated. For WNV, 100 µL of mouse anti-WNV NS1 antibody (1:1000) (NovusBio, Colorado, USA) was added to each well and incubated for 1 hour in the 37°C incubator. The washing step was repeated, followed by the addition of 100 µL horseradish peroxidase (HRP) conjugated goat-anti mouse secondary antibody (Seracare, Massachusetts, USA) to each well in a 1:1000 dilution and the plate incubated for 1 hour at 37°C. The washing step was repeated. For WSLB, 100 µL of a 1:100 dilution rabbit anti-WSLB NS1 sera (1 µg/mL), provided by our collaborators from WUR, was added, followed by the addition of 100 µL goat anti-rabbit IgG secondary antibody (Merck, New Jersey, USA). The washing step was once again repeated, and the plate incubated for 1 hour at 37°C. For the detection step of each of the respective ELISAs, 100 µL 2,2'-Azinobis [3- ethylbenzothiazoline-6-sulfonic acid]- diammonium salt (ABTS) was added to each well and the plate incubated in a dark chamber for 30 minutes at room temperature. After the 30 minutes, 100 µL 1% SDS was added to the wells to stop the reaction. Readings were taken at optical density (OD) of 405 nanometers (nm) (Mindray MR-96A microplate reader (Mindray, Hong Kong, China). Refer to figure 5.3 and figure 5.4 for the setup of the WNV and WSLB ELISA setup.

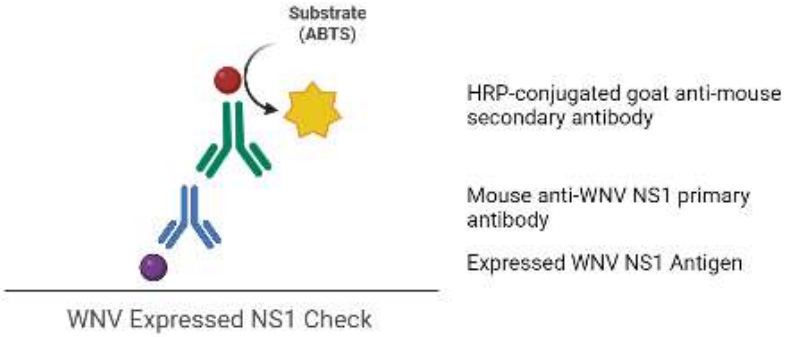

Figure 5.3: WNV ELISA setup. A graphic representation of the ELISA set-up to compare the expressed and imported WNV NS1 antigen.

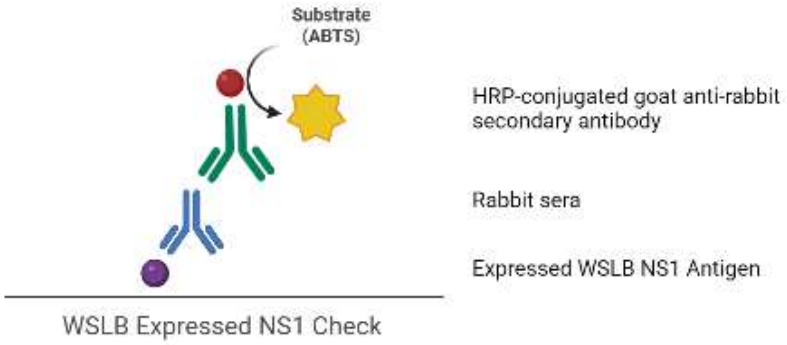

Figure 5.4: WSLB ELISA setup. A graphic representation of the ELISA set-up to compare the expressed and imported WSLB NS1 antigen.

5.3 Results

5.3.1 WNV NS1 protein expression

Several rounds of transfection and amplification had to take place before there seemed to be recombinant protein expressed by the baculovirus system. Polymerase chain reactions and SDS-PAGE gels were used to monitor the expression of the WNV and WSLB NS1 gene and protein respectively. Conventional one-step PCRs were set in place to check presence of the NS1 gene after each round of amplification. For WNV, a PCR was developed and optimized and checked against the WNV NS1 plasmid produced, as well as a WNV control (WNV HS101/08 culture) on an agarose gel to determine efficiency of the assay. A band of approximately 500 bp were expected. The results can be seen in Figure 5.5. The DNA was extracted from the WNV NS1 P1 cells and supernatant and both of these and ran together with controls on an agarose gel with the conventional PCR explained previously to confirm transfection resulted in establishment of recombinant baculoviruses. Figure 5.5 shows the results obtained. Faint bands were detected in both the P1 cells' lane, as well as the P1 supernatant lane at approximately 500 bp. The plasmid control came up, but the WNV culture control did not come up. This confirmed that there is some level of WNV expression and can be amplified further before purifying and running an SDS-PAGE

gel.

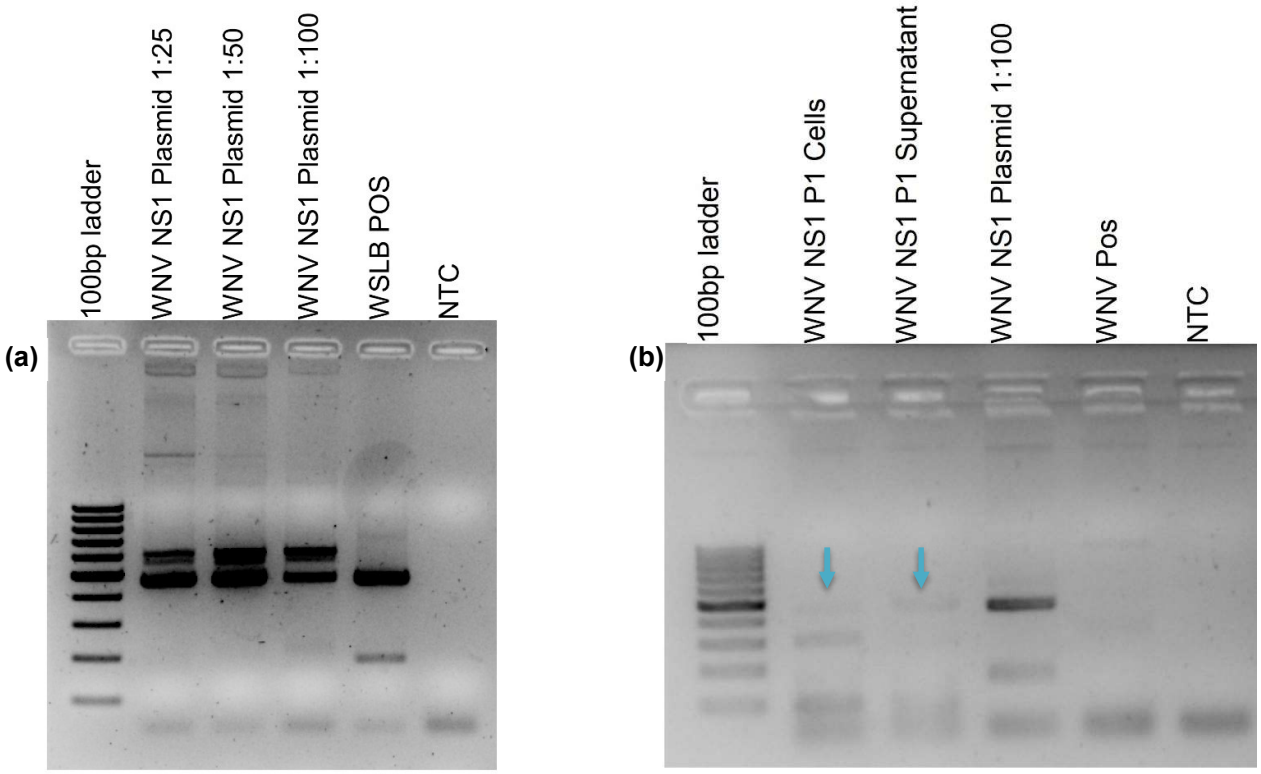

Figure 5.5: (a) WNV NS1 plasmid dilutions. An agarose gel showing the results of the WNV NS1 plasmid dilutions, to be used as a control in the PCR. **(b) WNV NS1 P1 Check.** An agarose gel showing the results of the extracted WNV NS1 P1 cells and supernatant. Faint bands formed at the same height as the plasmid control.

The WNV NS1 passage 1 was upscaled to bigger T75 flasks and higher passages, in order to increase the amount of protein present. After taking the WNV NS1 baculovirus to passage three in three different T75 flasks, the flasks were pooled, and protein purification took place. With regards to the protein purification, the protein is eluted in six fragments, with the protein expected to be in fraction 3 and fraction 4. The concentrations of the fractions were measured (Table 5.2) with the Nanodrop (ThermoFisher, Massachusetts, USA) and then ran on an SDS PAGE gel (Figure 5.6). Fractions 3 and 4 had the highest concentration, which is expected to have the recombinant expressed WNV NS1 protein. Compared to the supplied WNV NS1 protein from our WUR collaborators, which supplied protein's concentration was 1.43 mg/mL, the current study's protein concentration was 0.55 mg/mL: about a third of that of the supplied WUR protein. Faint bands in the lanes of the SDS-PAGE gel for fractions 3 and 4 were also observed at a size of approximately 55 kDa. The NS1 protein of flaviviruses has a size of 40-55 kDa.

Table 5.2: WNV NS1 fraction concentrations. A table showing the purified WNV NS1 protein concentrations, as measured on a Nanodrop.

Fraction	Concentration (mg/mL)	Purity (260/280)
1	0.12	2.34
2	0.07	1.61
3	0.55	1.69
4	0.31	1.81
5	0.05	3.01
6	0.01	2.70

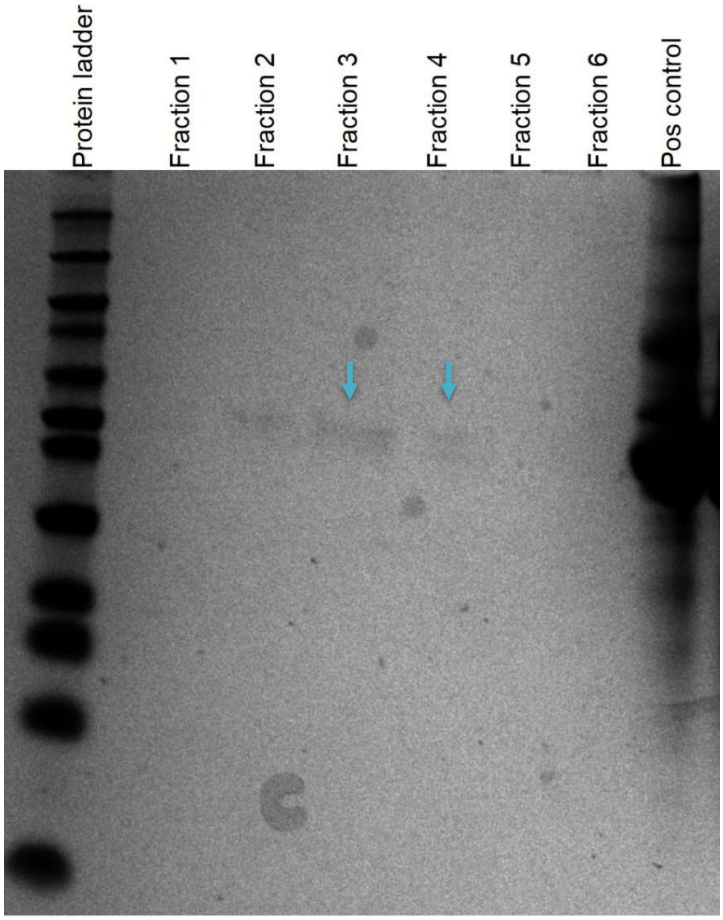

Figure 5.6: SDS-PAGE gel of purified WNV NS1 proteins. An SDS-PAGE gel showing the results of each fraction purified from the WNV NS1 protein. Fraction 3 and fraction 4 had faint bands forming.

An ELISA was also performed to compare the performance of the in-house expressed WNV NS1 compared to the provided WNV NS1 protein and the results can be seen in Figure 5.7 and Table 5.3. The in-house expressed WNV NS1 protein resulted in very low OD values, compared to the antigen expressed by WUR.

Table 5.3: WNV NS1 antigen check ELISA. A table showing OD values obtained when using the in-house expressed NS1 antigen, compared to the imported WUR NS1 antigen.

WNV NS1 antigen check		OD Values		
		WNV Antigen	Mock Antigen	Net OD
In-house expressed		0.156	0.074	**0.082**
WUR imported		1.325	0.081	**1.244**
Negative control	No antigen	0.075	x	**0.075**
	No anti-WNV NS1	0.076	x	**0.076**
	No secondary	0.082	x	**0.082**

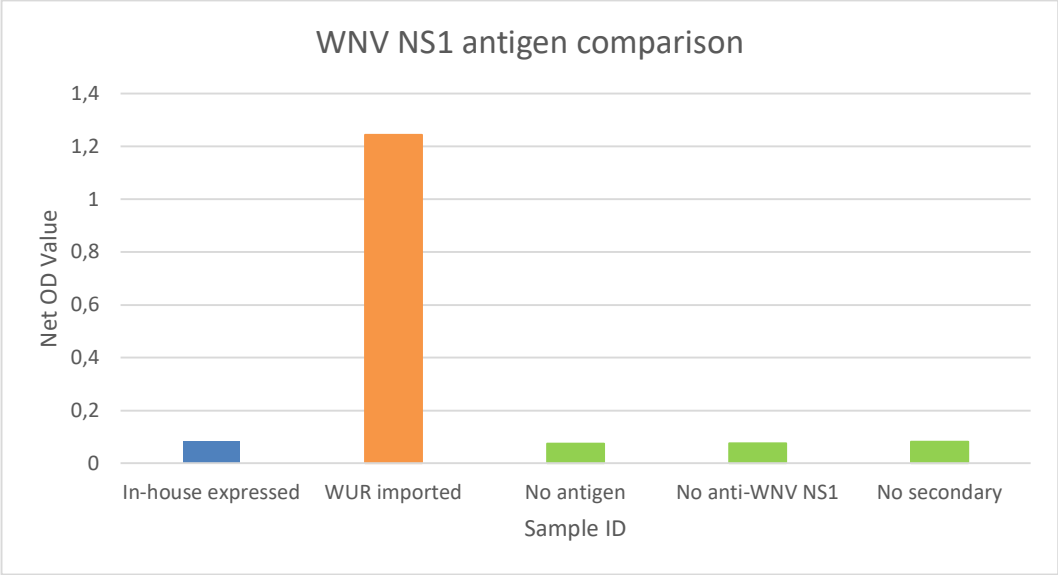

Figure 5.7: Graph showing the net OD values obtained for the WNV NS1 antigen comparison ELISA. The graph shows that the WNV NS1 imported antigen results in much higher OD values compared to the in-house expressed antigen.

5.3.2 WSLB NS1 protein expression

The same principle and steps were applied to expressing the WSLB NS1 protein. A conventional one-step PCR were set in place to check presence of protein after each round of amplification. For WSLB, a PCR was developed and optimised and checked against the WSLB NS1 plasmid produced, as well as a WSLB control (WSLB AV259 P3 culture) on an agarose gel to determine efficiency of the assay. A band of approximately 500 bp were expected. The results can be seen in Figure 5.8. The WSLB culture control came up at the expected size, but none of the plasmid dilutions formed bands where expected. In the 1:25 dilution lane a band formed, but it remained in the well. The reason for this could be that there is no WSLB NS1 DNA present in the plasmid or that the plasmid is of too big in size to effectively run on the agarose gel. In Figure 5.8 the second passage of the WSLB culture was ran on an agarose gel, with only the culture control coming up and the plasmid control once again fluorescing in the well, while no other bands were observed on the gel. This suggested that there was no insert in the plasmid.

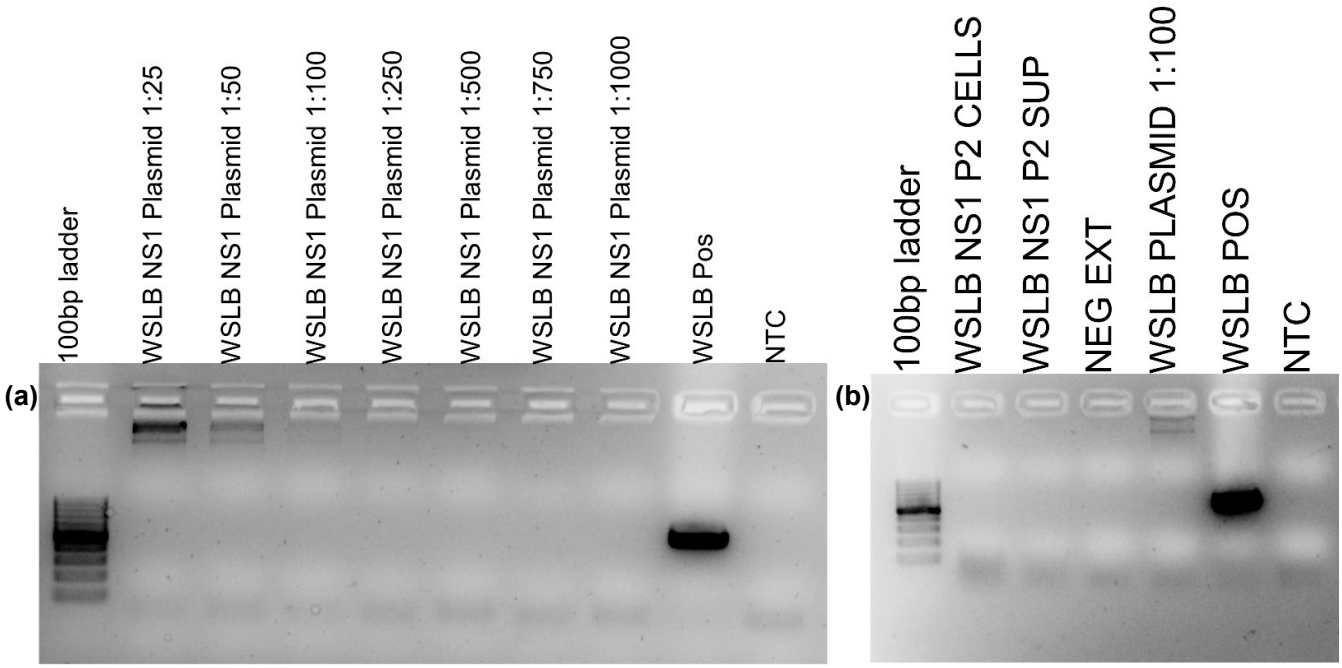

Figure 5.8: (a) WSLB NS1 plasmid dilutions. An agarose gel showing the results of the WSLB NS1 plasmid dilutions, to be used as a control in the PCR. **(b) WSLB NS1 P2 Check.** An agarose gel showing the results of the extracted WNV NS1 P1 cells and supernatant. No bands formed in the extracted cells or supernatant lanes or the plasmid control. A WSLB culture control formed a band.

The WSLB NS1 baculovirus culture was upscaled to three T75 flasks in order to purify the protein and run on an SDS-PAGE gel. The concentrations of each fraction were measured on the Nanodrop (Table 5.4), and the SDS-PAGE gel results can be seen in Figure 5.9.

Table 5.4: WSLB NS1 fraction concentrations. A table showing the purified WSLB NS1 protein concentrations, as measured on a Nanodrop.

Fraction	Concentration (mg/ml)	Purity (260/280)
1	0.04	0.96
2	0.08	0.79
3	0.14	1.31
4	0.10	1.12
5	0.12	0.92
6	0.05	0.77

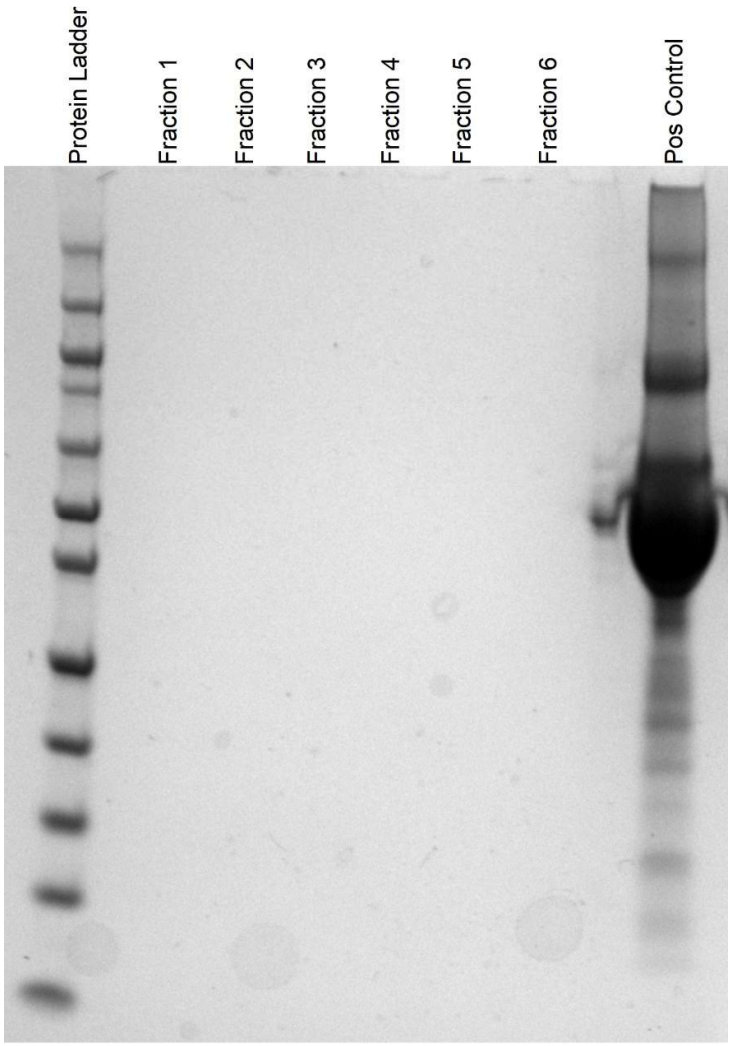

Figure 5.9: SDS-PAGE gel of purified WSLB NS1 proteins. An SDS-PAGE gel showing the results of each fraction purified from the WSLB NS1 protein. No bands were observed, indicating that there was no expression of the WSLB NS1 protein.

An ELISA was also performed to compare the performance of the in-house expressed WSLB NS1 compared to the provided WSLB NS1 protein and the results can be seen in Figure 5.10 and Table 5.5.

Table 5.5: WSLB NS1 antigen check ELISA. A table showing OD values obtained when using the in-house expressed NS1 antigen, compared to the imported WUR NS1 antigen.

WSLB NS1 antigen check		**OD Values**		
		WNV Antigen	**Mock Antigen**	**Net OD**
NS1	In-house expressed	0.291	0.413	**0.001**
	WUR imported	1.078	0.094	**0.984**
Negative control	No antigen	0.072	x	**0.072**
	No rabbit sera	0.071	x	**0.071**
	No secondary	0.071	x	**0.071**

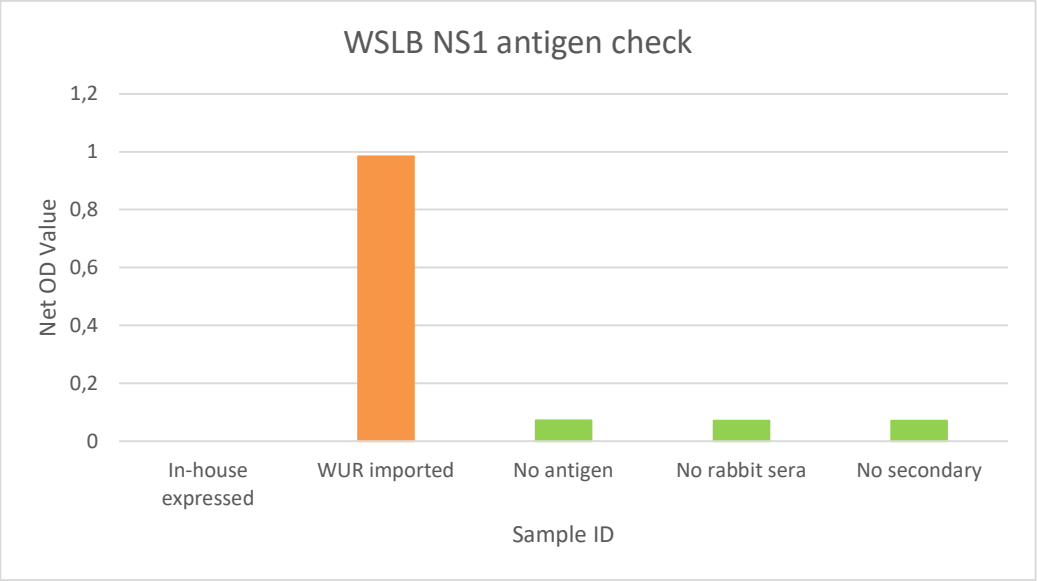

Figure 5.10: Graph showing the net OD values obtained for the WSLB NS1 antigen comparison ELISA. The graph shows that the WSLB NS1 imported antigen results in much higher OD values compared to the in-house expressed antigen.

5.4 Discussion

Enzyme linked immunosorbent assays provide a valuable tool in the detection and diagnosis of virus infection. The ability to produced recombinant proteins will ensure that future ELISAs are safe (as there is no live virus), low background (only virus antigens are present) and specific (single viral proteins can be used) (Scholz et al., 2017). The ability to synthesise recombinant proteins in the laboratory allows easy scale up for the commercial manufacture of ELISA kits. The clear advantage of recombinant protein/peptide is that high quality assurance is ensured, especially with peptides as these can be manufactured synthetically, in the absence of any other proteins (Scholz, 2017). This latter point being the most crucial advantage of recombinant based proteins ELISAs in that even if a virus cannot be cultured, provided gene sequence is available, it is possible to rapidly respond to emerging viruses and new viral strains of existing pathogens (Scholz, 2017).

The purpose of this study was to express WNV and WSLB NS1 proteins, while making use of the baculovirus expression system, to use in downstream applications. This would allow for the use of in-house ELISA development, to reduce the need for commercial ELISA kits. With regards to the WNV NS1 expression, bands were seen after the P2 infection on an agarose gel, which indicated that the baculovirus has successfully recombined with the WNV NS1 plasmid and expresses WNV NS1 proteins. The cultures were amplified and eventually purified to run on an SDS PAGE gel. Faint bands also formed on the SDS-PAGE gel and the highest concentration measured was 0.55 mg/mL.

Compared to the WUR WNV NS1 protein (1.43 mg/mL), this seemed like a good result. When an ELISA was performed to compare the efficiency of the in-house expressed WNV NS1 and the WUR WNV NS1, it was clear that even when added at the same concentration, the in-house expressed antigen was not good enough to use in downstream applications and that the imported NS1 antigen will be used for ELISA development.

With regards to the WSLB NS1 expression, bands were not seen on the agarose gel, not even when only the plasmid was used as a control. This could be explained by the size of the plasmid, but dilutions did not make a difference to the DNA being stuck in the well. A different explanation could be that there was no plasmid DNA present in the extracted cell and supernatant control, due to unsuccessful transfection. Nevertheless, the WSLB cultures were still amplified, and the protein purified. The highest concentration obtained was 0.14 mg/mL and compared to the WUR WSLB NS1 protein (7.6 mg/mL), the attempt at expressing WSLB NS1 in-house was unsuccessful. The SDS-PAGE gel showed no bands formed, the ELISA to compare the two antigens confirmed this. Wesselsbron virus NS1 was not expressed using the baculovirus expression system.

The reason for the low concentrations of WNV and WSLB NS1 proteins expressed in-house could be due to host factors like differences between distinct insect cell lines that may cause the differences in the efficiency of protein production, post translational folding, or that there was never sufficient recombination when transfection took place (Liu, 2013). Another reason could also be that the amplification had to have gone up several more passages until litres of supernatant could be collected for protein purification. Our WUR collaborators have a very good expression laboratory in place, which could explain why ours was not as successful as theirs.

5.5 Conclusion

WNV and WSLB NS1 proteins were not successfully expressed using the baculovirus expression system. For downstream applications, the WUR expressed antigens will be used in ELISA development.

Chapter 6 – Establishment of serological assays to detect the presence of WNV in humans

6.1 Introduction

To diagnose flavivirus-associated disease, laboratory testing is required and can be done through directly detecting the infectious agent or detecting antibodies against it (Musso and Despres, 2020). Due to the low levels of viraemia present at the time of clinical signs, detecting ribonucleic acid (RNA) in samples is limited to only a few days (Hobson-Peters, 2012). In order to detect recent infections, immunoglobulin M (IgM) antibodies need to be detected or an increase in immunoglobulin G (IgG) antibodies. Detection of IgG to an endemic virus alone is not proof that it is the cause of infection, and only useful for sero-prevelance studies. Due to cross reactivity between flaviviruses, serum neutralisation assays are needed as confirmation of specific viruses. Thus, using serological assays like IgM enzyme linked immunosorbent assays (ELISAs) or immunofluorescence assay (IFAs) or paired serum for IgG assays followed by serum neutralisation assays, are recommended for diagnosis of flavivirus infection (Musso and Despres, 2020).

In South Africa, human cerebrospinal fluid (CSF) specimens in hospitals in the Tshwane region, Pretoria, using reverse transcriptase polymerase chain reaction (RT-PCR), IgM ELISA and tissue culture infectious dose ($TCID_{50}$) neutralisation assays in 2009 detected WNV in 19.4% (40/206) of unsolved cases of neurological disease in patients (Zaayman, 2012). A serosurvey of veterinarians from across South Africa reported 12.5% (10/125) seropositivity in 2011-2012 (van Eeden, 2014).

Serological tools for flavivirus infection mostly rely on detecting anti-envelope (E) or anti-non-structural protein 1 (NS1) antibodies, since the E and NS1 proteins are the most immunodominant (Endale et al., 2021). The interpretation of serological results has proven to be challenging at times, due to the cross-reactivity inherent in the Japanese Encephalitis virus (JEV) serogroup (Crill and Chang, 2004). Studies have shown that the highest cross-reactivity takes places with IgG capture assays compared to IgM capture assays (Endale et al., 2021). It also revealed that assays based on the E protein have higher cross-reactivity than assays based on the NS1 protein (Stettler et al., 2016). The E protein elicits a cross-reactive neutralisation antibody, while NS1 induces a non-neutralising virus-specific antibody response and serves as a good diagnostic marker

for flavivirus species-specific infection (Stettler et al., 2016).

Macdonald (Macdonald, 2005) and Saxena (Saxena, 2013)) developed two NS1 antigen-capture ELISAs; however, these assays do not effectively distinguish West Nile virus (WNV) from other flavivirus infections or standardisation because the antibodies used in these assays are either a flavivirus NS1 protein cross-reactive monoclonal antibody (MAb) or a WNV-NS1 polyclonal antibody (Macdonald, 2005; Saxena, 2013). This results in poor specificity in detecting WNV or intra- and inter- laboratory variability caused by batch-to-batch variations in polyclonal antisera (Ding, 2014).

There are various methods to produce antigenic material for an ELISA (Spencer, 2007). Inactivated whole virus can be used or individual proteins produced through recombinant gene expression. One such method is through the baculovirus expression vector system (BEVS) as described in chapter 5.

A commercial IgM ELISA is available for humans against WNV but is expensive and has to be imported into South Africa. The aim of this aspect of the project was to develop in-house IgG and IgM ELISAs for WNV in humans.

6.2 Materials and Methods

6.2.1 Clinical Samples

Samples used to develop, optimise and validate the WNV IgG, and IgM ELISA were selected based on the outcome of the commercial WNV IgM ELISA kit for humans (Euroimmun, Lübeck, Germany) and neutralisation assays (Refer to Chapter 3 and Appendix Table A3).

6.2.2 Expressed NS1 Antigen

Researchers at Wageningen University & Research (WUR) expressed the WNV NS1 antigen using the baculovirus expression system and exported it to the Zoonotic arbo- and respiratory virus (ZARV) research lab in South Africa to use in the development of the ELISAs (Oymans, 2020).

6.2.3 IgG ELISA against WNV

To coat the MaxiSorp medium absorption plate (Thermo Fisher, Massachusetts, USA), 100 µL of the NS1 antigen WNV (1.43 mg/mL) was diluted in phosphate buffered saline (PBS, pH7) (Merck, New Jersey, USA) and added to each well at a concentration of 2

µg/mL, followed by overnight incubation at 4°C. Microtitre plates used for coating are special plates with a modified surface to allow for high binding capacity and ensures proper antibody orientation (Rajna and Irena, 2020). It is very important that the whole surface of the well bottom must be covered, to prevent low absorbance reads, while on the other hand excess antigen will be washed away, also resulting in lower signal.The following day, the plate was washed six times with 300 µL 0.1% Tween®20 (Sigma Aldrich, Missouri, USA) using an automatic plate washer (Mindray MW-12A, Vacutex, South Africa). Next 200 µL of 10% Skim milk diluted in PBS, pH7, (SPAR, Pretoria, South Africa) was added to each well (blocking step) and the plate incubated for 1 hour at 37°C (Series 2000, Scientific Engineering, Johannesburg, South Africa). The washing step was then repeated. The serum sample was diluted in 2% skim milk using a 1:50 ratio and 100 µL of diluted sample added in duplicate to the plate. The plate was incubated for 1 hour at 37°C, followed by the washing step. Next, 100 µL horseradish peroxidase (HRP) conjugated goat anti-human IgG secondary antibody (Sigma Aldrich, Missouri, USA) was added to each well in a 1:1000 dilution and the plate incubated for 1 hour at 37°C followed by washing. For the detection step, 100 µL 2,2'-Azinobis [3- ethylbenzothiazoline-6-sulfonic acid]-diammonium salt (ABTS) (SurModics, Minnesota, USA) was added to each well and the plate incubated in a dark chamber for 30 minutes at room temperature (20-22°C). After the 30 minutes, 100 µlL 1% sodium dodecyl sulphate (SDS) (Amresco, Idaho, USA) was added to the wells to stop the reaction. Readings were taken at a wavelength of 405 nm using the Mindray MR-96A microplate reader (Mindray, Hong Kong, China). Figure 6.1 gives a graphic representation of the setup of the WNV IgG Human ELISA.

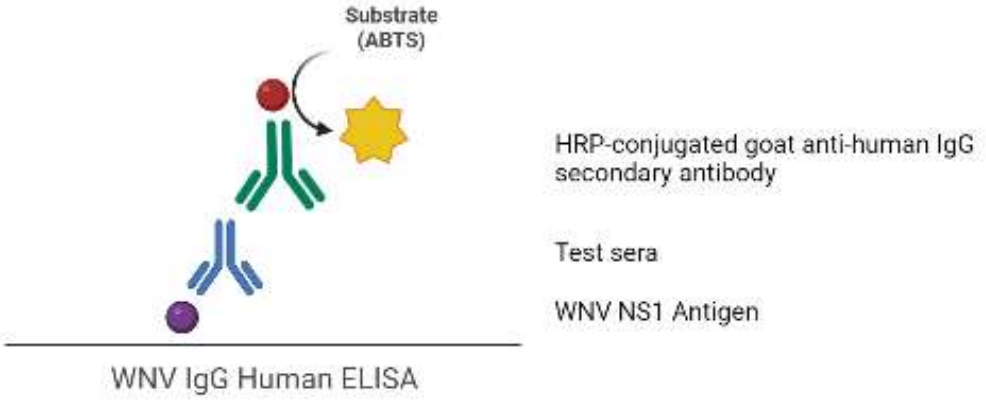

Figure 6.1: WNV IgG Human ELISA Setup. The figure shows the setup of the WNV IgG Human ELISA that starts with coating the plate with the WNV NS1 antigen, followed by the addition of test sera and lastly the HRP-conjugated goat anti-human IgG secondary antibody. Picture made by BioRender.

6.2.4 Capture antibody IgM ELISA for WNV

To coat the MaxiSorp medium absorption plate (Thermo Fisher, Massachusetts, USA), goat anti-human IgM (0.5 µg/mL) (SeraCare, Massachusetts, USA) was diluted in PBS, pH7, and 100 µL added to each well on the plate. The plate was incubated overnight at 4°C. To wash the plate, 300 µL of 0.1% Tween (SigmaAldrige, Missouri, USA) was added to each well and repeated six times using an automatic plate washer. Next 200 µL of 10% Skim milk diluted in PBS, pH7 (SPAR, Pretoria, South Africa) was added to each well for the blocking step and the plate incubated for 1 hour at 37°C followed by washing. The sera were diluted in 2% skim milk using a 1:100 ratio and 100 µL of the diluted sample added in duplicate to the plate. The plate was incubated for 1 hour at 37°C, followed by the washing step. Next, 100 µL of the NS1 antigen WNV (2 µL/mL), diluted in 2% skim milk, was added to each well and incubated for 1 hour at 37°C. After the 1-hour incubation, the plate was washed six times with 200 µL 0.01% Tween (SigmaAldrige, Missouri, USA). Next 100 µL of the mouse monoclonal primary antibody, anti-West Nile virus NS1 (Abcam, Cambridge, UK) was added to each well in a 1:1000 dilution. Finally, 100 µL HRP conjugated goat anti-mouse secondary antibody (SeraCare, Massachusetts, USA) was added to each well in a 1:1000 dilution and the plate incubated for 1 hour at 37°C. The washing step was repeated. For the detection step, 100 µL ABTS was added to each well and the plate incubated in a dark chamber for 30 minutes at room temperature (20-22°C). After the 30 minutes, 100 µL 1% SDS (Amresco, Idaho, USA) was added to the wells to stop the reaction. Readings were taken at a wavelength of 405 nm using the Mindray MR-96A microplate reader (Mindray, Hong Kong, China). A visual representation of the assay can be seen in Figure 6.2.

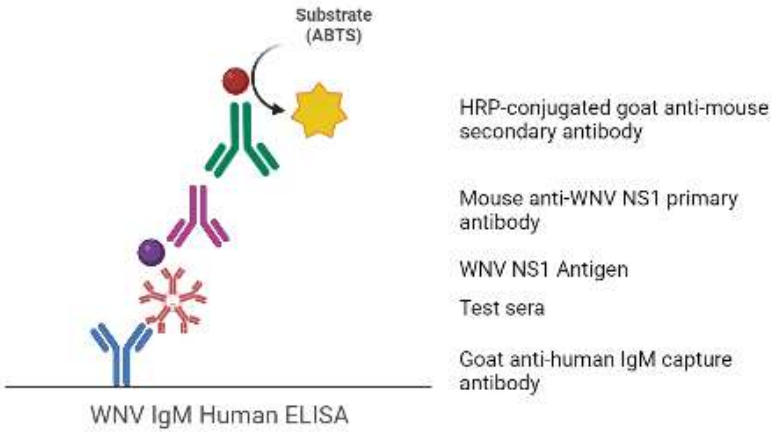

Figure 6.2: WNV IgM Human ELISA original setup. The figure shows the setup of the original WNV IgM Human ELISA that starts with coating the plate with the goat anti-human IgM capture antibody, followed by the addition of test sera, the WNV NS1 antigen, then mouse anti-WNV NS1 antibody and lastly the HRP-conjugated goat anti-mouse IgG secondary antibody. Picture made by BioRender.

The next step was to re-evaluate the setup of the WNV IgM Human ELISA to attempt to reduce the background activity shown in Figure 6.8. It now made use of a more direct approach, very similar to the WNV IgG Human ELISA in the previous section making use of HRP-conjugated rabbit anti-human secondary antibody. (Figure 6.3). The secondary antibody is from the Euroimmun kit and it does not state what the dilution of the antibody is, so will be referred to as undiluted from here on.

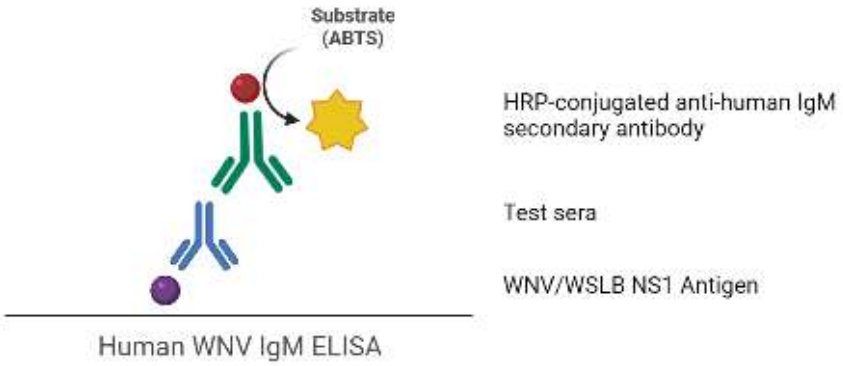

Figure 6.3: WNV IgM Human ELISA with the new setup. The figure shows the setup of the WNV IgM Human ELISA using a more direct approach. The plate was coated with antigen, followed by the addition of test sera and lastly conjugated rabbit anti-human IgM secondary antibodies. Image made with BioRender.

6.2.5 Checkerboard titrations

Optimisation of ELISAs is essential to ensure accurate detection of a target antibody response. Since ELISA is a multistep procedure, each component can be individually tested prior to the use of the assay on clinical specimens. Optimisation aids in establishing ideal concentrations of each assay reagent and condition for each step. Factors that should be tested include the concentration of the antigen used for coating, buffer used, sample dilution and antibody concentrations.The process of checkerboard titration involves the dilution of two reagents against each other to examine the activities inherent at all the resulting combinations (Figure 6.4). By running each well with a different ratio of antibody to antigen for example, you can find not only the optimal concentration of each, but the optimal ratio of concentrations as well. Using the information gleaned from the checkerboard assay, you can perform your ELISA experiment with the optimal concentrations for your application and get better results. With regards to optimisation of the assays in this study, the concentration of the antigen, as well as diluent, PBS or carbonate buffer, was tested until the optimal conditions were established. Incubation time for blocking was compared – 1 hour at 37°C compared to

overnight at 4°C. The dilutions and concentration of primary and secondary antibodies were tested to establish the optimal concentration to use.

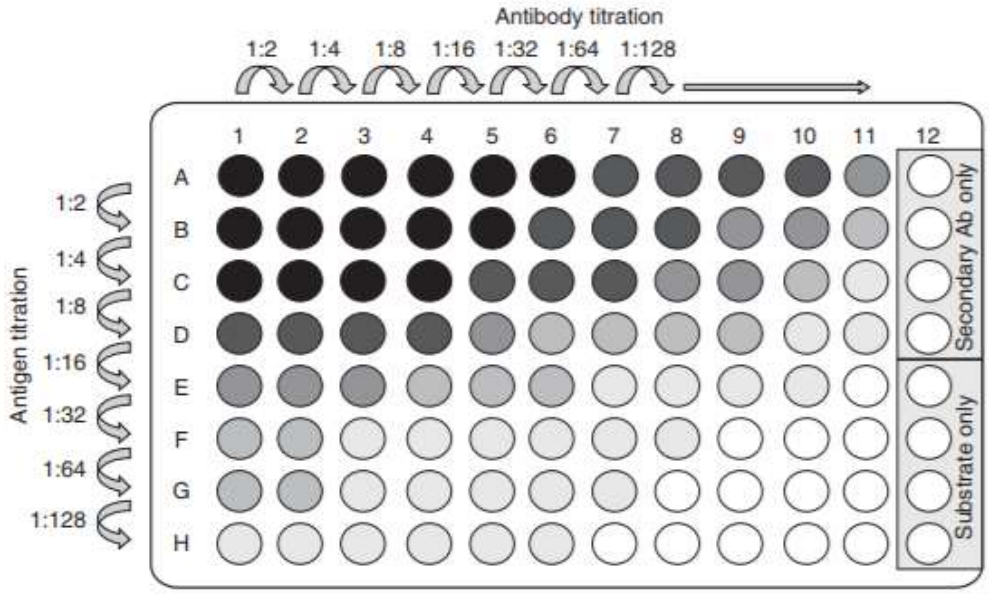

Figure 6.4: Checkerboard titration plate layout. The figure shows the layout of the ELISA plate for a checkerboard titration.

6.2.6 Statistical analysis

In literature, the cut-off value is determined using two or three standard deviations above and below the mean value of the negative sample set, but since the data was not normally distributed an alternative method had to be used. MedCalc (https://www.medcalc.org/) is a statistical software package for biomedical research. The receiver operating curve (ROC) curve connects the coordinate points using "1 – specificity (false positive rate)" as the x-axis and "sensitivity" as the y-axis for all cut-off values measured from the test results. The area under curve (AUC) is widely used to measure the accuracy of diagnostic tests. The closer the ROC curve is to the upper left corner of the graph, the higher the accuracy of the test since in the upper left corner, the sensitivity = 1 and the false positive rate = 0 (specificity = 1). The area under the curve (AUC) is an effective measuring tool for sensitivity and specificity that describes the validity of a diagnostic test (Haijan-Tilaki, 2013). The ideal ROC curve has an AUC of 1.0 (Nahm, 2022). The Youden Index (J) refers to the distance between the 45° diagonal in the coordinate (0,1) direction. The cut-point that achieves this maximum is referred to as the optimal cut-point (*c*) because it is the cut-point that optimises the biomarker's differentiating ability when equal weight is given to sensitivity and specificity (Ruopp, 2008). Youden's J statistic can be calculated as

follows, and represents the value that is optimal for cut-off:

$$J = Se + Sp - 1$$

MedCalc (MedCalc Statistical Software Ltd, Flanders, Belgium) provides a sample size estimation for a single diagnostic test and includes various analytical techniques to determine the optimal cut-off value. Four runs of negative only samples on the in-house assay were performed and the previously obtained positive results included to determine the cut-off value.

Table 6.1: AUC value interpretation. The table shows the interpretation of the AUC and what it means for a diagnostic test to be meaningful. Obtained from Nahm, 2022.

Area under the curve (AUC)	Interpretation
0.9 ≤ AUC	Excellent
0.8 ≤ AUC < 0.9	Good
0.7 ≤ AUC < 0.8	Fair
0.6 ≤ AUC < 0.7	Poor
0.5 ≤ AUC < 0.6	Fail

For a diagnostic test to be meaningful, the AUC must be greater than 0.5. Generally, an AUC ≥ 0.8 is considered acceptable.

Commercial kits make use of ratios to determine the cut-off value, but their tests have been validated with a lot more samples and panels to determine the optimal cut-off value. In this case, it is better to work out the cut-off value for each assay making use of the ROC curve and Youden Index determined by MedCalc, but for interest's sake the ratios will be shown as a comparison to the commercial kits. The ratio is determined as WNV antigen/Mock antigen. For the Euroimmun WNV IgM ELISA kit, a ratio of ≥ 1.1 was considered positive and < 0.8 was considered negative. Values in-between 0.8 and 1.1 were deemed borderline.

6.3 Results

6.3.1 WNV IgG ELISA development and optimisation

For the WNV IgG Human ELISA, the medium absorption microtitre plates (ThermoFisher, Massachusetts, USA) was coated with the WNV NS1 antigen. A checkerboard titration was performed to determine the optimal concentrations of coating the plate with the WNV NS1 antigen, as well as the dilution factor of the serum and the secondary HRP-conjugated goat anti-human IgG secondary antibody. It was determined that coating the plate with 4 µg/mL NS1 antigen yielded optimal results, as well as diluting serum in 1:50 to ensure detection, but due to limited availability of the WNV NS1 antigen, a dilution of 3 µg/mL was used . Finally, an optimal dilution of

1:2500 was determined to detect antibodies best and allow for slow colour development.

After optimal concentrations of antigen and secondary antibody were determined, an IgG run was performed to determine if the assay works. The samples used to validate the WNV IgG Human ELISA were obtained from the results of a commercial IgM ELISA from Euroimmun (Euroimmun, Lübeck, Germany) (Chapter 3). These samples were confirmed with neutralisation assays to rule out cross reaction to other arboviruses, and an assumption was made that some IgM positive samples will also already have IgG antibodies present against WNV (Ehrenstein, 2000). For this assay, three controls were included: (1) omitting the WNV NS1 antigen but adding all other reagents; (2) omitting the serum but adding all other reagents and (3) omitting the secondary antibody but adding all other reagents. Table 6.2 shows the OD values obtained from the results of this experiment, while Figure 6.5 shows the visual representation.

Table 6.2: Net OD values obtained with the in-house WNV IgG Human ELISA. The table shows the net OD values obtained during validation of the in-house WNV IgG Human ELISA. Positive and negative samples used were selected based on the neutralisation assay outcomes.

WNV IgG Human ELISA		OD Values			Ratio
		WNV Antigen	Mock Antigen	Net OD	
Positive sera	ZRUA2067/22	1.29	0.35	**0.94**	**3.72**
	ZRUA1541/21	0.62	0.10	**0.52**	**6.10**
	ZRUA2099/22	1.34	0.16	**1.18**	**8.18**
	ZRUA1601/21	1.23	0.16	**1.07**	**7.65**
	ZRUA1607/21	0.82	0.20	**0.62**	**4.07**
	ZRUA1611/21	0.93	0.15	**0.78**	**6.12**
	ZRUA1652/21	1.14	0.31	**0.83**	**3.73**
	ZRUA2067/22	0.82	0.12	**0.70**	**6.92**
	ZRUA2099/22	0.94	0.13	**0.81**	**7.36**
	ZRUA1550/21	0.76	0.20	**0.56**	**3.78**
Negative sera	ZRUA1560/21	0.31	0.26	**0.05**	**1.19**
	ZRUA1565/21	0.23	0.18	**0.05**	**1.29**
	ZRUA1581/21	0.37	0.15	**0.22**	**2.48**
	ZRUA2221/22	0.22	0.16	**0.06**	**1.40**
	ZRUA2253/22	0.53	0.26	**0.27**	**2.01**
	ZRUA1496/21	0.10	0.12	**0.00**	**0.86**
	ZRUA1513/21	0.24	0.23	**0.01**	**1.05**
	ZRUA1514/21	0.16	0.14	**0.02**	**1.11**
	ZRUA1485/21	0.12	0.32	**0.00**	**0.36**
	ZRUA1506/21	0.12	0.22	**0.00**	**0.55**
	ZRUA1527/21	0.15	0.10	**0.05**	**1.43**
	ZRUA1534/21	0.32	0.19	**0.14**	**1.71**
Negative control	No antigen	0.07	x	**0.07**	**x**
	No serum	0.07	x	**0.07**	**x**
	No secondary	0.06	x	**0.06**	**x**

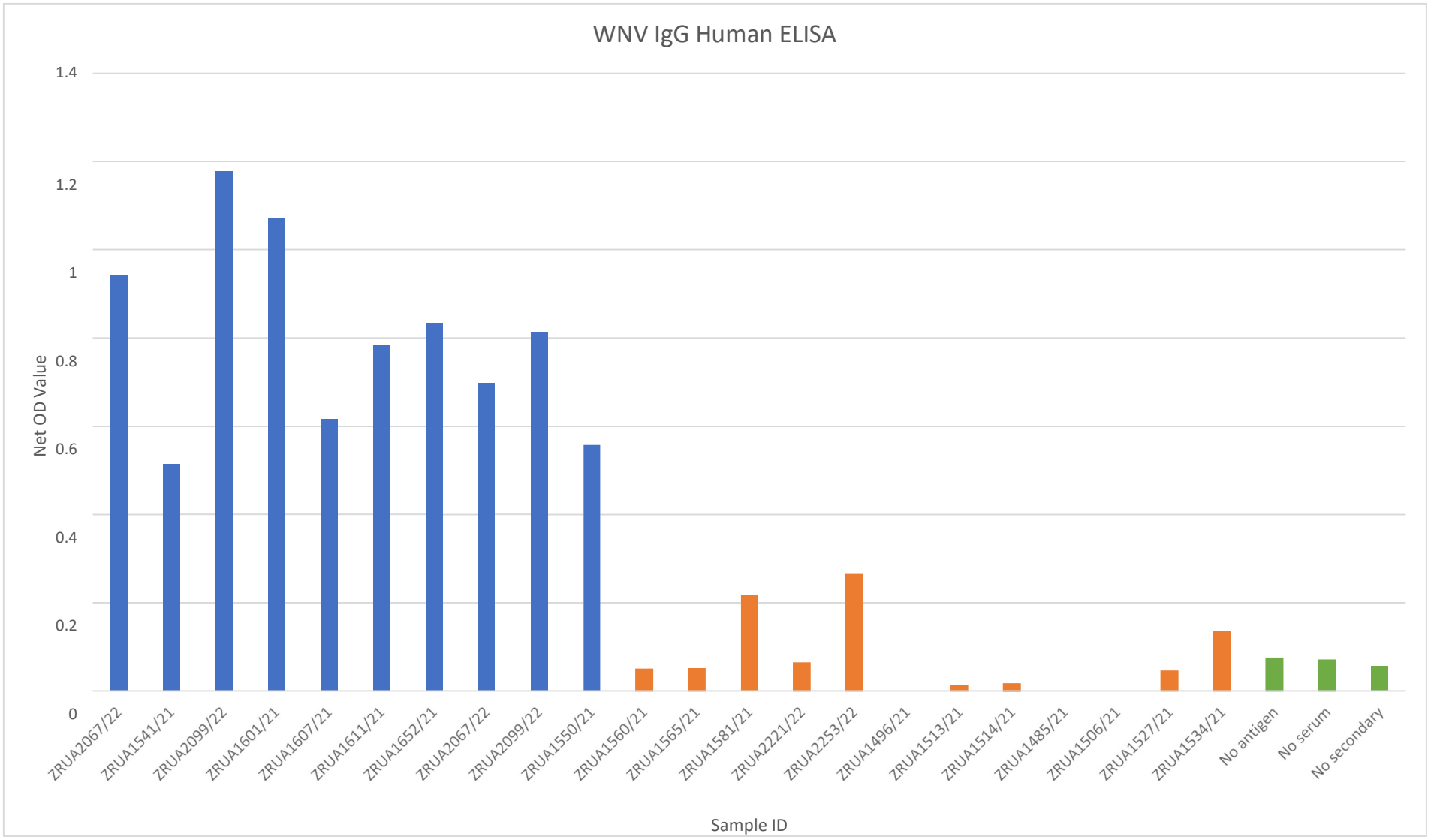

Figure 6.5: Net OD values obtained with the in-house WNV IgG Human ELISA. The bar shows the net OD values obtained during validation of the in-house WNV IgG Human ELISA. Positive (blue bars) and negative samples (orange bars) were selected based on the neutralisation assay outcomes. Negative controls (green bars) were included to monitor the interaction of the antibodies with each other.

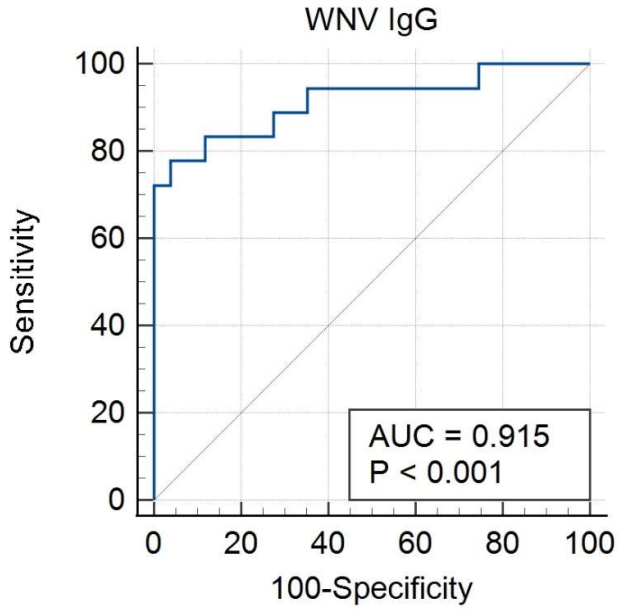

Figure 6.6: ROC curve for the in-house WNV IgG Human ELISA. The figure shows the ROC curve obtained for the in-house WNV IgG Human ELISA. An AUC value of 0.915 was obtained with a p value of <0.001. The ROC curve was generated using MedCalc.

An ROC curve was used to determine the trade-off between sensitivity and specificity for the experimental ELISA. By making use of MedCalc, the ROC curve was generated, as seen in Figure 6.6. The sample size used to construct the ROC curve was 18 positive samples and 13 negative samples that were repeated four times for reproducibility, thus yielding 51 negative results to be used. The AUC value obtained was 0.915, which can be interpreted as excellent and a Youden's Index of 0.7386 was determined.

The sensitivity of the assay was determined to be 77.78%, while the specificity was 96.08% (Table 6.4). Comparing the cut-off value to the net OD values obtained, 8/10 samples were positive, with 12/12 samples negative (Table 6.3).

Table 6.3: Cut-off value of in-house WNV IgG Human ELISA. The table shows the net OD values obtained during validation of the in-house WNV IgG Human ELISA, as well as what the cut-off value was 73.86 (YI) and if the sample is classified as positive or negative.

WNV IgG Human ELISA		Net OD	Percentage (YI – 73.86)	Outcome	
				Commercial	In-house
Positive sera	ZRUA2067/22	**0.94**	94.3	Positive	Positive
	ZRUA1541/21	**0.52**	51.5	Positive	Negative
	ZRUA2099/22	**1.18**	117.7	Positive	Positive
	ZRUA1601/21	**1.07**	107	Positive	Positive
	ZRUA1607/21	**0.2**	61.7	Positive	Positive
	ZRUA1611/21	**0.78**	78.4	Positive	Positive
	ZRUA1652/21	**0.83**	83.4	Positive	Positive
	ZRUA2067/22	**0.70**	69.8	Positive	Borderline
	ZRUA2099/22	**0.81**	81.4	Positive	Positive
	ZRUA1550/21	**0.56**	55.8	Positive	Negative
Negative sera	ZRUA1560/21	**0.05**	4.9	Negative	Negative
	ZRUA1565/21	**0.05**	5	Negative	Negative
	ZRUA1581/21	**0.22**	21.8	Negative	Negative
	ZRUA2221/22	**0.06**	6.3	Negative	Negative
	ZRUA2253/22	**0.27**	26.5	Negative	Negative
	ZRUA1496/21	**0.00**	0.1	Negative	Negative
	ZRUA1513/21	**001**	1.2	Negative	Negative
	ZRUA1514/21	**0.2**	1.6	Negative	Negative
	ZRUA1485/21	**0.00**	0.1	Negative	Negative
	ZRUA1506/21	**0.00**	0.1	Negative	Negative
	ZRUA1527/21	**0.05**	4.5	Negative	Negative
	ZRUA1534/21	**0.14**	13.5	Negative	Negative

Table 6.4: Sensitivity and Specificity of in-house WNV IgG Human ELISA. The table shows the sensitivity and the specificity of the in-house WNV IgG Human ELISA, comparing the commercial IgM ELISA results with the in-house developed IgG ELISA.

WNV IgG Human ELISA	Confirmed pos	Confirmed neg
In-house ELISA pos	8	0
In-house ELISA neg	2	12

6.3.2 WNV IgM ELISA Development

The initial setup of the WNV IgM Human ELISA was based on coating the plate with goat anti-human IgM, followed by test sera and the WNV NS1 antigen, then a primary antibody mouse anti-WNV NS1 and lastly the HRP-conjugated goat anti-mouse secondary antibody. Figure 6.7 shows the results obtained from an initial run using the original setup. The OD values obtained were below 0.3, for both the positive (blue bars) and negative samples (orange bars), with no distinction between the two sets. The negative controls (green bars) had OD values ranging from 0.1 and 0.3, which indicates that there was high background, with some reagents reacting with each other. Optimisation steps included increasing the concentration of the goat anti-human IgM capture antibody, as well as increasing the amount of WNV NS1 antigen added to each well, but this did not make a difference.

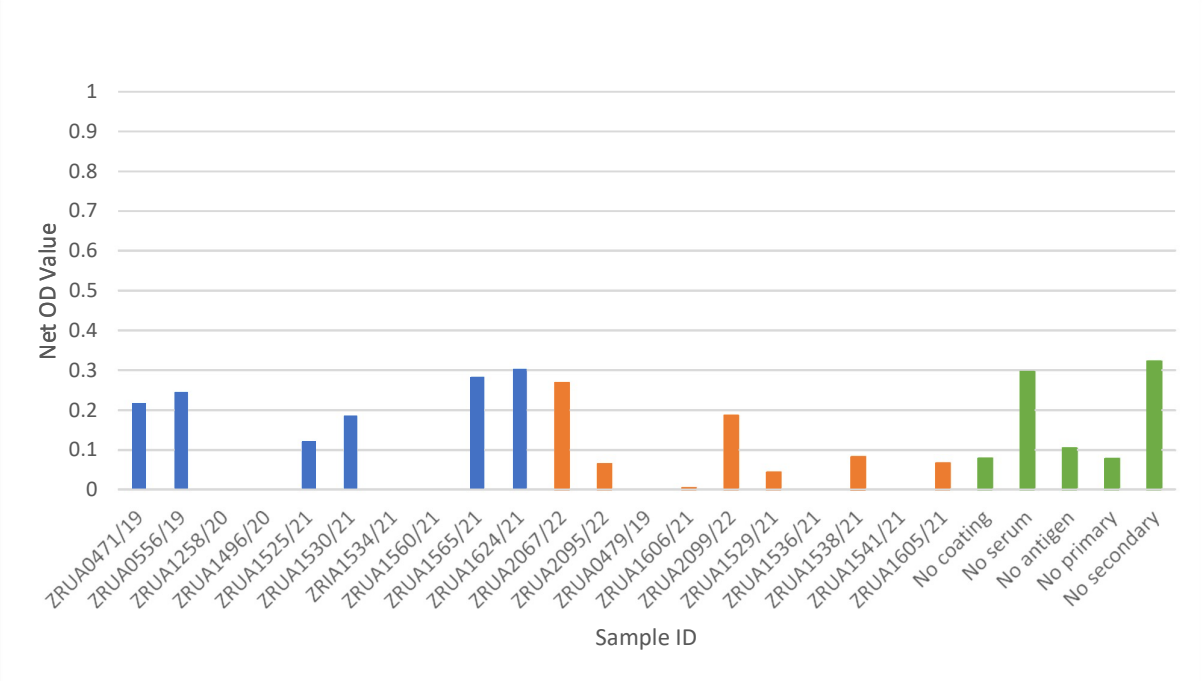

Figure 6.7: WNV IgM Human ELISA with the original setup. The figure shows the results obtained when using the goat anti-human IgM capture antibody to coat the plate with the WNV IgM Human ELISA. No difference observed between the positive samples (blue bars) and the negative samples (orange bars). The negative controls also had a high OD value.

Figure 6.8 shows the optimisation steps for the new setup of the WNV IgM Human ELISA. Different concentrations of coating the plate with WNV NS1 antigen was done – 2 µg/mL, 3 µg/mL, and 4 µg/mL. The dilutions of the HRP-conjugated rabbit anti-

human IgM secondary antibody were undiluted, 1:50 and 1:100. It was decided that 2 µg/mL for the NS1 antigen and undiluted for the conjugate yielded the most optimal results.

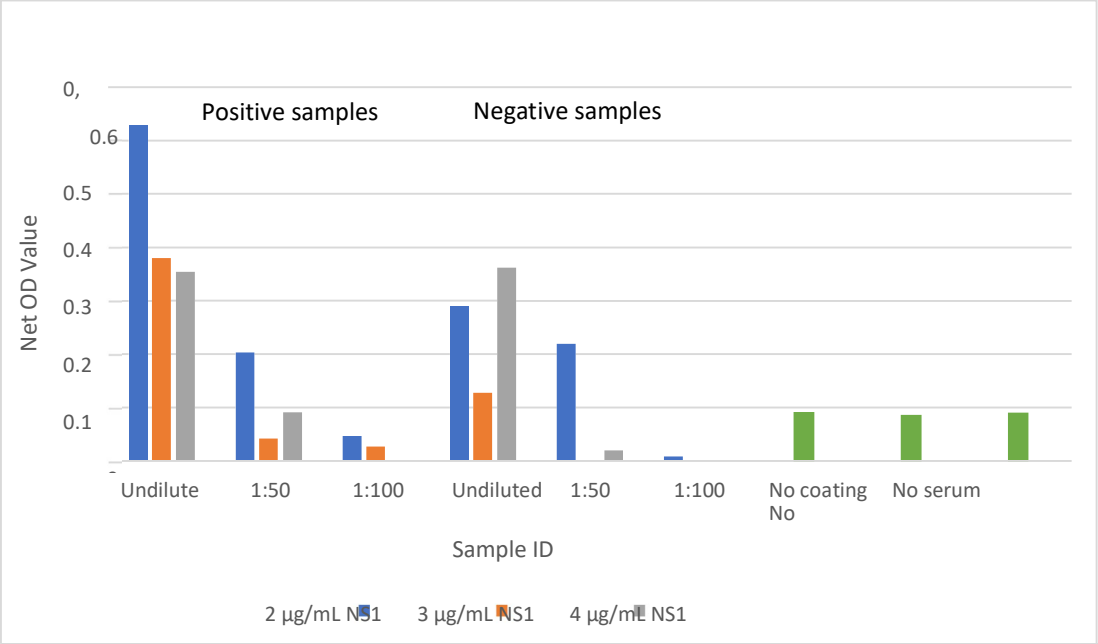

Figure 6.8: WNV IgM Human ELISA checkerboard titrations. The figure shows the results obtained when testing the NS1 antigen at different concentrations, as well as serum sample dilutions to determine the optimal conditions. The secondary antibody was tested undiluted (blue bars), 1:50 dilution (orange bars) and 1:100 dilution (grey bars). Negative controls were included (green bars).

After the determination of the most optimal conditions for the assay, a run was performed with positive and negative samples that were confirmed with the commercial WNV IgM ELISA, as well as neutralizsation assays. Table 6.5 shows the net OD values obtained from the run; Figure 6.9 is a graphical representation of the results.

Table 6.5: Net OD values obtained with the in-house WNV IgM Human ELISA. The table shows the net OD values obtained during validation of the in-house WNV IgM Human ELISA. Positive and negative samples were selected based on the neutralization assay outcomes.

WNV IgM Human ELISA		OD Values			Ratio
		WNV Antigen	Mock Antigen	Net OD	
Positive sera	ZRUA0471/19	1.17	1.03	**0.14**	**1.13**
	ZRUA1258/20	0.33	0.44	**0.00**	**0.75**
	ZRUA1496/20	0.21	0.3	**0.00**	**0.70**
	ZRUA1525/21	1.32	0.44	**0.88**	**2.98**
	ZRUA1530/21	0.88	0.31	**0.57**	**2.88**
	ZRUA1249/20	0.62	0.16	**0.46**	**3.83**
	ZRUA1235/20	0.12	0.09	**0.03**	**1.38**
	ZRUA1515/21	0.83	0.72	**0.11**	**1.15**
	ZRUA1526/21	1.66	1.19	**0.47**	**1.39**
	ZRUA1252/20	0.22	0.10	**0.12**	**2.20**
	ZRUA1258/20	0.41	0.24	**0.16**	**1.67**
	ZRUA1606/21	1	0.59	**0.41**	**1.69**
	ZRUA1496/21	0.18	0.12	**0.06**	**1.55**
	ZRUA1513/21	0.93	0.27	**0.67**	**3.51**
	ZRUA1514/21	0.80	0.62	**0.18**	**1.28**
	ZRUA1585/21	0.64	0.57	**0.07**	**1.12**
	ZRUA0467/19	0.20	0.15	**0.04**	**1.29**
	ZRUA0478/19	0.12	0.11	**0.01**	**1.13**
Negative sera	ZRUA2067/22	0.71	0.80	**0.00**	**0.88**
	ZRUA2095/22	0.52	0.30	**0.22**	**1.75**
	ZRUA0476/19	0.63	0.27	**0.36**	**2.36**
	ZRUA1606/21	0.76	0.53	**0.23**	**1.44**
	ZRUA2099/22	0.87	0.50	**0.37**	**1.74**
	ZRUA1529/21	0.18	0.28	**0.00**	**0.66**
	ZRUA1536/21	0.26	0.45	**0.00**	**1.58**
	ZRUA1538/21	0.86	0.75	**0.12**	**1.16**
	ZRUA1541/21	0.43	0.41	**0.02**	**1.04**
	ZRUA1605/21	0.34	0.20	**0.14**	**1.68**
Negative control	No coating	0.07	x	**0.07**	**x**
	No serum	0.07	x	**0.07**	**x**
	No secondary	0.07	x	**0.07**	**x**

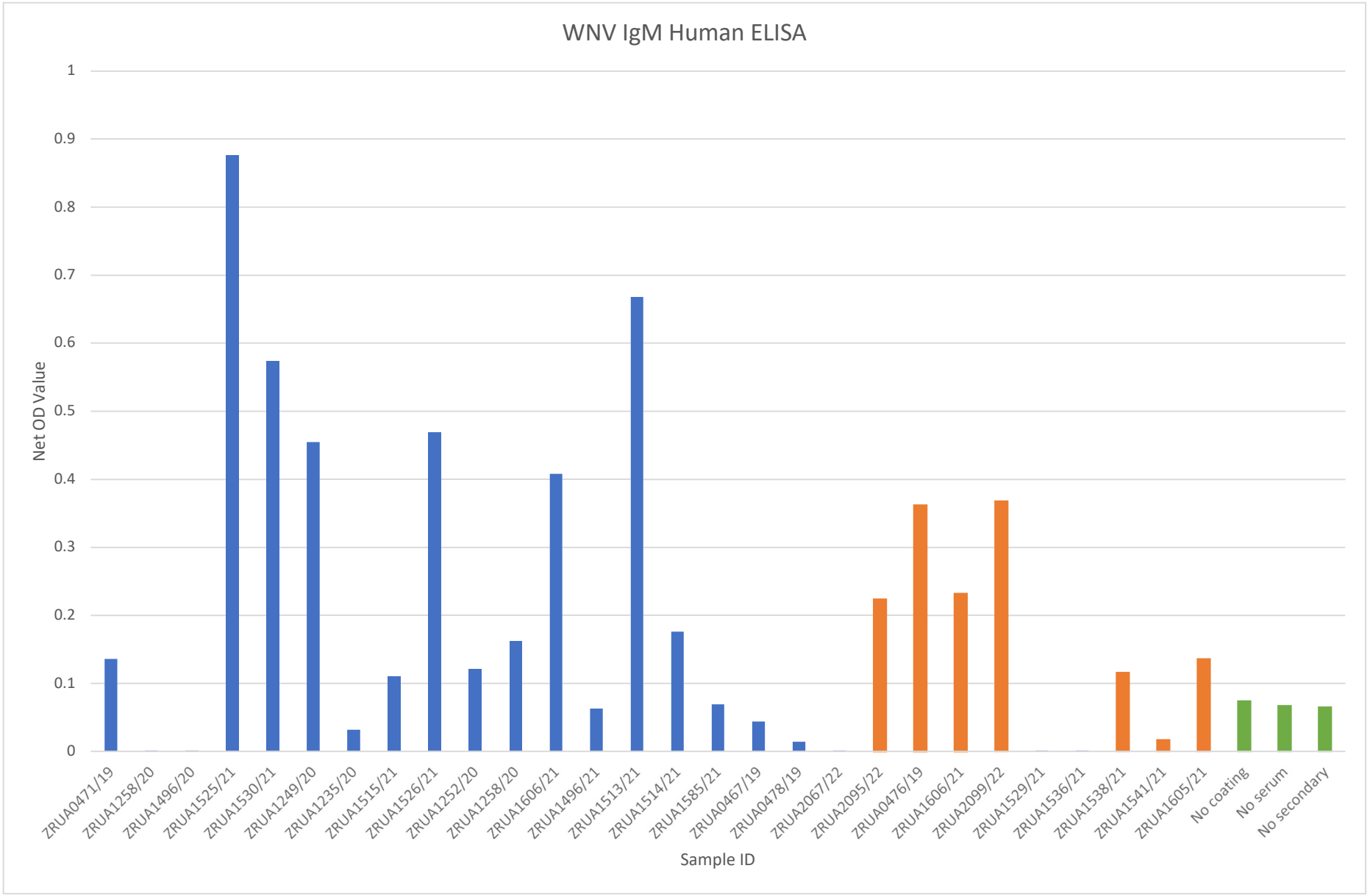

Figure 6.9: Net OD values obtained with the in-house WNV IgM Human ELISA. The bar shows the net OD values obtained during validation of the in-house WNV IgM Human ELISA. Positive (blue bars) and negative samples (orange bars) were selected based on the neutralisation assay outcomes.

Subsequently, four runs of negative samples only were performed on different days under different conditions to test repeatability and reproducibility, as well as to determine the cut-off value of the assay. Statistical software, MedCalc, was used to draw an ROC curve. Figure 6.10 shows the graph obtained:

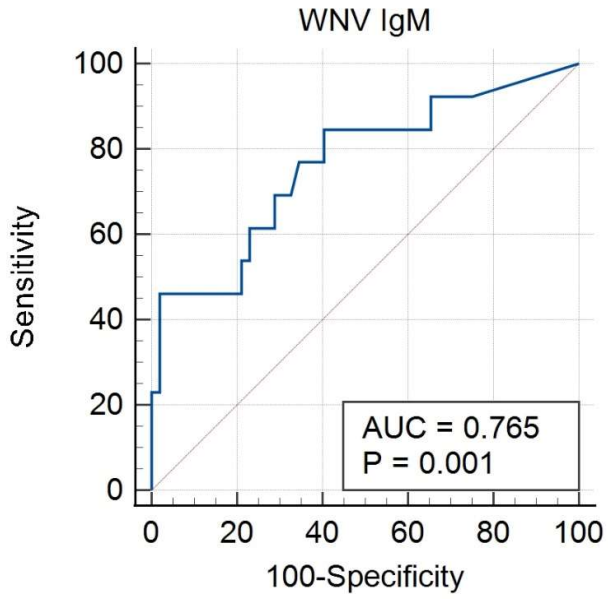

Figure 6.10: ROC curve for the WNV IgM Human ELISA. The figure shows the ROC curve obtained for the WNV IgM Human ELISA. An AUC value of 0.765 was obtained with a p value of <0.001. The ROC curve was generated using MedCalc.

The ROC curve was generated by making use of 13 positive samples and 52 negative samples that were repeated four times. The AUC value obtained was 0.765, which is classified as good. A Youden Index (J) of 0.4423 was achieved. The sensitivity was determined to be 84.62%, while the specificity was 59.62%. Comparing the cut-off value to the net OD values obtained, 6/24 samples (25%) were positive, with 10/10 samples (100%) being negative (Table 6.6). For further optimisation, Eurosorb (Euroimmun, Lübeck, Germany) was included to dilutethe samples, since it pellets IgG antibodies out, resulting in more IgM antibodies available in the serum. Table 6.6 shows the results obtained after including Eurosorb. Previous experiments were done without the use of Eurosorb and the sensitivity and specificity increased after the inclusion of Eurosorb.

Table 6.6: Cut-off value of in-house WNV IgM Human ELISA. The table shows the net OD values obtained during validation of the in-house WNV IgM Human ELISA, as well as what the cut-off value was 44.23 (YI) and if the sample is classified as positive or negative.

WNV IgM Human ELISA		Net OD	Percentage (YI - 44.23)	Outcome	
				Commercial	In-house
Positive sera	ZRUA0471/19	0.14	13.6	Positive	Negative
	ZRUA1258/20	0.00	0.1	Positive	Negative
	ZRUA1496/20	0.00	0.1	Positive	Negative
	ZRUA1525/21	0.88	87.6	Positive	Positive
	ZRUA1530/21	0.58	57.4	Positive	Positive
	ZRUA1249/20	0.46	45.5	Positive	Positive
	ZRUA1235/20	0.03	3.2	Positive	Negative
	ZRUA1515/21	0.11	11	Positive	Negative
	ZRUA1526/21	0.47	46.9	Positive	Positive
	ZRUA1252/20	0.12	12.1	Positive	Negative
	ZRUA1258/20	0.16	16.2	Positive	Negative
	ZRUA1606/21	0.41	40.8	Positive	Borderline
	ZRUA1496/21	0.06	6.3	Positive	Negative
	ZRUA1513/21	0.67	66.8	Positive	Positive
	ZRUA1514/21	0.18	17.6	Positive	Negative
	ZRUA1585/21	0.07	6.9	Positive	Negative
	ZRUA0467/19	0.04	4.4	Positive	Negative
	ZRUA0478/19	0.01	1.4	Positive	Negative
Negative sera	ZRUA2067/22	0.00	0.1	Negative	Negative
	ZRUA2095/22	0.22	22.4	Negative	Negative
	ZRUA0476/19	0.36	36.2	Negative	Negative
	ZRUA1606/21	0.23	23.2	Negative	Negative
	ZRUA2099/22	0.37	36.8	Negative	Negative
	ZRUA1529/21	0.00	0.1	Negative	Negative
	ZRUA1536/21	0.00	0.1	Negative	Negative
	ZRUA1538/21	0.12	11.6	Negative	Negative
	ZRUA1541/21	0.02	1.7	Negative	Negative
	ZRUA1605/21	0.14	13.6	Negative	Negative

Table 6.7: Sensitivity and specificity of in-house WNV IgM Human ELISA. The table shows the sensitivity and the specificity of the in-house WNV IgM Human ELISA, comparing the commercial IgM ELISA results with the in-house developed IgM ELISA.

WNV IgM Human ELISA	Confirmed pos	Confirmed neg
In-house ELISA pos	6	0
In-house ELISA neg	18	10

6.4 Discussion

Detection of WNV through molecular testing can be challenging, due to the short viraemia in infected animals, which makes the use of serological assays, like paired serum 2 weeks apart and IgG ELISA or an IgM ELISA 7 days after the onset of signs, a more effective means of confirming infection. Enzyme linked immunosorbent assays are highly sensitive, economical immunodiagnostic assays that can detect both antigens and antibodies depending on the setup (Sahu, 2022). These assays are widely used to detect the acute and exposure levels of WNV infection in humans and animals by using serum or plasma samples (Sahu, 2022). The IgM antibody appears between 5-7 days post-infection and remains in the serum for up to one month, which is why it is a good indicator of acute infection, while IgG antibodies have a long half-life, making it ideal for determining previous exposure (Sahu, 2022).

The aim of this study was to develop and validate a recombinant NS1 baculovirus expressed antigen-based IgG and IgM ELISA for the serodiagnosis of WNV in humans. There are commercial WNV IgM and IgG Human ELISAs available from Euroimmun (Euroimmun, Lübeck, Germany) but these are expensive and have to be imported.

In both assays, a cut-off value had to be determined to distinguish between positive and negative samples. Net OD values were obtained using PBS coated wells to consider the non-specific reactivity or background noise. By using the statistical software, MedCalc (MedCalc Software Ltd, Flanders, Belgium), a ROC curve was constructed, and the Youden Index provided the cut-off value for the assay. Sensitivity and specificity, as well as p-values were provided by the software to determine efficacy of the assays.

Standardisation of the WNV IgG Human ELISA was attempted using checkerboard titrations to determine the optimal dilution of the coating NS1 antigen, serum, as well as HRP-conjugated secondary antibody. A run was performed using a panel of positive and negative samples, as well as a negative only run to determine reproducibility. There were little to no difference between the negative repeat runs, which indicates high reproducibility. The ROC curve was constructed using MedCalc and the AUC value of 0.915 was achieved. This was interpreted as excellent. There is not a commercial WNV IgG ELISA available in the laboratory to compare the in-house result to, which is a limitation of the study. However, only two of the samples that tested positive by the commercial IgM assay did not come up with the IgG assay, which reduced the calculated sensitivity to 77%. This may however be due to these two samples not having IgG antibodies when the sample was taken. In general, the IgG assay therefore performed

well and could be used in a research setting to investigate seroprevalence.

When it comes to the standardisation of the WNV IgM Human ELISA, it was a much more challenging task. The original setup of the IgM ELISA was based on the test sera being sandwiched between an anti-human coating antibody and an anti-NS1 antibody for detection. This resulted in very low OD values, indicative more of background than any detection. The coating antibody used was a polyclonal goat anti-human antibody, which could possibly be interacting with the secondary HRP-conjugated goat anti-mouse antibody; however, this would likely have resulted in higher background noise. Another possible explanation could be that the mouse anti-WNV NS1 primary antibody does not bind properly to the recombinant expressed WNV NS1 antigen. This could be due to the recombinant antigen not being biologically active and can thus not be used in ELISAs. Many different optimisation steps were attempted to try and better the assay, but ultimately it was decided that it is not effectively detecting any WNV IgM antibodies, and a new setup was required.

The new setup for the WNV IgM Human ELISA used a more direct approach, which started by coating the plate with the WNV NS1 antigen, followed by the addition of the test sera and lastly HRP-conjugated anti-human IgM antibody from Euroimmun (Euroimmun, Lübeck, Germany). The conjugate was part of the commercial WNV IgM ELISA kit from Euroimmun and was the only available antibody for the new setup. Alternatively, the goat anti-human IgM capture antibody can be added after the test sera, followed by HRP-conjugated donkey anti-goat secondary antibody (Sahu, 2022). Various optimisation steps were performed ultimately leading to the use of a panel of positive and negative sera on the developed assay. The ROC curve generated, resulted in an AUC of 0.765 and a Youden's Index of 0.4423, which can be interpreted as good. The sensitivity and specificity of the commercial WNV IgM Human ELISA (Euroimmun) was 94.4% and 99.8% respectively. The commercial WNV IgM ELISA from Euroimmun's target antigen is the E protein, while the in-house developed IgM ELISA targets the NS1 protein, which may contribute to the difference in sensitivity and specificity of the two assays. Two studies generated antibodies against WNV NS1 protein and investigated the secretion of WNV NS1 during WNV infection using an ELISA assay (Macdonald, 2005; Fisher, 2023;). The NS1 protein was detected up to day five in infected hamsters and up to three days post-infection in mice, which suggested that the levels of NS1 during infection is low (Fisher et al., 2023). The commercial WNV IgM and IgG ELISA available on the market targets the E protein, so the introduction of a NS1-based serology assay should be investigated with regards to diagnosis and determining differentiation between the viruses

of the flavivirus family (Fisher et al., 2023). However, looking at the results obtained with the study, it is clear that the commercial IgM assays against the E protein is much more sensitive and specific than the NS1 assays. According to recent studies NS1 based diagnosis cannot replace other serology, especially when the diagnosis is made long after the infection, due to its low sensitivity (Fisher et al., 2023). The data from our study suggest that the IgG ELISA could possibly be used if paired sera is available to identify an increase in antibodies in acute infections.

There are several strengths and limitations of this study. It was possible to successfully develop an IgG ELISA to use in determining the seroprevalence of WNV in humans. A limitation of the WNV IgG Human ELISA was the lack of available serum, since the only serum available was known positive and negatives from the WNV IgM commercialELISA kit confirmed with neutralisation assays. However, the ELISA was optimised and validated with consistent results being obtained. For the in-house IgM ELISA, it was attempted to standardise using a polyclonal capture antibody, goat anti-human IgM, and included a primary and secondary antibody, but very low signal was obtained with little to no difference between the positive and negative samples. It has previously been reported that monoclonal antibodies are preferred as a capture antibody while developing a capture ELISA (Sahu, 2022). By changing the setup of the IgM ELISA, better results were obtained with high OD values for the positive samples and lower distinct OD values. The limitation with this setup, was the use of the commercial ELISA kit's HRP-conjugated anti-human IgM secondary antibody, since they do not provide information regarding how the antibody was produced, as well as its concentration.

6.5 Conclusion

The baculovirus expressed NS1 protein was useful for establishing an IgG ELISA but was not sensitive enough to use in an IgM ELISA format to detect antibodies in serum from humans. The IgG assay has demonstrated relatively high sensitivity and specificity, but the IgM assay was not as sensitive as the commercial WNV ELISA, which targets the E protein.

Chapter 7 – Establishment of serological assays to detect the presence of WNV and WLSB antibodies in horses, cattle and as a species independent setup

7.1 Introduction

West Nile virus (WNV) is endemic in Africa and spread to tropical, as well as moderate or temperate climate regions across all continents with an increasing number of infections in humans and animals in the Americas, specifically the United States (US), Canada and Mexico, and Europe especially the Mediterranean regions (Pierson and Diamond, 2020). West Nile virus infects many species including humans, horses, birds and wildlife- a few cases have also been reported in cattle and dogs in South Africa (SA) that was detected through polymerase chain reaction (PCR), so the incidence is not known in the absence of serological assays (Venter, 2017; Steyn, 2019). Wesselsbron virus (WLSB) is endemic to Africa and has been detected serologically in Thailand (CFSPH, 2017). It mainly affects cattle and sheep and is associated with abortions, but limited studies are available on its importance in other animals (Diagne, 2017). It was detected in horses with neurological signs in 2022 (refer to Chapter 4) as well as in 2009, but has not been well described (Human, 2009). After an incubation period of 3 to 15 days, WNV infection in horses lead to a short viraemic phase with low virus titres (Castillo-Olivares and Wood, 2004). Molecular assays like real-time reverse transcriptase polymerase chain reaction (RT-PCR) can be used to confirm infection, but cases are often missed due to the short viraemia of WNV. With regards to WSLB, serological tests that have been described include hemagglutination inhibition, complement fixation and virus neutralisation tests (Weyer, 2013). Serological assays have been established to detect acute WNV and WSLB in horses and other animals, either through detection of immunoglobulin M (IgM) or using paired serum of 2-3 weeks apart to detect an increase in immunoglobulin G (IgG) antibodies (Beck, 2017; Oymans, 2020).

There is a commercial WNV IgM Equine enzyme linked immunosorbent assay (ELISA) available from InBios (Seattle, Washington, US), but it is expensive to purchase and must be imported from the US No IgM ELISA is available for other species. For this reason, the aim of this study was to evaluate the baculovirus expressed non-structural protein 1 (NS1) proteins detection of WNV IgM and IgG in horses and cattle as well as a species independent setup.

The aim of this study was to develop an in-house IgG and IgM ELISA for WNV that is as sensitive and specific as the commercial kit and adapt the assay for detection of WNV in cattle. Second, we wanted to develop an IgG and IgM ELISA for WSLB to use in surveillance of horses and livestock.

7.2 Materials and Methods

7.2.1 Clinical Samples

Samples used to develop, optimise, and validate the WNV IgG, and IgM ELISA were selected based on the outcome of the commercial WNV IgM ELISA kit for equines (InBios, Seattle, USA) and serum neutralisation assays (See Chapter 5). For WSLB ELISA development, rabbit sera were used as a positive control, since there was not any available positive serum available. The rabbit sera were produced by our collaborators at Wageningen University & Research (WUR) in the Netherlands and had a final concentration of 1 mg/mL, which allowed for a concept ELISA to be developed (Oymans et al., 2020). With regards to the bovine IgM ELISA, cattle sera from 2010-2022 were screened with serum neutralisation assays for WNV and WSLB (See Appendix Table A3).

7.2.2 Expressed NS1 Antigen

Wageningen University & Research expressed the WNV and WSLB NS1 antigen and exported it to us to use in the development of the ELISAs.

7.2.3 IgG ELISA targeting WNV and WSLB

To coat the MaxiSorp medium absorption plate (Thermo Fisher, Massachusetts, USA), 100 µL of the NS1 antigen WNV (1.43 mg/mL) and WSLB (7.6 mg/mL) respectively was added to each well at a concentration of 2 µg/mL and incubated overnight at 4 °C (Series 2000, Scientific Engineering, Johannesburg, South Africa). With regards to optimisation, the amount of antigen needed to coat the ELISA plates the protein solution was diluted in either PBS or carbonate buffer at various dilutions to determine the optimal coating buffer. Each sample was added in duplicate with one well coated with the NS1 antigen and the other well coated with phosphate buffer saline (PBS) (Merck, New Jersey, USA), imitating a mock antigen to determine background of the sample. The following day, the plate was washed six times with 300 µL 0.1% Tween®20 (Sigma Aldrich, Missouri, USA), using an automatic platewasher (Mindray MW-12A, Vacutec, South Africa). Next 200 µL of 10% skim milk (SPAR, Pretoria, South Africa) was added to each well for the blocking step and the plate incubated for

1 hour at 37°C. The washing step was repeated. The sera were diluted in 2% skim milk using a 1:100 ratio and 100 µL doubling dilutions added to the plate. Various dilutions were tested as part of optimisation. The plate was incubated for 1 hour at 37°C, followed by the washing step. After establishing conditions for coating and the correct buffers to use, concentration of the secondary antibody were experimented with, the HRP-conjugated goat anti-equine antibody (NovusBio, Colorado, USA) were prepared for proper titration of antibody concentration. The ideal concentration should provide the highest signal with the lowest amount of background noise. The recommended use is at a dilution of 1:10 000. Next, 100µL horseradish peroxidase (HRP) conjugated rabbit-anti equine secondary antibody (Sigma Aldrich,Missouri, USA), was added to each well in a 1:1000 dilution and the plate incubated for 1 hour at 37°C. The washing step was repeated. For the detection step,100 µL 2,2'-Azinobis [3-ethylbenzothiazoline-6-sulfonic acid]-diammonium salt (ABTS) (SurModics, Minnesota, USA) was added to each well and the plate incubated in a dark chamber for 30 minutes at room temperature (20-22°C). After the 30 minutes, 100 µL 1% sodium dodecyl sulphate (SDS) (Amresco, Idaho, USA), was added to the wells to stop the reaction. Readings were taken at a wavelength of 405 nm Mindray MR-96A microplate reader (Mindray, Hong Kong, China). Figure 7.1 shows the schematic representation of the WNV IgG Equine ELISA setup, with Figure 7.2 showing the WSLB IgG ELISA setup. After the optimal conditions were determined, a run was performed using previously confirmed positive and negative samples to determine if the assay works. The samples used to validate the WNV IgG Equine ELISA were obtained from the results of the commercial IgM ELISA (refer to Chapter 4). These samples were confirmed with neutralisation assays to confirm the virus specificity as WNV or WSLB, and it was assumed that a positive neutralization assay result indicates the presence of IgG or IgM antibodies.

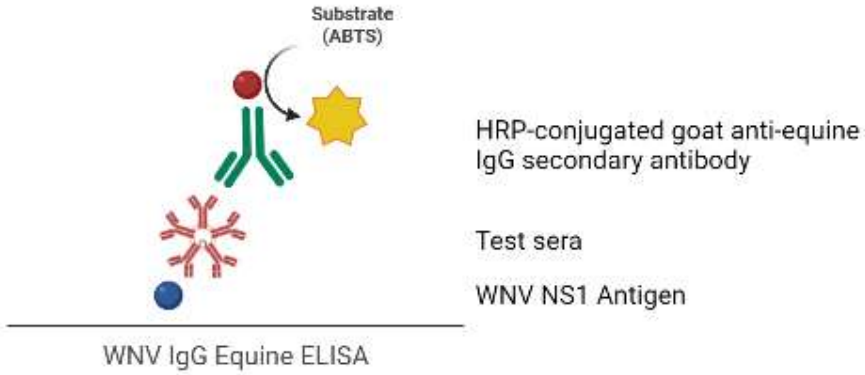

Figure 7.1: WNV IgG Equine ELISA Setup. The figure shows the setup of the WNV IgG Equine ELISA that starts with coating the plate with the WNV NS1 antigen, followed by the addition of test sera and lastly the HRP-conjugated goat anti-equine IgG secondary antibody. Picture made by BioRender.

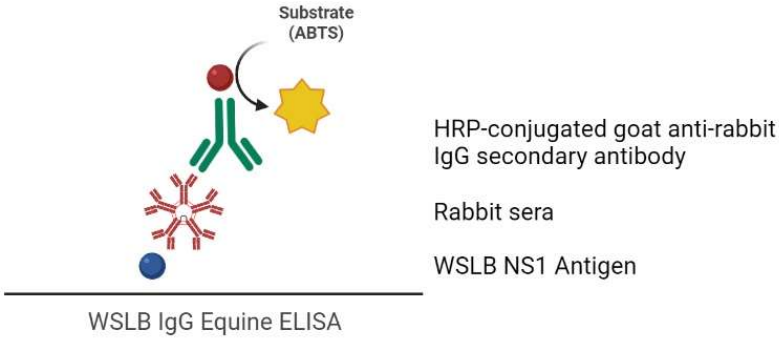

Figure 7.2: WSLB IgG Equine ELISA Setup. The figure shows the setup of the WSLB IgG Equine ELISA that starts with coating the plate with the WSLB NS1 antigen, followed by the addition of test sera and lastly the HRP-conjugated goat anti-rabbit IgG secondary antibody. Picture made by BioRender.

7.2.4 Equine IgM ELISA targeting WNV and WSLB

The MaxiSorp medium absorption plate (Thermo Fisher, Massachusetts, USA) was coated with a mouse anti-equine IgM capture antibody (Figure 7.4). To determine whether the sensitivity will increase, the coating antibody was changed to a mouse anti-equine IgM capture antibody. The mouse anti-equine IgM antibody (NovusBio,Colorado, USA) is a polyclonal antibody used to ensure detection of IgM antibodies in equine samples and is recommended to be used at a concentration of 0.5 µg/mL by the manufacturers. The polyclonal antibody selected for detection of WNV in the IgM ELISA has the advantage that they rarely fail to bind to the antigen (Rajna, 2020). Enzyme linked immunosorbent assay sensitivity can be increased by using indirect detection using polyclonal antibodies, due to higher levels of polyclonal antibody that binds to the target antigen (Rajna and Irena, 2020). A more direct approach was decided on and was made up on the basis of the WNV IgG Equine ELISA (Figure 7.3) Optimisation steps included antigen concentration, sample dilution, as well

as primary and secondary antibody dilutions, as explained in section 2.2. To coat the plate, 100 µL of the NS1 antigen WNV and WSLB respectively (2 µL/mL) was added to each well and incubated overnight at 4°C. The following day, the plate waswashed six times with 300 µL 0.1% Tween (Thermo Fisher Scientific, Massachusetts, USA) using an automatic plate washer (Mindray MW-12A, Vacutec, South Africa). Next 200 µL of 10% skim milk (SPAR, Pretoria,South Africa) was added to each well for the blocking step and the plate incubated for 1 hour at 37°C. The washing step was repeated. The sera were diluted in 2% skim milk using a 1:100 ratio and 100 µL doubling dilutions added to the plate. Eurosorb was included to dilute the samples,since it pellets IgG antibodies out, resulting in more IgM antibodies available in the serum. The plate was incubated for 1 hour at 37°C, followed by the washing step.Next 100 µL of mouse anti-equine IgM antibody (0.5 ng/mL) (NovusBio, Colorado, USA) was added to each well and incubated for 1 hour at 37°C. The washing step was repeated, followed by the addition of 100 µL HRP conjugated goat-anti mouse secondary antibody (Seracare,Massachusetts, USA) to each well in a 1:1000 dilution and the plate incubated for 1 hour at 37°C. The washing step was repeated. For the detection step, 100 µL ABTS was added to each well and the plate incubated in a dark chamber for 30 minutes at room temperature (20-22°C). After the 30 minutes, 100 µL 1% SDS was added to the wells to stop the reaction. Photometric measurement was performed using the Mindray MR-96A microplate reader (Mindray, Hong Kong, China) at a wavelength of 450 nm.

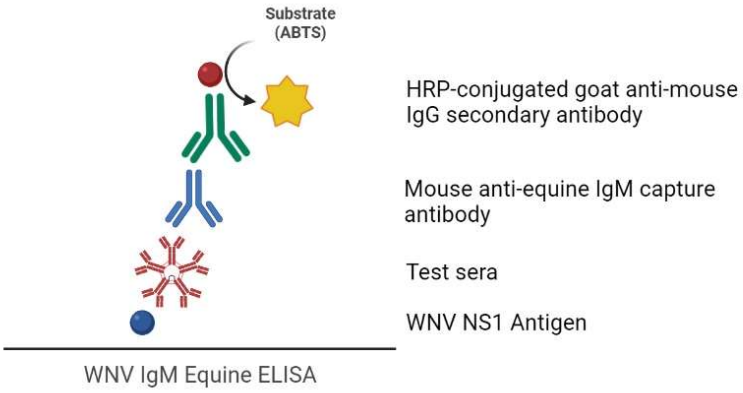

Figure 7.3: WNV IgM Equine ELISA Setup. The figure shows the setup of the WNV IgM Equine ELISA that starts with coating the plate with the WNV NS1 antigen, followed by the addition of test sera, then mouse anti-equine IgM capture antibody and lastly the HRP-conjugated goat anti-mouse IgG secondary antibody. Picture made by BioRender.

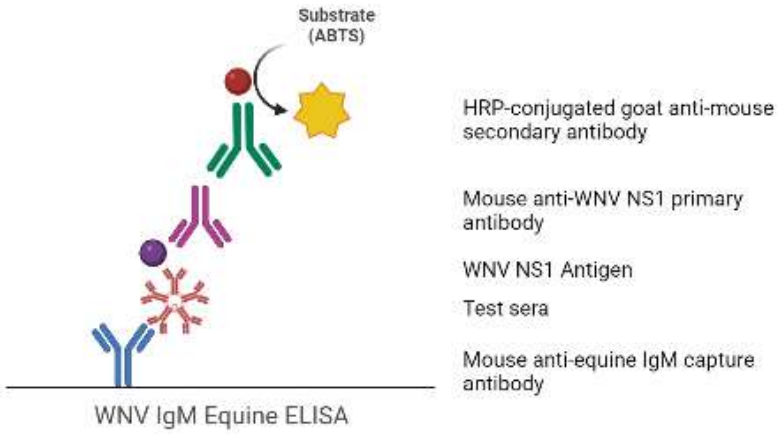

Figure 7.4: WNV IgM Equine ELISA Original Setup. The figure shows the setup of the original WNV IgM Equine ELISA that starts with coating the plate with the goat anti-equine/mouse anti-equine IgM capture antibody, followed by the addition of test sera, the WNV NS1 antigen, then mouse anti-WNV NS1 antibody and lastly the HRP-conjugated goat anti-mouse IgG secondary antibody. Picture made by BioRender.

7.2.5 Bovine IgM ELISA targeting WNV and WSLB

Coating of the plate with WNV and WSLB NS1 antigen was performed as explained for the equine ELISA in section 2.3, as well as blocking and washing steps.The MaxiSorp medium absorption plate (Thermo Fisher, Massachusetts, USA) was incubated for 1 hour at 37°C, followed by the washing step.Next 100 µL of goat anti-bovine IgM antibody (0.5ng/ml) (KPL, Seracare, Massachusetts, USA) was added to each well and incubated for 1 hour at 37°C. The washing step was repeat, followed by the addition of HRP conjugated donkey anti-goat secondary antibody (Invitrogen, Thermo Fisher Scientific, Massachusetts, USA). The recommended dilution is between 1:2000 and 1:20000. Various dilutions were tested in conjunction with the goat anti-bovine IgM antibody to determine the optimal concentration for detection. Finally, 1:1000 dilution of the secondary antibody was used and 100 µL added to each well and the plate incubated for 1 hour at 37°C. The washing step was repeated. For the detection step, 100 µL ABTS was added to each well and the plate incubated in a dark chamber for 30 minutes at room temperature (20-22°C). After the 30 minutes, 100 µL 1% SDS was added to the wells to stop the reaction. Readings were taken using the Mindray MR-96A microplate reader (Mindray, Hong Kong, China) at a wavelength of 450 nm. Refer to Figure 7.5 for the Bovine IgM ELISA setup.

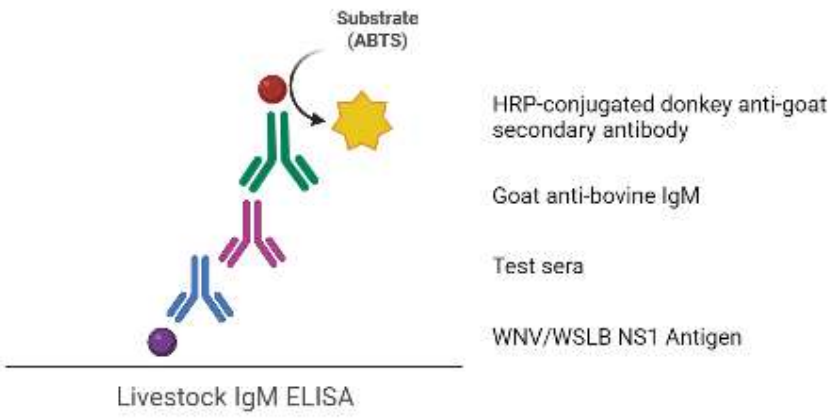

Figure 7.5: WNV/WSLB IgM Bovine ELISA Setup. The figure shows the setup of the WNV/WSLB IgM Bovine ELISA that starts with coating the plate with the WNV/WSLB NS1 antigen, followed by the test sera, then goat anti-bovine IgM antibody and lastly the HRP-conjugated donkey anti-goat IgG secondary antibody. Picture made by BioRender.

7.2.6 Species Independent IgG ELISA

To coat the MaxiSorp medium absorption plate (Thermo Fisher, Massachusetts, USA), 100 µL of the NS1 antigen WNV and WSLB respectively (2 µL/mL) was added to each well and incubated overnight at 4°C. The following day, the plate was washed six times with 300 µL 0.1% Tween using an automatic plate washer. Next 200µL of 10% Skim milk (SPAR, Pretoria,South Africa) was added to each well for the blocking stepand the plate incubated for 1 hour at 37°C. The washing step was repeated. The serum was diluted in 2% skim milk using a 1:100 ratio and 100 µL doubling dilutions added to the plate. The plate was incubated for 1 hour at 37°C, followed by the washing step. Next, 100 µL HRP conjugated Protein G antibody (EMD Millipore Corp, Massachusetts, USA) was added to each well in a 1:5000 dilution, as recommended by manufacturers, and the plate incubated for 1 hour at 37°C. The washing step was repeated. For the detection step, 100 µL ABTS was added to each well and the plate incubated in a dark chamber for 30 minutes at room temperature (20-22°C). After the 30 minutes, 100 µL 1% SDS was added to the wells to stop the reaction. Readings were taken at a wavelength of 405 nm using the Mindray MR-96A microplate reader (Mindray, Hong Kong, China). Refer to Figure 7.6 and Figure 7.7 for the schematic representation of the assay. Protein G is a bacterial cell wall protein that is produced by groups C and G streptococci and has the ability to bind at the Fc region of many immunoglobins (Pfaunmiller et al., 2016). This results in adsorbed antibodies that have a good orientation and high activity for binding to the target compounds (Pfaunmiller et al., 2016). Protein G can bind to many types of immunoglobulins allowing it to be used inassays with a wide range of antibodies, targets,

and samples (Akerström et al., 1985). It has been determined that Protein G successfully binds to IgG antibodies from rabbits, rats, humans, goat, cow and equine species (Akerström et al., 1985).

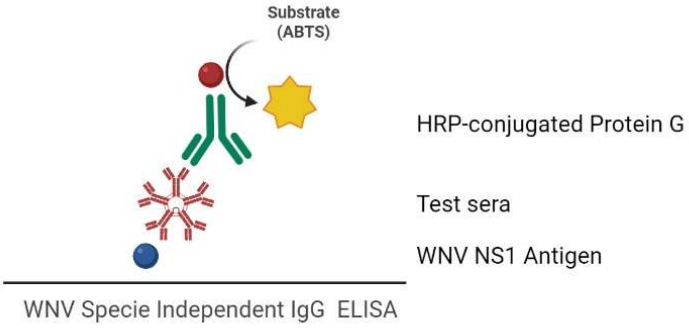

Figure 7.6: WNV Specie Independent IgG ELISA Setup. The figure shows the setup of the WNV Specie independent IgG ELISA that starts with coating the plate with the WNV NS1 antigen, followed by the addition of test sera and lastly the HRP-conjugated Protein G secondary antibody. Picture made by BioRender.

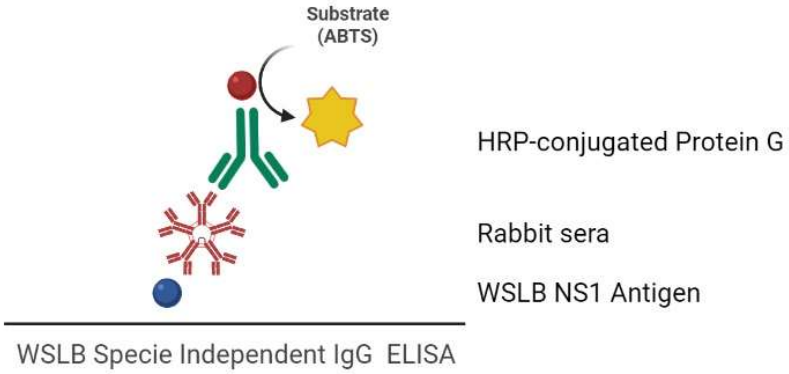

Figure 7.7: WSLB Specie Independent IgG ELISA Setup. The figure shows the setup of the WSLB Specie independent IgG ELISA that starts with coating the plate with the WSLB NS1 antigen, followed by the addition of test sera and lastly the HRP-conjugated Protein G secondary antibody.

2.2.8 Statistical analysis

The statistical analysis on each ELISA was determined exactly the same as in Chapter 6. Once again, the ratios were shown (WNV antigen/Mock antigen) as a comparison to the commercial kit from InBios (InBios, Seattle, USA). Specimens with a ratio of ≥ 3 were considered positive, and those with a ratio of ≤ 2 were considered negative as defined by the kit. Specimens with a ratio of < 3.0 but > 2.0 were considered borderline but possible positives. The cut-off value for each assay was determined individually through a receiver operating curve (ROC) curve and Youden-index (J). The ROC curve connects the coordinate points using “1 – specificity (false positive rate)” as the x-axis and “sensitivity”

as the y-axis for all cut-off values measured from the test results. The closer the ROC curve is to the upper left corner of the graph, the higher the accuracy of the test since in the upper left corner, the sensitivity = 1 and the false positive rate = 0 (specificity = 1). The ideal ROC curve thus has an area under the curve (AUC = 1.0). The Youden Index refers to the distance between the 45° diagonal in the coordinate (0,1) direction. The cut-point that achieves this maximum is referred to as the optimal cut-point (c) because it is the cut-point that optimizes the biomarker's differentiating ability when equal weight is given to sensitivity and specificity (Ruopp, 2008). Youden's J statistic can be calculated as follows, and represents the value that is optimal for cut-off:

$$J = Se + Sp-1$$

Four runs of negative only samples were performed on the in-house ELISAs to obtain a set of negative samples that measures reproducibility of the assay. The positive results used are the OD values obtained from the validation run. This results in a sample set that was used to determine the cut-off value of the respective assays.

7.3 Results

7.3.1 WNV IgG ELISA Development

Figure 7.8 shows the various concentrations of WNV NS1 antigen, provided byWageningen University & Research, used to coat the plate, comparing the absorbance to the amount of antigen used for coating. An optimal dilution of 2 µg/mL for the antigen was determined to be best for coating the plate, with the highest OD values observed, while also using the antigen sparingly. Different dilutions of serum samples were tested, and the results obtained can be seen in Figure 7.8. By making use of 2 µg/mL WNV NS1 antigen, the 1:100 dilution of serum samples allowed for distinction between the positive and negative sera, with low background and efficient detection.

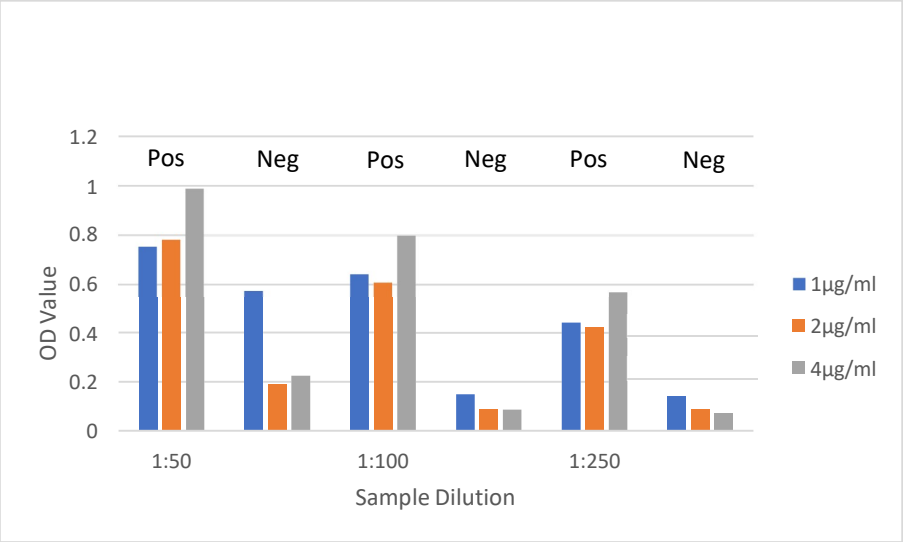

Figure 7.8: Antigen concentration and serum sample dilutions. The NS1 antigen is recommended to use at a concentration of 2 ug/mL, while serum samples are recommended to be diluted 1:100. The graph shows different serum dilution and antigen concentration to determine the optimal combination.

An experiment was also performed using a positive and negative set of samples comparing the effect of diluting the WNV NS1 antigen in PBS or carbonate buffer for coating. The NS1 antigen diluted in PBS had lower OD values observed, compared to the NS1 antigen diluted in bicarbonate buffer. Antigen diluted in bicarbonate buffer had very high OD values and little to no difference was observed between the samples, indicating that there are high background and nonspecific binding involved, whereas the antigen diluted in PBS, had lower background. Thereafter, it was decided that diluting the antigen in PBS is the best option. Figure 7.9 shows the different OD values obtained using different concentrations of the secondary antibody. To reduce background and prevent too quick colour development, the 1:1000 dilution was selected to detect the presence of WNV antibodies in the samples, 10x more than the recommended amount.

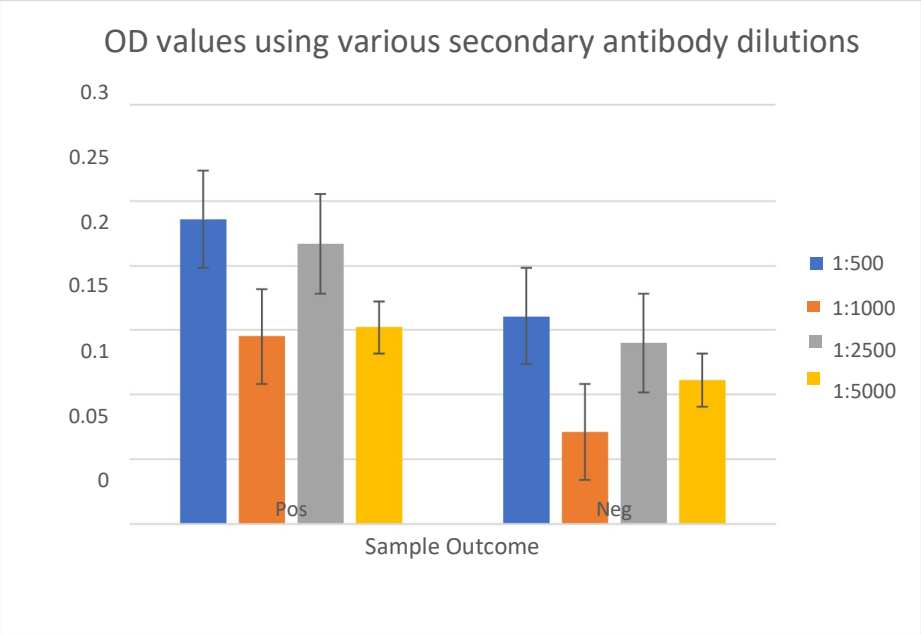

Figure 7.9: WNV IgG Equine ELISA secondary antibody dilutions. The HRP-conjugated rabbit anti-equine IgG secondary antibody is used for detection and is recommended to be used at a dilution of 1:1000. Three other dilutions were tested – 1:500, 1:2500 and 1:5000.

Table 7.1 shows the respective OD values obtained from the run, while Figure 7.10 shows a graphical representation of the results obtained from the WNV IgG Equine ELISA. A total of 26 positive samples were available for testing after being confirmed having neutralising antibodies against WNV. In addition, a negative panel of 13 serum sample was used and tested on the WNV IgGequine ELISA on four different occasions to determine reproducibility and draw a ROC to determine the cut-off value (Figure 7.11).

Table 7.1: Net OD values obtained with the in-house WNV IgG Equine ELISA. The table shows the net OD valuesobtained during validation of the in-house WNV IgG Equine ELISA. Positive and negative samples were selected based on the neutralisation assay outcomes.

WNV IgG Equine ELISA		OD Values			Ratio
		WNV NS1 Antigen	Mock Antigen	Net OD	
Positive sera	ZRU119/17	0.80	0.16	**0.65**	**5.12**
	ZRU096/21	0.65	0.16	**0.49**	**4.06**
	ZRU057/19	2.43	0.13	**2.30**	**18.95**
	ZRU063/19	2.02	0.10	**1.92**	**20.84**
	ZRU090/19	2.26	0.11	**2.14**	**20.13**
	ZRU058/20	2.21	0.12	**2.09**	**19.18**
	ZRU066/20	1.21	0.20	**1.01**	**6.01**
	ZRU122/20	1.65	0.10	**1.55**	**16.68**
	ZRU058/21	1.09	0.13	**0.96**	**8.29**
	ZRU094/19	1.43	0.14	**1.29**	**10.42**
	ZRU145/21	0.92	0.09	**0.83**	**10.65**
	ZRU146/21	1.03	0.10	**0.93**	**10.02**
	ZRU023/17	1.15	0.11	**1.04**	**10.54**
	ZRU057/20	2.22	0.10	**2.11**	**21.32**
	ZRU038/17	0.68	0.11	**0.56**	**6.04**
	ZRU082/17	1.77	0.35	**1.42**	**5.06**
	ZRU013/19	0.50	0.33	**0.18**	**1.54**
	ZRU027/19	2.03	0.23	**1.80**	**8.81**
	ZRU090/19	1.62	0.09	**1.53**	**18.16**
	ZRU145/21	1.06	0.09	**0.97**	**11.69**
	ZRU083/19	1.70	0.10	**1.59**	**16.31**
	ZRU057/20	1.49	0.09	**1.40**	**16.42**
	ZRU033/19	0.88	0.11	**0.77**	**7.74**
	ZRU035/19	1.88	0.10	**1.78**	**18.99**
	ZRU143/19	1.15	0.08	**1.06**	**13.98**
	ZRU146/21	1.12	0.09	**1.03**	**11.95**
Negative sera	ZRU012/22	0.84	0.29	**0.55**	**2.85**
	ZRU013/22	0.16	0.33	**0.16**	**0.51**
	ZRU011/17	0.87	0.11	**0.75**	**7.79**
	ZRU020/17	0.99	0.11	**0.88**	**9.03**
	ZRU072/17	0.29	0.28	**0.01**	**1.04**
	ZRU018/19	0.76	0.09	**0.67**	**8.17**
	ZRU007/22	0.83	0.08	**0.74**	**9.86**
	ZRU035/17	1.17	0.08	**1.09**	**14.49**
	ZRU082/17	1.61	0.18	**1.42**	**8.78**
	ZRU104/17	1.34	0.08	**1.26**	**17.36**
	ZRU119/17	0.47	0.08	**0.16**	**6.05**
	ZRU072/17	0.14	0.07	**0.07**	**1.92**
	ZRU079/17	0.14	0.07	**0.07**	**1.92**

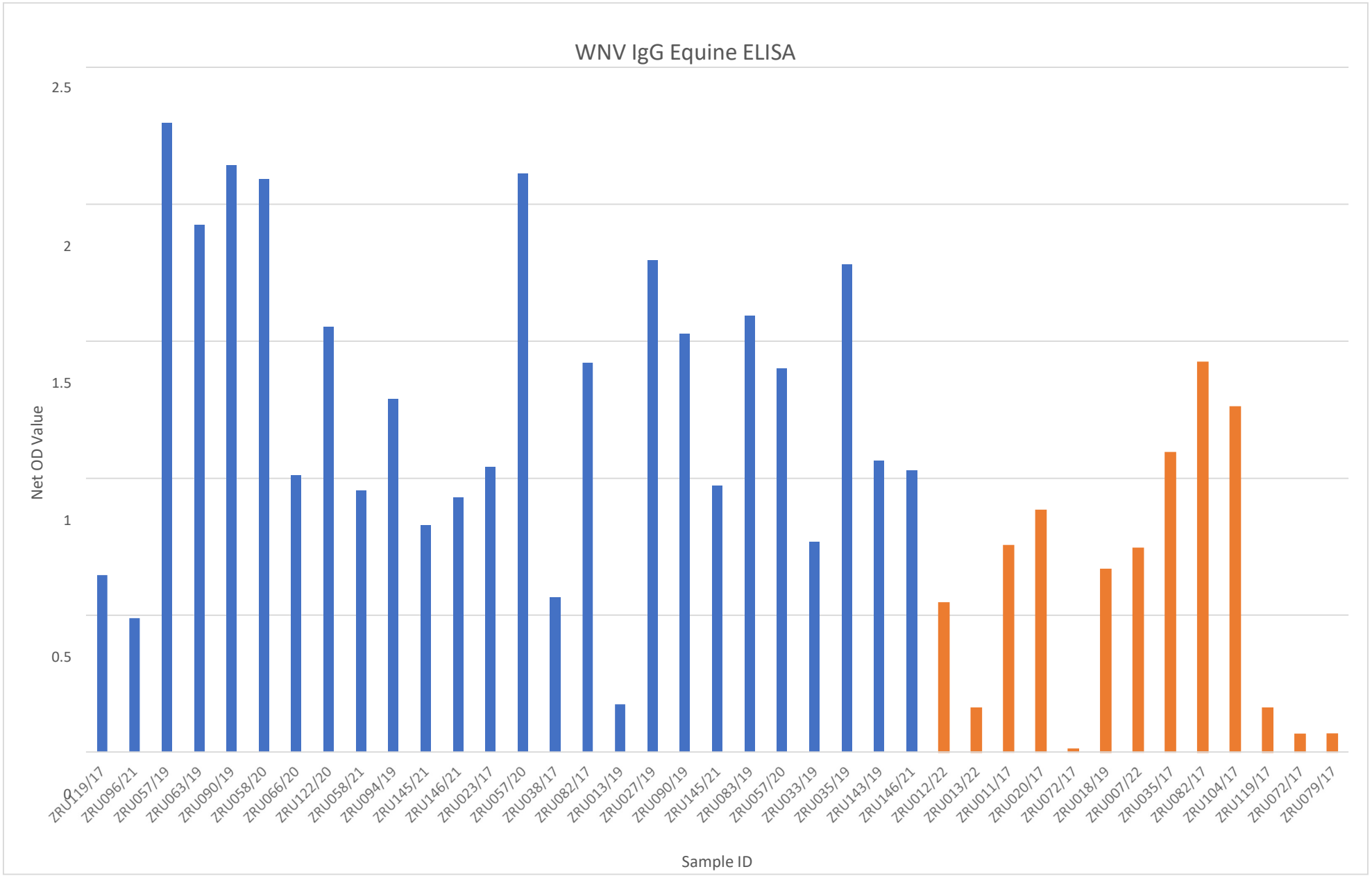

Figure 7.10: Net OD values obtained with the in-house WNV IgG Equine ELISA. The bar shows the net OD values obtained during validation of the in-house WNV IgG Equine ELISA.Positive and negative samples were selected based on the neutralisation assay outcomes.

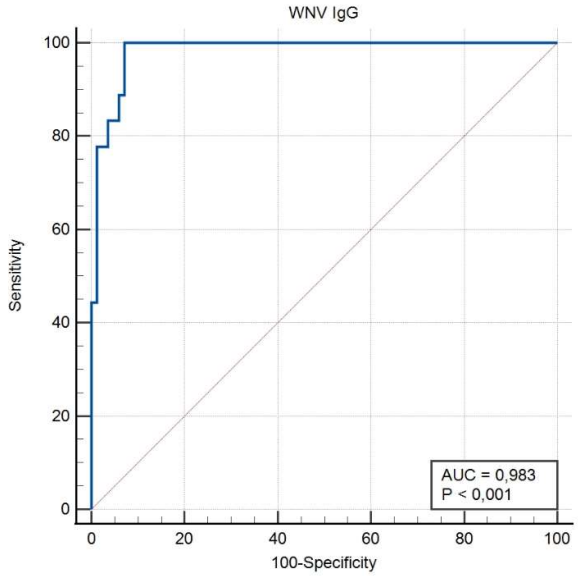

Figure 7.11: ROC curve for the in-house WNV IgG Equine ELISA. The figure shows the ROC curve obtained for the in-house WNV IgG Equine ELISA. An AUC value of 0.983 was obtained with a p value of <0.001. The ROC curve was generated using MedCalc.

By making use of MedCalc, the ROC curve was generated, as seen in Figure 7.11. The sample size usedto construct the ROC curve was 18 positive samples and 21 negative samples that were repeated on four different days for reproducibility, thus yielding 84 results to be used. The AUC value obtained was 0.983, which can be interpreted as excellent anda Youden's Index of 0.98286 was determined.

The sensitivity of the assay was determined to be 100%, while the specificity was 92.86% (Table 7.2 and Table 7.3).

Table 7.2: Cut-off value of in-house WNV IgG Equine ELISA. The table shows the net OD values obtained during validation of the in-house WNV IgG Equine ELISA, as well as what the cut-off value was (YI) and if the sample is classified as positive or negative.

WNV IgG Equine ELISA		Net OD Value	Cut-off value (YI - 92.8)		
				Commercial	In-house
Positive sera	ZRU119/17	0.65	64.6	Positive	Negative
	ZRU096/21	0.49	48.9	Positive	Negative
	ZRU057/19	2.30	229.8	Positive	Positive
	ZRU063/19	1.92	192.4	Positive	Positive
	ZRU090/19	2.14	214.3	Positive	Positive
	ZRU058/20	2.09	209.1	Positive	Positive
	ZRU066/20	1.01	101.2	Positive	Positive
	ZRU122/20	1.55	155.2	Positive	Positive
	ZRU058/21	0.96	95.5	Positive	Negative
	ZRU094/19	1.29	129	Positive	Positive
	ZRU145/21	0.83	83	Positive	Negative
	ZRU146/21	0.93	92.9	Positive	Negative
	ZRU023/17	1.04	104	Positive	Positive
	ZRU057/20	2.11	211.3	Positive	Positive
	ZRU038/17	0.56	56.4	Positive	Negative
	ZRU082/17	1.42	142.2	Positive	Positive
	ZRU013/19	0.18	17.5	Positive	Negative
	ZRU027/19	1.80	179.7	Positive	Positive
	ZRU090/19	1.53	152.7	Positive	Positive
	ZRU145/21	0.97	97.3	Positive	Negative
	ZRU083/19	1.59	159.2	Positive	Positive
	ZRU057/20	1.40	140.3	Positive	Positive
	ZRU033/19	0.77	76.8	Positive	Negative
	ZRU035/19	1.78	178.1	Positive	Positive
	ZRU143/19	1.06	106.4	Positive	Positive
	ZRU146/21	1.03	102.9	Positive	Positive
Negative sera	ZRU012/22	0.55	54.5	Negative	Negative
	ZRU013/22	0.16	16.1	Negative	Negative
	ZRU011/17	0.75	75.4	Negative	Negative
	ZRU020/17	0.88	88.3	Negative	Negative
	ZRU072/17	0.01	1.1	Negative	Negative
	ZRU018/19	0.67	66.7	Negative	Negative
	ZRU007/22	0.74	74.4	Negative	Negative
	ZRU035/17	1.09	109.3	Negative	Positive
	ZRU082/17	1.42	142.3	Negative	Positive
	ZRU104/17	1.26	126	Negative	Positive
	ZRU119/17	0.16	16.1	Negative	Negative
	ZRU072/17	0.07	6.5	Negative	Negative
	ZRU079/17	0.07	6.6	Negative	Negative

Table 7.3: Sensitivity and Specificity of in-house WNV IgG Equine ELISA. The table shows the sensitivity and thespecificity of the in-house WNV IgG Equine ELISA, comparing the commercial IgM ELISA results with the in-house developed IgG ELISA.

WNV IgG Equine ELISA	Confirmed pos	Confirmed neg
In-house ELISA pos	17	3
In-house ELISA neg	9	10

7.3.2 WNV IgM ELISA Development

The basis for the WNV IgM Equine ELISA is similar to that of the WNV IgG EquineELISA, so the optimisation steps done previously is similar, apart from the anti-equine IgM antibody required for the WNV IgM Equine ELISA. Initially, the setup of the WNV IgM Equine ELISA was different as we chose to use goat anti- equine IgM capture antibodies (NovusBio,Colorado, USA) to coat the plate.The results can be seen in Figure 7.12. There was no difference observed between thepositive and negative sera, as well as the negative control. High OD values were observed, which suggested that background detection was very high.

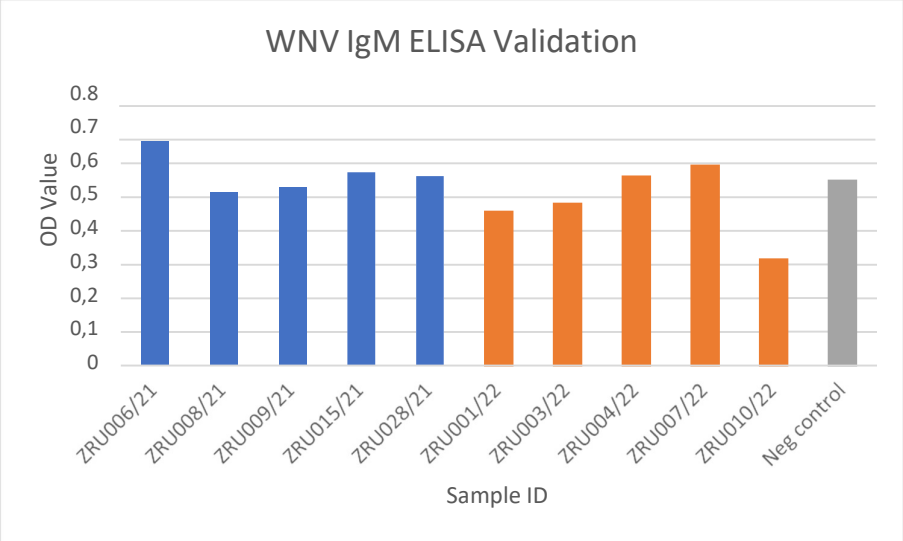

Figure 7.12: WNV IgM Equine ELISA with the original setup. The figure shows the results obtained when using the goat anti-equine IgM capture antibody to coat the plate with in the WNV IgM Equine ELISA. No difference observed between the positive samples (blue bars) and the negative samples (orange bars). The negative control also had a high OD value.

Coating the plate with the mouse anti-equine IgM capture antibody, very low OD values were observed across all samples (less than 0.2) as well as no difference observed between the positive and negative sera, as well as the negative control (Figure 7.13). The set-up was re-evaluated to attempt at making the assay more sensitive.

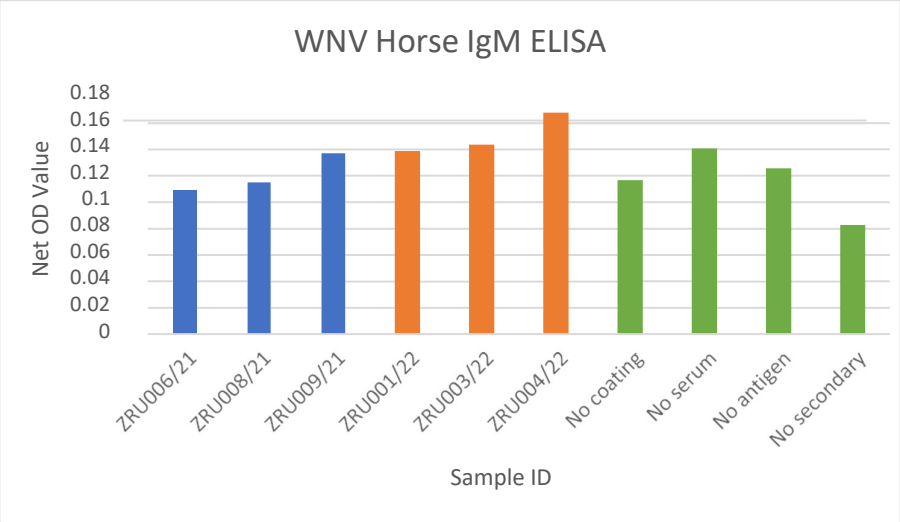

Figure 7.13: WNV IgM Equine ELISA with the new capture antibody. The figure shows the results obtained when using the mouse anti-equine IgM capture antibody to coat the plate. No difference was observed between the positive samples (blue bars) and the negative samples (orange bars). The negative controls also had a high OD value. Lower OD values were observed overall.

Figure 7.14 shows the outcome of the optimisation experiment. The blue bars represent the ZRU029/17. Using the mouse anti-equine IgM antibody at a concentration of 1 ng/mL per well yielded the most optimal results, with the positive sample having a high OD value, while the negative sample has a very low OD value, showing a big difference between the two samples, as well as very little background detected.

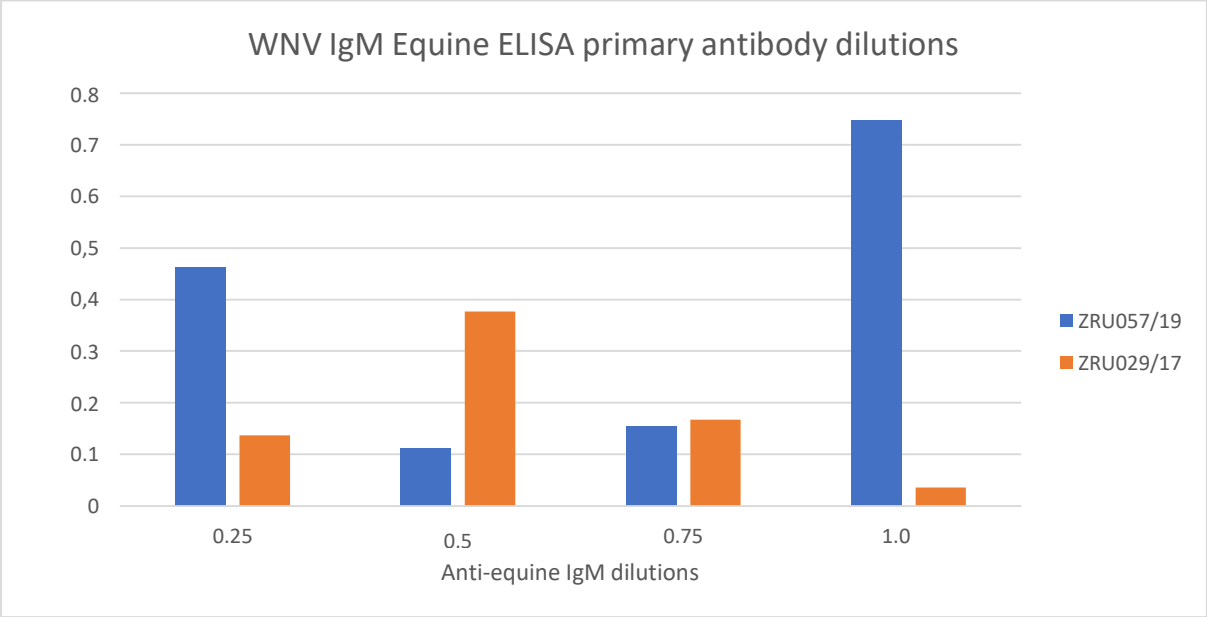

Figure 7.14: WNV IgM Equine ELISA primary antibody dilutions. The figure shows the results obtained when using the mouse anti-equine IgM capture antibody as a primary antibody and which dilution yields the optimal concentration. A positive sample (blue bars) and a negative sample (orange) was included.

Figure 7.15 shows the optimal concentration of the secondary antibody, HRP-conjugated goat anti-mouse IgG and it was determined that the 1:1000 dilution is the most efficient to use in this assay.

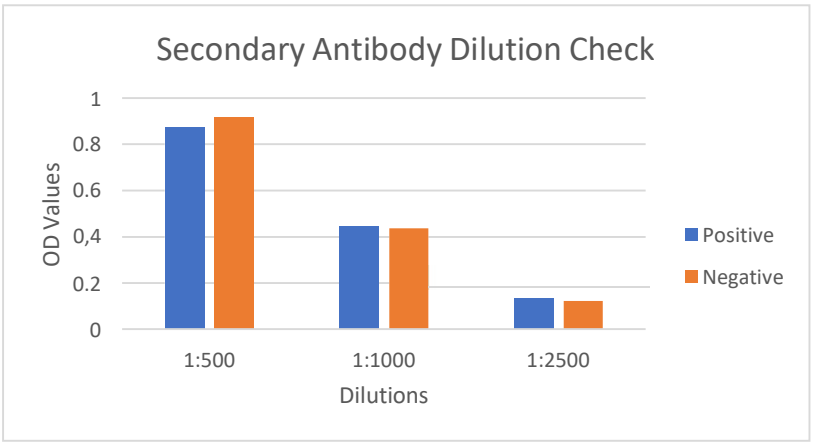

Figure 7.15: WNV IgM Equine ELISA secondary antibody dilutions. The HRP-conjugated goat anti-mouse IgG antibody was used as the secondary antibody and is recommended for use at a dilution of 1:1000. Two other dilutions were tested – 1:500 and 1:2500.

After the optimal concentrations were determined, an IgM run was performed to determine if the assay works. The samples used to validate the WNV IgM Equine ELISA were obtained from the results of the commercial IgM ELISA (refer to Chapter

5). These samples were confirmed with neutralization assays, and it was assumed that a positive neutralisation assay result indicates the presence of WNV specific IgM antibodies. Figure 7.16 shows the results of the WNV IgM Equine ELISA making use of 1 ng/mL mouse anti-equine IgM antibody. Low OD values were observed, with some samples having such high background, that the net OD value resulted in a negative value. The negative controls (green bars) had similar or even higher OD values than some of the samples, which indicates high background noise and unspecific binding.

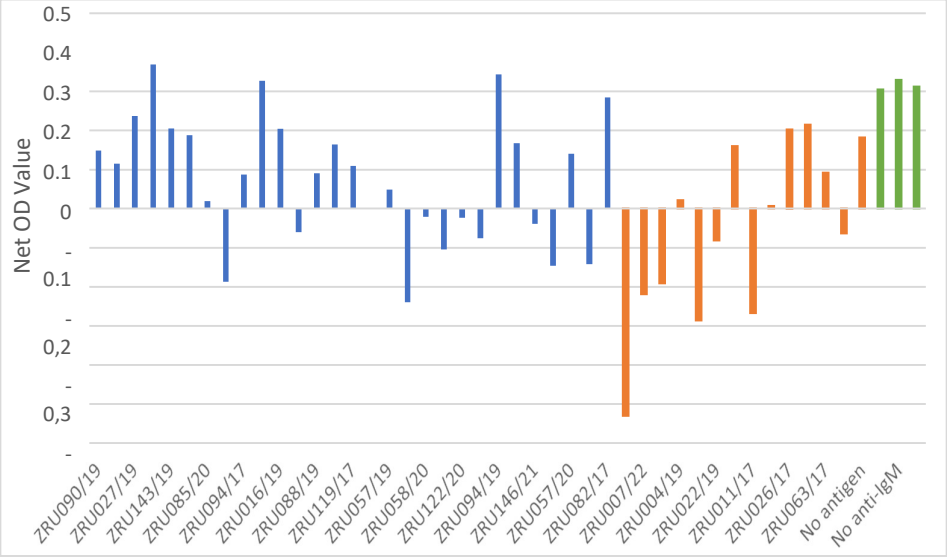

Figure 7.16: WNV IgM Equine ELISA with 1.0 ng/mL primary antibody dilution. The figure represents the net OD values obtained when using a concentration of 1.0 ng/mL mouse anti-equine IgM primary antibody. Several samples had a higher background OD value than what the sample had, thus resulting in a negative OD value. Low ODvalues were obtained. No difference between the positive samples (blue bars), negative samples (orange bars) and negative controls (green bars).

Very high background was observed, with little to no difference between the positive and negative sera. It was then decided to continue the validation with the original recommended mouse anti-equine IgM antibody dilution of 0.5 ng/mL per well to see if there is improvement. Figure 7.17 shows the results obtained after a WNV IgM Equine ELISA run with a sample set consisting of positive and negative samples, with Table 7.4 showing the net OD values obtained for the run.

Table 7.4: Net OD values obtained with the in-house WNV IgM Equine ELISA. The table shows the net OD values obtained during validation of the in-house WNV IgM Equine ELISA. Positive and negative samples were selected based on the neutralisation assay outcomes.

WNV IgM Equine ELISA		OD Values			Ratio
		WNV Antigen	Mock Antigen	Net OD	
Positive sera	ZRU090/19	0.56	0.45	**0.11**	**1.25**
	ZRU013/19	1.27	0.69	**0.59**	**1.86**
	ZRU027/19	0.96	0.43	**0.53**	**2.24**
	ZRU083/19	0.74	0.44	**0.30**	**1.68**
	ZRU143/19	0.87	0.32	**0.55**	**2.71**
	ZRU069/20	0.91	0.92	**0.00**	**0.99**
	ZRU085/20	1.18	0.85	**0.33**	**1.38**
	ZRU028/21	1.32	0.55	**0.77**	**0.59**
	ZRU094/17	1.02	0.54	**0.48**	**1.89**
	ZRU124/17	0.87	0.27	**0.60**	**3.18**
	ZRU016/19	0.90	0.24	**0.66**	**3.74**
	ZRU033/19	0.80	0.40	**0.40**	**2.01**
	ZRU088/19	0.61	0.33	**0.29**	**1.87**
	ZRU104/17	0.61	0.26	**0.35**	**2.38**
	ZRU119/17	0.70	0.34	**0.36**	**2.06**
	ZRU096/21	0.63	0.46	**0.17**	**1.37**
	ZRU063/19	0.62	0.29	**0.33**	**2.14**
	ZRU058/20	0.57	0.13	**0.44**	**4.55**
	ZRU066/20	0.75	0.68	**0.07**	**1.10**
	ZRU122/20	0.34	0.29	**0.06**	**1.19**
	ZRU058/21	0.95	0.76	**0.18**	**1.24**
	ZRU094/19	1.24	0.68	**0.56**	**1.83**
	ZRU145/21	0.32	0.40	**0.00**	**0.79**
	ZRU146/21	0.76	0.55	**0.21**	**1.38**
	ZRU023/17	0.99	0.37	**0.63**	**2.70**
	ZRU057/20	0.63	0.65	**0.00**	**0.97**
	ZRU038/17	0.70	0.70	**0.00**	**0.99**
	ZRU082/17	0.45	0.30	**0.15**	**1.50**
Negative sera	ZRU004/22	0.15	0.11	**0.04**	**1.39**
	ZRU007/22	0.26	0.21	**0.05**	**1.26**
	ZRU011/22	0.11	0.09	**0.02**	**1.19**
	ZRU004/19	1.01	0.94	**0.07**	**1.07**
	ZRU018/19	0.97	0.53	**0.45**	**1.85**
	ZRU022/19	1.31	1.12	**0.19**	**1.17**
	ZRU031/19	0.21	0.08	**0.13**	**2.51**
	ZRU013/22	0.59	0.35	**0.24**	**1.70**
	ZRU011/17	0.29	0.14	**0.15**	**2.09**
	ZRU020/17	0.63	0.44	**0.20**	**1.45**
	ZRU026/17	0.48	0.39	**0.09**	**1.22**
	ZRU029/17	0.63	0.58	**0.05**	**1.09**
Negative control	No antigen	0.24	x	**0.24**	**x**
	No serum	0.20	x	**0.19**	**x**
	No anti-IgM	0.28	x	**0.28**	**x**
	No secondary	0.18	x	**0.18**	**x**

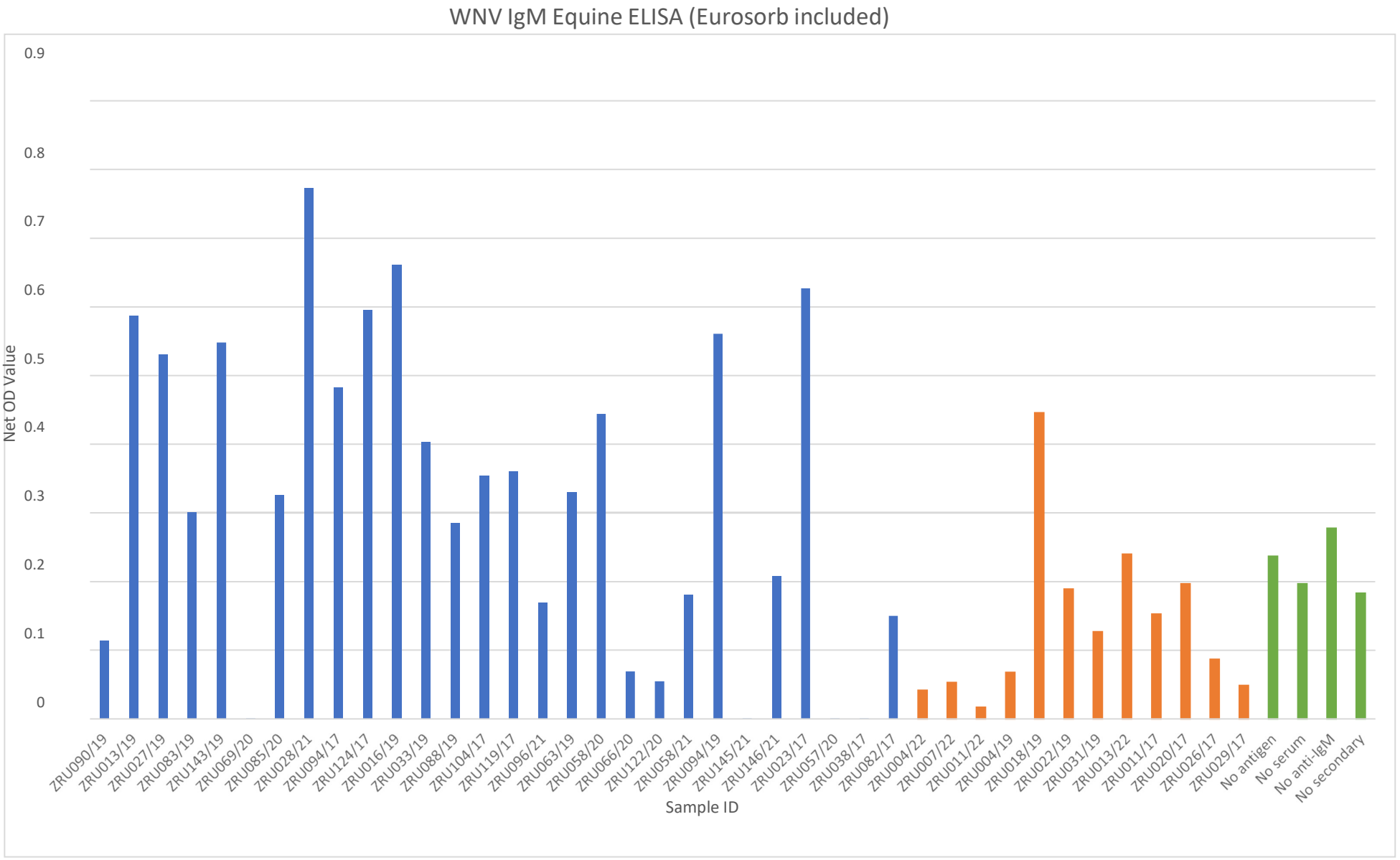

Figure 7.17: Net OD values obtained with the in-house WNV IgM Equine ELISA. The bar shows the net OD values obtained during validation of the in-houseWNV IgM Equine ELISA. Positive (blue bars) and negative samples (orange bars) were selected based on the neutralisation assay outcomes.

Subsequently, four runs of negative samples only were performed on different days to test reproducibility and determine the cut-off value, by drawing a ROC curve on MedCal (Figure 7.18).

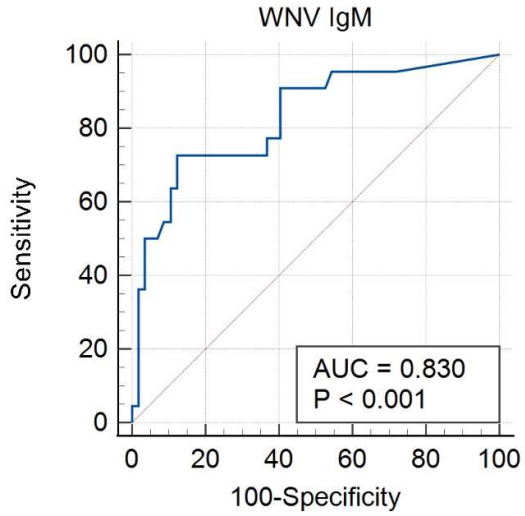

Figure 7.18: ROC curve for the in-house WNV IgM Equine ELISA. The figure shows the ROC curve obtained for the in-house WNV IgM Equine ELISA. An AUC value of 0.964 was obtained with a p value of <0.001. The ROC curve was generated using MedCalc.

The ROC curve was generated by making use of 14 positive samples and 13 negative samples that were repeated four times for reproducibility, thus yielding 52 negative OD values to use. The AUC value obtained was 0.830, which is classified as excellent and a Youden Index (J) of 0.6045 was determined. The sensitivity was determined to be 72.73%, while the specificity was 87.72%. Comparing the cut-off value to the net OD values obtained, 9/28 samples (32.14%) were positives, with all negative samples testing negative (Table 7.5).

Table 7.5: Cut-off value of in-house WNV IgM Equine ELISA. The table shows the net OD values obtained during validation of the in-house WNV IgM Equine ELISA, as well as what the cut-off value was (YI) and if the sample is classifiedas positive or negative.

WNV IgM Equine ELISA		Net OD Value	Percentage	Outcome	
			(YI - 60.45)	Commercial	In-house
Positive sera	ZRU090/19	0.11	11.4	Positive	Positive
	ZRU013/19	0.59	58.7	Positive	Borderline
	ZRU027/19	0.53	53.1	Positive	Borderline
	ZRU083/19	0.30	30.1	Positive	Negative
	ZRU143/19	0.55	54.8	Positive	Borderline
	ZRU069/20	0.00	0.1	Positive	Negative
	ZRU085/20	0.33	32.6	Positive	Negative
	ZRU028/21	0.77	77.3	Positive	Positive
	ZRU094/17	0.48	48.2	Positive	Negative
	ZRU124/17	0.60	59.6	Positive	Borderline
	ZRU016/19	0.66	66.2	Positive	Positive
	ZRU033/19	0.40	40.3	Positive	Negative
	ZRU088/19	0.29	28.5	Positive	Negative
	ZRU104/17	0.35	35.4	Positive	Negative
	ZRU119/17	0.36	36.1	Positive	Negative
	ZRU096/21	0.17	17	Positive	Negative
	ZRU063/19	0.33	33	Positive	Negative
	ZRU058/20	0.44	44.4	Positive	Negative
	ZRU066/20	0.07	6.9	Positive	Negative
	ZRU122/20	0.06	5.5	Positive	Negative
	ZRU058/21	0.18	18.1	Positive	Negative
	ZRU094/19	0.56	56.1	Positive	Borderline
	ZRU145/21	0.00	0.1	Positive	Negative
	ZRU146/21	0.21	20.8	Positive	Negative
	ZRU023/17	0.63	62.7	Positive	Positive
	ZRU057/20	0.00	0.1	Positive	Negative
	ZRU038/17	0.00	0.1	Positive	Negative
	ZRU082/17	0.15	15	Positive	Negative
Negative sera	ZRU004/22	0.04	4.2	Negative	Negative
	ZRU007/22	0.05	5.3	Negative	Negative
	ZRU011/22	0.02	1.7	Negative	Negative
	ZRU004/19	0.07	6.8	Negative	Negative
	ZRU018/19	0.45	44.6	Negative	Negative
	ZRU022/19	0.19	18.9	Negative	Negative
	ZRU031/19	0.13	12.7	Negative	Negative
	ZRU013/22	0.24	24	Negative	Negative
	ZRU011/17	0.15	15.3	Negative	Negative
	ZRU020/17	0.20	19.7	Negative	Negative
	ZRU026/17	0.09	8.7	Negative	Negative
	ZRU029/17	0.05	4.9	Negative	Negative

Table 7.6: Sensitivity and Specificity of in-house WNV IgM Equine ELISA. The table shows the sensitivity and thespecificity of the WNV IgM Equine ELISA, comparing the commercial IgM ELISA results with the in-house developed IgM ELISA.

WNV IgM Equine ELISA	Commercial pos	Commercial neg
In-house ELISA pos	9	0
In-house ELISA neg	19	12

7.3.3 WNV Bovine IgM ELISA

It was determined that the 1:5000 dilution is the most efficient to use in this assay (Figure 7.19).

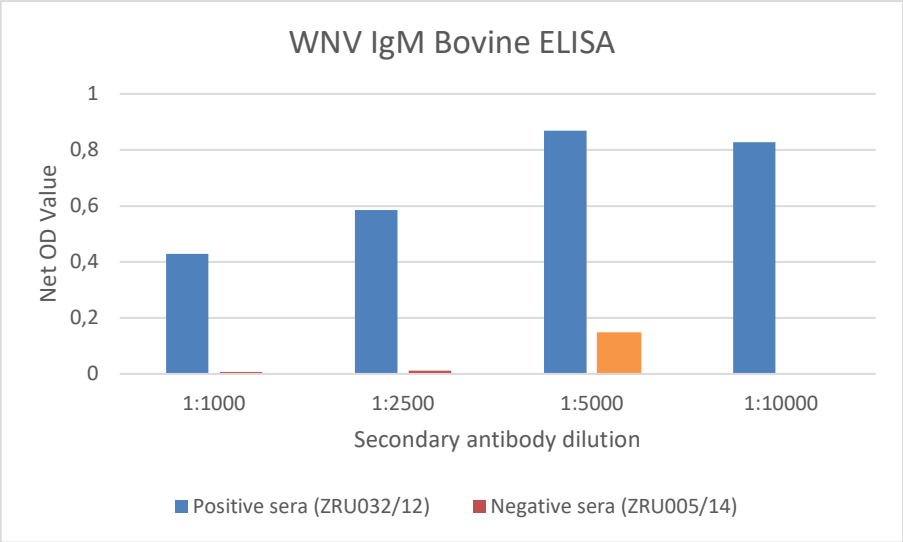

Figure 7.19: WNV IgM Bovine ELISA secondary antibody dilutions. The HRP-conjugated donkey anti-goat IgG antibody is used as the secondary antibody and is recommended for use at a dilution of between 1:2000 and 1:20 000. The dilutions that were tested included – 1:1000, 1:2500, 1:5000 and 1:10 000.

After the optimal concentrations were determined, an IgM run was performed to determine if the assay works. The samples used to validate the WNV IgM Bovine ELISA were obtained from the results of the neutralisation assays performed on livestock from 2012-2022 (Refer to Chapter 5). A positive neutralization result indicated the presence of antibodies. Figure 7.20 shows the results of the WNV IgM Bovine ELISA making use of 0.5 ng/mL goat anti-bovine IgM antibody. High OD values were observed. The negative controls that were included had very low OD values, indicating that there is not an interaction and unspecific binding between the antibodies used in the assay. Table 7.7 shows the Net OD values obtained for the run.

Table 7.7: Net OD values obtained with the in-house WNV IgM Bovine ELISA. The table shows the net OD values obtained during validation of the in-house WNV IgM Bovine ELISA. Positive and negative samples were selected based on the neutralisation assay outcomes.

WNV IgM Bovine ELISA		OD Values			Ratio
		WNV Antigen	Mock Antigen	Net OD	
Positive sera	ZRU108/22	1.81	1.17	**0.64**	**1.55**
	ZRU142/22	1.54	0.50	**1.04**	**3.07**
	ZRU032/12	1.44	0.46	**0.98**	**3.11**
	ZRU181/12	1.79	0.40	**1.38**	**4.45**
	ZRU022/12	1.62	0.41	**1.21**	**3.97**
	ZRU060/12	1.00	0.23	**0.78**	**4.41**
Negative sera	ZRU071/12	1.37	0.75	**0.63**	**1.84**
	ZRU189/12	2.02	1.35	**0.67**	**1.49**
	ZRU062/12	1.53	1.11	**0.42**	**1.38**
	ZRU035/13	1.38	0.99	**0.38**	**1.38**
	ZRU005/14	0.08	0.07	**0.00**	**1.05**
	ZRU173/15	1.30	0.44	**0.87**	**2.98**
Negative control	No antigen	0.08	x	**0.08**	**x**
	No serum	0.10	x	**0.10**	**x**
	No anti-IgM	0.07	x	**0.07**	**x**
	No secondary	0.28	x	**0.28**	**x**

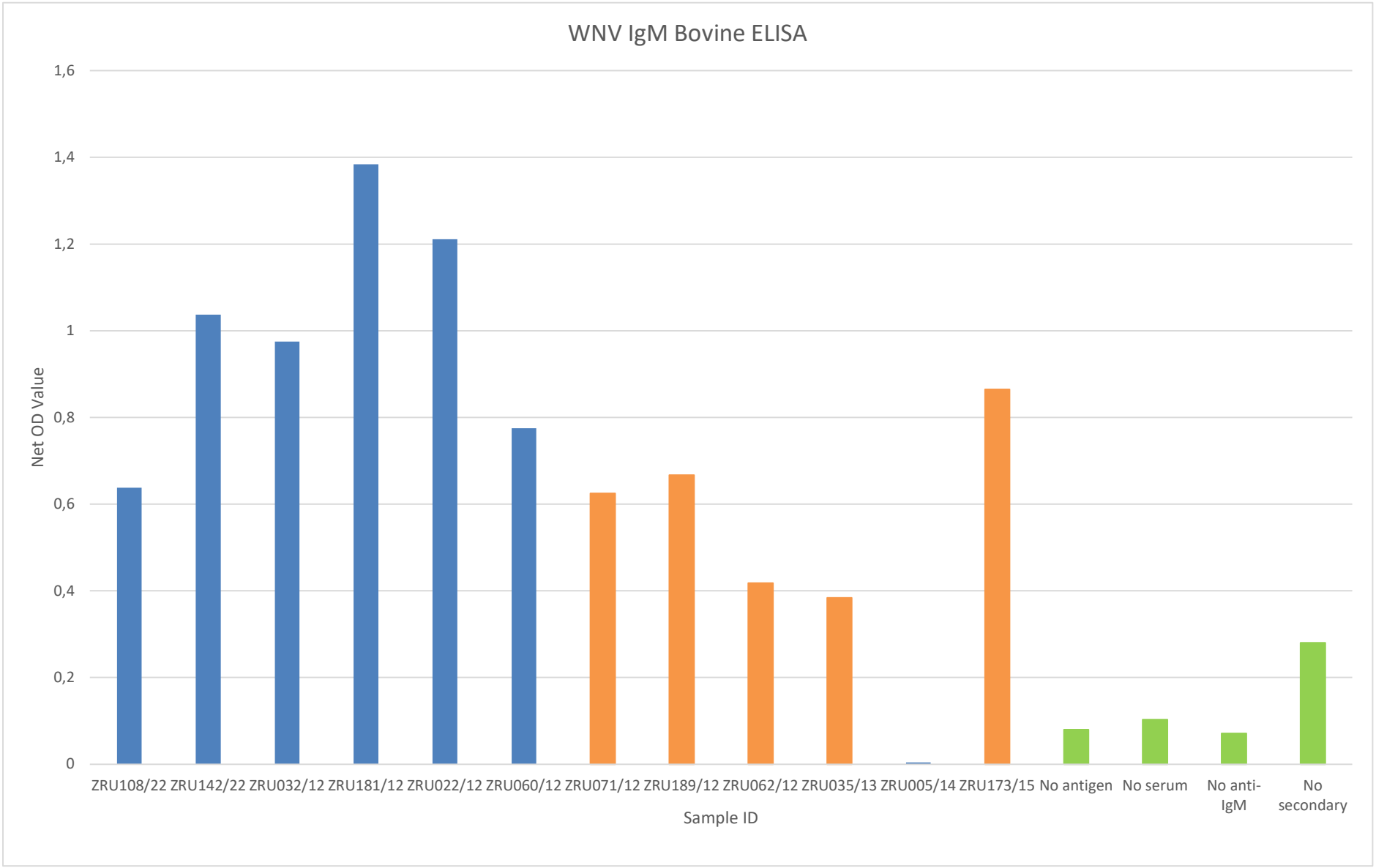

Figure 7.20: Net OD values obtained with the in-house WNV IgM Bovine ELISA. The bar shows the net OD values obtained during validation of the in-house WNV IgM Bovine ELISA.Positive (blue bars) and negative samples (orange bars) were selected based on the neutralisation assay outcomes.

Subsequently, four runs of negative samples only were performed on different days to test reproducibility and determine the cut-off value, by drawing a ROC curve on MedCalc. Figure 7.21 shows the ROC curve generated.

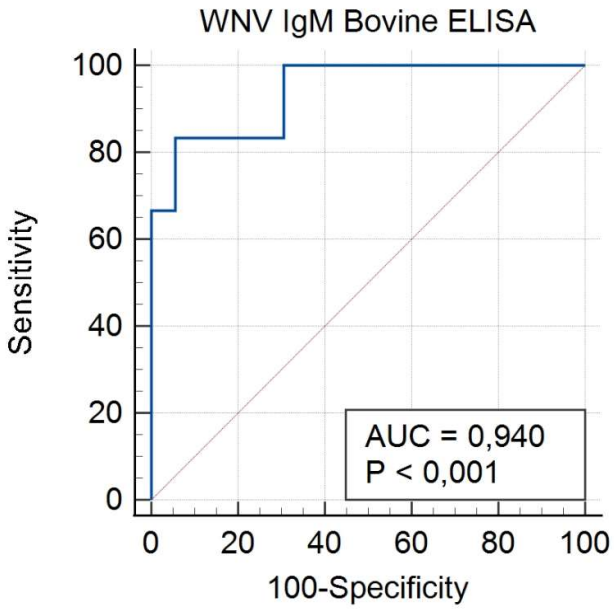

Figure 7.21: ROC curve for the in-house WNV IgM Bovine ELISA. The figure shows the ROC curve obtained for the in-house WNV IgM Bovine ELISA. An AUC value of 0.940 was obtained with a p value of <0.001. The ROC curve was generated using MedCalc.

The ROC curve was generated by making use of six positive samples and nine negative samples that were repeated four times for reproducibility, thus yielding 36 negative OD values to use. The AUC value obtained was 0.940, which is classified as excellent and a Youden Index (J) of 0.7778 was determined. The sensitivity was determined to be 83.3%, while the specificity was 94.4%. Comparing the cut-off value to the net OD values obtained, five of six samples (83.3%) were positive, and with the same number of negative samples testing negative (5/6; 83.3%) (Table 7.8 and Table 7.9).

Table 7.8: Cut-off value of in-house WNV IgM Bovine ELISA. The table shows the net OD values obtained during validation of the in-house WNV IgM Bovine ELISA, as well as what the cut-off value was (YI) and if the sample is classified as positive or negative.

WNV IgM Bovine ELISA		Net OD	Percentage	Outcome	
			(YI - 77.78)	Neutralization assay	In-House
Positive sera	ZRU108/22	0.64	63.8	Positive	Negative
	ZRU142/22	1.04	103.7	Positive	Positive
	ZRU032/12	0.98	97.5	Positive	Positive
	ZRU181/12	1.38	138.4	Positive	Positive
	ZRU022/12	1.21	121.1	Positive	Positive
	ZRU060/12	0.78	77.5	Positive	Positive
Negative sera	ZRU071/12	0.63	62.5	Negative	Negative
	ZRU189/12	0.67	66.7	Negative	Negative
	ZRU062/12	0.42	41.8	Negative	Negative
	ZRU035/13	0.38	38.4	Negative	Negative
	ZRU005/14	0.00	0.4	Negative	Negative
	ZRU173/15	0.87	86.5	Negative	Positive

Table 7.9: Sensitivity and specificity of in-house WNV IgM Bovine ELISA. The table shows the sensitivity and the specificity of the in-house WNV IgM Bovine ELISA, comparing the neutralisation assay results with the in-house developed IgM ELISA.

WNV IgM Bovine ELISA	Neut pos	Neut neg
In-house ELISA pos	5	1
In-house ELISA neg	1	5

7.3.4 WNV Species-independent IgG ELISA

Figure 7.22 depicts the results obtained by evaluating different dilutions of protein G (EMD Millipore Corp, Massachusetts, USA). The 1:2500 dilution (shown in orange) yielded the highest OD values for both the positive and negative samples, while the 1:5000 dilution (shown in grey) resulted in lower OD values, but there was a bigger difference between the positive and negative samples.

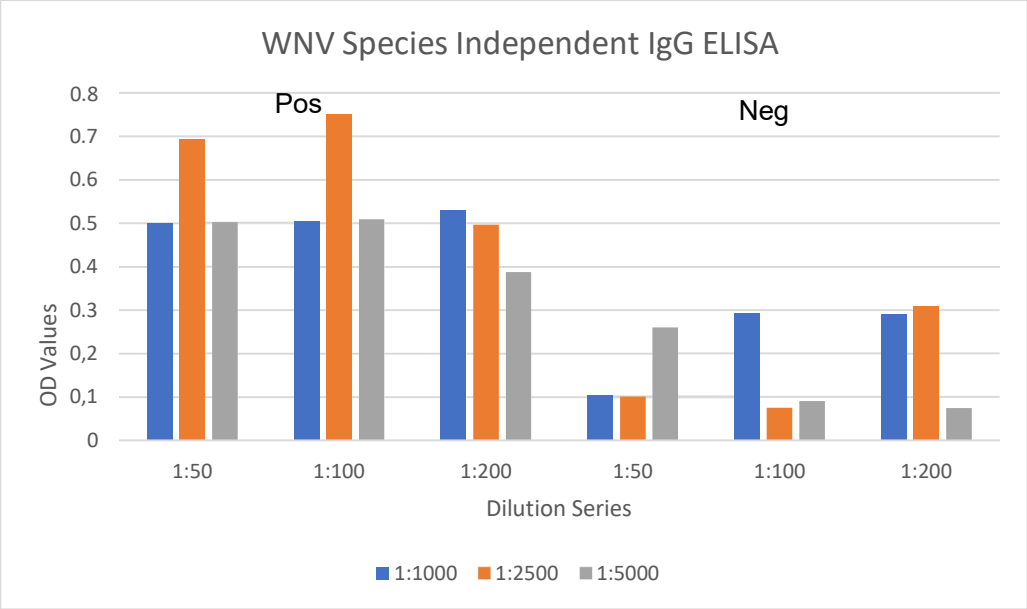

Figure 7.22: Checkerboard titration of the net OD values obtained for the WNV species independent IgG ELISA. The figure shows the results obtained from the checkerboard titration performed with different antigen concentration, dilution of samples and secondary antibody dilutions (protein G).

A panel of positive and negative equine and human samples, confirmed by commercial IgM ELISA kits were used to validate the WNV species-independent IgG ELISA. To test the sensitivity towards other species, real-time RT-PCR WNV positives were tested. This included a roan and two giraffe species. Figure 7.23 shows the results obtained for the WNV species-independent IgG ELISA. It was assumed that neutralisation positive samples would have IgG antibodies against WNV. Four runs of negative only samples were performed as well to determine reproducibility and draw a ROC curve. Figure 7.24 shows the ROC curve analysis.

The results obtained from the WNV Species-Independent IgG ELISA was able to detect the equine sample, as well as the giraffe samples. The human samples were also

detected., Figure 7.23 and Table 7.10 shows the results obtained from the assay, with Figure 7.24 showing the ROC curve generated.

Table 7.10: Net OD values obtained with the in-house WNV Species Independent IgG ELISA. The table shows the net OD values obtained during validation of the in-house WNV Species Independent IgG ELISA. Positive and negative samples were selected based on the neutralisation assay outcomes.

WNV Specie-Independent IgG ELISA			OD Values			Ratio
			WNV Antigen	Mock Antigen	Net OD	
Positive samples	Human	ZRUA1601/21	0.62	0.29	**0.33**	**2.16**
		ZRUA1611/21	0.54	0.32	**0.22**	**1.71**
		ZRUA1652/21	0.73	0.18	**0.55**	**4.06**
		ZRUA2099/22	0.56	0.25	**0.31**	**2.27**
		ZRUA2067/22	0.38	0.14	**0.24**	**2.75**
		ZRUA1541/21	0.32	0.09	**0.23**	**3.72**
	Horse	ZRU146/21	0.37	0.28	**0.09**	**1.33**
		ZRU063/19	0.50	0.09	**0.41**	**5.33**
		ZRU090/19	0.31	0.31	**0.00**	**0.99**
		ZRU058/20	1.03	0.13	**0.90**	**7.88**
		ZRU122/20	0.29	0.36	**0.00**	**0.78**
		ZRU057/20	0.79	0.33	**0.46**	**2.39**
		ZRU083/17	0.34	0.33	**0.02**	**1.05**
		ZRU024/19	0.26	0.22	**0.04**	**1.16**
		ZRU038/17	0.11	0.38	**0.00**	**0.29**
		ZRU087/17	0.71	0.10	**0.62**	**7.47**
	Other	ZRU061/16 (Roan)	0.25	0.28	**0.00**	**0.91**
		ZRU125/18 (Giraffe)	0.54	0.30	**0.24**	**1.79**
		ZRU165/18 (Giraffe)	0.48	0.29	**0.20**	**1.69**
		ZRU109/22 (Ovine)	0.49	0.08	**0.31**	**6.03**
		ZRU142/22 (Ovine)	0.48	0.18	**0.31**	**2.27**
Negative samples	Human	ZRUA2095/22	0.36	0.34	**0.03**	**1.08**
		ZRUA1529/21	0.08	0.07	**0.01**	**1.10**
		ZRUA1538/21	0.13	0.10	**0.03**	**1.34**
		ZRUA0471/19	0.35	0.14	**0.21**	**2.59**
		ZRUA1607/21	0.29	0.15	**0.14**	**1.95**
	Horse	ZRU020/17	0.31	0.13	**0.18**	**2.41**
		ZRU066/20	0.47	0.33	**0.15**	**1.45**
		ZRU018/19	0.37	0.22	**0.15**	**1.66**
		ZRU104/17	0.28	0.29	**0.00**	**0.97**
		ZRU079/17	0.08	0.07	**0.01**	**1.14**
Negative controls		No antigen	0.08	x	**0.08**	**x**
		No serum	0.16	x	**0.16**	**x**
		No secondary	0.11	x	**0.11**	**x**

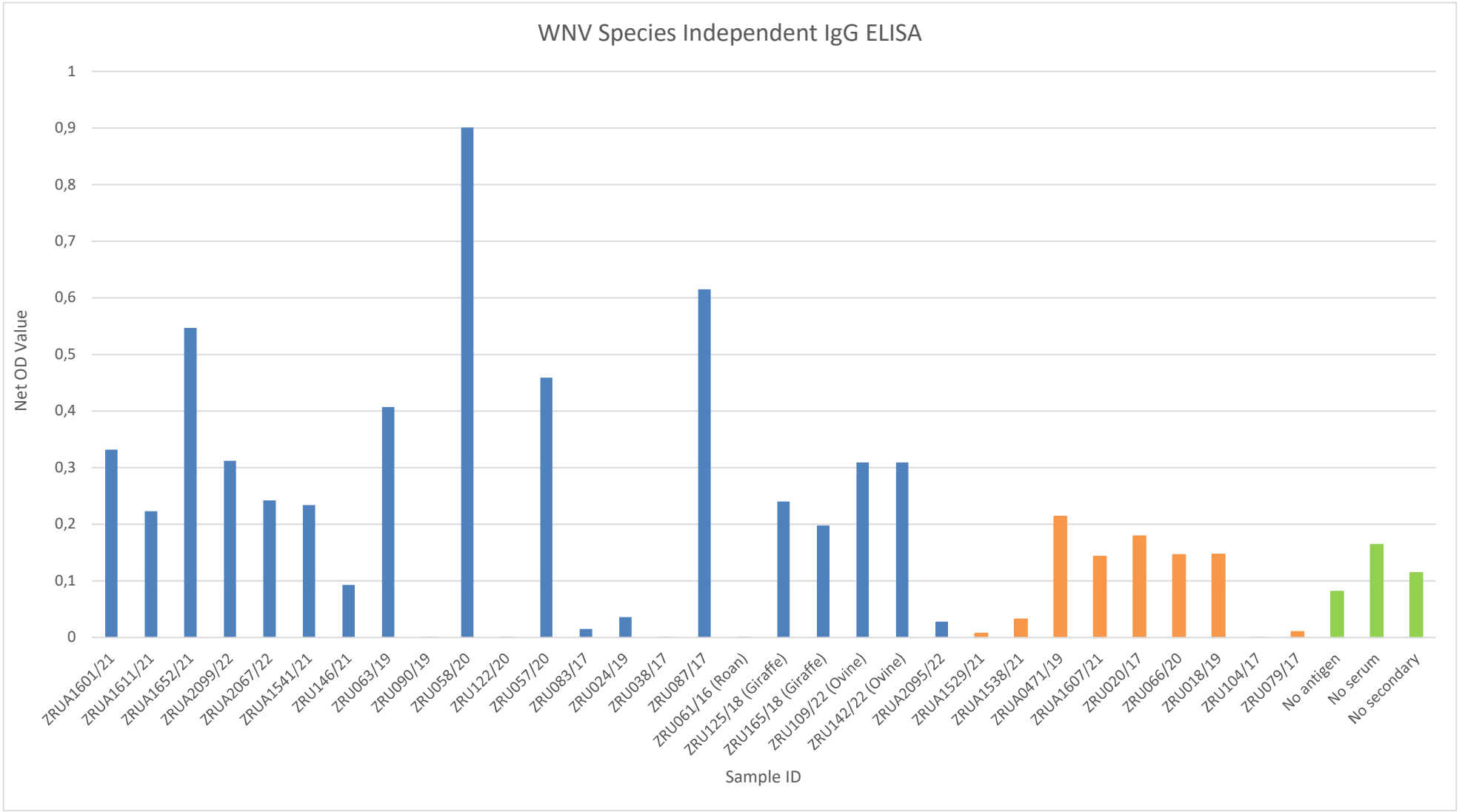

Figure 7.23: Net OD values obtained with the in-house WNV Species Independent IgG ELISA. The bar shows the net OD values obtained during validation of the in-house WNV Species Independent IgG ELISA. Positive (blue bars) and negative samples (orange bars) were selected based on the neutralisation assay outcomes.

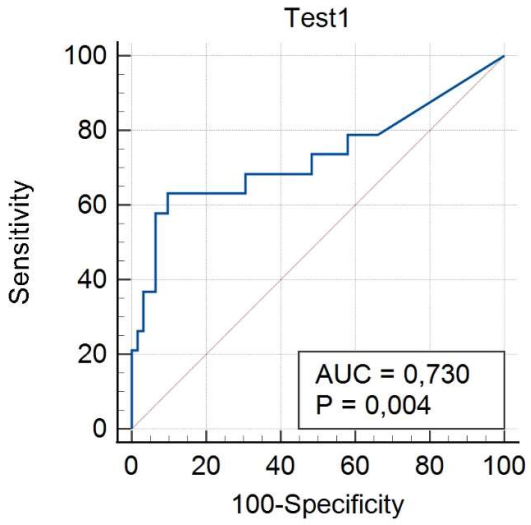

Figure 7.24: ROC curve for the in-house WNV Species Independent IgG ELISA. The figure shows the ROC curve obtained for the WNV Species Independent IgG ELISA. An AUC value of 0.730 was obtained with a p value of <0.004. The ROC curve was generated using MedCalc.

The ROC curve was generated by making use of 19 positive samples and 16 negative samples that were repeated four times for reproducibility, thus yielding 52 negative OD values to use. The AUC value obtained was 0.730, which is classified as fair and a Youden Index (J) of 0.5348 was determined. The sensitivity was determined to be 63.16%, while the specificity was 90.32% (Table 7.11 and Table 7.12).

Table 7.11: Cut-off value of in-house WNV Species Independent IgG ELISA. The table shows the net OD values obtained during validation of the WNV Species Independent IgG ELISA, as well as what the cut-off value was (YI) and if the sample is classified as positive or negative.

WNV Species-Independent IgG ELISA			Net OD Value	Percentage (YI - 53.48)	Commercial	In-house
Positive samples	Human	ZRUA1601/21	0.33	33.2	Positive	Negative
		ZRUA1611/21	0.22	22.3	Positive	Negative
		ZRUA1652/21	0.55	54.7	Positive	Positive
		ZRUA2099/22	0.31	31.2	Positive	Borderline
		ZRUA2067/22	0.24	24.2	Positive	Negative
		ZRUA1541/21	0.23	23.4	Positive	Negative
	Horse	ZRU146/21	0.09	9.3	Positive	Negative
		ZRU063/19	0.41	40.7	Positive	Positive
		ZRU090/19	0.00	0.1	Positive	Negative
		ZRU058/20	0.90	90.1	Positive	Positive
		ZRU122/20	0.00	0.1	Positive	Negative
		ZRU057/20	0.46	45.9	Positive	Borderline
		ZRU083/17	0.02	1.5	Positive	Negative
		ZRU024/19	0.04	3.6	Positive	Negative
		ZRU038/17	0.00	0.1	Positive	Negative
		ZRU087/17	0.62	61.5	Positive	Positive
	Other	ZRU061/16 (Roan)	0.00	0.1	RT-PCR positive	Negative
		ZRU125/18 (Giraffe)	0.24	24	RT-PCR positive	Negative
		ZRU165/18 (Giraffe)	0.20	19.8	RT-PCR positive	Negative
		ZRU109/22 (Ovine)	0.41	40.7	Neut positive	Negative
		ZRU142/22 (Ovine)	0.31	30.9	Neut positive	Negative
Negative samples	Human	ZRUA2095/22	0.03	2.8	Negative	Negative
		ZRUA1529/21	0.01	0.7	Negative	Negative
		ZRUA1538/21	0.03	3.2	Negative	Negative
		ZRUA0471/19	0.21	21.4	Negative	Negative
		ZRUA1607/21	0.14	14.3	Negative	Negative
	Horse	ZRU020/17	0.18	17.9	Negative	Negative
		ZRU066/20	0.15	14.6	Negative	Negative
		ZRU018/19	0.15	14.7	Negative	Negative
		ZRU104/17	0.00	0.1	Negative	Negative
		ZRU079/17	0.01	1	Negative	Negative

Table 7.12: Sensitivity and specificity of in-house WNV Species Independent IgG ELISA. The table shows the sensitivity and the specificity of the WNV Species Independent IgG ELISA, comparing the commercial IgM ELISA results with the in-house developed species independent IgG ELISA.

WNV Species-Independent IgG ELISA	Confirmed pos	Confirmed neg
In-house ELISA pos	6	0
In-house ELISA neg	15	10

7.3.5 WSLB IgG Equine ELISA

The WSLB IgG Equine ELISA has the exact same set-up as the WNV IgG Equine ELISA, with optimisation steps included in coating of the plate with WSLB NS1 antigen, serum sample dilutions and HRP-conjugated secondary antibody concentrations. Figure 7.25 shows the results obtained from the coating of the plate with WSLB NS1 at various concentrations, as well as comparing the effectiveness of PBS to bicarbonate buffer.

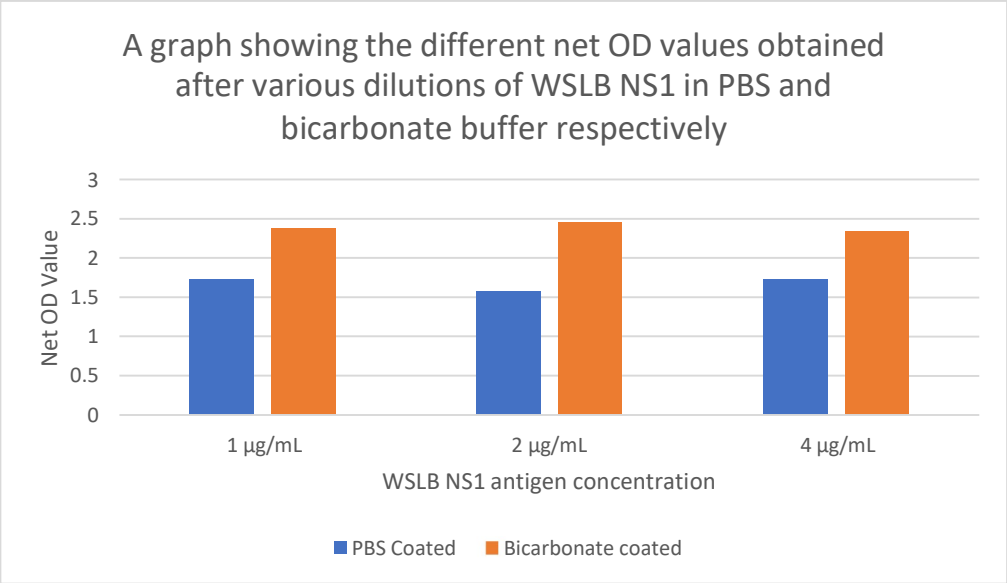

Figure 7.25: WSLB Antigen Dilution in PBS compared to bicarbonate buffer. The figure shows the net OD values obtained when coating the plate with various WSLB NS1 antigen concentrations, diluted in both PBS (blue bars) and bicarbonate buffer (orange bars).

As explained previously, there is no WSLB positive IgG or IgM samples that could be confirmed with neutralisation assays, so the test had to be optimised with rabbit sera. To demonstrate the sensitivity of the test, dilutions of the rabbit sera was made to determine the limit of detection, which can standardise it for use of samples. Figure 7.26 shows the results obtained from the experiment. The limit of detection was determined to be 1:5750 dilution of the 1 µg/mL rabbit sera.

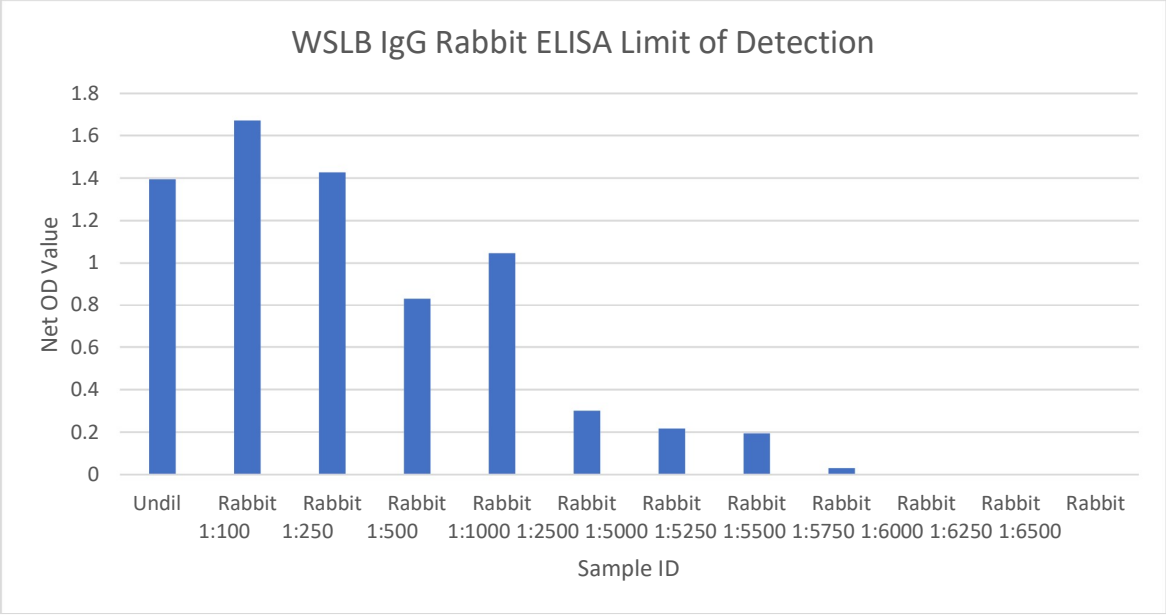

Figure 7.26: WSLB Rabbit IgG Limit of detection. The figure shows the net OD values obtained when diluting the rabbit sera from 1:100 to 1:25000 to determine the limit of detection of the assay.

Lastly, the optimal concentration of the HRP-conjugated goat anti-rabbit IgG secondary antibody had to be determined. Figure 7.27 shows the results obtained from the experiment with the 1:1000 dilution giving the optimal results.

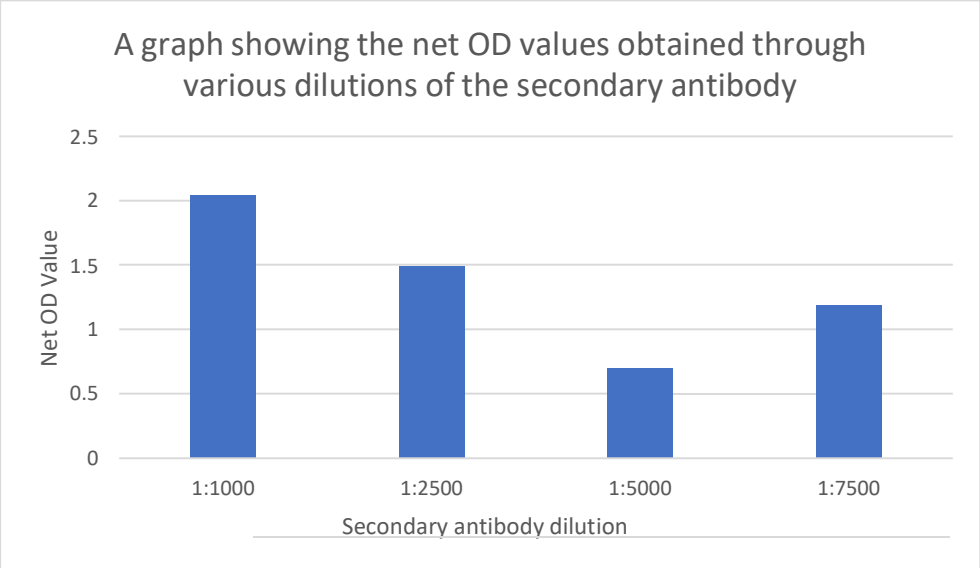

Figure 7.27: Secondary antibody dilution for the WSLB IgG Rabbit ELISA. The figure shows the net OD values obtained when diluting the goat anti-rabbit secondary antibody for the WSLB Equine IgG assay.

7.3.6 WSLB Bovine IgM ELISA

Figure 7.28 shows the various dilutions of the secondary antibody tested for the WSLB IgM Bovine ELISA. It was determined that the 1:2500 dilution is the most efficient to use in this assay.

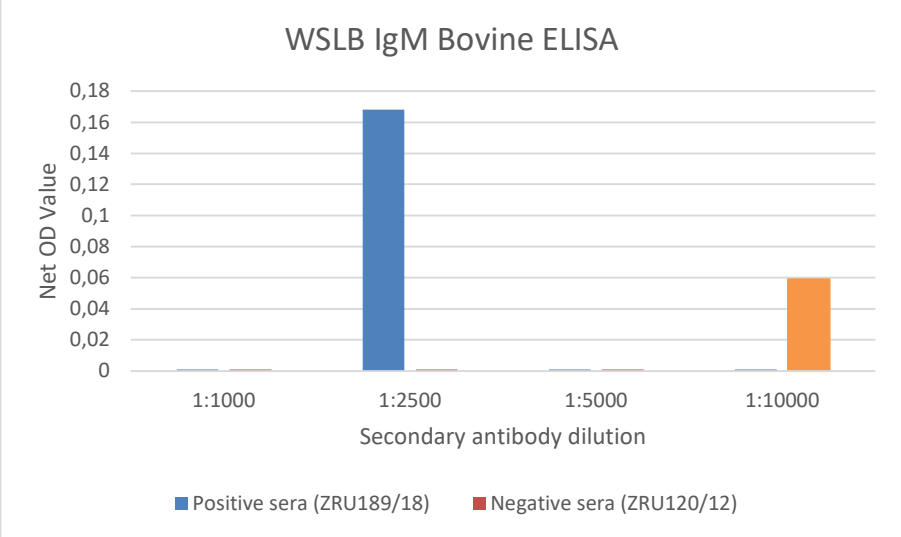

Figure 7.28: WNV IgM Bovine ELISA secondary antibody dilutions. The HRP-conjugated donkey anti-goat IgG antibody is used as the secondary antibody and is recommended to use at a dilution of between 1:2000 and 1:20 000. The dilutions that were tested included – 1:1000, 1:2500, 1:5000 and 1:10 000.

After the optimal concentrations were determined, an IgM run was performed to determine if the assay works. The samples used to validate the WNV IgM Bovine ELISA were obtained from the results of the neutralisation assays performed on livestock from 2012-2022 (Refer to Chapter 5). Figure 7.29 shows the results of the WSLB IgM Bovine ELISA making use of 0.5 ng/mL goat anti-bovine IgM antibody. Low OD values were observed, with some samples not even detected. Table 7.13 shows the OD values obtained for the assay.

Table 7.13: Net OD values obtained with the in-house WSLB IgM Bovine ELISA. The table shows the net OD values obtained during validation of the in-house WSLB IgM Bovine ELISA. Positive and negative samples were selected based on the neutralisation assay outcomes.

WSLB IgM Bovine ELISA		OD Values			Ratio
		WSLB Antigen	Mock Antigen	Net OD	
Positive sera	ZRU062/12	1.37	1.11	**0.26**	**1.24**
	ZRU071/13	1.27	1.10	**0.17**	**1.16**
	ZRU189/18	1.37	1.24	**0.13**	**1.11**
	ZRU181/12	0.63	0.63	**0.00**	**1.00**
	ZRU005/14	0.10	0.08	**0.02**	**1.26**
Negative sera	ZRU035/13	0.56	0.75	**0.00**	**0.75**
	ZRU157/16	0.98	1.04	**0.00**	**0.95**
	ZRU132/17	0.67	0.33	**0.33**	**2.01**
	ZRU224/18	0.42	1.41	**0.00**	**0.30**
	ZRU173/15	0.87	1.20	**0.00**	**0.72**
	ZRU120/12	0.95	0.96	**0.00**	**0.99**
Negative control	No antigen	0.08	x	**0.08**	**x**
	No serum	1.78	x	**1.78**	**x**
	No anti-IgM	0.07	x	**0.07**	**x**
	No secondary	0.06	x	**0.06**	**x**

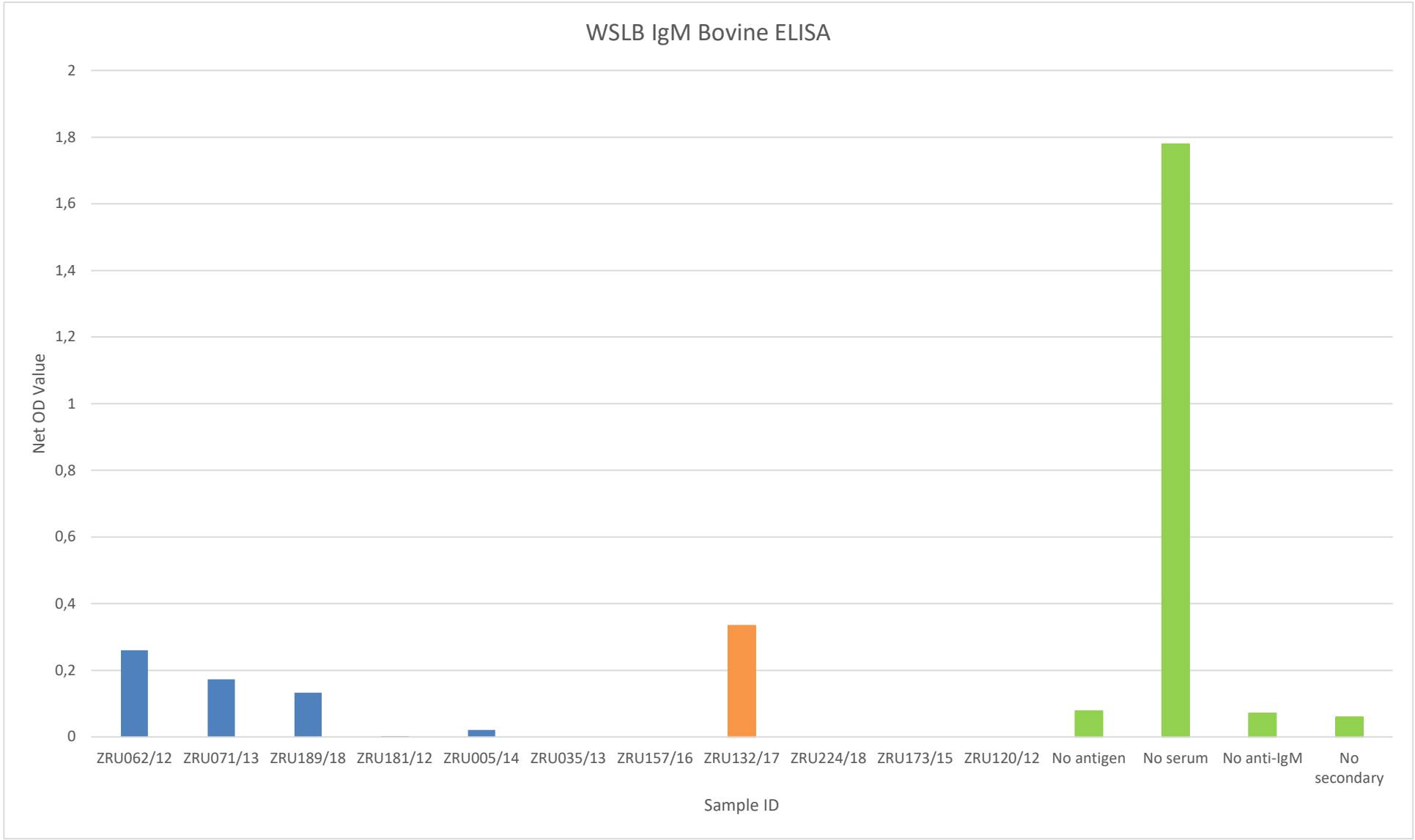

Figure 7.29: Net OD values obtained with the in-house WSLB IgM Bovine ELISA. The bar shows the net OD values obtained during validation of the in-house WSLB IgM Bovine ELISA. Positive (blue bars) and negative samples (orange bars) were selected based on the neutralisation assay outcomes.

7.3.7 WSLB Species Independent IgG ELISA

The optimal protein G concentration was determined to detect IgG antibodies using a dilution series for the WNV species independent ELISA at a concentration of 1:5000 to determine the limit of detection of the assay (Figure 7.30). The limit of detection was determined to be 1:3250 dilution of the 1 µg/mL rabbit sera.

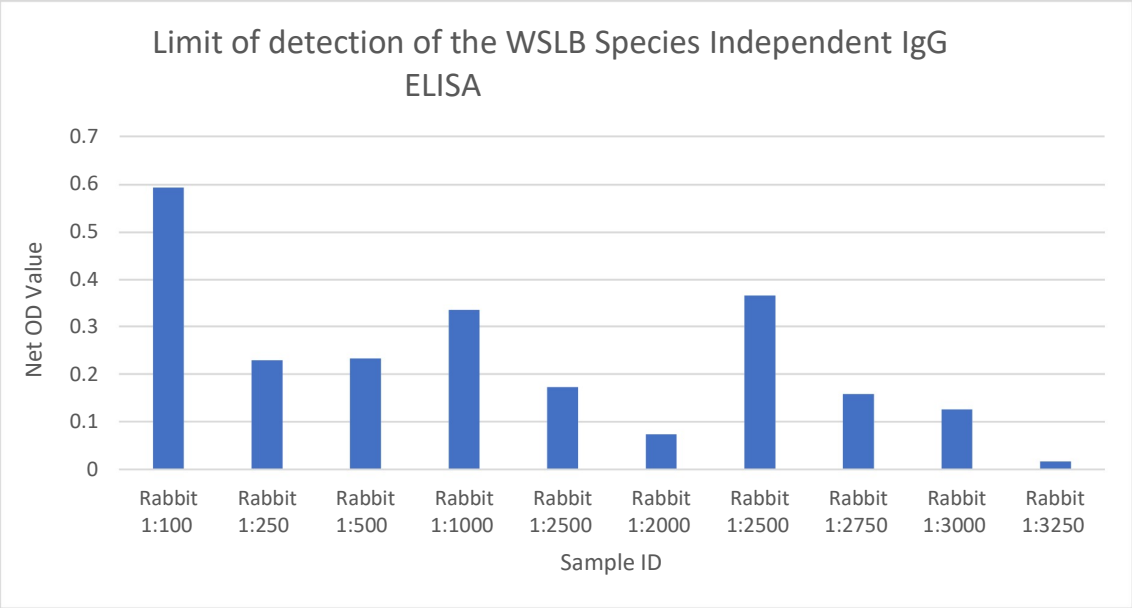

Figure 7.30: WSLB Species Independent IgG Limit of detection. The figure shows the net OD values obtained when diluting the rabbit sera from 1:100 to 1:3500 to determine the limit of detection of the assay.

7.4 Discussion

Detection of flaviviruses, WNV and WSLB, by RT-PCR or virus isolation is challenging due to the short viraemic phase in infected animals, which is why the use of serological assays (IgG and IgM) are effective to confirm infection (McVey et al., 2015). Distinguishing between previous infection, vaccination and acute infection can be a challenge especially with regards to IgG ELISAs in endemic countries (Sahu, 2022). Immunoglobulin M antibodies appear after 5-7 days post-infection indicating a new or recent infection and remain in the serum for up to one month, compared to IgG antibodies which have long half-life (Lustig et al., 2018).

The aim of the study was to develop and validate recombinant NS1 protein-based IgM and IgG ELISAs for serodiagnosis of WNV and WSLB respectively. There is a commercial WNV IgM Equine ELISA available from InBios that is highly specific and sensitive and approved by the United States Department of Agriculture (USDA);

however it is expensive and must be imported, which is why an in-house WNV ELISA would be very beneficial. The WNV IgG Equine ELISA had a relative diagnostic sensitivity and specificity of 65.4% and 23.1%, respectively. The ZARV laboratory does not have a commercial WNV IgG Equine ELISA available to compare the in-house developed ELISA to,so the sensitivity and specificity could not be compared to that of an available commercial assay . Serum neutralisation assays do not distinguish between IgM and IgG (Chan, 2022). Since these were all sick animals that had been confirmed as negative with the IgM commercial ELISA it is possible that some may only have IgG antibodies.

An attempt was made to develop and standardise an in-house capture IgM ELISA for serodiagnosis of WNV in equines. Goat-anti equine IgM polyclonal antibody was used as capture antibody, but there were no significant differences between the OD values of positive and negative sera, which could be due to the antibody binding nonspecifically with the serum or the primary and secondary antibodies. Similar observations were made by other research groups while developing capture IgM antibodies and the authors suggested the use of monoclonal antibodies (Atre et al., 2019; Sahu et al., 2022). With the goat anti-equine IgM capture antibody not working, the capture antibody was switched to a polyclonal mouse anti-equine IgM antibody to try and improve the sensitivity of the assay. The same results were obtained with similar OD values for both the positive and negative sera, thus not being able to distinguish between the two sample sets. The reason for the high background and unspecific binding could also be due to the coating antibody interacting with the mouse anti-WNV NS1 primary antibody and HRP-conjugated goat anti-mouse secondary antibody. It was then decided to adjust the setup of the ELISA using a more direct approach and coating the wells with WNV NS1 antigens. After the optimal concentrations and dilutions were determined, a run was performed with a set of positive and negative sera. A significant difference ($p<0.5$) was observed between the OD values of positive and negative samples with minimum background observed. The sensitivity of the assay was determined to be 62.5%, while the specificity was 66.25%. The low diagnostic sensitivity achieved might be due to various factors, including the authenticity of the NS1 protein, antibody concentrations or even choice of blocking agent or due to the presence of high amounts of IgG antibodies (Sahu, 2022). Comparing the in-house WNV IgM equine ELISA to the commercial ELISA available from InBios, it is less sensitive than what is available. The assays differ in the target protein, with E protein and NS1 protein used respectively, which may contribute to

slightly different results. An AUC value of 0.65 was obtained, which is classified as poor according to the classifying index (Nahm, 2022). Receiver operating curves above the diagonal line are considered to have reasonable discriminating ability to diagnose patients with and without the disease (Mandrekar, 2009).

A WNV IgM Bovine ELISA was developed, with a sensitivity of 83.33% and a specificity of 94.44%. The AUC value was 0.940. Overall, this assay is very sensitive and has the ability to correctly identify IgM antibodies in bovine samples and can possibly be used as an in-house assay, since there is not a commercial assay to compare the results to. The number of WNV seropositive serum samples available to test was; however, limited and further validation would be required to confirm the sensitivity. An alternative setup would be to replace the detection antibody in the commercial test to an anti-bovine IgM specific antibody.

With regards to the WNV Species-Independent IgG ELISA, a sensitivity of 63.16% was achieved, with a specificity of 90.32%. The AUC value was 0.730. More samples are required to obtain a better, more specific species-independent IgG ELISA, but due to limited sample availability, further validation is required. Overall, this assay is not as sensitive as it could be but have the ability to detect IgG antibodies in various different species. In the case of the WNV Species-Independent IgG ELISA, it is used to screen for seroprevalence of WNV in various species, so sensitivity is considered more important when a disease is highly contagious or associated with complications, while in contrast specificity is more important than specificity when a test is required to confirm whether the diagnosis is risky (Nahm, 2022). The lower sensitivity may make serum neutralisation assays more suitable as a screening tool in a research setting though.

For WLSB a concept ELISA was developed showing the limit of detection (LoD) of the assay, but further development is required. Since WSLB positive serum was not available, neurological cases submitted from livestock between 2012 and 2022 was screened by virus neutralization tests (VNT). After performing neutralisation assays on livestock samples against WSLB, 5/23 positives were identified, and an attempt made at developing a WSLB IgM Bovine ELISA to use in-house. The samples had very low OD values and the control where the serum was omitted, yielded very high OD values. This could indicate that there are no IgM antibodies present, but the fact that the no serum negative control had such a high OD value, indicates that the WSLB NS1

antigen interacted with the anti-bovine IgM antibodies and the assay is not effective, due to unspecific binding. This is concerning and results in a non-specific assay that is not efficient enough for use as an in-house ELISA. Similar results were found for IgG and species independent ELISAs. It bound well to rabbit sera from animals used to raise antibodies to the recombinant NS1 protein; however, this may also be targeted to the polyhistidine-tag (His-tag) region (Oymans, 2020). It is therefore possible that the protein was not similar enough to the authentic protein to be recognised by naturally infected animal sera.

There are several strengths and limitations of the study. A WNV IgG Equine ELISA was developed, but the specificity appears to be low while the WNV IgM Equine ELISA and the WNV Species-independent IgG ELISA are not as sensitive as the commercial kit available or compared to the equine specific IgG ELISA, respectively. A WNV bovine IgM ELISA was developed and showed very promising results to be used as an in-house ELISA; however, the WSLB bovine IgM ELISA development was unsuccessful. A big limitation of the study was the availability of positive and negative samples for both WNV and WSLB. For WNV, only an IgM kit was available and neutralisation assays performed to confirm presence of antibodies, so to confirm the WNV IgM Equine ELISA was easy, but to validate the WNV IgG Equine ELISA and Species Independent IgG ELISA, validation had to be done using neutralisation assay positive and negative samples, which could result in false positives and negatives. For WSLB, there is no commercial ELISA assay available to obtain a pool of positive and negative samples, as well as a minimal number of cases over the past 10 years in South Africa with available sera. The use of VNT did confirm the presence of WNV and WSLB antibodies in livestock with neurological signs, and WNV IgM could be confirmed in several suggesting that this virus likely contributes to more clinical cases in livestock than previously recognised.

7.5 Conclusion

Various ELISAs were evaluated using the baculovirus expressed NS1 protein to measure IgG and IgM antibodies in serum from WNV and WSLB infections. The WNV IgM Equine ELISA did not have a good enough sensitivity and specificity compared to the commercial WNV IgM Equine ELISA from InBios to replace it as an in-house assay. However, the WNV IgM Bovine ELISA showed very promising results. As concluded, the WSLB antigen seemed to be problematic, and assays were not able to be developed.

Chapter 8 – Concluding remarks

Arboviral diseases are among the most important emerging infectious diseases worldwide (Gubler, 2002). In South Africa, important arboviruses include members of the *Flaviviridae* family, specifically West Nile virus (WNV) and Wesselsbron virus (WSLB). While surveillance for WNV in equines and humans are well-established, WSLB is a neglected flavivirus in South Africa. The epidemiology of these viruses, as well as their disease description as animal pathogens remain poorly described in South Africa (Venter, 2018).

The study's primary focus was to evaluate available and novel diagnostic methods for the diagnosis of WNV and WSLB through molecular and serological testing. The availability of sensitive tests will allow epidemiological investigations into the prevalence of these viruses in neurological infections in South Africa. Commercial WNV immunoglobulin M (IgM) enzyme linked immunosorbent assay (ELISA) kits were used to investigate the epidemiology of WNV infection in humans and horses over 2 years and to better understand the disease presentation in acute neurological cases of unknown cause. Virus neutralisation assays were used to establish panels of serum for testing of novel serological assays. The use of molecular and serological assays allowed the identification (or detection) of WNV in humans and horses and retrospectively in livestock and detection of WSLB virus infections in horses, exotic birds and livestock.

In this study, 143 samples, which included EDTA, plasma and serum from hospitalised patients presenting with neurological symptoms of unexplained cause or fever, were screened over the arboviral season (January-June) in 2021 and 2022 from two sentinel sites, Mpumalanga and Gauteng. West Nile virus was identified in 10.34% of patients in 2021 and 2.44% of patients in 2022. The likelihood of WNV infection was higher in males, individuals older than 50 years; however, this was not statistically significant, compared to physical labourers being 2.16 times more likely to be infected with WNV. A higher proportion of WNV infections were detected in the rural Mpumalanga sites, which suggests suitable mosquito breeding conditions and more vector-host interactions.

Disease presentation included symptoms like general WNV fever symptoms, as well as more serious disease, with all patients being hospitalised in this study. Neurological

symptoms like headaches and meningitis, seizures and flaccid paralysis were reported in 37.76% of cases, which were not well-described in WNV infections in South Africa before. No fatalities were reported, with 68.5% of patients making a full recovery after infection. These findings confirm that WNV is often overlooked, and health practitioners should take it into consideration as a cause for febrile and neurological disease, especially during the arboviral season.

When looking at animal data, WNV has been reported as a cause of neurological disease in 3-11% of equine cases, 1.5% of livestock cases and 0.5% of wildlife cases in average over 8 years (Venter, 2017). Between 2021 and 2022, 338 animal cases were submitted displaying fever, neurological signs, or sudden unexpected death. With regards to molecular testing, all animals were screened with a pan-flavi real-time reverse transcriptase polymerase chain reaction (RT-PCR) to detect any positive WNV or WSLB cases. Over the two years, only one WNV case was identified with RT-PCR, while two WSLB cases were identified. These positive cases were subjected to sequencing and phylogenetic analysis and confirmed as WNV lineage 2. With regards to serological testing, all equine samples with available plasma or serum, were subjected to testing on the commercial WNV IgM ELISA kit from InBios. Out of the 166 samples tested, 12 samples came up as positive and 10/12 were confirmed with neutralisation assays. No co-infections were reported. A positivity rate of 11.69% (9/77) was obtained for 2021 and 1.12% (1/89) for 2022.

Only equine samples tested positive for WNV, and this can be due to the awareness and alertness of WNV amongst owners when observing neurological signs, while it is difficult to actively monitor wildlife and livestock, which could result in missed cases. However, since serological assays are only available for horses, cases may also be missed in other species. The majority of clinical signs reported included ataxia, blindness and seizures. The PCR positive case aborted and had a severely deformed foal and had to be euthanised. Of the remaining cases that were identified with IgM, no fatalities were reported; however, cases with signs reported like seizures, paralysis, blindness and recumbency are very serious and there is a good chance that these horses had to be euthanised eventually. Interestingly to note, is the fact that 100% of the WNV positive cases were unvaccinated, suggesting that vaccination of equines need to be prioritised to prevent severe disease.

Wesselsbron virus was identified in two cases, one a toucan and another in a horse,

both presenting with neurological signs. Wesselsbron virus has only been described in a horse twice before, when it was identified by the Zoonotic arbo- and respiratory virus (ZARV) team in 2008 (Accession numbers JN226797 and JN226798) (Human, 2011). In the previous cases, one case had died and one had neurological signs but survived (Human, 2011). These cases highlight the lack of knowledge of the hosts range or severity of WSLB in other species and show how important its surveillance in South Africa is. The NS5 region was sequenced and clustered closely to the Senegal strain. Further investigation is however, required to know more about the WSLB strain circulating in South Africa.

These results indicate that WNV and WSLB cases are missed when only relying on one diagnostic method. This is why it was important to ensure that there is an effective WSLB real-time RT-PCR in place for detection, as well as serological assays for both WNV and WSLB for detection of IgM and IgG antibodies. The one-step real-time RT-PCR assay showed good sensitivity and specificity, with a limit of detection of $10^{-2.667}$ viral genome copies/µL when tested on WSLB cultures and $2.068x10^{3}$ viral genome copies/µL when making use of a positive control. This assay can be used to confirm whether a positive result on the pan-flavivirus assay, is in fact a WSLB positive. The detection limit of the plasmid tested on the HybProbe nested PCR was determined to be $5.509x10^{-2}$ viral genome numbers/reaction. Comparing the HybProbe nested PCR with the one-step real-time WSLB specific RT-PCR, it was determined that the one step real-time RT-PCR is sensitive enough to replace the HybProbe nested PCR as a WSLB confirmational PCR.

With regards to the serological assays, an IgG, IgM and species-independent IgG assay was developed for WNV and validated making use of known positive and negative samples that were obtained through commercial ELISA kit results and neutralisation assays. Comparing the in-house developed ELISAs to the commercial IgM ELISA, the sensitivity and specificity is not equal or better than the commercially available kit. This can be due to the difference in target antigen, which is NS1 for the in-house ELISA, compared to the E protein for the commercial ELISA. For the WSLB ELISAs, it was only possible to validate and determine a limit of detection using rabbit sera, which is a positive control, due to a lack of available positive samples. When testing livestock samples with neutralisation assays against WSLB and WNV, it was made evident that these viruses do circulate under cattle and causes symptoms like fever, ataxia,

recumbency and nasal discharge was reported for WNV, while samples positive for WSLB neutralising antibodies reported signs like recumbency, seizures, abortions in ovines, and anaemia.

In conclusion, WNV and WSLB infections were identified in animals presenting with febrile, neurological and respiratory signs between 2021 and 2022 in South Africa. West Nile virus was identified in horses and humans and WSLB Infection was identified in a horse, as well as an avian species (toucan). Gauteng, KwaZulu-Natal and the Western Cape reported the highest number of positive cases and can be considered as hotspots for WNV outbreaks. The study also highlights the importance of vaccination against WNV in equines. Humans are just as vulnerable to WNV infections as animals and the study highlights that hospitalised human cases of febrile and neurological disease are being missed. Prevention methods should be applied, to prevent mosquito bites especially in areas where mosquito breeding sites have optimal conditions. By making use of molecular and serological assays in conjunction, a better understanding of WNV and WSLB disease prevalence in South Africa can be obtained and may assist in the prevention, diagnosis, treatment and control of the endemic flaviviruses. Unfortunately, baculovirus expressed NS1 antigens for WNV and WSLB do not appear to be ideal for WNV and WSLB ELISA development, so commercial ELISA kits for WNV are still the optimal choice with regards to serological testing.

Appendices

Appendix Table A1: Extent of personal contribution to the overall study

Chapter	Species	Years included in the study	Years screened by the candidate	Number screened by candidate/total number included in the study
3	Humans	2021-2022	2021-2022	Part of a team involved in screening ANDEMIA specimens (2021-2022), ANDEMIA IgM serology = 143/183
5	Animals	2021-2022	2021-2022	Part of a team involved in routine animal diagnostics, screening animals for various arboviruses (2021-2022), IgM serology on equines = 166/231, rotation schedule for extraction of viral RNA and RT-PCR testing

Appendix Table A2: Pathogens targeted by the Chipron array card, indicating genome target area and the primer and probe sequences.

Target pathogen	Target gene	Primer/Probe name	Orientation	Primer/probe sequence (5'-3')
West Nile virus	5'UTR-capsid junction	Forward primer	Sense	CTGTGTGAGCTGACAAACTTAGT
		Reverse primer	Antisense	GCGTTTTAGCATATTGACAGCC
		Probe	Sense	GAAGATTTCGATGTCTAAGAAACCA
Rift Valley fever virus	M segment	Forward primer	Sense	AGGGCATTAAAAGCCATCATT
		Reverse primer	Antisense	ACTGCTAAGGCTGGAAGGACTGT
		Probe	Sense	AGCAAATAGGGAGAGAAACCATG
Chikungunya virus	Non-structural protein 1	Forward primer	Sense	TGTACGTGGACATAGACGCTGA
		Reverse primer	Antisense	AACGCTCTAGCATTAGCATGGTC
		Probe	Sense	GTTTGAGGTGGAACCTAGGCA
Sindbis virus	Structural protein E2	Forward primer	Sense	AAATGCGGCGACTACAARA
		Reverse primer	Antisense	CTTYCCTTGKGCGGTGTG
		Probe	Sense	ACCAAACGAAGTGGGTCTTCAACT
Rubella virus	Non-structural protein	Forward primer	Sense	GAAACTCCTAGATGAGGTTCTTGC
		Reverse primer	Antisense	ATGAGGACGTGTAGGGCTTCTTT
		Probe	Sense	TATAACTTAACCGTCGGCAGTTG
Crimean Congo haemorrhagic fever virus	S segment	Forward	Sense	ACGCCCACAGTGTTCYCTTGAG
		Reverse 1	Antisense	GACATCACAATTTCACCAGG
		Reverse 2	Antisense	TGGARTCCTTYTGTGCATCA
		Probe 1	Sense	GGACTTGTGGACACTTTCACAAACTCC
		Probe 2	Sense	GGGCTTGTGGACACCTTCACAAACTC
Cytomegalovirus	UL83 gene	Forward primer	Sense	TTGGGACACAACACCGTAAAG
		Reverse primer	Antisense	TTCGTGTTTCCCACCAAGG
		Probe	Sense	CTGGTCACCTATCACCTGCATC
Measles virus	H gene	Forward primer	Sense	AGCATGTACCGAGTGTTTGAAGTAG
		Reverse primer	Antisense	AAGCATGTCTCCATTCGCAA
		Probe	Sense	ATAGACAGGCTTTACCTCTCATCTCA
Mumps virus	Nucleocapsid	Forward primer	Sense	GGCTACCCATTGATATTCAGYTATG
		Reverse primer	Antisense	TGTTGAACCGGAGGAACAAA
		Probe	Sense	ACAGAGTAGCAGATGATCTAGGCC
Herpes simplex	Glycoprotein D	Forward primer	Sense	GGATGCCTCTCTCAAGATGG
		Reverse primer	Antisense	TGTTGTAGGAGCATTCGGTGT

Appendix Table A2 cont: Pathogens targeted by the Chipron array card, indicating genome target area and the primer and probe sequences.

virus 1		Probe	Sense	AGGCAACTGTGCTATCCCCATC
Target pathogen	**Target gene**	**Primer/Probe name**	**Orientation**	**Primer/probe sequence (5'-3')**
Herpes simplex virus 2	Glycoprotein D	Forward primer	Sense	CGCCAAATACGCCTTAGCAG
		Reverse primer	Antisense	TTGTAGGGGCACTCGGTGT
		Probe	Sense	TGTGTACTACGCAGTGCTGGAA
Varicella Zoster virus	ORF 29	Forward primer	Sense	ATGTCCTAGAGGAGGTTTTATCTGC
		Reverse primer	Antisense	ACTCATCGTCTGTAAGACTTAACCA
		Probe	Sense	CCAAGTTCGCGGTATAATTGTC
Rabies virus	Nucleoprotein	Forward primer	Sense	TACAATGGATGCCGACAAGAT
		Reverse primer	Antisense	GAGCCCAATTCCCTTCTACAT
		Probe	Sense	GGTGGTCTCTTTGAAGCCTGA
Epstein-Barr virus	LMP2a gene	Forward primer	Sense	AGGAACGTGAATCTAATGAAGAGC
		Reverse primer	Antisense	ATGAGTCATCCCGTGGAGAGTA
		Probe	Sense	AGTCTGTACTTGGGATTGCAACA
JC virus	T antigen	Forward primer	Sense	AATGGGTCTCCCCATACCAA
		Reverse primer	Antisense	GCTTTTGCTTTTAATCTGGTTTAGG
		Probe	Sense	CTAAATCCAGCCTTTCTTTCCAC
Enterovirus	5'UTR	Forward primer	Sense	CGGTACCTTTGTGCGCCTGT
		Reverse primer	Antisense	TTAGGATTAGCCGCATTCAG
		Probe	Sense	ACATGGTGTGAAGAGCCTATTGAGCTA
Dengue virus	3'UTR	Forward primer	Sense	AGACTAGYGGTTAGAGGAGACC
		Reverse primer	Antisense	CTGTGCCTGGAATGATGCTG
		Probe	Sense	CGCTGGGAGAGACCAGAGAT
Rickettsia spp.	OMPa gene	Forward primer	Sense	TGAGTAGTAGCGGGGCACTC
		Reverse primer	Antisense	CAGCCGTTATCTCATTCCA
		Probe	Sense	GCATTTAGTGATAATGTTGGCAATA
Borrelia burgdorferi	Flagellin gene	Forward primer	Sense	TCAGATGCAGACAGAGGTTCTATAC
		Reverse primer	Antisense	GCAATAGCTTCATCTTGGTTTG
		Probe	Sense	CTGATCAAGCTCAATATAACCAAATG
Brucella spp.	OMPa gene	Forward primer	Sense	GGCGCTGGCTACTTCTACATT
		Reverse primer	Antisense	TGGAATTCSGATTCGTCGATA
		Probe	Sense	TACGTCCGTTACGACGTAAAGGG

Appendix Table A2 cont: Pathogens targeted by the Chipron array card, indicating genome target area and the primer and probe sequ

Target pathogen	Target gene	Primer/Probe name	Orientation	Primer/probe sequence (5'-3')
Adenovirus	Hexon gene	Forward primer	Sense	CCCCAGTGGTCTTACATGCACATC
		Reverse primer	Antisense	GCCACGGTGGGGTTTCTAAACTT
		Probe	Sense	GGAGTACCTGAGCCCGGGTCTG
Coxiella burnetii	Com1 gene	Forward primer	Sense	TTTAGTAGAAGCATCCCAAGCATT
		Reverse primer	Antisense	TTGGCAGCGTATTGCGATT
		Probe	Sense	CCGCGTTGTCTTCAAAGAACT
Leptospira spp.	FlaB gene	Forward primer	Sense	TGCTGTGGACAAGACGATGAA
		Reverse primer	Antisense	CACCAGCGCAGATACTTCCA
		Probe	Sense	TCCAGACTTCGAATGGTATCTACAG
Mycobacterium tuberculosis	IS6110	Forward primer	Sense	GTAGGCGTCGGTGACAAAGG
		Reverse primer	Antisense	CAAAGTGTGGCTAACCCTGAAC
		Probe	Sense	CGACACATAGGTGAGGTCTGCTA
Neisseria meningitidis	CTRa gene	Forward primer	Sense	GTGTTCCGCTATACGCCATT
		Reverse primer	Antisense	CGCATCAGCCATATTCACAC
		Probe	Sense	GATAAATGGATTGCTCAAGGTTATG
Plasmodium falciparum	Parc178 gene	Forward primer	Sense	AGGAACTCGACTGGCCTACA
		Reverse primer	Antisense	CCAGCGACAGCGGTTATACT
		Probe	Sense	ACGCCTGACATGGATGGATA
Flavivirus genus	Non-structural protein 5	Forward primer	Sense	AACATGATGGGRAARAGRGARAA
		Reverse primer	Antisense	GTGTCCCAGCCGGCGGTGTCATCAGC
		Probe 1	Sense	GCAATATGGTACATGTGGCTGG
		Probe 2	Sense	GCCATATGGTTCATGTGGCTG
Hepatitis A virus	5'UTR	Forward primer	Sense	TTCAACGCCGAAGGACTG
		Reverse primer	Antisense	GTTTGCCCTAAGCACAGAGAG
		Probe	Sense	TCTCATCCAGTGGATGCATTG
Hepatitis B virus	S protein	Forward primer	Sense	CTCGTGGTGGACTTCTCTCAA
		Reverse primer	Antisense	ACAAACGGGCAACATACCTT
		Probe	Sense	TGCCTCATCTTCTTGTTGGTTC

Appendix Table A3: WNV neutralisation assay details of the WNV positive and borderline ANDEMIA samples 2021-2022

ZRUA number	WNV IgM ELISA Results	WNV micro-VNT results		
		1:8	1:16	1:32
ZRUA1484/21	Borderline	-	-	-
ZRUA1485/21	Borderline	-	-	-
ZRUA1496/21	Positive	-	-	-
ZRUA1504/21	Positive	-	-	-
ZRUA1506/21	Borderline	+	+	+
ZRUA1514/21	Positive	+	-	-
ZRUA1515/21	Positive	+	+	+
ZRUA1525/21	Positive	+	+	+
ZRUA1526/21	Positive	-	+	+
ZRUA1527/21	Positive	-	-	-
ZRUA1530/21	Positive	+	+	+
ZRUA1534/21	Positive	-	-	-
ZRUA1539/21	Borderline	+	+	+
ZRUA1544/21	Borderline	+	+	+
ZRUA1547/21	Borderline	+	+	+
ZRUA1552/21	Borderline	+	+	+
ZRUA1601/21	Positive	+	+	+
ZRUA1603/21	Borderline	+	+	+
ZRUA1624/21	Positive	-	-	-
ZRUA1652/21	Positive	-	-	-
ZRUA1560/21	Positive	-	-	-
ZRUA1566/21	Positive	+	+	+
ZRUA1569/21	Positive	+	+	+
ZRUA1581/21	Borderline	-	-	-
ZRUA2221/22	Borderline	-	-	-
ZRUA2251/22	Positive	+	+	+
ZRUA2253/22	Positive	-	-	-

Appendix Table A4: WNV and WSLB neutralisation assay details of the livestock samples screened for WNV and WSLB neutralising antibodies between 2010-2022 to obtain a positive and negative pool for ELISA validation.

Sample ID	Animal Type	WNV result	WSLB result
ZRU132/21	Bovine (Brahman)	Not tested	Negative
ZRU173/15/4	Bovine (Cow)	Negative	Negative
ZRU157/16	Bovine (Cattle)	Negative	Negative
ZRU132/17	Caprine (Goat)	Negative	Negative
ZRU224/18	Bovine (Dexter)	Negative	Negative
ZRU035/13	Bovine (Cattle)	Negative	Negative
ZRU044/13	Bovine (Cattle)	Negative	1:8 positive
ZRU108/22	Bovine (Bonsmara)	1:32 positive	Negative
ZRU109/22	Ovine	1:32 positive	1:32 positive
ZRU142/22	Ovine (Sheep)	1:32 positive	Negative
ZRU032/12	Bovine (Friesian)	1:32 positive	Negative
ZRU049/12	Bovine (Friesian)	Not tested	Negative
ZRU181/12/1	Bovine (Bonsmara)	1:16 positive	1:16 positive
ZRU189/18	Bovine (Red Wagyu)	Negative	1:16 positive
ZRU224/18	Bovine (Dexter)	Not tested	Negative
ZRU022/13	Bovine (Cattle)	1:8 positive	Negative
ZRU023/13	Bovine (Cattle)	Negative	Negative
ZRU033/13	Bovine (Cattle)	Negative	Negative
ZRU060/13	Bovine (Nguni)	1:8 positive	Negative
ZRU062/13	Bovine (Cattle)	Negative	1:8 positive
ZRU071/13/1	Bovine (Cattle)	Not tested	1:8 positive
ZRU120/13	Bovine (Holstein Fries)	Negative	Negative
ZRU005/14	Bovine (Calf)	Negative	1:32 positive

Appendix Table A5: WNV neutralisation assay details of the WNV IgM positive and borderline equine samples 2021-2022

ZRU number	WNV IgM ELISA Results	WNV micro-VNT results		
		1:8	1:16	1:32
ZRU006/21	Positive	+	+	+
ZRU008/21	Positive	+	+	+
ZRU009/21	Positive	+	+	+
ZRU015/21	Positive	+	+	+
ZRU028/21	Positive	+	+	+
ZRU029/21	Positive	-	-	-
ZRU058/21	Positive	+	+	+
ZRU096/21	Positive	+	+	+
ZRU145/21	Positive	+	+	+
ZRU146/21	Positive	+	+	+
ZRU031/22	Positive	+	+	+
ZRU063/22	Positive	+	+	+
ZRU066/22	Borderline	-	-	-

UNIVERSITEIT VAN PRETORIA
UNIVERSITY OF PRETORIA
YUNIBESITHI YA PRETORIA

Faculty of Health Sciences

Institution: The Research Ethics Committee, Faculty Health Sciences, University of Pretoria complies with ICH-GCP guidelines and has US Federal wide Assurance.

- FWA 00002567, Approved dd 18 March 2022 and Expires 18 March 2027.
- IORG #: IORG0001762 OMB No. 0990-0278 Approved for use through August 31, 2023.

Faculty of Health Sciences **Research Ethics Committee**

23 March 2023

Approval Certificate
Annual Renewal

Dear Ms C Lourens,

Ethics Reference No.: 181/2021 – Line 2
Title: Establishment of serological assays to investigate the incidence of West Nile and Wesselsbron flavivirus infections in Africa

The **Annual Renewal** as supported by documents received between 2023-02-20 and 2023-03-15 for your research, was approved by the Faculty of Health Sciences Research Ethics Committee on 2023-03-15 as resolved by its quorate meeting.

Please note the following about your ethics approval:

- Renewal of ethics approval is valid for 1 year, subsequent annual renewal will become due on 2024-03-23.
- Please remember to use your protocol number (181/2021) on any documents or correspondence with the Research Ethics Committee regarding your research.
- Please note that the Research Ethics Committee may ask further questions, seek additional information, require further modification, monitor the conduct of your research, or suspend or withdraw ethics approval.

Ethics approval is subject to the following:

- The ethics approval is conditional on the research being conducted as stipulated by the details of all documents submitted to the Committee. In the event that a further need arises to change who the investigators are, the methods or any other aspect, such changes must be submitted as an Amendment for approval by the Committee.

We wish you the best with your research.

Yours sincerely

On behalf of the FHS REC, Professor C Kotzé
MBChB, DMH, MMed(Psych), FCPsych, Phd
***Acting Chairperson**: Faculty of Health Sciences Research Ethics Committee*

The Faculty of Health Sciences Research Ethics Committee complies with the SA National Act 61 of 2003 as it pertains to health research and the United States Code of Federal Regulations Title 45 and 46. This committee abides by the ethical norms and principles for research, established by the Declaration of Helsinki, the South African Medical Research Council Guidelines as well as the Guidelines for Ethical Research: Principles Structures and Processes, Second Edition 2015 (Department of Health)

Research Ethics Committee
Room 4-60, Level 4, Tswelopele Building
University of Pretoria, Private Bag x323
Gezina 0031, South Africa
Tel +27 (0)12 356 3084
Email: deepeka.behari@up.ac.za
www.up.ac.za

Fakulteit Gesondheidswetenskappe
Lefapha la Disaense tša Maphelo

Appendix Figure A1: Human ethical approval certificate for the study

UNIVERSITEIT VAN PRETORIA
UNIVERSITY OF PRETORIA
YUNIBESITHI YA PRETORIA

Faculty of Veterinary Science
Animal Ethics Committee

18 May 2023

Approval Certificate
Annual Renewal
(EXT2)

AEC Reference No.: 181/2021 Line 2
Title: Establishment of serological assays to investigate the incidence of West Nile and Wesselsbron flavivirus infections in Africa
Researcher: Ms C Lourens
Student's Supervisor: Prof M Venter

Dear Ms C Lourens,

The **Annual Renewal** as supported by documents received between 2023-04-17 and 2023-05-02 for your research, was approved by the Animal Ethics Committee on its quorate meeting of 2023-05-02.

Please note the following about your ethics approval:

1. The use of species is approved:

Species	Approved
Mammalia – various (Equine, wildlife, livestock)	700
Samples	Approved
Blood (serum, plasma, wb) (samples from live animals)	200
Blood (serum, plasma, wb) - Retrospective/ Stored (H155-19)	20
CSF - Retrospective/ Stored (H155-19)	50
CSF - (samples from live animals)	50
Organs - Retrospective/ Stored (H155-19)	100
Organs- (samples from live animals)	100

2. Ethics Approval is valid for 1 year and needs to be renewed annually by 2024-05-18.
3. Please remember to use your protocol number (181/2021) on any documents or correspondence with the AEC regarding your research.
4. Please note that the AEC may ask further questions, seek additional information, require further modification, monitor the conduct of your research, or suspend or withdraw ethics approval.
5. All incidents must be reported by the PI by email to Ms Marleze Rheeder (AEC Coordinator) within 3 days, and must be subsequently submitted electronically on the application system within 14 days.
6. The committee also requests that you record major procedures undertaken during your study for own-archiving, using any available digital recording system that captures in adequate quality, as it may be required if the committee needs to evaluate a complaint. However, if the committee has monitored the procedure previously or if it is generally can be considered routine, such recording will not be required.

Ethics approval is subject to the following:

- The ethics approval is conditional on the research being conducted as stipulated by the details of all documents submitted to the Committee. In the event that a further need arises to change who the investigators are, the methods or any other aspect, such changes must be submitted as an Amendment for approval by the Committee.

Room 6-13, Arnold Theiler Building, Onderstepoort
Private Bag X04, Onderstepoort 0110, South Africa
Tel +27 12 529 8434
Fax +27 12 529 8321
Email: marleze.rheeder@up.ac.za

Fakulteit Veeartsenykunde
Lefapha la Disaense tša Bongakadiruiwa

We wish you the best with your research.

Yours sincerely

Prof V Naidoo
CHAIRMAN: UP-Animal Ethics Committee

Appendix Figure A2: Animal ethical approval certificate for the study

References

Abudurexiti, A., Adkins, S., Alioto, D., Alkhovsky, SV., Avsic-Zupanc, T., Ballinger, MJ., Bente, DA., Beer, M., Bergeron, E., Blair, CD., Briese, T., Buchmeier, MJ., Burt, FJ., Calisher, CH., Chang, C., Charrell, RN., Choi, IR., Clegg, JCS., De La Torre, JC., De Lamballerie, X., Deng, F., Di Serio, F., Digiaro, M., Drebot, MA., Duan, X., Ebihara, H., Elbeaino, T., Ergunay, K., Fulhorst, CF., Garrison, AR., Gao, GF., Gonzalez, JJ., Groschup, MH., Gunther, S., Haenni, AL., Hall, RA., Hepojoki, J., Hewson, R., Hu, Z., Hughes, HR., Jonson, MG., Junglen, S., Klempa, B., Klingstrom, J., Kou, C., Laenen, L., Lambert, AJ., Langevin, SA., Liu, D., Lukashevich, IS., Luo, T., Lu, C., Maes, P., De Souza, WM., Marklewitz, M., Martelli, GP., Matsuno, K., Mielke-Ehret, N., Minutolo, M., Mirazimi, A., Moming, A., Mulbach, HP., Naidu, R., Navarro, B., Nunes, MRT., Palacios, G., Papa, A., Pauvolid-Correa, A., Paweska, JT., Qiao, J., Radoshitzky, SR., Resende, RO., Romanowski, V., Sall, AA., Salvato, MS., Sasaya, T., Shen, S., Shi, X., Shirako, Y., Simmonds, P., Sironi, M., Song, JW., Spengler, JR., Stenglein, MD., Su, Z., Sun, S., Tang, S., Turina, M., Wang, B., Wang, C., Wang, H., Wang, J., Wei, T., Whitfield, AE., Zerbini, FM., Zhang, J., Zhang, L., Zhang, Y., Zhang, YZ., Zhang, Y., et al. (2019). Taxonomy of the order Bunyavirales: update 2019. *Arch Virol,* 164**,** 1949-1965.

Akerstrom, B., Brodin, T., Reis, K. and Bjorck, L. (1985). Protein G: a powerful tool for binding and detection of monoclonal and polyclonal antibodies. *The Journal of Immunology,* 135**,** 2589-2592.

Amato, L., Dente, MG., Calistri, P. and Delich, S. (2020). Integrated Early Warning Surveillance: Achilles' Heel of One Health? *Microorganisms,* 8.

ANDEMIA. (2021). *About the African Network for improved Diagnostics, Epidemiology and Management of Common Infectious Agents* [Online]. Available: https://www.andemia.org/about-andemia/ [Accessed 23 March 2021].

Aspock, H., Behr, C., Combes, C., Daugschies, A., De Bont, J., Dobler, G., Dubremetz, J., Freeman, J., Frenkel, J., Gessner, A., Gustafsson, M., Haas, W., Hanel, H., Hansen, O., Harder, A., Julsing, M., Kaneshiro, E., Kayser, O., Kohler, P., Lehmacher, W., Londershausen, M., Mackenstedt, U., Maule, A., Mehlhorn, H., Pereira Da Silva, L., Raether, W., Reither-Owona, I., Richter, D., Rollinghoff, M., Schaub, G., Schnieder, T., Seitz, H., Smulian, A., Spielman, A., Spindler, K., Taraschewski, H., Tielens, A., Turberg, A., Vercruysse, J., Walldorf, V. and Werndorfer, W. (2008). Arboviruses. *In:* MEHLHORN, H. (ed.) *Encyclopedia of Parasitology.* 3 ed. Germany: Springer.

Atre, T., Phillips, RL., Modjarrad, K., Regules, JA. and Bergmann-Leitner, ES. (2019). Development and characterization of a Zaire Ebola (ZEBOV) specific IgM ELISA. *J Immunol Methods,* 468**,** 29-34.

Bai, F., Thompson, EA., Vig, PJS. and Leis, AA. (2019). Current Understanding of West Nile Virus Clinical Manifestations, Immune Responses, Neuroinvasion, and Immunotherapeutic Implications. *Pathogens,* 8.

Bakonyi, T. and Haussig, JM. (2020). West Nile virus keeps on moving up in Europe. *Euro Surveill,* 25.

Bakos, I., Mahdi, M., Kardos, L., Nagy, A. and Varkonyi, I. (2022). Clinical spectrum and CSF findings in patients with West-Nile virus infection, a retrospective cohort review. *Diagnostics (Basel),* 12.

Barnard, B. (1997). Antibodies against some viruses of domestic animals in southern African wild animals. *Onderstepoort Journal of Veterinary Research,* 6**,** 95-110.

Barzon, L., Pacenti, M., Franchin, E., Pagni, S., Lavezzo, E., Squarzon, L., Martello, T., Russo, F., Nicoletti, L., Rezza, G., Castilletti, C., Capobianchi, MR., Salcuni, P., Cattai, M., Cusinato, R. and PALU, G. (2013). Large human outbreak of West Nile virus infection in north-eastern Italy in 2012. *Viruses,* 5**,** 2825-39.

Beasly, D. (2011). Vaccines and immunotherapeutics for the prevention and treatment of infections with West Nile virus. *Immunotherapy,* 3**,** 269-285.

Beck, C., Lowenski, S., Durand, B., Bahuon, C., Zientara, S. and Lecollinet, S. (2017). Improved reliability of serological tools for the diagnosis of West Nile fever in horses within Europe. *PLoS Negl Trop Dis,* 11**,**e0005936.

Beckham, JD. and Tyler, KL. (2015). Arbovirus Infections. *Continuum (Minneap Minn),* 21**,** 1599-611.

Benjelloun, A., El Harrak, M., Calistri, P., Loutfi, C., Kabbaj, H., Conte, A., Ippoliti, C., Danzetta, ML. and Belkadi, B. (2017). Seroprevalence of West Nile virus in horses in different Moroccan regions. *Vet Med Sci,* 3**,** 198-207.

Bernkopf, H., Levine, S. and Nerson, R. (1953). Isolation of West Nile Virus in Israel. *The Journal of Infectious Diseases,* 93**,** 207-218.

Bertram, FM., Thompson, PN. and Venter, M. (2020). Epidemiology and Clinical Presentation of West Nile Virus Infection in Horses in South Africa, 2016-2017. *Pathogens,* 10.

Bird, BH. and Mazet, JAK. (2018). Detection of Emerging Zoonotic Pathogens: An Integrated One Health Approach. *Annu Rev Anim Biosci,* 6**,** 121-139.

Blazevic, J., Rouha, H., Bradt, V., Heinz, FX. and Stiasny, K. (2016). Membrane Anchors of the Structural Flavivirus Proteins and Their Role in Virus Assembly. *J Virol,* 90**,** 6365-6378.

Bollati, M., Alvarez, K., Assenberg, R., Baronti, C., Canard, B., Cook, S., Coutard, B., Decroly, E., De Lambellerie, X., Gould, EA., Grard, G., Grimes, JM., Hilgenfeld, R., Jansson, AM., Malet, H.,Mancini, EJ., Mastrangelo, E., Mattevi, A., Milani, M., Moureau, G., Neyts, J., Owens, RJ., Ren, J., Selisko, B., Speroni, S., Steuber, H., Stuart, DI., Unge, T. and Bolognesi, M. (2010). Structure and functionality in flavivirus NS-proteins: perspectives for drug design. *Antiviral Res,* 87**,** 125-48.

Bowen, R. and Nemeth, N. (2007). Experimental infections with West Nile virus. *Curr Opin Infect Dis,* 20**,** 293-297.

Burt, F., Grobbelaar, A., Leman, P., Anthony, F., Gibson, G. and Swanepoel, R. (2002). Phylogenetic relationships of Southern African West Nile virus isolates. *Emerg Infect Dis,* 8**,** 820-826.

Burt, F., Goedhals, D. and Mathengtheng, L. (2014). Arboviruses in southern Africa: are we missing something? *Future Virology,* 9**,** 993–1008.

Busch, MP., Kleinman, SH., Tobler, LH., Kamel, HT., Norris, PJ., Walsh, I., Matud, JL., Prince, HE., Lanciotti, RS., Wright, DJ., Linnen, JM. and Caglioti, S. (2008). Virus and antibody dynamics in acute west nile virus infection. *J Infect Dis,* 198**,** 984-93.

Calisher, CH., Karabatsos, N., Dalrymple, JM., Shope, RE., Porterfield, JS., Westaway, EG. and Brandt, WE. (1989). Antigenic Relationships between Flaviviruses as Determined by Cross-neutralization Tests with Polyclonal Antisera. *Journal of General Virology,* 70**,** 37-43.

Calistri, P., Giovannini, A., Hubalek, Z., Ionescu, A., Monaco, F., Savini, G. and Lelli, R. (2010). Epidemiology of West Nile in Europe and in the Mediterranean Basin. *The Open Virology Journal,* 4**,** 29-37.

Campbell, G., Ceianu, C. and Savage, H. (2001). Epidemic West Nile encephalitis in Romania: waiting for history to repeat itself. *Ann New York Acad Sci,* 951**,** 94-101.

Castillo-Olivares, J. and Wood, J. (2004). West Nile virus infection of horses. *Vet Res,* 35**,** 467-83.

CDC. 2018. *WNV disease cases and presumptive viremic blood donors by state 2018* [Online]. Available: https://www.cdc.gov/westnile/statsmaps/finalmapsdata/index.html [Accessed 8 July 2021].

CDC. 2021a. *Center for Disease Control* [Online]. [Accessed 29 March 2021].

CDC. 2021b. *Preliminary Maps & Data for 2020* [Online]. Available: https://www.cdc.gov/westnile/statsmaps/preliminarymapsdata2020/index.html [Accessed 29 June 2021].

CDC. 2021c. *West Nile virus disease cases reported to CDC by state of residence, 1999-2019* [Online]. Available: https://www.cdc.gov/westnile/statsmaps/cumMapsData.html [Accessed 1 June 2021].

CDC. 2023. *Preliminary WNV Maps and Data for 2022* [Online]. Available: https://www.cdc.gov/westnile/statsmaps/preliminarymapsdata2022/index.html [Accessed 30 May 2023].

CFSPH. 2017. *Wesselsbron Disease* [Online]. [Accessed March 2021].

Cha, GW., Cho, JE., Ju, YR., Hong, YJ., Han, MG., Lee, WJ., Choi, EY. and Jeong, YE. (2014). Comparison of four serological tests for detecting antibodies to Japanese encephalitis virus after vaccination inchildren. *Osong Public Health Res Perspect,* 5**,** 286-91.

Chan, KR., Ismail, AA., Thergarajan, G., Raju, CS., Yam, HC., Rishya, M. and Sekaran, SD. (2022). Serological cross-reactivity among common flaviviruses. *Front Cell Infect Microbiol,* 12**,** 975398.

Chippaux, JP. and Chippaux, A. (2018). Yellow fever in Africa and the Americas: a historical and epidemiological perspective. *J Venom Anim Toxins Incl Trop Dis,* 24**,** 20.

Chung, WM., Buseman, CM., Joyner, SN., Hughes, SM., Fomby, TB., Luby, JP. and Haely, RW. (2013). The 2012 West Nile encephalitis epidemic in Dallas, Texas. *JAMA,* 310**,** 297-307.

Ciota, AT. (2017). West Nile virus and its vectors. *Curr Opin Insect Sci,* 22**,** 28-36.

Ciota, AT. and Kramer, LD. (2013). Vector-virus interactions and transmission dynamics of West Nile virus. *Viruses,* 5**,** 3021-47.

Coetzer, J., Theodoridis, A. and Van Heerden, A. (1978). Wesselsbron disease, pathological, haematological and clinical studies in natural cases and experimentally infected new-born lambs. *Onderstepoort Journal ofVeterinary Research,* 45**,** 93-106.

Coffey, LL., Forrester, N., Tsetsarkin, K., Vasilakis, N. and Weaver, SC. (2013). Factors shaping the adaptive landscape for arboviruses: implications for the emergence of disease. *Future Microbiol,* 8**,** 155-76.

Colpitts, TM., Conway, MJ., Montgomery, RR. and Fikrig, E. (2012). West Nile Virus: biology, transmission,and human infection. *Clin Microbiol Rev,* 25**,** 635-48.

Cornel, AJ., Lee, Y., Almeida, APG., Johnson, T., Mouatcho, J., Venter, M., De Jager, C. and Braack, L. (2018). Mosquito community composition in South Africa and some neighboring countries. *Parasites & Vectors,* 11**,** 331.

Cotar, AI., Falcuta, E., Dinu, S., Necula, A., Birlutiu, V., Ceianu, CS. and Prioteasa, FL. (2018). West Nile virus lineage 2 in Romania, 2015-2016: co-circulation and strain replacement. *Parasit Vectors,* 11**,** 562.

Crill, WD. and Chang, GJ. (2004). Localization and characterization of flavivirus envelope glycoprotein cross-reactive epitopes. *J Virol,* 78**,** 13975-86.

Crowther, J. (2002). Stages in ELISA. *The ELISA guidebook.* New Jersey: Humana Press.

Danis, K., Papa, A., Papnikolaou, E., Dougas, G., Terzaki, I., Baka, A., Vrioni, G., Kapsimali, V., Tsakris, A., Kansouzidou, A., Tsiodras, S., Vakalis, N., Bonovas, S. and Kremastinou, J. (2011a). Ongoing outbreak of West Nile virus infection in humans, Greece, July to August 2011. *Eurosurveillance,* 16**,** 1-5.

Danis, K., Papa, A., Theocharopoulos, G., Dougas, G., Athanasiou, M., Detsis, M., Baka, A., Lytras, T., Mellou, K., Bonovas, S. and Panagiotopoulos, T. (2011b.) Outbreak of West Nile virus infection in Greece, 2010. *Emerg Infect Dis,* 17**,** 1868-72.

Diagne, MM., Faye, M., Faye, O., Sow, A., Balique, F., Sembene, M., Granjon, L., Handschumacher, P., Faye, O., Diallo, M. and Sall, AA. (2017). Emergence of Wesselsbron virus among black rat and humans in Eastern Senegal in 2013. *One Health,* 3**,** 23-28.

Ding, XX., Li, XF., Deng, YQ., Guo, YH., Hao, W., Che, XY., Qin, CF. and Fu, N. (2014). Development of a Double Antibody Sandwich ELISA for West Nile Virus Detection Using Monoclonal Antibodies against Non-Structural Protein 1. PLOS ONE, 9, e108623.

Droll, DA., Krishna Murthy, HM. and Chambers, TJ. (2000). Yellow fever virus NS2B-NS3 protease: charged-to-alanine mutagenesis and deletion analysis define regions important for protease complex formation and function. *Virology,* 275**,** 335-47.

ECDC. 2022. *Weekly updates: 2022 WNV transmission season* [Online]. Available: https://www.ecdc.europa.eu/en/west-nile-fever/surveillance-and-disease-data/disease-data-ecdc [Accessed 30 May 2023].

Ehrenstein, M., Cook, H. and Neuberger, M. (2000). Deficiency in Serum Immunoglobulin (Ig)M Predisposes to Development of IgG Autoantibodies. *J. Exp. Med.,* 191**,** 1253-1257.

Endale, A., Medhin, G., Darfiro, K., Kebede, N. and Legesse, M. (2021). Magnitude of Antibody Cross-Reactivity in Medically Important Mosquito-Borne Flaviviruses: A Systematic Review. *Infect Drug Resist,* 14**,** 4291-4299.

Fall, G., Di Paola, N., Faye, M., Dia, M., Freire, CCDM., Loucoubar, C., Zanotto, PMDA., Faye, O. and Sall, AA. (2017). Biological and phylogenetic characteristics of West African lineages of West Nile virus. *PLOS Neglected Tropical Diseases,* 11**,** e0006078.

Faye, M., Seye, T., Patel, P., Diagne, CT., Diagne, MM., Dia, M., Thiaw, FD., Sall, AA. and Faye, O. (2022). Development of Real-Time Molecular Assays for the Detection of Wesselsbron Virus in Africa. *Microorganisms,* 10.

Felderbaum, RS. (2015). The baculovirus expression vector system: A commercial manufacturing platform for viral vaccines and gene therapy vectors. *Biotechnol J,* 10**,** 702-14.

Foil, L. and Gorham, J. (2000). Mechanical transmission of disease agents by arthropods *In:* ELDRIDGE, B. & EDMAN, J. (eds.) *Medical Entomology.* Dordrecht: Springer.

Frierson, G. (2010). The Yellow Fever Vaccine: A History. *Yale Journal of Biology and Medicine,* 83**,** 77-85.

Frost, MJ., Zhang, J., Edmonds, JH., Prow, NA., Gu, X., Davis, R., Hornitzky, C., Arzey, KE., Finlaison, D., Hick, P., Read, A., Hobson-Peters, J., May, FJ., Doggett, SL., Haniotis, J., Russell, RC., Hall, RA., Khromykh, AA. and Kirkland, PD. (2012). Characterization of virulent West Nile virus Kunjin strain, Australia, 2011. *Emerg Infect Dis,* 18**,** 792-800.

Gan, SD. and Patel, KR. (2013). Enzyme immunoassay and enzyme-linked immunosorbent assay. *J Invest Dermatol,* 133**,** e12.

Garcia-Bocanegra, I., Jaen-Tellez, JA., Napp, S., Arenas-Montes, A., Fernandez-Morente, M., Fernandez-Molera, V. and Arenas, A. (2012). Monitoring of the West Nile virus epidemic in Spain between 2010 and 2011. *Transbound Emerg Dis,* 59**,** 448-55.

Gbenga, A., Witbooi, P. and Okosun, K. (2016). Modeling and analyzing the impact of temperature and rainfall on mosquito population dynamics over KwaZulu-Natal province, South Africa. *International Journal of Biomathematics,* 10.

Gebhard, LG., Filomatori, CV. and Gamarnik, AV. (2011). Functional RNA elements in the dengue virus genome. *Viruses,* 3**,** 1739-56.

Giladi, M., Metzkor-Cotter, E., Martin, D., Siegman-Igra, Y., Korczyn, A., Rosso, R., Berger, S., Campbell, G. and Lanciotti, R. (2001). West Nile encephalitis in Israel 1999: the New York connection. *Emerg Infect Dis,* 7**,** 659-661.

Glasner, DR., Puerta-Guardo, H., Beatty, PR. and Harris, E. (2018). The Good, the Bad, and the Shocking: The Multiple Roles of Dengue Virus Nonstructural Protein 1 in Protection and Pathogenesis. *Annu Rev Virol,* 5**,** 227-253.

Gould, D., Gunakasem, P., Marshall, J. and Nisalak, A. (1967). Ecology of arboviruses in Thailand. *Annual progress report,* 1**,** 43-71.

Gould, LH. and Fikrig, E. (2004). West Nile virus: a growing concern? *J Clin Invest,* 113**,** 1102-7.

Gould, E., Pettersson, J., Higgs, S., Charrel, R. and De Lamballerie, X. (2017). Emerging arboviruses: Why today? *One Health,* 4**,** 1-13.

Granwehr, BP., Lillibridge, KM., Higgs, S., Mason, PW., Aronson, JM., Campbell, GA. and Barrett, ADT. (2004). West Nile virus: where are we now? *The Lancet Infectious Diseases,* 4**,** 547-556.

Grard, G., Moureau, G., Charrel, RN., Lemasson, JJ., Gonzalez, JP., Gallian, P., Gritsun, TS., Holmes, EC., Gould, EA. and De Lamballerie, X. (2007). Genetic characterization of tick-borne flaviviruses: new insights into evolution, pathogenetic determinants and taxonomy. *Virology,* 361**,** 80-92.

Gubler, D. (2002). The global emergence/resurgence of arboviral diseases as public health problems. *Archives of Medical Research,* 22**,** 330-342.

Gubler, DJ. (2007). The continuing spread of West Nile virus in the western hemisphere. *Clin Infect Dis,* 45**,** 1039-46.

Habarugira, G., Suen, WW., Hobson-Peters, J., Hall, RA. and Bielefeldt-Ohmann, H. (2020). West Nile Virus: An Update on Pathobiology, Epidemiology, Diagnostics, Control and "One Health" Implications. *Pathogens,* 9.

Haijan-Tilaki, K. (2013). Receiver Operating Characteristic (ROC) Curve Analysis for Medical Diagnostic Test Evaluation. *Caspian J Intern Med,* 4**,** 627-635.

Hardcastle, AN., Osborne, JCP., Ramshaw, RE., Hulland, EN., Morgan, JD., Miller-Petrie, MK., Hon, J., Earl, L., Rabinowitz, P., Wasserheit, JN., Gilbert, M., Robinson, TP., Wint, GRW., Shirude, S., Hay, SI. and Pigott, DM. (2020). Informing Rift Valley Fever preparedness by mapping seasonally varying environmental suitability. *Int J Infect Dis,* 99**,** 362-372.

Hayes, C. (1989). West Nile fever: Epidemiology and Ecology. *In:* MONATH, T. (ed.) *The Arboviruses.*

Hayes, E., Sejvar, J., Zaki, S., Lanciotti, R., Bode, A. and Campbel, G. (2005). Virology, Pathology, and Clinical Manifestations of West Nile Virus Disease. *Emerg Infect Dis,* 11**,** 1174-1179.

Heymann, C., Kokernot, R. and De Meillon, B. (1958). Wesselsbron virus infections in man. *SA Medical Journal,* 32**,** 543-545.

Hobson-Peters, J. (2012). Approaches for the development of rapid serological assays for surveillance and diagnosis of infections caused by zoonotic flaviviruses of the Japanese encephalitis virus serocomplex. *J Biomed Biotechnol,* 2012**,** 379738.

Holbrook, MR. (2017). Historical Perspectives on Flavivirus Research. *Viruses,* 9.

Holland, P., Abramson, R., Watson, R. and Gelfand, D. (1991). Detection of specific polymerase chain reaction product by utilizing the 5′—3' exonuclease activity of Thermus aquaticus DNA polymerase. *Proceedings of the National Academy of Sciences of the United States of America,* 88**,** 7276-7280.

Hubalek, Z. and Halouzka, J. (1999). West Nile Fever—a Reemerging Mosquito Borne Viral Disease in Europe. *Emerg Infect Dis,* 5**,** 643-650.

Hubalek, Z., Tomesek, M., Kosina, M., Sikutova, S., Strakova, P. and Rudolf, I. (2019). West Nile virus outbreak in captive and wild raptors, Czech Republic 2018. *Zoonoses Public Health,* 66**,** 978-981.

Human, S., Leman, P., Kemp, A., Paweska, J. and Venter, M. (2008) Molecular characterization of Wesselsbron virus from animals and humans in South Africa. 8th Annual Conference of the South African Society of Veterinary epidemiology and preventative medicine.

Human, S. (2011). *Characterization of zoonotic flavi- and alphaviruses in sentinel animals in South Africa.* MSc Medical Virology, University of Pretoria.

Jankovic, S. (2008). Public Health SurveillancePublic health surveillance. *In:* KIRCH, W. (ed.) *Encyclopedia ofPublic Health.* Dordrecht: Springer Netherlands.

Jones, R., Kulkarni, MA., Davidson, TMV., Team, RLR. and Talbot, B. (2020). Arbovirus vectors of epidemiological concern in the Americas: A scoping review of entomological studies on Zika, dengueand chikungunya virus vectors. *PLoS One,* 15**,** e0220753.

Jupp, P. (2014). Mosquitoes as vectors of human disease in South Africa. *SA Fam Practice,* 47**,** 68-72.

Jupp, P., Blackburn, N., Thompson, D. and Meenehan, G. (1986). Sindbis and West Nile virus infections in theWitwatersrand-Pretoria region. *SAMJ,* 70**,** 218-220.

Jupp, P. and Kemp, A. (1998). Studies of an outbreak of Wesselsbron virus in the Free State province, South Africa. *Journal of the American Mosquito Control Association,* 14**,** 40-45.

Justines, G. and Shope, R. (1969). Wesselsbron virus infection in a laboratory worker, with virus recovery from athroat washing. *Health Lab Sci.,* 6**,** 46-49.

Karabatsos, N., and Rockefeller, F. (1985). *International catalogue of arboviruses, including certain other viruses of vertebrates,* San Antonio, Tex., American Society of Tropical Medicine and Hygiene for the Subcommittee on Information Exchange of the American Committee on Arthropod-borne Viruses.

Karim, K. (2019). Polymerase Chain Reaction (PCR): Principle and Applications. *In:* MADAN, L. N., OANA-MARIA, B., CORNEL, B. & SHYMAA, E. (eds.) *Synthetic Biology.* Rijeka: IntechOpen.

Keusch, G., Pappaioanou, M., Gonzalez, M. and Scott, KTP. (2009). Achieving an Effective Zoonotic Disease Surveillance System. *In:* CAPACITY, C. O. A. S. G., OF, F. S. A. R. T. E. D. & ORIGIN, Z. (eds.) *Sustaining Global Surveillance and Response to Emerging Zoonotic Diseases* Washington DC, USA: National Academies Press.

Khan, E., Barr, KL., Farooqi, JQ., Prakoso, D., Abbas, A., Khan, ZY., Ashi, S., Imtiaz, K., Aziz, Z., Malik, F., Lednicky, JA. and Long, MT. (2018). Human West Nile Virus Disease Outbreak in Pakistan, 2015- 2016. *Front Public Health,* 6**,** 20.

Khromykh, AA., Varnavski, AN., Sedlak, PL. and Westaway, EG. (2001). Coupling between replication and packaging of flavivirus RNA: evidence derived from the use of DNA-based full-length cDNA clones of Kunjin virus. *J Virol,* 75**,** 4633-40.

Kitai, Y., Shoda, M., Kondo, T. and Konishi, E. (2007). Epitope-blocking enzyme-linked immunosorbent assay to differentiate west nile virus from Japanese encephalitis virus infections in equine sera. *Clin Vaccine Immunol,* 14**,** 1024-31.

Kodani, M. and Winchell, JM. (2012). Engineered combined-positive-control template for real-time reverse transcription-PCR in multiple-pathogen-detection assays. *J Clin Microbiol,* 50**,** 1057-60.

Kokernot, R., Paterson, H. and De Meillon, B. (1958). Studies on the transmission of Wesselsbron virus by Aedes (Ochlerotatus) caballus (THEO.). *SA Medical Journal,* 32**,** 546-548.

Komar, N., Langevin, S., Hinten, S., Nemeth, N., Edwards, E., Hettler, D., Davis, B., Bowen, R. and Bunning, M. (2003). Experimental infection of North American birds with the New York 1999 strain of West Nile Virus. *Emerging Infectious Diseases,* 9**,** 311-322.

Komar, N. (2001). West Nile virus surveillance using sentinel birds. *Ann N Y Acad Sci,* 951**,** 58-73.

Kralik, P. and Ricchi, M. (2017). A Basic Guide to Real Time PCR in Microbial Diagnostics: Definitions, Parameters, and Everything. *Front Microbiol,* 8**,** 108.

Kuno, G. (2003). Serodiagnosis of Flaviviral Infections and Vaccinations in Humans. *Advances in Virus Research Volume 61.*

Lanciotti, RS., Ebel, GD., Deubel, V., Kerst, AJ., Murri, S., Meyer, R., Bowen, M., McKinney, N., Morrill, WE., Crabtree, MB., Kramer, LD. and Roehrig, JT. (2002). Complete genome sequences and phylogenetic analysis of West Nile virus strains isolated from the United States, Europe, and the Middle East. *Virology,* 298**,** 96-105.

Laureti, M., Narayanan, D., Rodriguez-Andres, J., Fazakerley, JK. and Kedzierski, L. (2018). Flavivirus Receptors: Diversity, Identity, and Cell Entry. *Front Immunol,* 9**,** 2180.

Le Roux, J. (1959). The Histopathology of Wesselsbron virus in sheep. *Onderstepoort Journal of Veterinary Research,* 28**,** 237-243.

LI, J. 2003. Asymmetric flaccid paralysis: A neuromuscular presentation of West Nile virus infection. *Annals of Neurology,* 53**,** 703.

Liang, G., Gao, X. and Gould, EA. (2015). Factors responsible for the emergence of arboviruses; strategies, challenges, and limitations for their control. *Emerg Microbes Infect,* 4**,** e18.

Liu, F., Wu, X., Li, L., Liu, Z. and Wang, Z. (2013). Use of baculovirus expression system for generation of virus-like particles: Successes and challenges. *Protein Expression and Purification,* 90**,** 104-116.

Lifescience. 2021. *LightCycler® TaqMan® Master* [Online]. Available: https://www.lifescience.roche.com/en_za/products/lightcycler-TaqMan-master.html [Accessed 31 March 2021].

Lindebach, B. and Rice, C. (2003). Molecular biology of flaviviruses. *Advances in virus research,* 59**,** 23-61.

Liu, J., Ochieng, C., Wiersma, S., Stroher, U., Towner, JS., Whitmer, S., Nichol, ST., Moore, CC., Kersch, GJ., Kato, C., Sexton, C., Peterson, J., Massung, R., Hercik, C., Crump, JA., Kibiki, G., Maro, A., Mijaga, B., Gratz, J., Jacob, ST., Banura, P., Scheld, WM., Juma, B., Onyango, CO., Montgomery, JM., Houpt, E. and Fields, B. (2016). Development of a TaqMan Array Card for Acute-Febrile-Illness Outbreak Investigation and Surveillance of Emerging Pathogens, Including Ebola Virus. *J Clin Microbiol,* 54**,** 49-58.

Llorente, F., Garcia-Irazabal, A., Perez-Ramirez, E., Cano-Gomez, C., Sarasa, M., Vazquez, A. and Jimenez-Clavero, MA. (2019). Influence of flavivirus co-circulation in serological diagnostics and surveillance: A model of study using West Nile, Usutu and Bagaza viruses. *Transbound Emerg Dis,* 66**,** 2100-2106.

Long, M., Ostlund, E., Porter, M. and Crom, R. (2002). Equine West Nile Encephalitis: Epidemiological and Clinical Review for Practitioners. *AAEP Proceedings,* 48**,** 1-6.

Lorenz, IC., Allison, SL., Heinz, FX. and Helenius, A. (2002). Folding and dimerization of tick-borne encephalitis virus envelope proteins prM and E in the endoplasmic reticulum. *J Virol,* 76**,** 5480-91.

Lustig, Y., Mannasse, B., Koren, R., Katz-Likvornik, S., Hindiyeh, M., Mandelboim, M., Dovrat, S., Soffer, D. and Mendelson, E. (2016). Superiority of West Nile Virus RNA Detection in Whole Blood for Diagnosis of Acute Infection. *J Clin Microbiol,* 54**,** 2294-7.

Lustig, Y., Kaufman, Z., Mannasse, B., Koren, R., Katz-Likvornik, S., Orshan, L., Glatman-Freedman, A. and Mendelson, E. (2017). West Nile virus outbreak in Israel in 2015: phylogenetic and geographic characterization in humans and mosquitoes. *Clin Microbiol Infect,* 23**,** 986-993.

Lustig, Y., Sofer, D., Bucris, ED. and Mendelson, E. (2018). Surveillance and Diagnosis of West Nile Virus in the Face of Flavivirus Cross-Reactivity. *Front Microbiol,* 9**,** 2421.

MacDonald, J., Tonry, J., Hall, RA., Williams, B., Palacios, G., Ashok, MS., Jabado, O., Clark, D., Tesh, RB., Briese, T. and Lipkin, WI. (2005). NS1 Protein Secretion during the Acute Phase of West Nile Virus Infection. *Journal of Virology,* 79**,** 13924-13933.

MacIntyre, C. (2022). *Investigation of the molecular epidemiology of West Nile virus at the human-animal interface in South Africa.* MSc Medical Virology, University of Pretoria.

MacIntyre, CDM., Guarido, MM., Riddin, MA., Johnson, T., Braack, L., Schrama, M., Gorsich, E., Almeida, AP. G. and Venter, M. (2023). Survey of West Nile and Banzi Viruses in Mosquitoes, South Africa, 2011-2018. *Emerg Infect Dis,* 29**,** 164-169.

MacKenzie, J., Barrett, A. and Deubel, V. (2002). The Japanese Encephalitis Serological Group of Flaviviruses: a Brief Introduction to the Group. *Current Topics in Microbiology and Immunology.* Berlin, Heidelberg: Springer.

MacKenzie, J., Jones, M. and Young, P. (1996). Immunolocalization of the dengue virus nonstructural glycoprotein NS1 suggests a role in viral RNA replication. *Virology,* 220**,** 232-240.

Madden, K. (2003). West Nile virus infection and its neurological manifestations. *Clinical Medicine & Research,* 1**,** 145-150.

Madewell, ZJ. (2020). Arboviruses and Their Vectors. *South Med J,* 113**,** 520-523.

Mandrekar, J. (2009). Receiver Operating Characteristic Curve in Test Assessment. *Journal of Thoracic Oncology,* 5**,** 1315-1316.

Marra, P., Griffing, S., Caffrey, C., Kilpatrick, A., Mclean, R., Brand, C., Saito, E., Dupius, A., Kramer, L. and Novak, R. (2004). West Nile Virus and Wildlife. *BioScience,* 54**,** 393-402.

Martinez, D., Murray, KO., Reyna, M., Arafat, RR., Gorena, R., Shah, UA. and Debboun, M. (2017). West Nile Virus Outbreak in Houston and Harris County, Texas, USA, 2014. *Emerg Infect Dis,* 23**,** 1372-1376.

Mavrouli, M., Vrioni, G., Kapsimali, V., Tsiamis, C., Mavroulis, S., Pervanidou, D., Billinis, C., Hadjichristodoulou, C. and Tsakris, A. (2019). Reemergence of West Nile Virus Infections in Southern Greece, 2017. *Am J Trop Med Hyg,* 100**,** 420-426.

Mazeaud, C., Freppel, W. and Chatel-Chaix, L. (2018). The Multiples Fates of the Flavivirus RNA Genome During Pathogenesis. *Front Genet,* 9**,** 595.

McIntosh, B. (1980). *The epidemiology of arthropod-borne viruses in Southern Africa.* DSc Dissertation, University of Pretoria.

McVey, D., Wilson, W. and Gay, C. (2015). West Nile Virus. *Rev. Sci. Tech. Off. Int. Epiz.,* 34**,** 431-439.

Melnick, JL. (1951). Isolation from Human Sera in Egypt of a Virus Apparently Identical to West Nile Virus. *Experimental Biology and Medicine,* 77**,** 661.

Modis, Y., Ogata, S., Clements, D. and Harrison, S. (2003). Structure of the dengue virus envelope protein after membrane fusion. *Nature,* 472**,** 313-319.

Molini, U., Franzo, G., Nel, H., Khaiseb, S., Ntahonshikira, C., Chiwome, B., Baines, I., Madzingira, O., Monaco, F., Savini, G. and D'Alterio, N. (2021). West Nile Virus Seroprevalence in a Selected Donkey Population of Namibia. *Front Vet Sci,* 8**,** 681354.

Monaco, F., Lelli, R., Teodori, L., Pinoni, C., Di Gennaro, A., Polci, A., Calistri, P. and Savini, G. (2010). Re-emergence of West Nile virus in Italy. *Zoonoses Public Health,* 57**,** 476-86.

Monastiri, A., Mechri, B., Vazquez-Gonzalez, A., Ar Gouilh, M., Chakroun, M., Loussaief, C., Mastouri, M., Dimassi, N., Boughzala, L., Aouni, M. and Serra-Cobo, J. (2018). A four-year survey (2011-2014) of West Nile virus infection in humans, mosquitoes and birds, including the 2012 meningoencephalitis outbreak in Tunisia. *Emerg Microbes Infect,* 7**,** 28.

Moureau, G. (2007). A Real-Time RT-PCR Method for the Universal Detection and Identification of Flaviviruses. *Vector-Borne and Zoonotic Diseases,* 7**,** 467.

Moureau, G., Cook, S., Lemey, P., Nougairede, A., Forrester, NL., Khasnatinov, M., Charrel, RN., Firth, AE., Gould, EA. and De Lamballerie, X. (2015). New insights into flavivirus evolution, taxonomy and biogeographic history, extended by analysis of canonical and alternative coding sequences. *PLoS One,* 10**,** e0117849.

Mukhopadhyay, S., Kuhn, RJ. and Rossmann, MG. (2005). A structural perspective of the flavivirus life cycle. *Nat Rev Microbiol,* 3**,** 13-22.

Musso, D. and Despres, P. (2020). Serological Diagnosis of Flavivirus-Associated Human Infections. *Diagnostics (Basel),* 10.

Murgue, B., Murri, S., Triki, H., Deubel, V. and Zeller, H. (2001). West Nile in the Mediterranean Basin: 1950-2000. *Ann New York Acad Sci,* 951**,** 117-126.

Murgue, B., Murri, S., Zientara, S., Durand, B., Durand, J. and Zeller, H. (2000). West Nile outbreak in horses in Southern France, 2000: The return after 35 years. *Emerg Infect Dis,* 7**,** 692-696.

Murray, K. (2006). Risk factors for encephalitis and death from West Nile virus infection. *Epidemiology and Infection,* 134**,** 1325.

Nahm, FS. (2022). Receiver operating characteristic curve: overview and practical use for clinicians. *Korean Journal of Anesthesiology,* 75**,** 25-36.

Nash, D., Mostashari, F., Fine, A., Miller, J., O'Leary, D., Murray, K., Huang, A., Rosenberg, A., Greenberg, A., Sherman, M., Wong, S. and Campbell, G. (2001). The outbreak of West Nile Virusinfection in the New York City area in 1999. *N Engl J Med,* 344**,** 1807-1814.

OBP. 2021. *Wesselsbron disease vaccine* [Online]. Available: https://www.obpvaccines.co.za/products[Accessed March 2021].

Oluwayelu, D., Adebiyi, A. and Tomori, O. (2018). Endemic and emerging arboviral diseases of livestock inNigeria: a review. *Parasit Vectors,* 11**,** 337.

One Health High-Level Expert Panel., Adisasmito, WB., Almuhairi, S., Behravesh, CB., Bilivogui, P., Bukachi, SA., Casas, N., Cediel Becerra, N., Charron, DF., Chaudhary, A., Ciacci Zanella, JR., Cunningham, AA., Dar, O., Debnath, N., Dungu, B., Farag, E., Gao, GF., Hayman, DTS., Khaitsa, M., Koopmans, MPG., Machalaba, C., Mackenzie, JS., Markotter, W., Mettenleiter, TC., Morand, S., Smolenskiy, V. and Zhou, L. (2022). One Health: A new definition for a sustainable and healthy future. *PLoS Pathog,* 18**,** e1010537.

Oymans, J., Van Keulen, L., Wichgers Schreur, PJ. and Kortekaas, J. (2020). Early Pathogenesis of Wesselsbron Disease in Pregnant Ewes. *Pathogens,* 9.

Palomares, LA., Estrada-Moncada, S. and Ramirez, OT. (2004). Production of Recombinant Proteins. *In:* Balbas, P. and Lorence, A. (eds.) *Recombinant Gene Expression: Reviews and Protocols.* Totowa, NJ: Humana Press.

Patel, P., Landt, O., Kaiser, M., Faye, O., Koppe, T., Lass, U., Sall, A. and Niedrig, M. (2013). Development of panflavi RT-PCR. *Virology,* 10**,** 1-11.

Pealer, N., Marfin, A., Peterson, L., Lanciotti, R., Page, P., Stramer, S., Stobierski, M., Signs, K., Newman, B., Kapoor, H., Goodman, J. and Chamberland, M. (2003). Transmission of West Nile Virusthrough blood transfusion in the United States in 2002. *N Engl J Med,* 349**,** 1236-1245.

Papa, A., Anastasiadou, A. and Delianidou, M. (2015). West Nile virus IgM and IgG antibodies three years post-infection. *Hippokratia,* 19**,** 34-36.

Peterson, L. and Marfin, A. (2002). West Nile virus: A primer for the clinician. *Annals of Internal Medicine,* 137**,** 173-179.

Peterson, LR., Brault, AC. and Nasci, RS. (2013). West Nile virus: review of the literature. *JAMA,* 310**,** 308-15.

Pfaunmiller, EL., Anguizola, JA., Milanuk, ML., Carter, N. and Hage, DS. (2016). Use of protein G microcolumns in chromatographic immunoassays: A comparison of competitive binding formats. *J Chromatogr B Analyt Technol Biomed Life Sci,* 1021**,** 91-100.

Pierson, TC. and Diamond, MS. (2020). The continued threat of emerging flaviviruses. *Nat Microbiol,* 5**,** 796-812.

Platonov, A., Shipulina, G., Shupulina, O., Tyutunnik, E., Frolochkina, T., Lanciotti, R., Yazyshina, S., Platonova, O., Obukhov, I., Zhukov, A., Vengerov, Y. and Pokrovskii, V. (2001). Outbreak of West Nile virus infection, Volgograd Region, Russia, 1999. *Emerg Infect Dis,* 7**,** 128-132.

Poidinger, M., Hall, R. and MacKenzie, J. (1996). Molecular Characterization of the Japanese Encephalitis Serocomplex of the Flavivirus Genus. *Virology,* 218**,** 417-421.

Popovic, N., Milosevic, B., Urosevic, A., Poluga, J., Lavadinovic, L., Nedelijkovic, J., Jevtovic, D. and Dulovic, O. (2013). Outbreak of West Nile virus infections among humans in Serbia, August to October 2012. *Eurosurveillance,* 18**,** 1-8.

Rajna, M. and Irena, Z. (2020). Optimization, Validation and Standardization of ELISA. *In:* GYULA, M. (ed.) *Norovirus.* Rijeka: IntechOpen.

Rathore, APS. and St John, AL. (2020). Cross-Reactive Immunity Among Flaviviruses. *Front Immunol,* 11**,** 334.

Reisen, W., Fang, Y. and Martinez, V. (2005). Avian host and mosquito (Diptera: Culicidae) vector competence determine the efficiency of West Nile and St. Louis Encephalitis virus transmission. *J. Med. Entomol.,* 42**,** 367Ð375.

Riccardo, F., Bolici, F., Fafangel, M., Jovanovic, V., Socan, M., Klepac, P., Plavsa, D., Vasic, M., Bella, A., Diana, G., Rosi, L., Pezzotti, P., Andrianou, XD., Di Luca, M., Venturi, G., Maraglino, F., Pervanidou, D., Cenviarelli, O., Baka, A., Young, J., Bakonyi, T., Rezza, G. and Suk, JE. (2020). West Nile virus in Europe: after action reviews of preparedness and response to the 2018 transmission season in Italy, Slovenia, Serbia and Greece. *Global Health,* 16**,** 47.

Rudolph, KE., Lessler, J., Moloney, RM., Kmush, B. and Cummings, DA. (2014). Incubation periods of mosquito-borne viral infections: a systematic review. *Am J Trop Med Hyg,* 90**,** 882-91.

Sahu, A., Dhanze, H., Singh, V., Mehta, D., Gupta, M., Singh, M., Vinod, VK. and Gulati, BR. (2022). Development of IgM-ELISA for diagnosis of recent infection of Japanese encephalitis virus in equines. *Biologicals,* 75**,** 16-20.

Sambri, V., Capobianchi, M., Charrel, R., Fyodorova, M., Gaibani, P., Gould, E., Niedrig, M., Papa, A., Pierro, A., Rossini, G., Varani, S., Vocale, C. and Landini, MP. (2013). West Nile virus in Europe: emergence, epidemiology, diagnosis, treatment, and prevention. *Clin Microbiol Infect,* 19**,** 699-704.

Saxena, D., Kumar, JS., Parida, M., Sivakumar, RR. and Patro, IK. (2013). Development and evaluation of NS1 specific monoclonal antibody based antigen capture ELISA and its implications in clinical diagnosis of West Nile virus infection. *Journal of Clinical Virology,* 58**,** 528-534.

Scholz, J. and Suppmann, S. (2017). A new single-step protocol for rapid baculovirus-driven protein production in insect cells. *BMC Biotechnol,* 17**,** 83.

Schubert, G., Achi, V., Ahuka, S., Belarbi, E., Bourhaima, O., Eckmanns, T., Johnstone, S., Kabore, F., Kra, O., Mendes, A., Ouebraogo, AS., Poda, A., Some, AS., Tomczyk, S., Couacy-Hymann, E., Kayembe JM., Meda, N., Muyembe Tamfum, JJ., Ouangraoua, S., Page, N., Venter, M., Leendertz, FH., Akoua-Koffi, C. and Consortium, A. (2021). The African Network for Improved Diagnostics, Epidemiology and Management of common infectious Agents. *BMC Infect Dis,* 21**,** 539.

Schwarz, ER. and Long, MT. (2023). Comparison of West Nile Virus Disease in Humans and Horses: Exploiting Similarities for Enhancing Syndromic Surveillance. *Viruses,* 15.

Schweitzer, BK., Chapman, NM. and Iwen, PC. (2009). Overview of theFlaviviridaeWith an Emphasis on the Japanese Encephalitis Group Viruses. *Laboratory Medicine,* 40**,** 493-499.

Sejvar, JJ., Curns, AT., Welburg, L., Jones, JF., Lundgren, LM., Capuron, L., Pape, J., Reeves, WC. And Campbel, GL. (2008). Neurocognitive and functional outcomes in persons recovering from West Nilevirus illness. *J Neuropsychol,* 2**,** 477-99.

Semenza JC., Tran, A., Espinosa, L., Sudre, B., Domanovic, D. and Paz, S. (2016). Climate change projections of West Nile virus infections in Europe: implications for blood safety practices. *Environ Health,* 15 Suppl 1**,** 28.

Sevvana, M. and Kuhn, RJ. (2020). Mapping the diverse structural landscape of the flavivirus antibody repertoire. *Curr Opin Virol,* 45**,** 51-64.

Shao, L., Devenport, M. and Jacobs-Lorena, M. (2001). The peritrophic matrix of hematophagous insects. *Archives of Insect Biochemistry and Physiology,* 47**,** 119-125.

Shope, RE. and Meegan, JM. (1997). Arboviruses. *In:* EVANS, A. S. & KASLOW, R. A. (eds.) *Viral Infections ofHumans: Epidemiology and Control.* Boston, MA: Springer US.

Sikkema, RS., Schrama, M., Van Den Berg, T., Morren, J., Munger, E., Krol, L., Van Der Beek, JG., Blom, R., Chestakova, I., Van Der Linden, A., Boter, M., Van Mastrigt, T., Molenkamp, R., Koenraadt, CJ., Van Den Brand, JM., Oude Munnink, BB., Koopmans, MP. and Vand Der Jeugd, H. (2020). Detection of West Nile virus in a common whitethroat (Curruca communis) and Culex mosquitoes in the Netherlands, 2020. *Euro Surveill,* 25.

Smit, JM., Moesker, B., Rodenhuis-Zybert, I. and Wilschut, J. (2011). Flavivirus cell entry and membrane fusion. *Viruses,* 3**,** 160-71.

Smith, DR. (2017). Waiting in the wings: The potential of mosquito transmitted flaviviruses to emerge. *Crit Rev Microbiol,* 43**,** 405-422.

Smithburn, KCK. (1957). Studies on arthropod-borne viruses of Tongaland. IX. Isolation of Wesselsbron virus from a naturally infected human being and from Aedes (Banksinella) circumluteolus Theo. *The South African journal of medical sciences,* 22**,** 113-20.

Sotelo, E., Llorente, F., Rebollo, B., Camanus, A., Venteo, A., Gallardo, C., Lubisi, A., Rodriguez, MJ., Sanz, AJ., Figuerola, J. and Jimenez-Clavero, MA. (2011). Development and evaluation of a new epitope-blocking ELISA for universal detection of antibodies to West Nile virus. *J Virol Methods,* 174**,** 35-41.

Spencer, KA., Osorio, FA. and Hiscox, JA. (2007). Recombinant viral proteins for use in diagnostic ELISAs to detect virus infection. *Vaccine,* 25**,** 5653-9.

Stettler, K., Beltramello, M., Espinosa, D., Graham, V., Cassotta, A., Bianchi, S., Vanzetta, F., Minola, A., Jaconi, S., Mele, F., Foglierini, M., Pedotti, M., Simonelli, L., Dowall, S., Atkinson, B., Percivalle, E., Simmons, C., Varani, L., Blum, J., Baldanti, F., Cameroni, E., Hewson, R., Harris, E., Lanzavecchia, A., Sallusto, F. and Corti, D. (2016). Specificity, cross-reactivity, and function of antibodies elicited by Zika virus infection. *Science,* 353**,** 823-826.

Steyn, J., Botha, E., Stivaktas, VI., Buss, P., Beechler, BR., Myburgh, JG., Steyl, J., Williams, J. and Venter, M. (2019). West Nile Virus in Wildlife and Nonequine Domestic Animals, South Africa, 2010-2018. *Emerg Infect Dis,* 25**,** 2290-2294.

Sule, WF., Oluwayelu, DO., Hernandez-Triana, LM., Fooks, AR., Venter, M. and Johnson, N. (2018). Epidemiology and ecology of West Nile virus in sub-Saharan Africa. *Parasit Vectors,* 11**,** 414.

Swanepoel, R. (1989). Wesselsbron Virus Disease. *In:* PRESS, C. (ed.) *The Arboviruses: Epidemiology and Ecology.* 1 ed.

Tajudeen, YA., Oladipo, HJ., Olandunjoye, IO., Yusuf, RO., Sodiq, H., Omotosho, AO., Adesuyi, DS., Yusuff, SI. and El-Sherbini, MS. (2022). Emerging Arboviruses of Public Health Concern in Africa: Priorities for Future Research and Control Strategies. *Challenges,* 13**,** 60.

Talk, S. (2020). *West Nile Virus in Horses: Symptoms, Treatment and Prevention* [Online]. Farnam. Available: https://www.farnam.com/stable-talk/west-nile-virus-in-horses [Accessed 23 April 2020].

Tomar, S. (2017). Flavivirus Protease: An Antiviral Target. *Viral Proteases and Their Inhibitors***,** 137.

Tomori, O., Monath, T., O'Connor, E., Lee, V. and Cropp, B. (1981). Arbovirus Infections among Laboratory Personnel in Ibadan, Nigeria. *Am J Trop Med Hyg,* 30**,** 855-861.

Ulbert, S. (2019). West Nile virus vaccines - current situation and future directions. *Hum Vaccin Immunother,* 15**,**2337-2342.

Van Eeden, C., Swanepoel, R. and Venter, M. (2014). Antibodies against West Nile and Shuni Viruses in Veterinarians, South Africa. *Emerging Infectious Disease journal,* 20**,** 1409.

Van Leur, SW., Heunis, T., Munnur, D. and Sanyal, S. (2021). Pathogenesis and virulence of flavivirus infections. *Virulence,* 12**,** 2814-2838.

Vazquez, A., Herrero, L., Negredo, A., Hernandez, L., Sanchez-Seco, MP. and Tenorio, A. (2016). Real time PCR assay for detection of all known lineages of West Nile virus. *J Virol Methods,* 236**,** 266-270.

Venter, M. (2018). Assessing the zoonotic potential of arboviruses of African origin. *Curr Opin Virol,* 28**,** 74-84.

Venter, M., Pretorius, M., Fuller, J., Botha, E., Rakgotho, M., Stivaktas, V., Weyer, C., Romito, M. and Williams, J. (2017a). West Nile virus lineage 2 in horses and other animals with neurological diseases in South Africa (2008-2015): a One Health approach for defining the epidemiology *Emerg Infect Dis,* 23**,** 2060-2064.

Venter, M., Pretorius, M., Fuller, JA., Botha, E., Rakgotho, M., Stivaktas, V., Weyer, C., Romito, M. and Williams, J. (2017b.) West Nile Virus Lineage 2 in Horses and Other Animals with Neurologic Disease, South Africa, 2008-2015. *Emerg Infect Dis,* 23**,** 2060-2064.

Venter, M., Zaayman, D., Van Niekerk, S., Stivaktas, V., Goolab, S., Weyer, J., Paweska, JT. and Swanepoel, R. (2014). Macroarray assay for differential diagnosis of meningoencephalitis in southern Africa. *J Clin Virol,* 60**,** 50-6.

Weatherhead, JE., Miller, VE., Garcia, MN., Hasbun, R., Salazar, L., Dimachkie, MM. and Murray, KO. (2015). Long-term neurological outcomes in West Nile virus-infected patients: an observational study. *Am J Trop Med Hyg,* 92**,** 1006-1012.

Weaver, SC. and Barrett, AD. (2004). Transmission cycles, host range, evolution, and emergence of arboviral disease. *Nat Rev Microbiol,* 2**,** 789-801.

Weinbren, KK. (1959). Regeneration of the liver. *Gastroenterology,* 37**,** 657-678.

Weiss, D., Carr, D., Kellachan, J., Tan, C., Phillips, M., Bresnitz, E. and Layton, M. (2001). Clinical findings of West Nile virus infection in hospitalized patients, New York and New Jersey 2000. *Emerg Infect Dis,* 7**,** 654-658.

Weiss, K., Haig, D. and Alexander, R. (1956). Wesselsbrons virus- A virus not previously described, associated with abortion in domestic animals. *Onderstepoort Journal of Veterinary Research,* 27**,** 183-195.

Weissenbock, H., Hubalek, Z., Bakonyi, T. and Nowotny, N. (2010). Zoonotic mosquito-borne flaviviruses: Worldwide presence of agents with proven pathogenicity and potential candidates of future emerging diseases. *Veterinary Microbiology,* 140**,** 271-280.

Weyer, J., Thomas, J., Leman, PA., Grobbelaar, AA., Kemp, A. and Paweska, JT. (2013). Human cases of Wesselsbron disease, South Africa 2010-2011. *Vector Borne Zoonotic Dis,* 13**,** 330-6.

WOAH (2022). Trade measures, Import/Export procedures and Veterinary certification. *Terrestrial Animal Health Code.*

Wu, P., Yu, X., Wang, P. and Cheng, G. (2019). Arbovirus lifecycle in mosquito: acquisition, propagation and transmission. *Expert Rev Mol Med,* 21**,** e1.

Zaayman, D. and Venter, M. (2012). West Nile virus neurologic disease in humans, South Africa, September 2008-may 2009. *Emerg Infect Dis,* 18**,** 2051-4.

Zhang, Y., Zhang, W., Ogata, S., Clements, D., Strauss, JH., Baker, TS., Kuhn, RJ. and Rossmann, MG. (2004). Conformational changes of the flavivirus E glycoprotein. *Structure,* 12**,** 1607-18.

Ziegler, U., Santos, PD., Groschup, MH., Hattendorf, C., Eiden, M., Hoper, D., Eisermann, P., Keller, M., Michel, F., Klopfleisch, R., Muller, K., Werner, D., Kampen, H., Beer, M., Frank, C., Lachmann, R., Tews, BA., Wylezich, C., Rinder, M., Lachmann, L., Grunewald, T., Szentiks, CA., Sieg, M., Schmidt-Chanasit, J., Cadar, D. and Luhken, R. (2020). West Nile Virus Epidemic in Germany Triggered by Epizootic Emergence, 2019. *Viruses,* 12.

Zou, S., Foster, G., Dodd, R., Peterson, L. and Stramer, S. (2010). West Nile Fever characteristics among viremic persons identified through blood donor screening. *The Journal of Infectious Diseases,* 202**,** 135